PB-231 266

HYPOLIMNION AERATION WITH COMMERCIAL OXYGEN-VOLUME II, BUBBLE PLUME GAS TRANSFER

R. E. Speece, et al

Texas University
Austin, Texas

December 1973

DISTRIBUTED BY:

NTIS
National Technical Information Service
U. S. DEPARTMENT OF COMMERCE
5285 Port Royal Road, Springfield Va. 22151

RESEARCH REPORTING SERIES

Research reports of the Office of Research and Monitoring, Environmental Protection Agency, have been grouped into five series. These five broad categories were established to facilitate further development and application of environmental technology. Elimination of traditional grouping was consciously planned to foster technology transfer and a maximum interface in related fields. The five series are:

1. Environmental Health Effects Research
2. Environmental Protection Technology
3. Ecological Research
4. Environmental Monitoring
5. Socioeconomic Environmental Studies

This report has been assigned to the ENVIRONMENTAL PROTECTION TECHNOLOGY series. This series describes research performed to develop and demonstrate instrumentation, equipment and methodology to repair or prevent environmental degradation from point and non-point sources of pollution. This work provides the new or improved technology required for the control and treatment of pollution sources to meet environmental quality standards.

PB 231 266

SELECTED WATER RESOURCES ABSTRACTS
INPUT TRANSACTION FORM

1. Report No.

2.

W74-16526

Hypolimnion Aeration with Commercial Oxygen - Vol. II - Bubble Plume Gas Transfer,

5. Report Date

8. Performing Organization Report No.

Speece, R.E.; Rayyan, F.; Murfee, G.

EPA Project
16080 FYW

Texas University,
~~The University of Texas at Austin~~
Austin, ~~Texas 78712~~

13. Type of Report and Period Covered

12. Sponsoring Organization

Environmental Protection Agency, Technology Series ~~report number~~,
EPA-660/2-73-025b, December 1973. 150p, 77 fig, 2 tab, 14 ref

This study deals with a proposed scheme for restoration and maintenance of dissolved oxygen in the hypolimnion of stratified impoundments without disturbing the stratification. Commercial oxygen is an economical alternative to air as an oxygen source for hypolimnion aeration. In addition, it possesses many other advantages, the main one being avoidance of nitrogen gas supersaturation and its related toxicity to fish.

Laboratory and lake studies were conducted to demonstrate the gas transfer dynamics of a bubble plume generated by the injection of pure oxygen bubbles within the hypolimnion. The experimental results verified the practicality of the original concept - hypolimnion aeration which preserves stratification. Efficient oxygen absorption was achieved within the hypolimnion.

Mathematical models were formulated and calibrated by experimental data. The calibrated model was then used to predict the oxygen transfer and hydrodynamic characteristics of the bubble plume for various oxygen injection rates and injection depths. The sensitivity of the model to the various input parameters was shown. (EPA)

(See also W74-16535)

17a. Descriptors

Water Quality, ~~Modeling~~, *Hypolimnion, *Aeration, Stratification, Water Quality Control, *Texas, Model studies, *Bubbles, Dissolved oxygen, *Oxygenation, Absorption

17b. Identifiers

*Lake Travis (Tex.), *Gas transfer

Copy Available from GPO Sup Doc as EP1.23: 660/2-73-025b $ [illegible]; microfiche from NTIS as PB $1.45

17c. COWRR Field & Group 05D, 05G

19. Security Class. (Report)

20. Security Class. (Page)

21. No. of Pages

22. Price

Send To:

WATER RESOURCES SCIENTIFIC INFORMATION CENTER
U.S. DEPARTMENT OF THE INTERIOR
WASHINGTON, D. C. 20240

R. E. Speece	The University of Texas at Austin

.ia

Reproduced by
NATIONAL TECHNICAL
INFORMATION SERVICE
U S Department of Commerce
Springfield VA 22151

157

EPA-660/2-73-025b
December 1973

HYPOLIMNION AERATION
WITH
COMMERCIAL OXYGEN

VOLUME II
BUBBLE PLUME GAS TRANSFER

By

R. E. Speece
George Murfee
The University of Texas at Austin

Project 16080 FYW
Program Element 1B2045

Project Officer

Lowell E. Leach
Robert S. Kerr Environmental Research Laboratory
Ada, Oklahoma 74820

Prepared for
OFFICE OF RESEARCH AND DEVELOPMENT
U.S. ENVIRONMENTAL PROTECTION AGENCY
WASHINGTON, D.C. 20460

For sale by the Superintendent of Documents, U.S. Government Printing Office, Washington, D.C. 20402 - Price $1.60

ic

EPA Review Notice

This report has been reviewed by the Environmental Protection Agency and approved for publication. Approval does not signify that the contents necessarily reflect views and policies of the Environmental Protection Agency, nor does mention of trade names or commercial products constitute endorsement or recommendation for use.

ABSTRACT

Hypolimnion aeration can be a desirable alternative to destratification for maintenance of good hypolimnion water quality characteristics. Injection of commercial oxygen can be designed to achieve efficient oxygen absorption within the hypolimnion, thus maintaining the stratified conditions. Stratified conditions are very desirable when the cold water resource needs to be preserved.

A mathematical model was developed for predicting the gas transfer characteristics of a bubble plume within an impoundment. Particular attention was given to evaluation of the gas transfer coefficient K_L, as a function of bubble size. With smaller bubble sizes, the buoyant velocity of the bubbles is lower, thus prolonging the contact time which tends to increase gas transfer. However, the gas transfer coefficient, K_L, is a function of bubble size which tends to counter the beneficial effect of extended contact times. The net effect is that the fraction of oxygen mass absorbed in a given rise height can be less for smaller bubbles than for larger ones, depending on the particular sizes.

Tables were compiled from the calibrated model. These tables predict the oxygen absorption characteristics which can be expected for various field situations.

This report was submitted in fulfillment of Project Number 16080 FYW under the partial sponsorship of the Office of Research and Monitoring, Environmental Protection Agency.

CONTENTS

Section		Page
I	CONCLUSIONS	1
II	RECOMMENDATIONS	3
III	INTRODUCTION	5
IV	OBJECTIVES OF INVESTIGATION	7
V	THEORY OF GAS ABSORPTION	9
VI	APPARATUS AND PROCEDURES	23
VII	RESULTS AND DISCUSSIONS	27
VIII	ACKNOWLEDGMENTS	85
IX	REFERENCES	87
X	LIST OF PUBLICATIONS	89
XI	APPENDICES	91

Preceding page blank

FIGURES

No.		Page
1	RELATIVE RESISTANCE TO GAS TRANSFER OF THE GAS AND LIQUID FILMS	10
2	LIQUID FILM COEFFICIENT VS DIAMETER	14
3	TERMINAL VELOCITY OF BUBBLES AS A FUNCTION OF BUBBLE RADIUS	15
4	FLOW CHART	17
5	EXPERIMENTAL SYSTEM	24
6	SPEECE'S MODIFICATION OF BARNHART'S FUNCTION	29
7	FRACTION OF ORIGINAL AMOUNT OF O_2 IN OFF-GAS VS DEPTH (USING SPEECE'S K_L FUNCTION)	31
8	OXYGEN COMPOSITION OF OFF-GAS VS DEPTH (USING SPEECE'S K_L FUNCTION)	32
9	FRACTION OF ORIGINAL AMOUNT OF O_2 IN OFF-GAS VS DEPTH (USING SPEECE'S K_L FUNCTION)	33
10	OXYGEN COMPOSITION OF OFF-GAS VS DEPTH (USING SPEECE'S K_L FUNCTION)	34
11	LIQUID FILM COEFFICIENT VS DIAMETER (MURFEE'S FUNCTION)	36
12	FRACTION OF ORIGINAL AMOUNT OF O_2 IN OFF-GAS VS DEPTH - PURE OXYGEN	37
13	OXYGEN COMPOSITION OF OFF-GAS VS DEPTH - PURE OXYGEN	38
14	FRACTION OF ORIGINAL AMOUNT OF O_2 IN OFF-GAS VS DEPTH - PURE OXYGEN	39

FIGURES

No.		Page
15	OXYGEN COMPOSITION OF OFF-GAS VS DEPTH	40
16	FRACTION OF ORIGINAL AMOUNT OF O_2 IN OFF-GAS VS DEPTH - PURE OXYGEN	41
17	OXYGEN COMPOSITION OF OFF-GAS VS DEPTH - PURE OXYGEN	42
18	FRACTION OF ORIGINAL AMOUNT OF O_2 IN OFF-GAS VS DEPTH - PURE OXYGEN	43
19	OXYGEN COMPOSITION OF OFF-GAS VS DEPTH - PURE OXYGEN	44
20	FRACTION OF ORIGINAL AMOUNT OF O_2 IN OFF-GAS VS DEPTH - PURE OXYGEN	45
21	OXYGEN COMPOSITION OF OFF-GAS VS DEPTH - PURE OXYGEN	46
22	OXYGEN COMPOSITION OF OFF-GAS VS DEPTH - PURE OXYGEN	47
23	DIAMETER OF BUBBLE AS A FUNCTION OF DEPTH	48
24	DIAMETER OF BUBBLE AS A FUNCTION OF DEPTH	49
25	RELATIVE VOLUME OF GAS VS DEPTH (FRACTION)	51
26	RELATIVE VOLUME OF GAS VS DEPTH (FRACTION)	52
27	LIQUID FILM COEFFICIENT VS DIAMETER	53
28	FRACTION OF ORIGINAL AMOUNT OF O_2 IN OFF-GAS VS DEPTH	54
29	OXYGEN COMPOSITION OF OFF-GAS VS DEPTH - PURE OXYGEN	55
30	FRACTION OF ORIGINAL AMOUNT OF O_2 VS FRACTION OF INITIAL INJECTION DEPTH	57

FIGURES

No.		Page
31	OXYGEN COMPOSITION OF OFF-GAS VS FRACTION OF INITIAL INJECTION DEPTH	58
32	FRACTION OF ORIGINAL AMOUNT OF O_2 IN OFF-GAS VS DEPTH	59
33	OXYGEN COMPOSITION OF OFF-GAS VS DEPTH	60
34	FRACTION OF ORIGINAL AMOUNT OF O_2 IN OFF-GAS VS DEPTH	61
35	FRACTION OF ORIGINAL AMOUNT OF O_2 IN OFF-GAS VS DEPTH	63
36	OXYGEN COMPOSITION OF OFF-GAS VS FRACTION OF DEPTH	64
37	FRACTION OF ORIGINAL AMOUNT OF O_2 IN OFF-GAS VS DEPTH	65
38	OXYGEN COMPOSITION OF OFF-GAS VS DEPTH	66
39	CENTER LINE VELOCITY VS HEIGHT ABOVE DIFFUSER	67
40	FRACTION OF ORIGINAL AMOUNT OF O_2 IN OFF-GAS VS DEPTH	68
41	RISE HEIGHT REQUIRED TO ACHIEVE INDICATED ABSORPTION EFFICIENCY VS BUBBLE DIAMETER	71
42	NITROGEN IN OFF-GAS VS DEPTH - PURE OXYGEN	77
43	NITROGEN IN OFF-GAS VS DEPTH - PURE OXYGEN	78
44	NITROGEN IN OFF-GAS VS DEPTH - PURE OXYGEN	79
45	NITROGEN IN OFF-GAS VS DEPTH - PURE OXYGEN	80
46	NITROGEN IN OFF-GAS VS DEPTH - AIR	81

FIGURES

No.		Page
47	NITROGEN IN OFF-GAS VS DEPTH - AIR	82
48	NITROGEN IN OFF-GAS VS DEPTH - AIR	83
49	NITROGEN IN OFF-GAS VS DEPTH - AIR	84
50	FRACTION OF ORIGINAL AMOUNT OF O_2 IN OFF-GAS VS DEPTH - PURE OXYGEN	94
51	RELATIVE VOLUME OF GAS VS DEPTH - PURE OXYGEN	95
52	FRACTION OF ORIGINAL AMOUNT OF O_2 IN OFF-GAS VS DEPTH - PURE OXYGEN	96
53	RELATIVE VOLUME OF GAS VS DEPTH - PURE OXYGEN	97
54	FRACTION OF ORIGINAL AMOUNT O_2 IN OFF-GAS VS DEPTH - PURE OXYGEN	98
55	RELATIVE VOLUME OF GAS VS DEPTH - PURE OXYGEN	99
56	FRACTION OF ORIGINAL AMOUNT OF O_2 IN OFF-GAS VS DEPTH - PURE OXYGEN	100
57	RELATIVE VOLUME OF GAS VS DEPTH - PURE OXYGEN	101
58	FRACTION OF ORIGINAL AMOUNT OF O_2 IN OFF-GAS VS DEPTH - PURE OXYGEN	102
59	RELATIVE VOLUME OF GAS VS DEPTH - PURE OXYGEN	103
60	FRACTION OF ORIGINAL AMOUNT OF O_2 IN OFF-GAS VS DEPTH - PURE OXYGEN	104
61	RELATIVE VOLUME OF GAS VS DEPTH - PURE OXYGEN	105
62	FRACTION OF ORIGINAL AMOUNT OF O_2 IN OFF-GAS VS DEPTH - PURE OXYGEN	106

FIGURES

No. Page

63 RELATIVE VOLUME OF GAS VS DEPTH - PURE OXYGEN 107

64 FRACTION OF ORIGINAL AMOUNT OF O_2 IN OFF-GAS VS DEPTH - AIR 108

65 RELATIVE VOLUME OF GAS VS DEPTH - AIR 109

66 FRACTION OF ORIGINAL AMOUNT OF O_2 IN OFF-GAS VS DEPTH - AIR 110

67 RELATIVE VOLUME OF GAS VS DEPTH - AIR 111

68 FRACTION OF ORIGINAL AMOUNT OF O_2 IN OFF-GAS VS DEPTH - AIR 112

69 RELATIVE VOLUME OF GAS VS DEPTH - AIR 113

70 FRACTION OF ORIGINAL AMOUNT OF O_2 IN OFF-GAS VS DEPTH - AIR 114

71 RELATIVE VOLUME OF GAS VS DEPTH - AIR 115

72 FRACTION OF ORIGINAL AMOUNT OF O_2 IN OFF-GAS VS DEPTH - AIR 116

73 RELATIVE VOLUME OF GAS VS DEPTH - AIR 117

74 FRACTION OF ORIGINAL AMOUNT OF O_2 IN OFF-GAS VS DEPTH - AIR 118

75 RELATIVE VOLUME OF GAS VS DEPTH - AIR 119

76 FRACTION OF ORIGINAL AMOUNT OF O_2 IN OFF-GAS VS DEPTH - AIR 120

77 RELATIVE VOLUME OF GAS VS DEPTH - AIR 121

TABLES

No.		Page
1	SUMMARY OF DATA	28
2	RISE HEIGHTS FOR GIVEN % ABSORPTION, INJECTION DEPTH, AND INITIAL BUBBLE DIAMETER	72

SECTION I

CONCLUSIONS

The concept of in-place hypolimnion aeration by injecting commercial oxygen bubbles has been validated. The rise height required for efficient absorption to be achieved within the hypolimnion has been defined. A relationship between the liquid film coefficient and bubble diameter has been developed for bubble diameters of approximately 0.2 and 2.0 mm. This relationship has been verified by use of a computer model and data obtained in a field study.

A methodology for the design of an in-place hypolimnion aeration system has been developed which can be of practical value to engineers faced with the problem of improving the quality of hypolimnetic releases.

SECTION II

RECOMMENDATIONS

It is recommended that additional studies be conducted to verify intermediate points defining the relationship between the gas transfer coefficient, K_L, and bubble diameter. A full-scale, well instrumented field installation needs to be made to demonstrate these laboratory and pilot-scale studies.

Preceding page blank

SECTION III

INTRODUCTION

Stratification of impounded waters causes deleterious changes to occur in the quality of the hypolimnion waters. If the stratification period is sufficiently long, an anaerobic condition will result. The dissolved oxygen in the hypolimnion is depleted due to microbial activity and reaeration will not occur because the hypolimnion is isolated from the atmosphere. Under these conditions, precipitated iron and manganese will return to solution, carbon dioxide will accumulate, and hydrogen sulfide will be produced resulting in taste and odor problems and color. To alleviate these problems some method of aerating the hypolimnion is called for.

Destratification of the reservoir has been one method used to aerate the hypolimnion. However, certain drawbacks are associated with this solution. Large volumes of water must be moved to accomplish the destratification. The beneficial cold water resource which the hypolimnion waters represent is destroyed. Algal productivity will be increased due to the return to the epilimnion of the nutrients which have collected in the hypolimnion. The water will be supersaturated with nitrogen causing adverse effects on trout and salmon if the concentration exceeds 104% of saturation.

Selective withdrawal of water from predetermined depths is another method which can be used to control the quality of the water discharged below an impoundment or withdrawn as a water supply. The warm epilimnion waters containing a high concentration of dissolved oxygen can be withdrawn and mixed with a chemically low-quality hypolimnetic release and thereby result in a compromise in the overall quality of the water. However, certain disadvantages are inherent in the use of this system. The capital cost and operating cost is high. An operational method must be employed to insure the release of water of sufficient quality to meet the downstream use demands. The various levels of release also must be monitored closely to prevent the accumulation of nutrients in the reservoir. It is apparent that in many cases a method must be used which improves the quality of the hypolimnion releases.

Penstock injection of commercial oxygen is another plausible alternative. Of primary importance, this method involves the least capital expenditure. Closer control of the dissolved oxygen concentration would be realized because all of the discharge water must pass through the penstock. The major disadvantage is that application can only be made during the period of peaking power production.

Preceding page blank

Speece (1) has proposed an in-place hypolimnion aeration system whereby the cold temperature of the hypolimnetic waters is not destroyed while the dissolved oxygen concentration is increased. Oxygen bubble injection deep within a reservoir is a desirable method for improvement of the quality of the water within the hypolimnion for several reasons. First, if the oxygen bubbles are within certain ranges in size and the depth of injection is sufficiently deep the bubbles will be completely absorbed before reaching the bottom of the metalimnion and no mixing will occur. With the thermal stratification maintained, a system of diffusers can be constructed allowing a build-up of an oxygenated pocket around a municipal or industrial water supply intake. This will result in quality rectification of the withdrawn water without aerating the entire hypolimnion. Oxygen gas is a more feasible gas to use than air because the dissolved nitrogen concentrations are not increased in the reservoir and more complete absorption of the total volume of gas injected will be realized, thereby reducing the potential for mixing to occur between the hypolimnion and the metalimnion for the cases where the maximum injection depth is relatively shallow.

This report covers several phases of a study directed toward research and demonstration of the concept of hypolimnion aeration with commercial oxygen. Laboratory and field experiments were conducted to gather data with which to calibrate a gas transfer model which could predict gas absorption characteristics within a bubble plume in an impoundment. Mass balances were made of the gas in bubble plumes after various rise heights, both in laboratory columns and in a stratified impoundment. One of the major considerations was to develop an empirical relationship between the gas transfer coefficient, K_L, and bubble diameter. After the gas transfer model was calibrated with the experimental data, it was used to determine the sensitivity of the bubble plume absorption characteristics to various parameters, e.g. dissolved nitrogen in the water, water temperature etc.

SECTION IV

OBJECTIVES OF INVESTIGATION

The principal objectives of this study were:

1. To investigate the effects of initial bubble size and injection depth on the mass transfer of oxygen in the field using:
    a. A diffuser capable of producing oxygen bubbles with diameters between 0.2 mm and 0.5 mm.
    b. A diffuser capable of producing oxygen bubbles with diameters between 1.0 mm and 2.0 mm.

2. To develop a relationship between liquid film coefficient and bubble diameter based on the data collected in field studies.

3. To develop a methodology for the design of a diffuser system of in-place hypolimnion aeration.

SECTION V

THEORY OF GAS ABSORPTION

Gas Mass-Transfer

The absorption rate of a gas into a liquid is basically governed by Fick's law of diffusion,

$$dm/dt = DA\,(dc/dx) \qquad (1)$$

where:
dm/dt = time rate of mass transfer
D = diffusivity of the gas
A = cross-sectional area across which diffusion occurs
dc/dx = the concentration gradient

This equation is not directly applicable to an aeration system because of the turbulent conditions present. As an oxygen bubble rises in water, the water mass surrounding the bubble is constantly being replaced; hence, the concentration gradient, dc/dx, will not be allowed to develop due to insufficient time. The dominant resistance to gas transfer is believed to occur at the interface between the gas and the liquid. The two film theory as proposed by Lewis and Whitman (2) in 1924, takes this resistance into account.

The two film theory assumes that at the interface a film of gas and a film of liquid is developed. As the gas is transferred, it passes through these two films by molecular diffusion (Figure 1). The time rate of mass-transfer of gas through the gas film must equal the rate through the liquid film and in turn must equal the rate of diffusion into the liquid. Assuming a steady-state condition:

$$dm/dt = -D_g A(dc/dx) = -D_1 A(dc/dx) \qquad (2)$$

where:
D_g = molecular diffusivity of the gas through the gas film
D_1 = molecular diffusivity of the gas through the liquid film
D = eddy or turbulent diffusivity of the gas in the main body of the liquid.

Preceding page blank

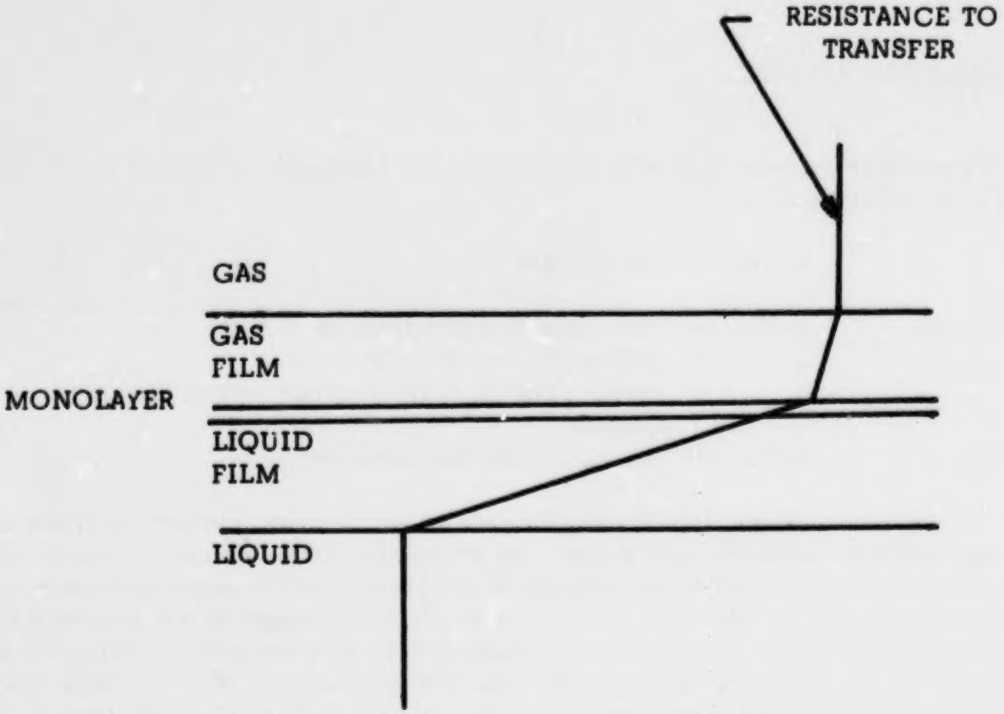
RESISTANCE TO TRANSFER
GAS
GAS FILM
MONOLAYER
LIQUID FILM
LIQUID

Fig. 1 RELATIVE RESISTANCE TO GAS TRANSFER OF THE GAS AND LIQUID FILMS

Treybal (3) showed that the gas film offers little resistance to mass-transfer compared to the liquid. Once the gas passes through the two films it is distributed by eddy or turbulent diffusion in the main body of liquid. The eddy or turbulent diffusivity, D, is much greater than the molecular diffusivity of gas through the two films.

Hence, the rate of mass-transfer is controlled by the limiting condition and

$$\frac{dm}{dt} = -D_L A \frac{dc}{dx} \tag{3}$$

The concentration gradient, dc/dx, is related to the deficiency between the saturation concentration of the gas in the liquid, C_S, and the concentration of the gas in the liquid, C_L.

$$\frac{dc}{dx} = C_S - C_L \tag{4}$$

Solving this equation with respect to a liquid film thickness, L,

$$\frac{dm}{dt} = \frac{-D_L A \left(C_S - C_L\right)}{L} \tag{5}$$

Letting $\frac{-D_L}{L} = K_L$, the liquid film coefficient.

$$\frac{dm}{dt} = K_L A \left(C_S - C_L\right) \tag{6}$$

From equation 6 it is obvious that the rate of mass-transfer is proportional to the deficit in concentration of gas in the liquid and the liquid film coefficient.

Higbie (4) argued that the two-film theory was inadequate because of the assumption of complete saturation of the liquid film and hence a steady-state process. Higbie states that the liquid film is constantly being replaced, therefore, the concentration of dissolved gas in the liquid film is equal to the concentration of dissolved gas in the liquid mass, C_L, at the time of replacement. Further, the residence time of the liquid film at the time of replacement is insufficient to allow complete saturation of the liquid film.

To account for this unsteady state condition, Higbie (4) proposed the penetration theory. He defined the liquid film coefficient by the equation,

$$K_L = 2\sqrt{\frac{D_L r}{\pi}} \qquad (7)$$

where: r = $1/t$ = rate of renewal of the liquid film.

Equation 7 gives an average value for K_L based on the assumption that the liquid mass is quiescent for the time period, t, and then is wholly mixed and then the process is again repeated.

Dankwertz (5) modified the penetration theory by redefining r as the average frequency of renewal. The equation for the liquid film coefficient then becomes:

$$K_L = \sqrt{D_L r} \qquad (8)$$

Dobbins (6) further modified the liquid film coefficient relation. He maintained that the liquid film is continuously being replaced. Dobbins combined the boundary conditions of a liquid film with thickness L and the Dankwertz K_L function:

$$K_L = \sqrt{D_L r}\ \coth\sqrt{rL^2/D_L} \qquad (9)$$

Dobbins' experiments verified this relationship. However, for an aeration system above a certain turbulence regime such as injection of gas bubbles into a liquid, $\coth\sqrt{rL^2/D_L}$ approaches unity and the value of K_L approaches $\sqrt{D_L r}$. Dankwertz's modification of the penetration theory is a special case of the more general function, equation 9.

Bubble Aeration

Eckenfelder (7) stated that oxygen transfer occurs during three phases of bubble life. At formation the liquid film is continuously being replaced and results in a higher absorption rate than in the second phase where the bubble is rising. During rise, the rate of mass-transfer is not only a function of the liquid film coefficient but also the terminal velocity which is a function primarily of the bubble size. Barnhart (8) has shown how the values of the liquid film coefficient, K_L, vary with the bubble diameter (Figure 2). The terminal velocity of the bubbles as a function of the bubble diameter has been reported by the David Taylor Modelling Basin Study (9) (Figure 3). The third phase in bubble life occurs when the bubble reaches the surface and bursts. The generalized equation for these three phases is:

$$\frac{dm}{dt} = (K_{LF}A_F + K_{LR}A_R + K_{LS}A_S)(C_S - C_L) \qquad (10)$$

where: the subscripts F, R, and S denote formation, rising and surface, respectively.

Subsequently, Calderbank (10) has found that the absorption rate at formation is less than that in the rising phase. Due to the fact that the time for mass-transfer at formation is of such short duration together with the lower absorption rate, the mass-transfer in the formation phase can be considered negligible.

Liquid Film Coefficient for Nitrogen

It has been found experimentally (11) that the liquid film coefficient for nitrogen is as follows:

$$K_L(N_2) = (0.89)\ K_L\ (O_2) \qquad (11)$$

Temperature Effects on K_L

The effect of temperature on K_L has been reported by Eckenfelder (7).

$$K_L(T) = K_L(20)\ 1.028^{(T-20)} \qquad (12)$$

Mathematical Model to Predict Mass-Transfer

Speece (1) developed a mathematical model to predict gas mass-transfer from an oxygen bubble injected at various depths into an impoundment. It

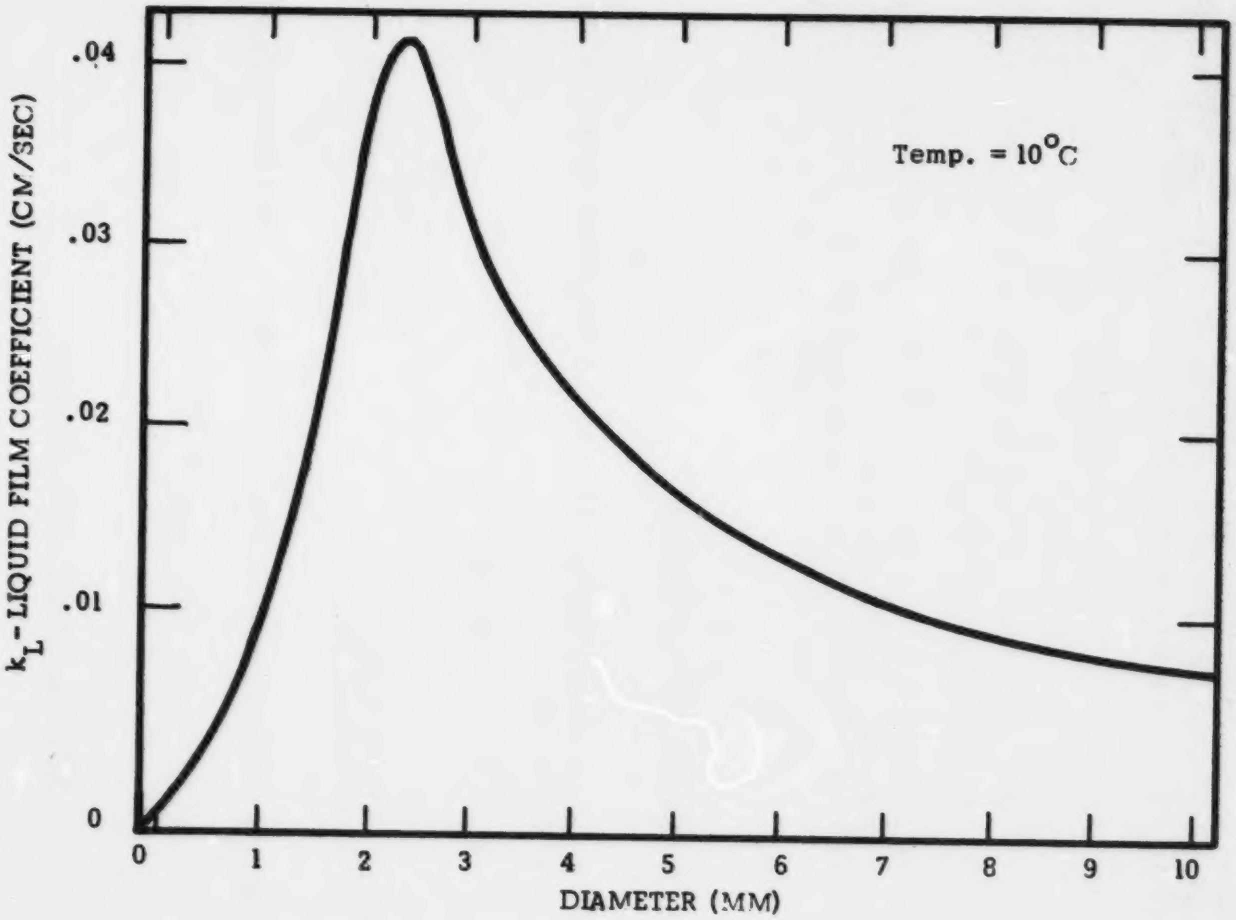

Fig. 2 k_L - LIQUID FILM COEFFICIENT VS DIAMETER

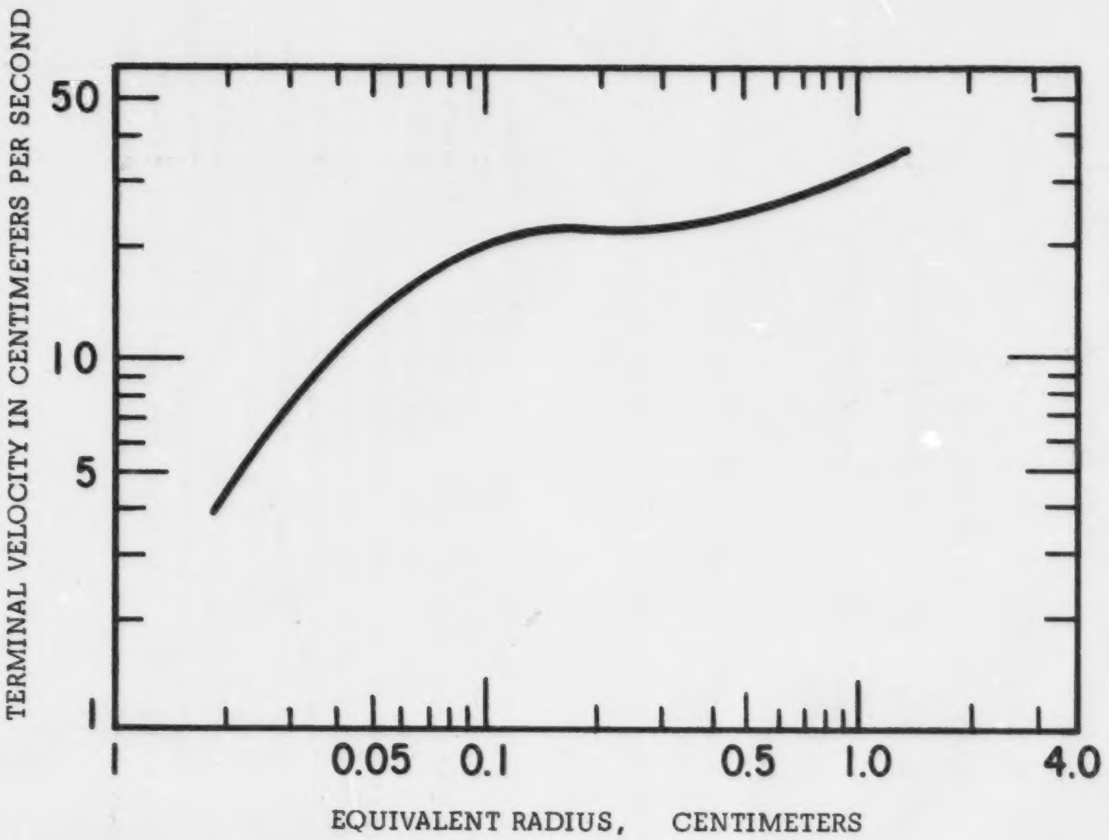

Fig. 3 TERMINAL VELOCITY OF BUBBLES AS A FUNCTION OF BUBBLE RADIUS

is based on the gas transfer equation:

$$\frac{dm}{dt} = K_L A \left(C_S - C_L\right) \qquad (13)$$

Equation 13 was incorporated into the model in the form:

$$\Delta M = K_L A \left(C_S - C_L\right) \Delta t$$

ΔM = mass of gas transferred, mg

K_L = 0.396 mm/sec for bubbles with diam < 1.2 mm

K_L = $0.396\ (\mathrm{DIAM}/1.2)^{0.5}$ mm/sec for bubbles with diam < 1.2 mm

A = interface area, $(\mathrm{mm})^2$

C_S = saturation concentration of the gas in the liquid, $\mathrm{mg}/(\mathrm{mm})^3$

C_L = actual concentration of the gas in the liquid, $\mathrm{mg}/(\mathrm{mm})^3$

t = time interval, seconds.

The model calculated oxygen transfer in the following manner. Initially, the concentrations of dissolved oxygen and dissolved nitrogen, the temperature of the water, the initial bubble diameter, and injection depth are set. The program calculates the mass of oxygen in the bubble, bubble surface area and the hydrostatic pressure. Next, the dissolved oxygen and dissolved nitrogen deficits are determined for the respective partial pressures inside the bubble. The weight of oxygen transferred and the weight of nitrogen transferred are then calculated. The new gas composition of the bubble was then determined. The distance the bubble traveled was calculated being a function of the velocity of rise and time increment, Δt. The new bubble diameter was determined and the procedure was repeated until the bubble reached the surface or was 95% absorbed. The model can predict oxygen and nitrogen transfer for air bubbles injected into the reservoir as well as for oxygen.

FLOW CHART

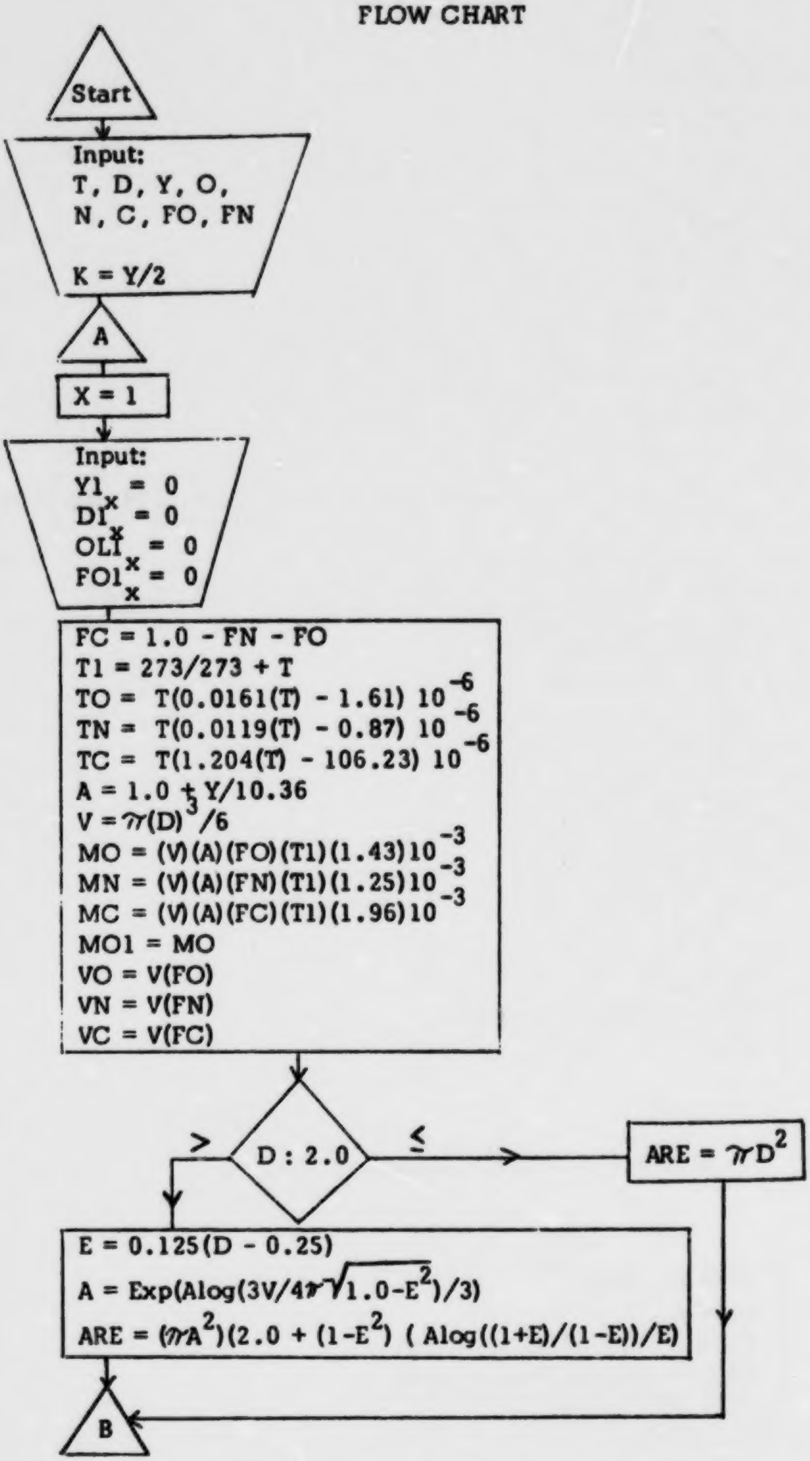
Start
Input:
T, D, Y, O,
N, C, FO, FN
K = Y/2
A
X = 1
Input:
Y1x = 0
DIx = 0
OLIx = 0
FO1x = 0
FC = 1.0 - FN - FO
T1 = 273/273 + T
TO = T(0.0161(T) - 1.61) 10^-6
TN = T(0.0119(T) - 0.87) 10^-6
TC = T(1.204(T) - 106.23) 10^-6
A = 1.0 + Y/10.36
V = π(D)^3/6
MO = (V)(A)(FO)(T1)(1.43)10^-3
MN = (V)(A)(FN)(T1)(1.25)10^-3
MC = (V)(A)(FC)(T1)(1.96)10^-3
MO1 = MO
VO = V(FO)
VN = V(FN)
VC = V(FC)
D : 2.0
>
≤
ARE = πD^2
E = 0.125(D - 0.25)
A = Exp(Alog(3V/4π√(1.0-E^2))/3)
ARE = (πA^2)(2.0 + (1-E^2) (Alog((1+E)/(1-E))/E)
B

Fig. 4

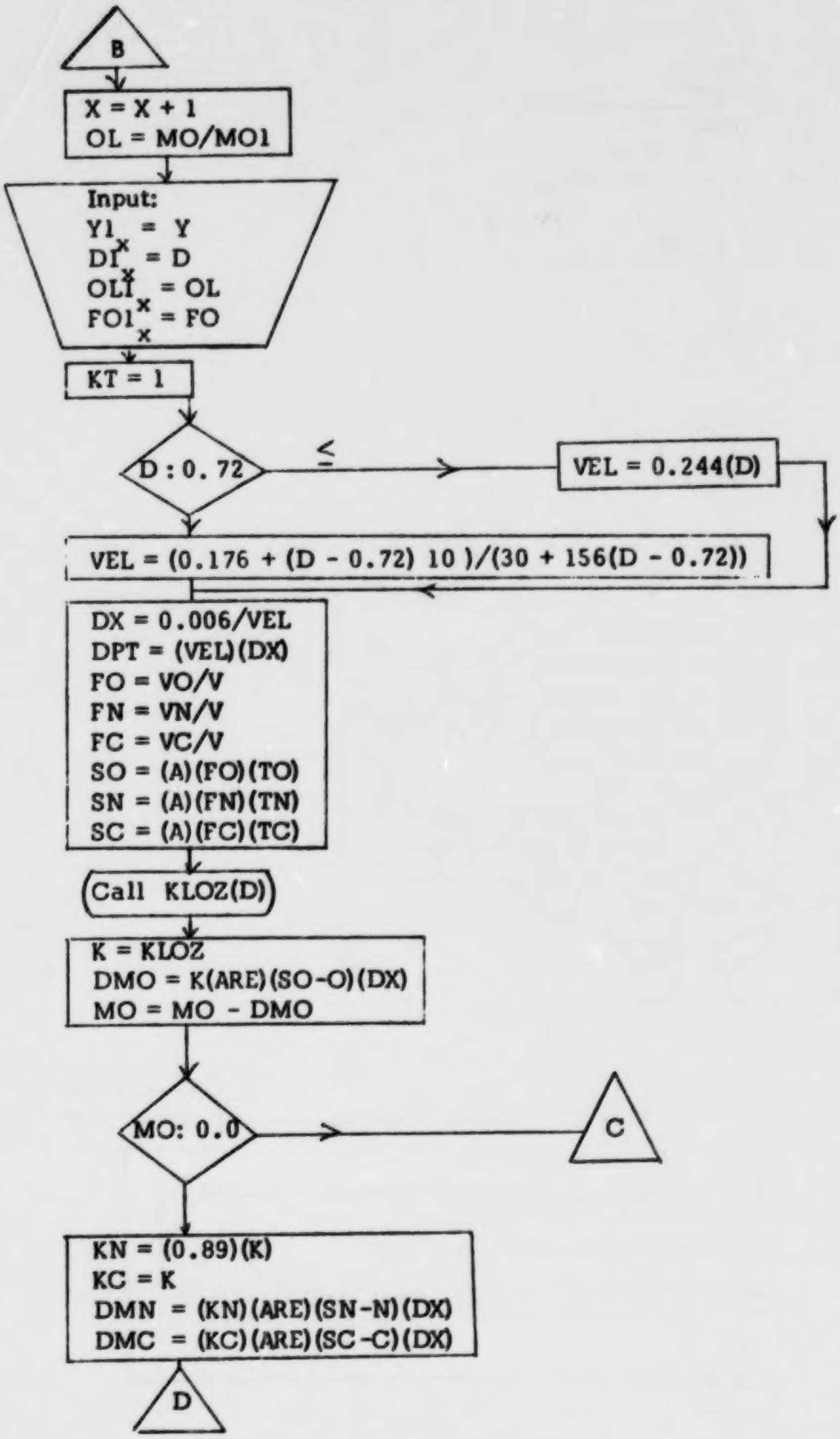
B
X = X + 1
OL = MO/MO1
Input:
Y1x = Y
DIx = D
OLIx = OL
FO1x = FO
KT = 1
D : 0.72
≤
VEL = 0.244(D)
VEL = (0.176 + (D - 0.72) 10)/(30 + 156(D - 0.72))
DX = 0.006/VEL
DPT = (VEL)(DX)
FO = VO/V
FN = VN/V
FC = VC/V
SO = (A)(FO)(TO)
SN = (A)(FN)(TN)
SC = (A)(FC)(TC)
Call KLOZ(D)
K = KLOZ
DMO = K(ARE)(SO-O)(DX)
MO = MO - DMO
MO: 0.0
C
KN = (0.89)(K)
KC = K
DMN = (KN)(ARE)(SN-N)(DX)
DMC = (KC)(ARE)(SC-C)(DX)
D

Fig. 4 (continued)

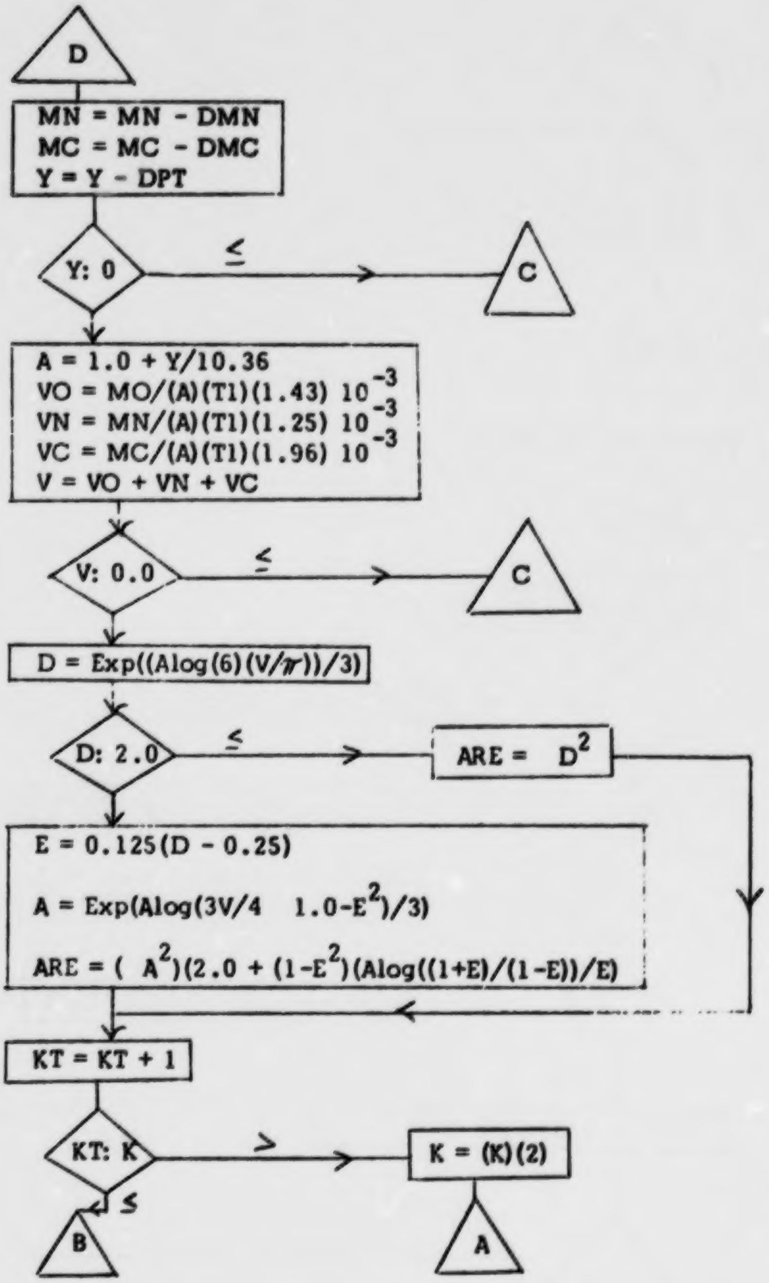
D
MN = MN - DMN
MC = MC - DMC
Y = Y - DPT
Y: 0
≤
C
A = 1.0 + Y/10.36
VO = MO/(A)(T1)(1.43) 10^-3
VN = MN/(A)(T1)(1.25) 10^-3
VC = MC/(A)(T1)(1.96) 10^-3
V = VO + VN + VC
V: 0.0
≤
C
D = Exp((Alog(6)(V/π))/3)
D: 2.0
≤
ARE = D^2
E = 0.125(D - 0.25)
A = Exp(Alog(3V/4 1.0-E^2)/3)
ARE = (A^2)(2.0 + (1-E^2)(Alog((1+E)/(1-E))/E)
KT = KT + 1
KT: K
>
K = (K)(2)
≤
B
A

Fig. 4 (continued)

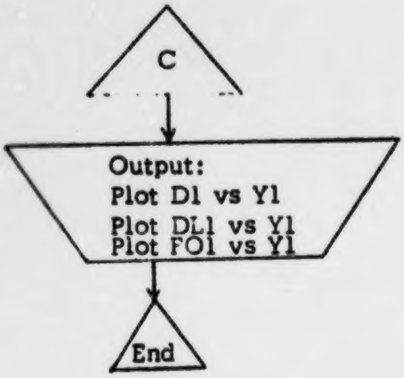
C
Output:
Plot D1 vs Y1
Plot DL1 vs Y1
Plot FO1 vs Y1
End

Subroutine, KLOZ(D):

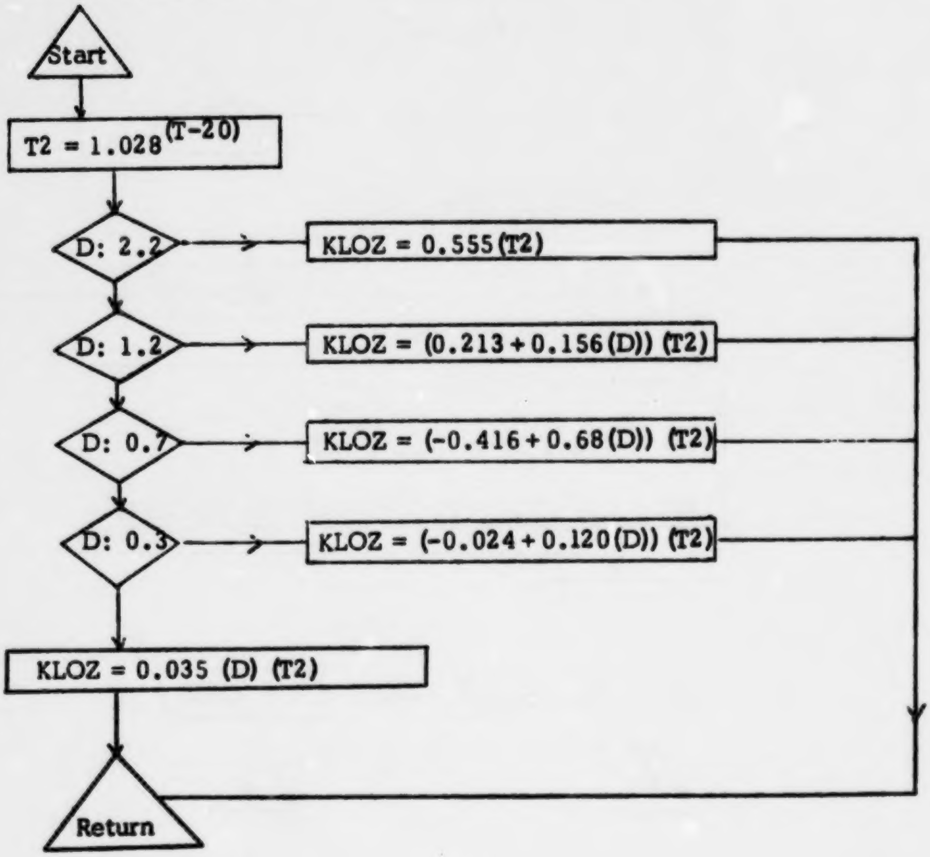
Start
T2 = 1.028^(T-20)
D: 2.2
KLOZ = 0.555(T2)
D: 1.2
KLOZ = (0.213 + 0.156(D)) (T2)
D: 0.7
KLOZ = (-0.416 + 0.68(D)) (T2)
D: 0.3
KLOZ = (-0.024 + 0.120(D)) (T2)
KLOZ = 0.035 (D) (T2)
Return

Fig. 4 (continued)

NOTATION FOR FIGURE 4

T = Temperature of the water, °C

D = Initial bubble diameter, mm

Y = Injection Depth, m

O = Concentration of dissolved oxygen, $mg/(mm)^3$

N = Concentration of dissolved nitrogen, $mg/(mm)^3$

C = Concentration of dissolved carbon dioxide, $mg/(mm)^3$

FO = Fraction of oxygen in the gas bubble

FN = Fraction of nitrogen in the gas bubble

FC = Fraction of carbon dioxide in the gas bubble

A = Pressure, atmospheres

V = Volume of bubble, $(mm)^3$

MO = O_2 in bubble, mg

MN = N_2 in bubble, mg

MC = CO_2 in bubble, mg

VO = Volume of O_2 in bubble, $(mm)^3$

VN = Volume of N_2 in bubble, $(mm)^3$

VC = Volume of CO_2 in bubble, $(mm)^3$

SO = Saturation concentration of dissolved oxygen, $mg/(mm)^3$

SN = Saturation concentration of dissolved nitrogen, $mg/(mm)^3$

SC = Saturation concentration of dissolved carbon dioxide, $mg/(mm)^3$

TO = Density of oxygen gas at one atmosphere, $mg/(mm)^3$

TN = Density of nitrogen gas at one atmosphere, $mg/(mm)^3$

ARE = Area of bubble, $(mm)^2$

OL = Oxygen remaining in bubble, mg

VEL = Terminal velocity of bubble, m/sec

DX = Step interval per iteration, m

DPT = Rise height per step interval, m

DMO = O_2 transferred per step interval, mg

DMN = N_2 transferred per step interval, mg

DMC = CO_2 transferred per step interval, mg

K = Liquid film coefficient for oxygen, mm/sec

KN = Liquid film coefficient for nitrogen, mm/sec

KL = Liquid film coefficient for carbon dioxide, mm/sec

$Y1_x$ = Plotted values of depth, m

$D1_x$ = Plotted values of bubble diameter, mm

$OL1_x$ = Plotted values of fraction of initial oxygen remaining in bubble

$FO1_x$ = Plotted values of fraction of bubble gas which is oxygen

SECTION VI

APPARATUS AND PROCEDURES

Reservoir Bubble Aeration System

The bubble aeration system used in the investigation at the reservoir site consisted of a polyvinyl chloride diffuser (capable of producing 1.0 -2.0 mm bubbles), a commercial oxygen cylinder, a pressure regulator, a flow meter, sheet metal gas collection hood, a sampling gear pump, a wet test meter, and an Orsat type gas analyzer (Figure 5).

Procedure for Reservoir Study

1. The dissolved oxygen and temperature profile for the injection depth and each ten foot increment above the injection depth was determined. A water sample was pumped up from each depth and the dissolved oxygen was measured by the azide modification of the Winkler method (12). The temperature was measured by a probe located at the water sample intake port.

2. The desired oxygen flow rate was established.

3. The off-gas system pump was started.

4. After an equilibrium condition was apparent (steady off-gas flow) the volume of off-gas was measured over a measured time period.

5. Three gas samples were taken for each test and the percent oxygen present was determined on the Orsat gas analyzer.

Lab Bubble Aeration System

The bubble aeration system used in the laboratory portion of the investigation consisted of essentially the same components as used in the reservoir study except a ceramic diffuser capable of producing smaller bubbles (between 0.2 mm and 0.50 mm) was used in place of the PVC diffuser.

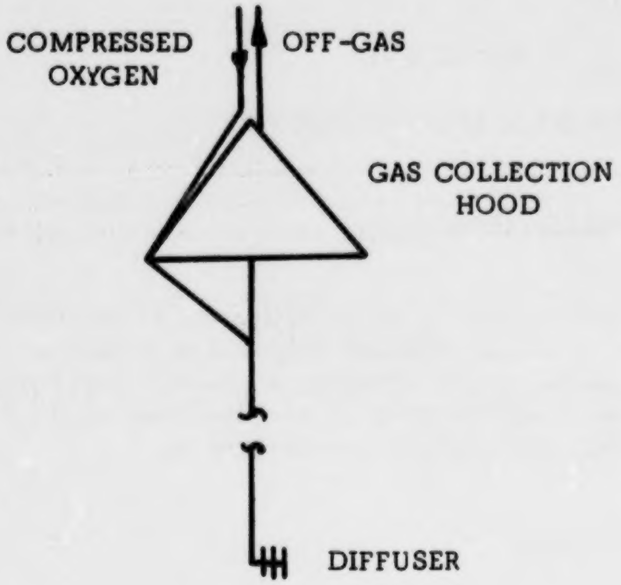
COMPRESSED OXYGEN
OFF-GAS
GAS COLLECTION HOOD
DIFFUSER

AERATION AND OFF-GAS COLLECTION SYSTEM

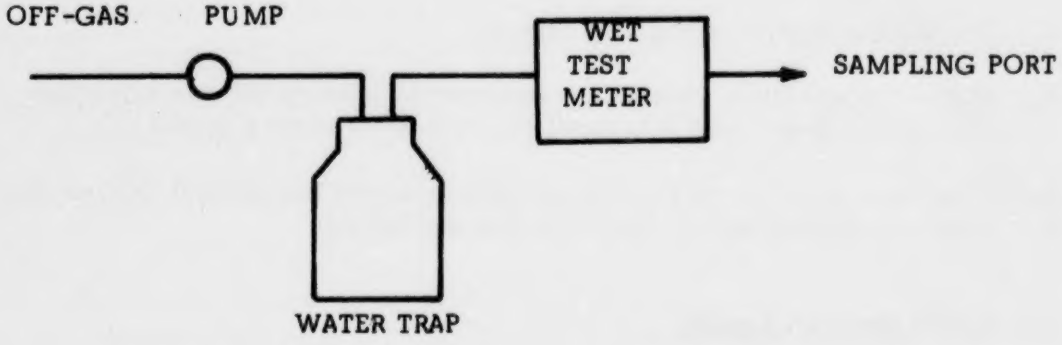
OFF-GAS
PUMP
WET TEST METER
SAMPLING PORT
WATER TRAP

OFF-GAS MEASURING AND SAMPLING SYSTEM

Fig. 5 EXPERIMENTAL SYSTEM

Procedure for Lab Study

1. Before each run the contents of the lab column were circulated through the flumes for twenty minutes to allow the water to become saturated with dissolved oxygen and dissolved nitrogen with respect to air.
2. The dissolved oxygen sample was taken from a depth of 5.0 meters and measured. The temperature was determined.
3. The rest of the procedure was the same as employed in the reservoir study.

Pressure Tank Laboratory Studies

One aspect of this project involved construction of a pressure tank fourteen feet high and thirty inches in diameter. This tank could be pressurized to a hydrostatic head of 200 feet. Thus, the absorption characteristics of bubbles injected as deep as 200 feet could be simulated for as much as fourteen feet of rise.

The column would be pressurized to the desired head and a given mass of oxygen would be injected. At a given height above the injection point, the bubbles would be harvested and the composition and mass determined. The change in mass of oxygen in the off-gas was then correlated with the increase in dissolved oxygen concentration of the water column.

Absorption characteristics in the laboratory pressure column were correlated with the field results. Test conditions were more easily controlled in the laboratory pressure column and test runs could be made more rapidly. In addition, field studies in Lake Travis were limited to ninety feet depth, while it was possible to simulate up to 200 feet in the lab.

The laboratory pressure column absorption results were used along with the field absorption studies to calibrate the oxygen absorption model.

SECTION VII

RESULTS AND DISCUSSION

The laboratory and field studies determined the dynamics of bubble mass and composition with rise height. In this section, the gas transfer prediction model is calibrated by the experimental results. The agreement between predictions of the calibrated model and actual results is shown. Then sensitivity of the model to various parameters is illustrated. The experimental results are summarized in Table 1.

The gas mass-transfer model

The liquid film coefficient, K_L, has been shown to vary with the bubble diameter and temperature. Hence, knowing these two values, as well as the injection depth and depth of gas collection, the results obtained for the fraction of original oxygen in the off-gas and oxygen composition of the off-gas were compared to the predicted results. It was found that the predicted efficiencies of oxygen absorption do not agree with the experimental measurements. Therefore, it was necessary to modify the mathematical function for determining K_L for bubble diameters less than 2.2 mm. Several curves were substituted in the model on a trial and error basis.

Speece's relationship for determining K_L covering the range of bubble diameters up to 2.2 mm is described as follows:

$$K_L = [(0.041)(D) + (0.096)(D)^2]\,T \qquad (14)$$

where: K_L = liquid film coefficient, mm/sec

D = diameter, mm

$T = (1.028)^{(TEMP-20)}$

Figure 6 is a graphical representation of this curve up to a 2.0 mm bubble diameter. This curve represents an extension of Barnharts curve to the origin. The diameter, D, is plotted on the abscissa and the liquid film coefficient, K_L, is plotted on the ordinate.

Preceding page blank

TABLE 1

Summary of Data

Range of Bubble Diam. mm	Inj. Depth, m.	Collection Depth, m	Oxygen Composition of Off-gas	Fraction of Orig. O_2 Mass in Off-gas
1.0 - 2.0	12.1	3.05	0.63 - 0.70 (9)*	0.15 - 0.20(3)
1.0 - 2.0	21.2	3.05	0.34 - 0.46(4)	0.07 - 0.09(2)
1.0 - 2.0	27.3	3.05	0.22(3)	-----
0.2 - 0.5	8.5	0.5	0.64 - 0.73(9)	0.55 - 0.56(3)
0.2 - 0.5	7.7	3.7	0.70 - 0.77(18)	0.62 - 0.69(6)
0.2 - 0.5	5.0	1.0	0.68 - 0.76(9)	0.63 - 0.69(3)

*The numbers in parenthesis following the results denote the number of observations included in the range of the results.

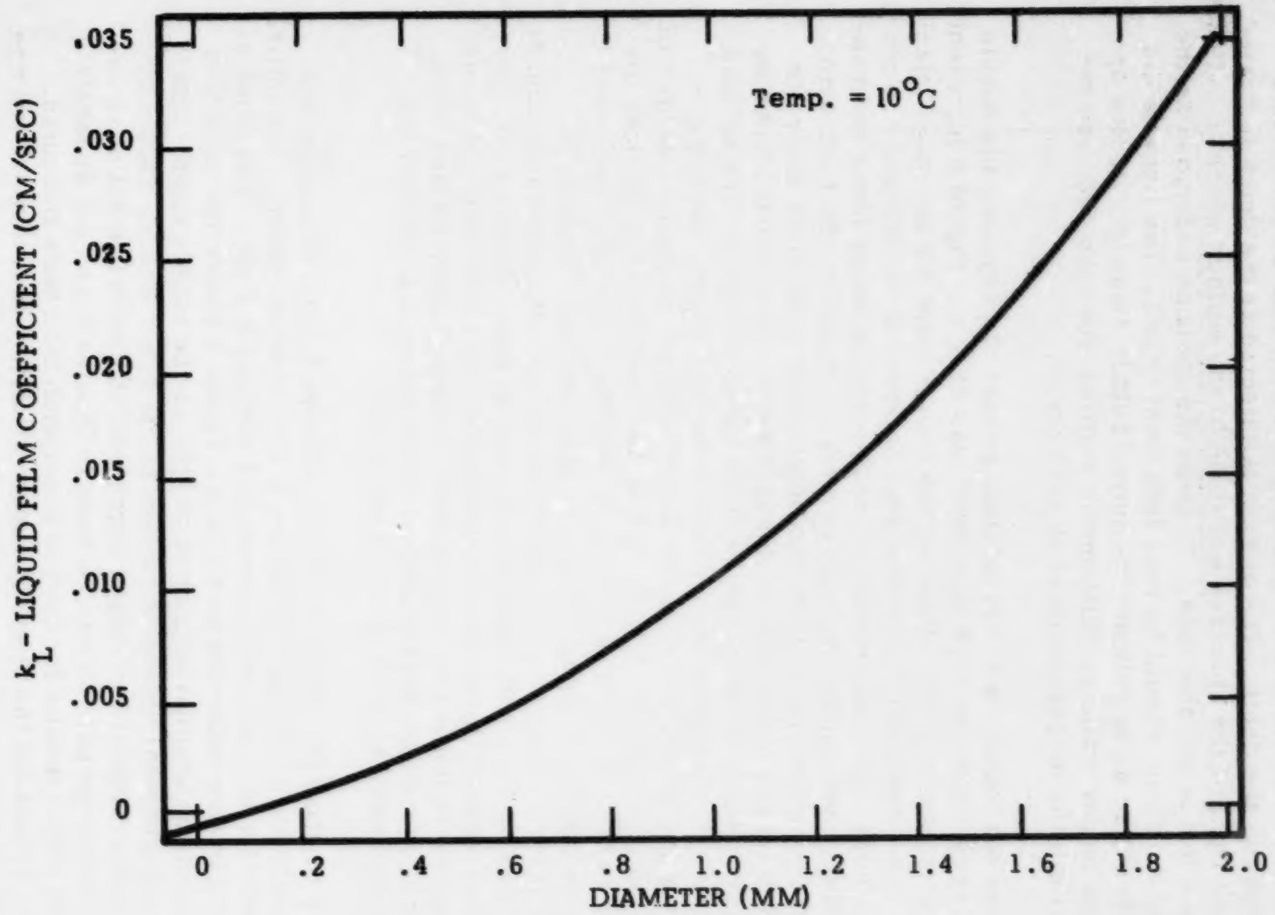

Fig. 6 k_L - LIQUID FILM COEFFICIENT VS DIAMETER

A note is necessary on the following graphs in which various parameters are plotted against the depth. The oxygen is injected at the depth indicated on the extreme right of the abscissa and rises to the surface which is indicated by the extreme left of the abscissa. To trace the changes undergone as the bubbles rise, the figure should be read from right to left. The lines of the figure are labeled so as to indicate the initial bubble diameter. It was assumed that the model would be sufficiently verified when the observed results were within the ranges depicted in each graph.

Figure 7 shows the reduction in the original amount of oxygen as the bubble rises for the case where the injection depth was 21.2 m. Figure 8 represents the oxygen composition in the bubble as the bubble rises for the same injection depth. The initial bubble diameter was believed to be between 1.0 mm and 2.0 mm; hence, two lines appear on each graph denoting these two bubble sizes. The values for the fraction of original oxygen in the bubble and the oxygen composition in the bubble as determined in the field study are included on the graphs. The data is represented by longitudinal blocks on each graph at the depth at which the samples were collected. The off-gas for this injection depth was collected at a depth of 3.05 m. Referring to Figure 7, the range of observed results for the fraction of original oxygen in the off-gas was 0.07 - 0.09. These values are plotted on the vertical line at the 3.05 m depth. For this case Speece's relationship between K_L and bubble diameter predicted results comparable to the observed results. Referring to Figure 8, the experimental values for the oxygen composition of the off-gas, 34% to 40%, were plotted. As can be seen, in this case, the model predicted a range of results approximately 15% higher than the range measured. Based on these two comparisons, it was determined that the K_L values were too low to accurately predict the oxygen mass-transfer for bubbles with diameters in the 1.0 - 2.0 mm range.

Figures 9 and 10 show the reduction in the original amount of oxygen and oxygen composition in the bubbles for the 8.5 m injection depth. The initial bubble diameter for this run was between 0.2 mm and 0.5 mm. The depth at which the off-gas was collected was 0.5 m. Figure 9 shows the reduction in the fraction of the original amount of oxygen as the bubble rises. The range of the experimental values is plotted at the 0.5 m depth. Figure 10 shows the oxygen composition versus depth with the experimental observations plotted on the graph. As can be seen in Figures 9 and 10, Speece's model predicts better results for oxygen absorption than were measured. Hence, the K_L values for the range of bubble diameters between 0.2 mm and 0.5 mm are higher than can be justified by the field studies.

Knowing that Speece's original function for the liquid film coefficient produces too liberal predictions in the model, a group of straight line approxi-

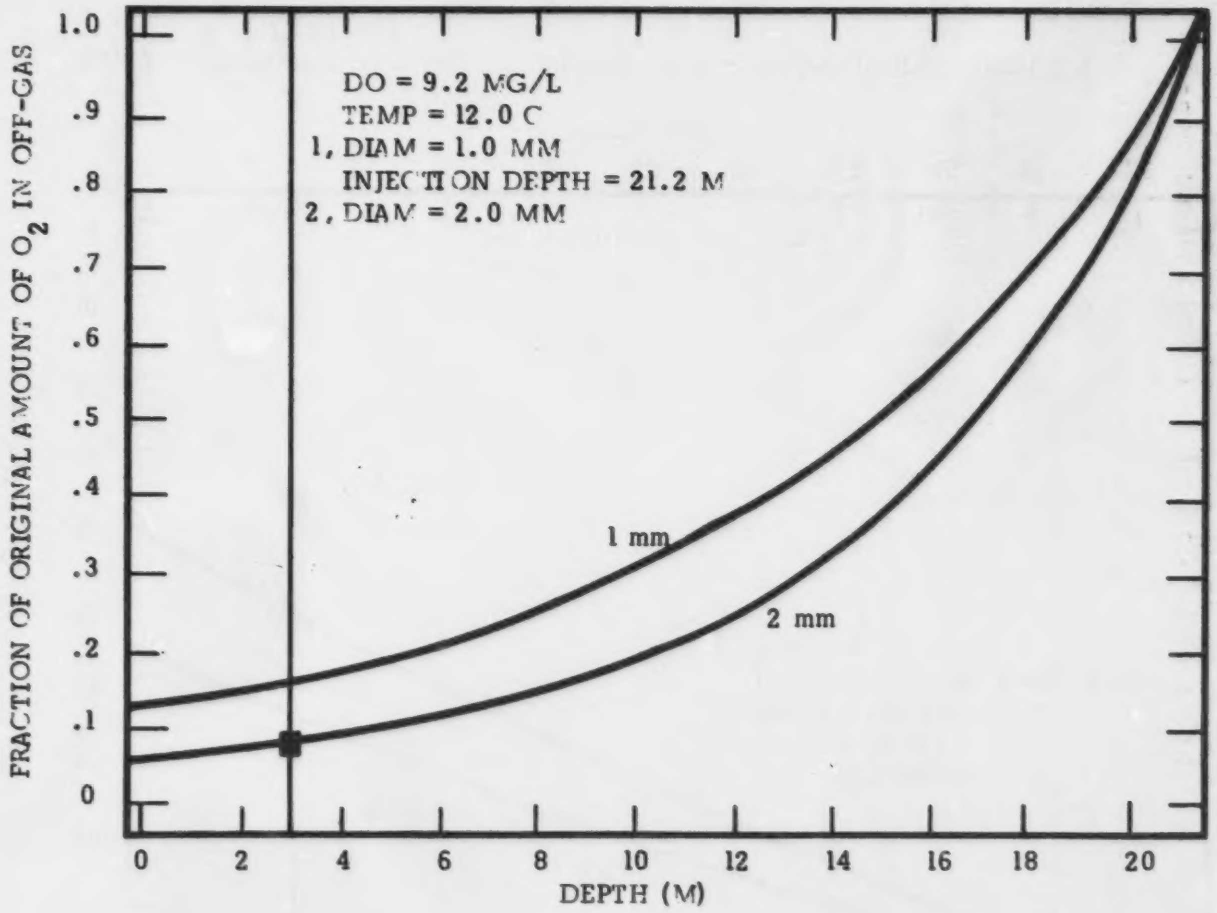

Fig. 7 FRACTION OF ORIGINAL AMOUNT OF O_2 IN OFF-GAS VS DEPTH (USING SPEECE'S k_L FUNCTION)

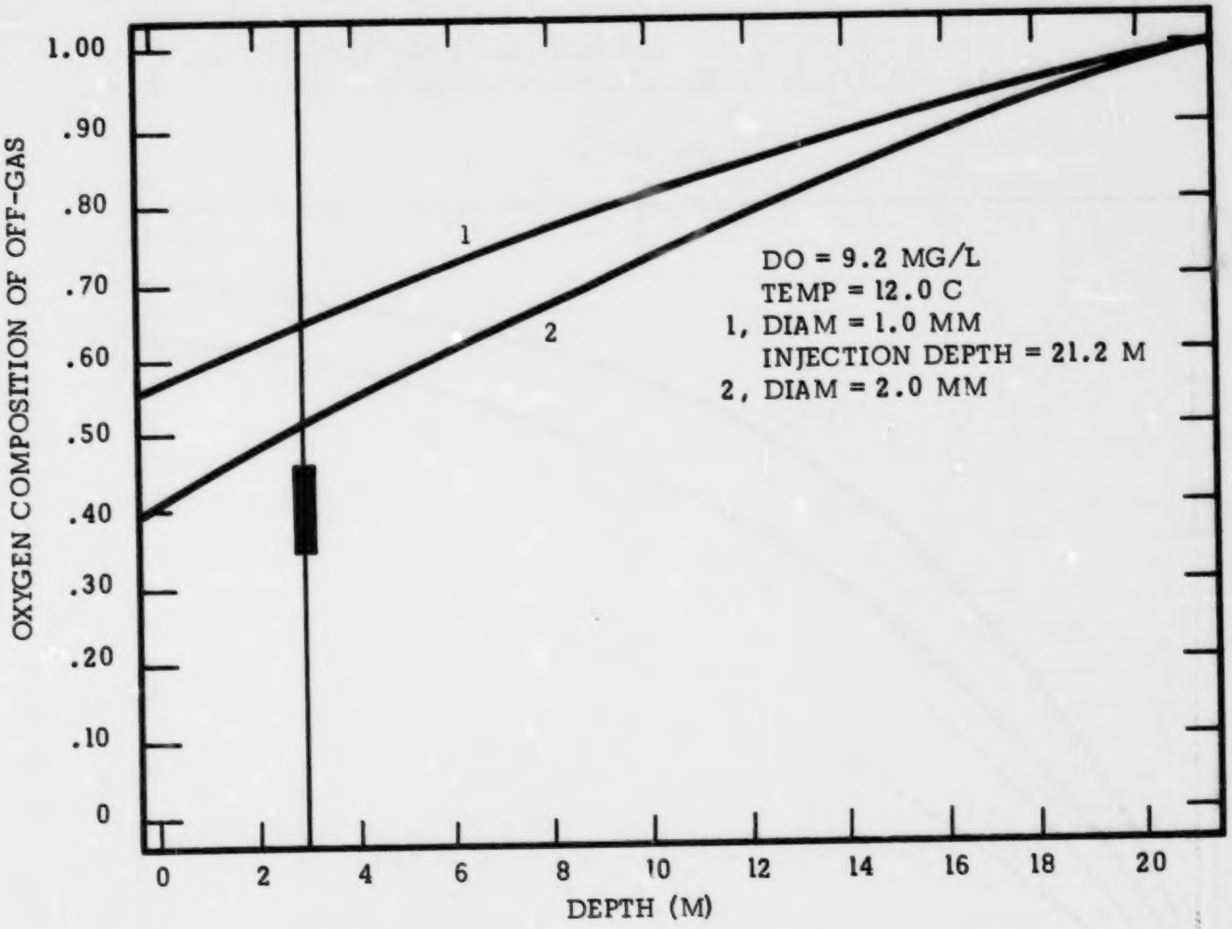

Fig. 8 OXYGEN COMPOSITION OF OFF-GAS VS DEPTH (USING SPEECE'S k_L FUNCTION)

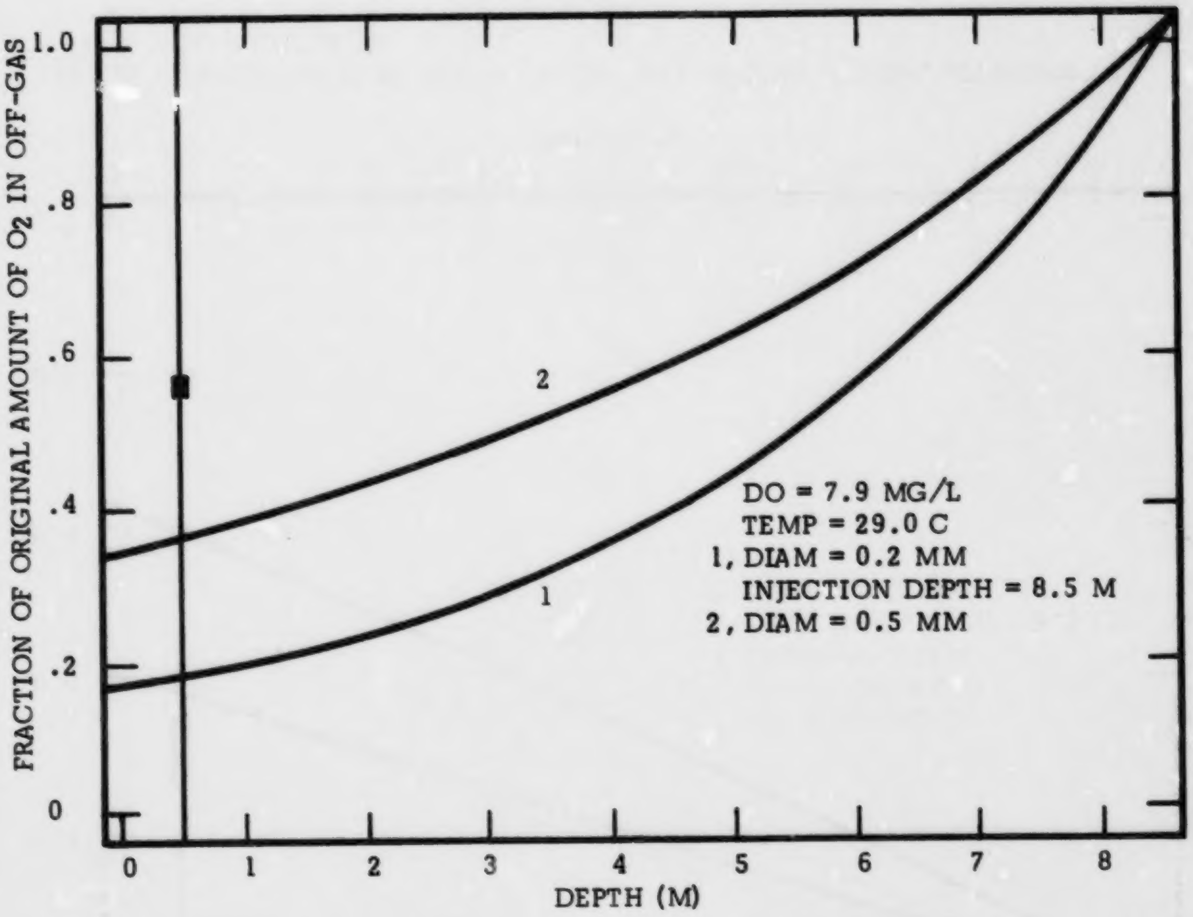

Fig. 9 FRACTION OF ORIGINAL AMOUNT OF O_2 IN OFF-GAS VS DEPTH (USING SPEECE'S k_L FUNCTION)

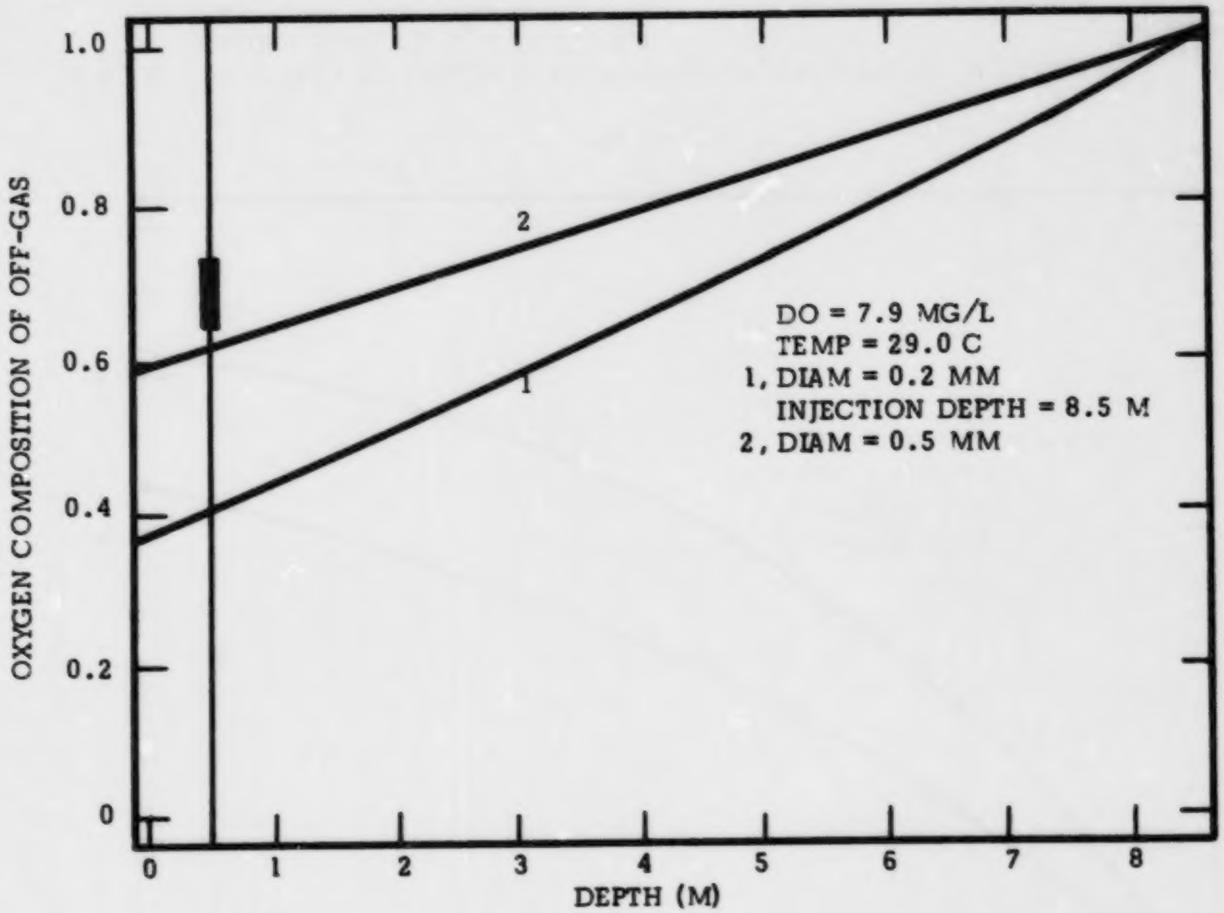

Fig. 10 OXYGEN COMPOSITION OF OFF-GAS VS DEPTH (USING SPEECE'S k_L FUNCTION)

mations were substituted for the K_L function for bubbles with diameters less than 2.2 mm. The K_L relationship for diameters less than 2.2 mm was divided into four sections:

for 0.0 mm to 0.3 mm,

$$K_L = (0.035)\ (D)\ (T) \qquad (15)$$

for 0.3 mm to 0.7 mm,

$$K_L = [(-0.044) + (0.175)\ (D)]\ (T) \qquad (16)$$

for 0.7 mm to 1.2 mm,

$$K_L = [(-0.486) + (0.78)\ (D)]\ (T) \qquad (17)$$

for 1.2 mm to 2.2 mm,

$$K_L = [(0.323) + (0.105)\ (D)]\ (T) \qquad (18)$$

Figure 11 presents these functions graphically.

Figures 12 through 22 are the graphs for each set of data collected in the study. The range of observed values are plotted on each graph at the depth of gas collection. The model with the new K_L function has been verified by the field studies. The data in each case falls within an acceptable range as predicted by the model.

The model has other capabilities that are of interest. The reduction in bubble diameter as the bubble rises can be followed. Figure 23 traces the size reduction for the 1.0 mm and 2.0 mm bubble injected at 21.2 m. Two processes are responsible for the charges in bubble volume. One, the hydrostatic pressure is being reduced linearly as the bubble rises; hence, the bubble volume will expand. Two, the processes of gas mass-transfer are allowing oxygen and nitrogen to be transferred out of or into the bubble.

Figure 24 shows the behavior of the bubble diameter with rise for the 0.2 mm and 0.5 mm. Notice the diameter remains approximately the same with depth for bubbles in this range.

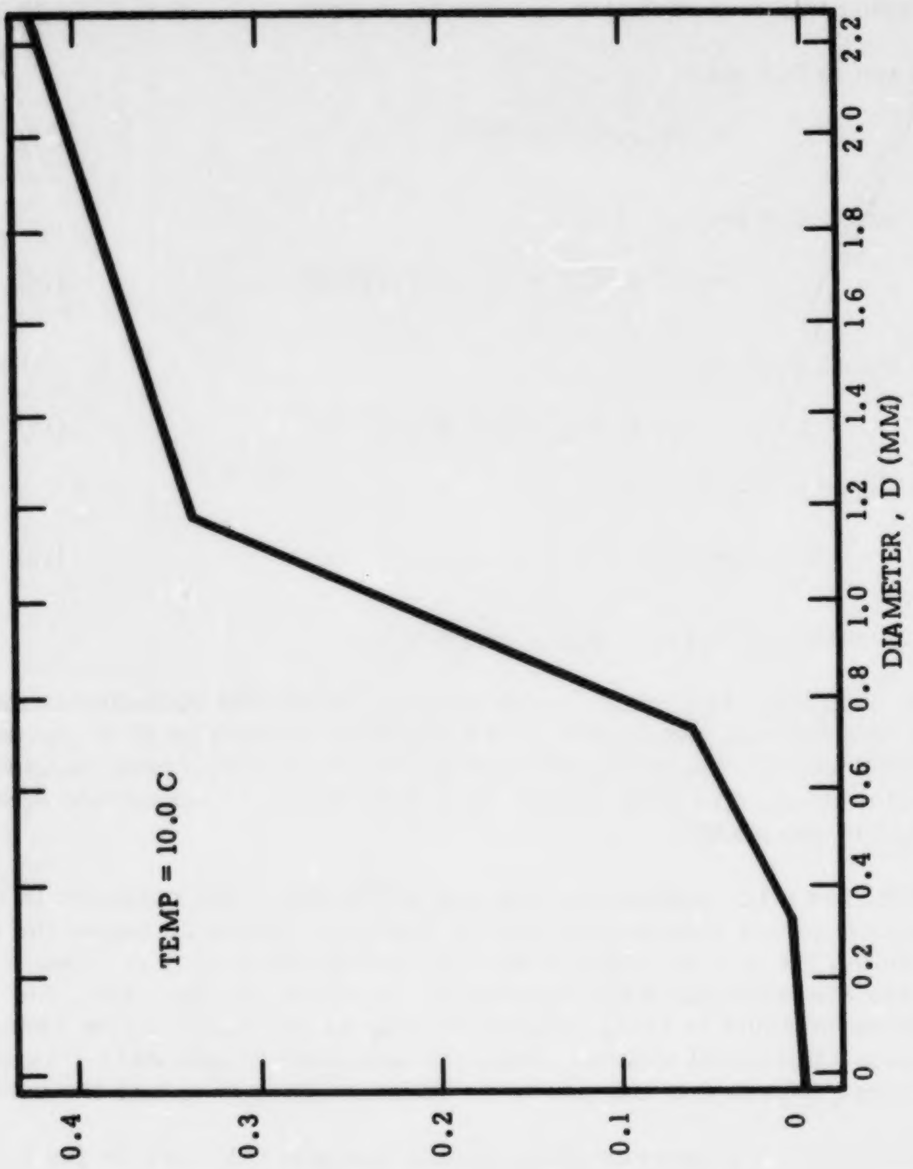

Fig. 11 LIQUID FILM COEFFICIENT VS DIAMETER

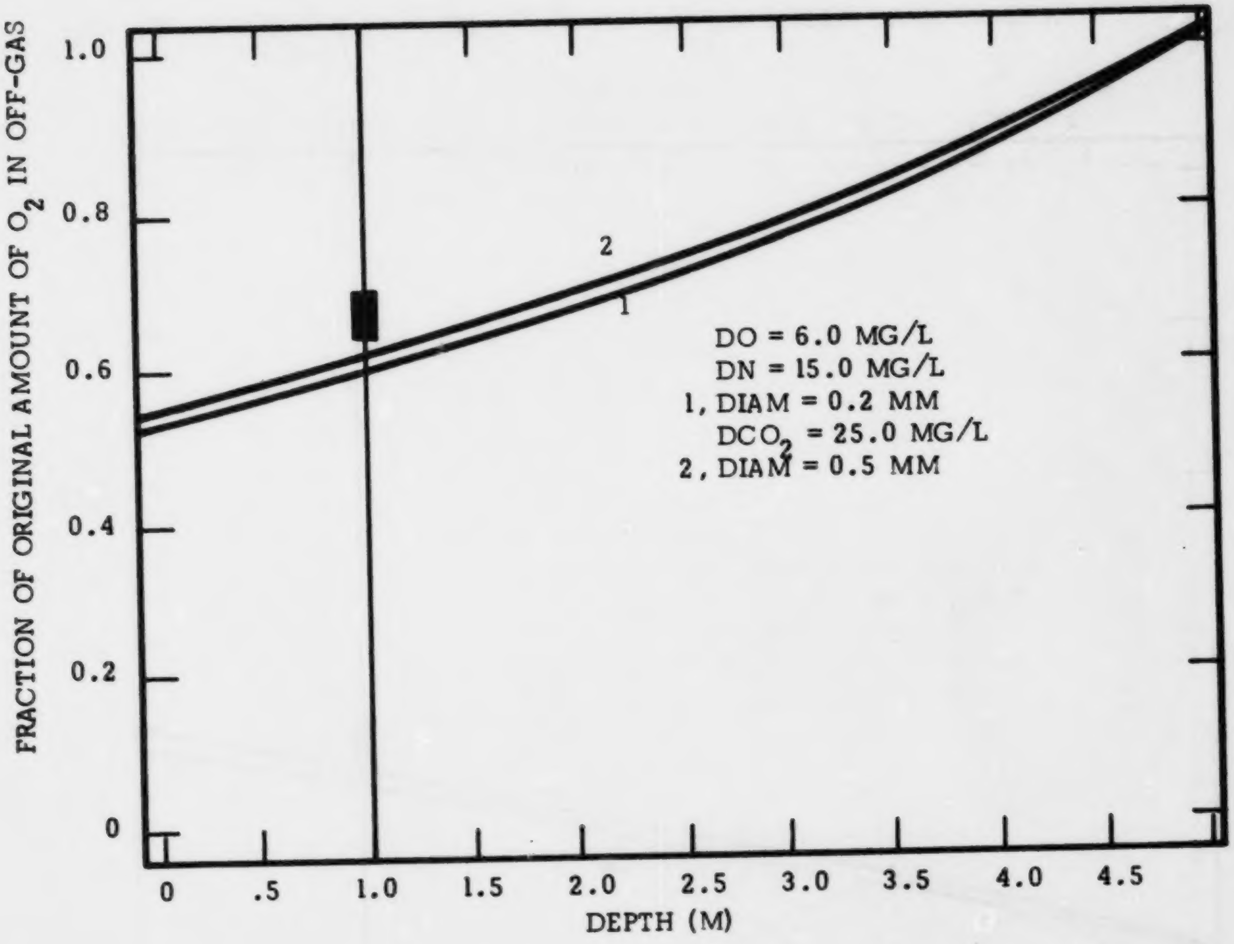

Fig. 12 FRACTION OF ORIGINAL AMOUNT OF O_2 IN OFF-GAS VS DEPTH PURE OXYGEN

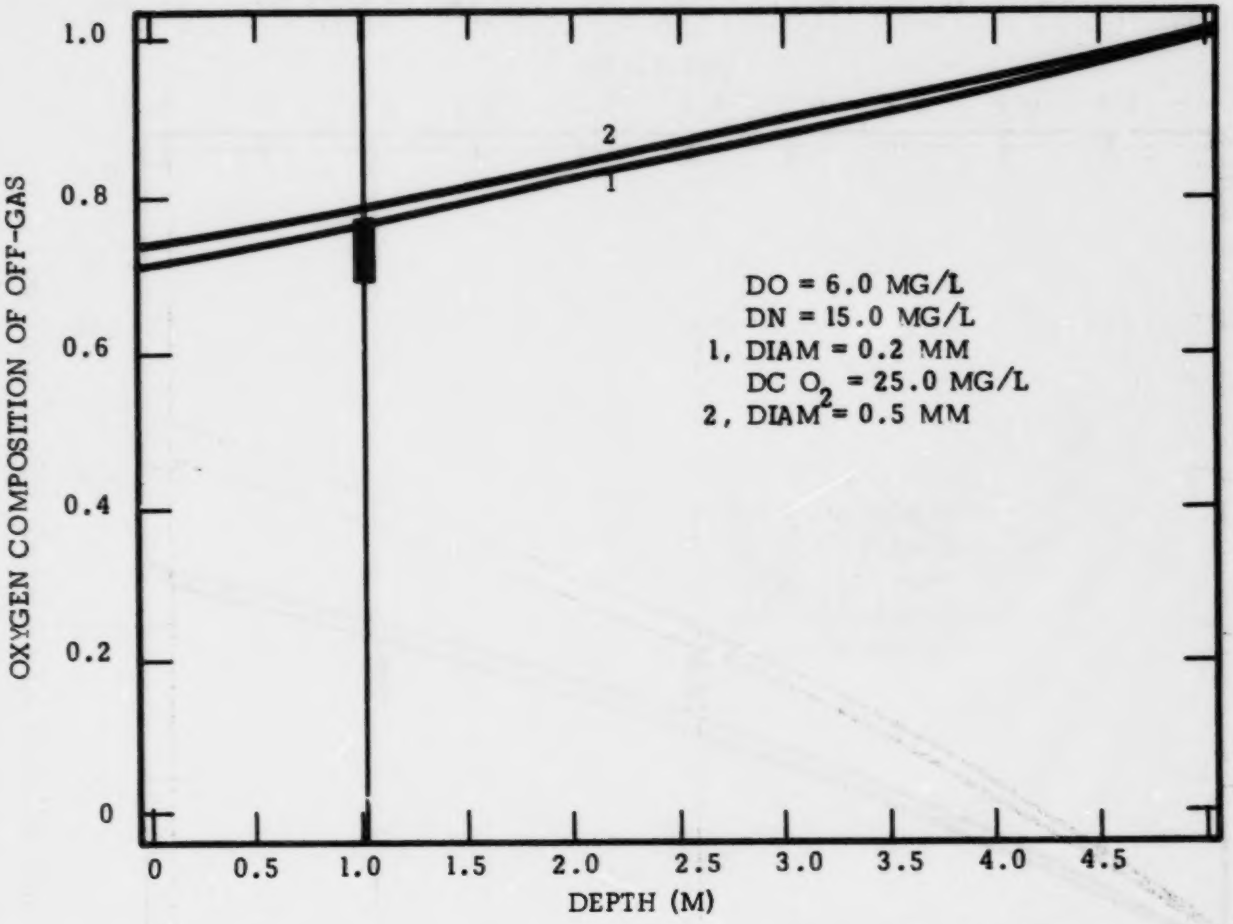

Fig. 13 OXYGEN COMPOSITION OF OFF-GAS VS DEPTH PURE OXYGEN

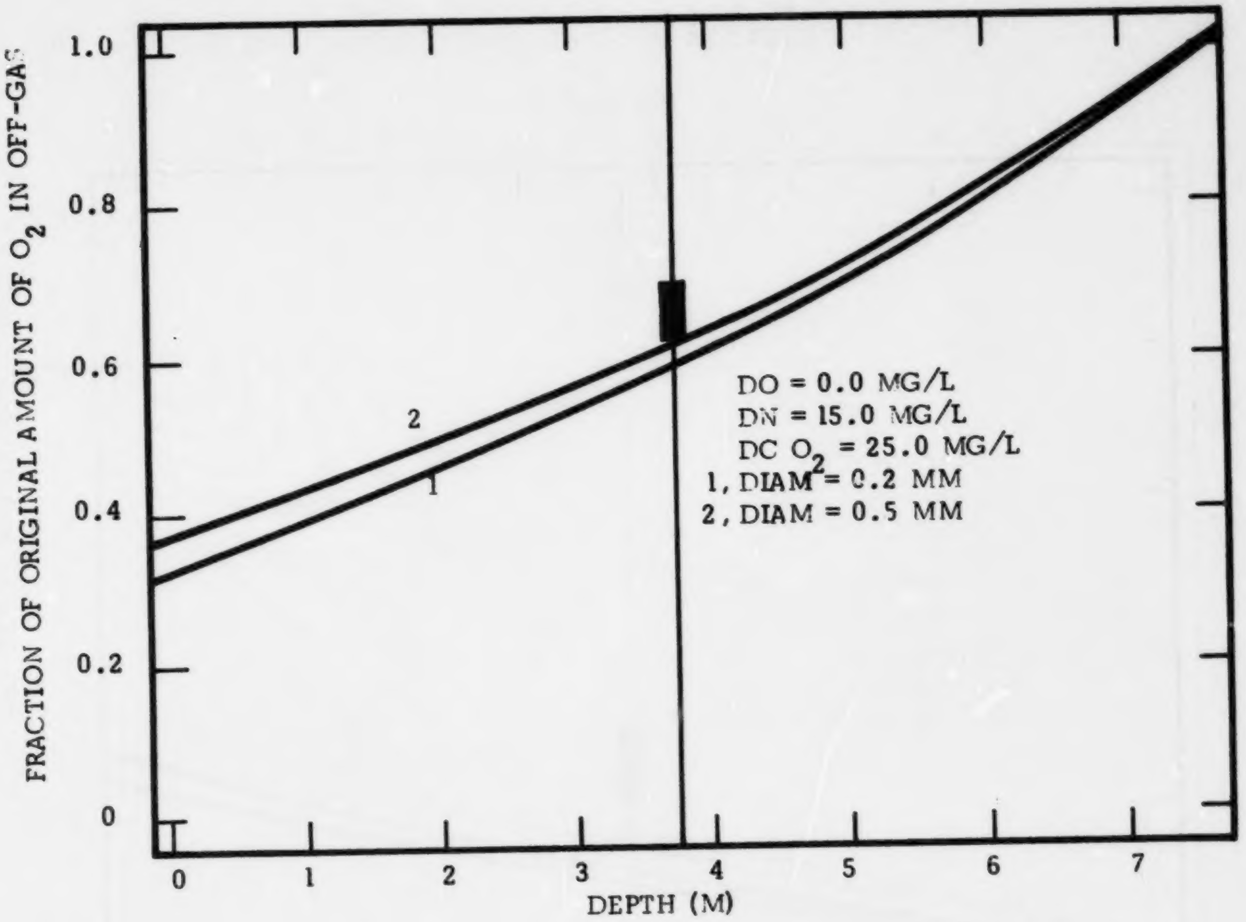

Fig. 14 FRACTION OF ORIGINAL AMOUNT OF O_2 IN OFF-GAS VS DEPTH PURE OXYGEN

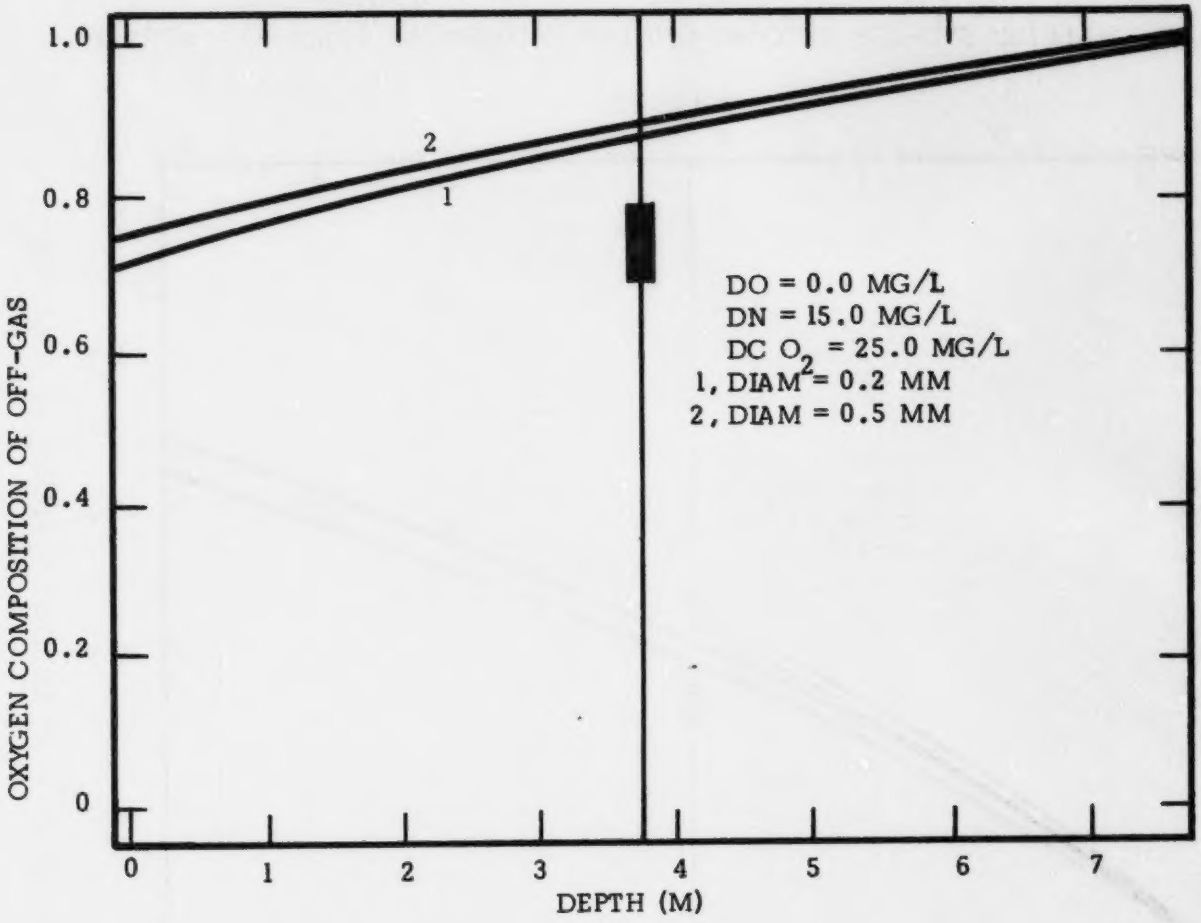

Fig. 15 OXYGEN COMPOSITION OF OFF-GAS VS DEPTH

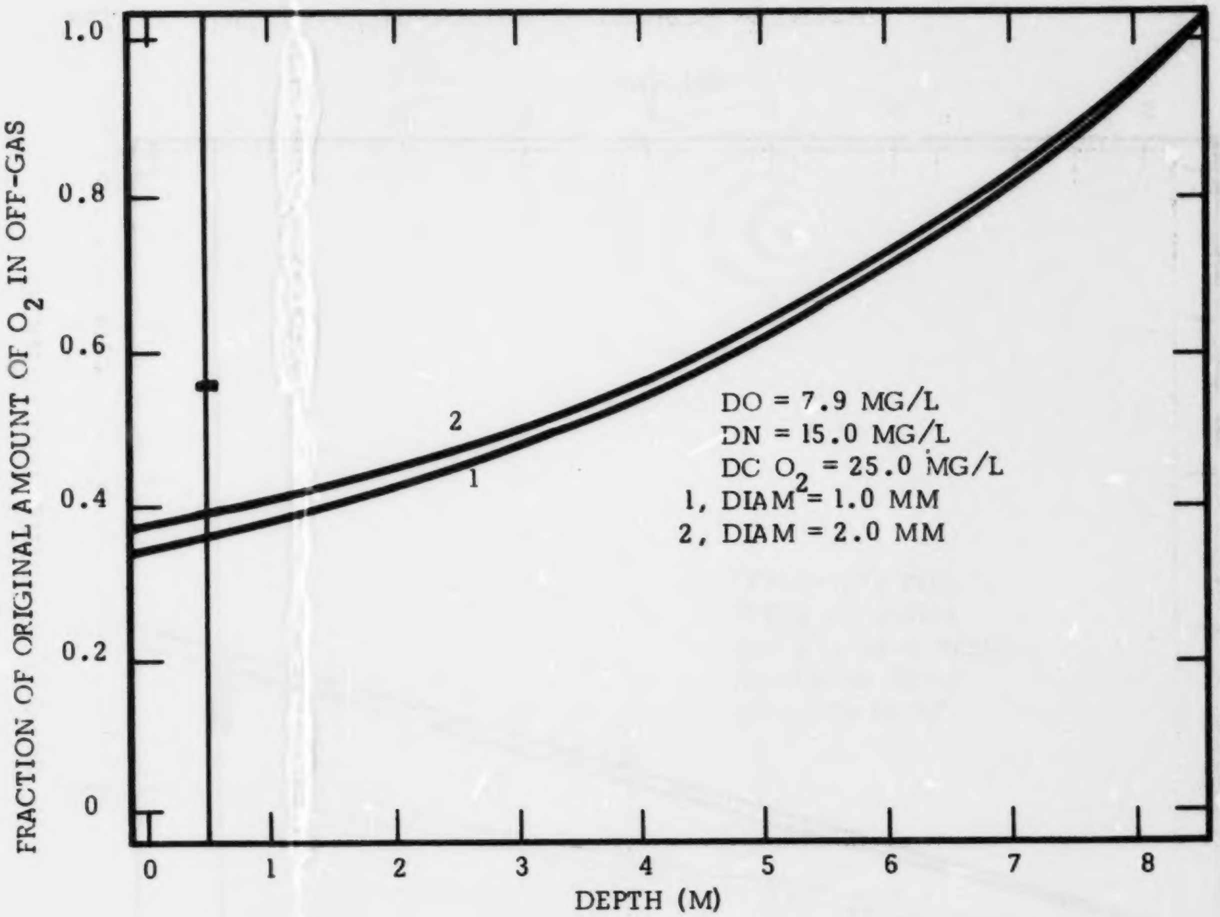

Fig. 16 FRACTION OF ORIGINAL AMOUNT OF O_2 IN OFF-GAS VS DEPTH PURE OXYGEN

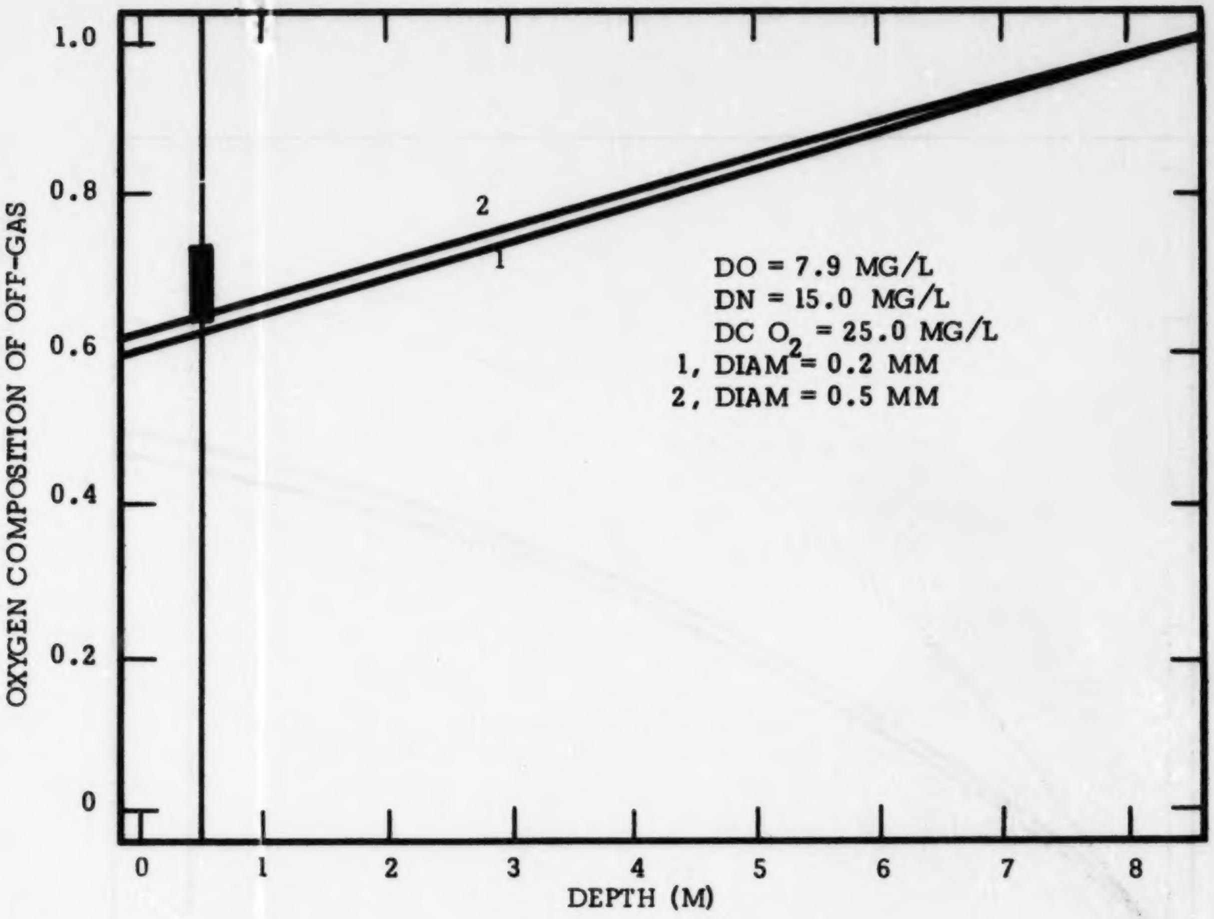

Fig. 17 OXYGEN COMPOSITION OF OFF-GAS VS DEPTH

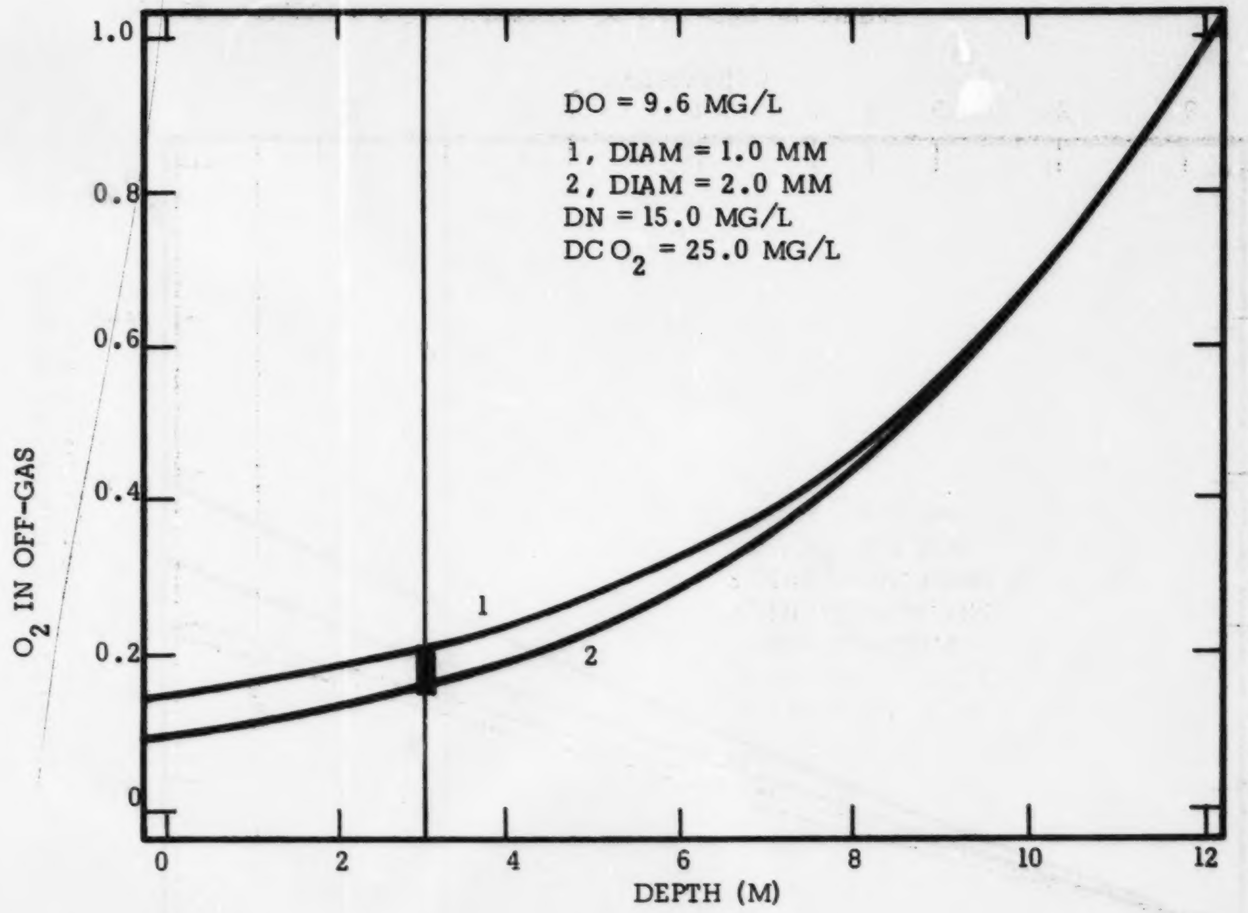

Fig. 18 FRACTION OF ORIGINAL AMOUNT OF O_2 IN OFF-GAS VS DEPTH - PURE OXYGEN

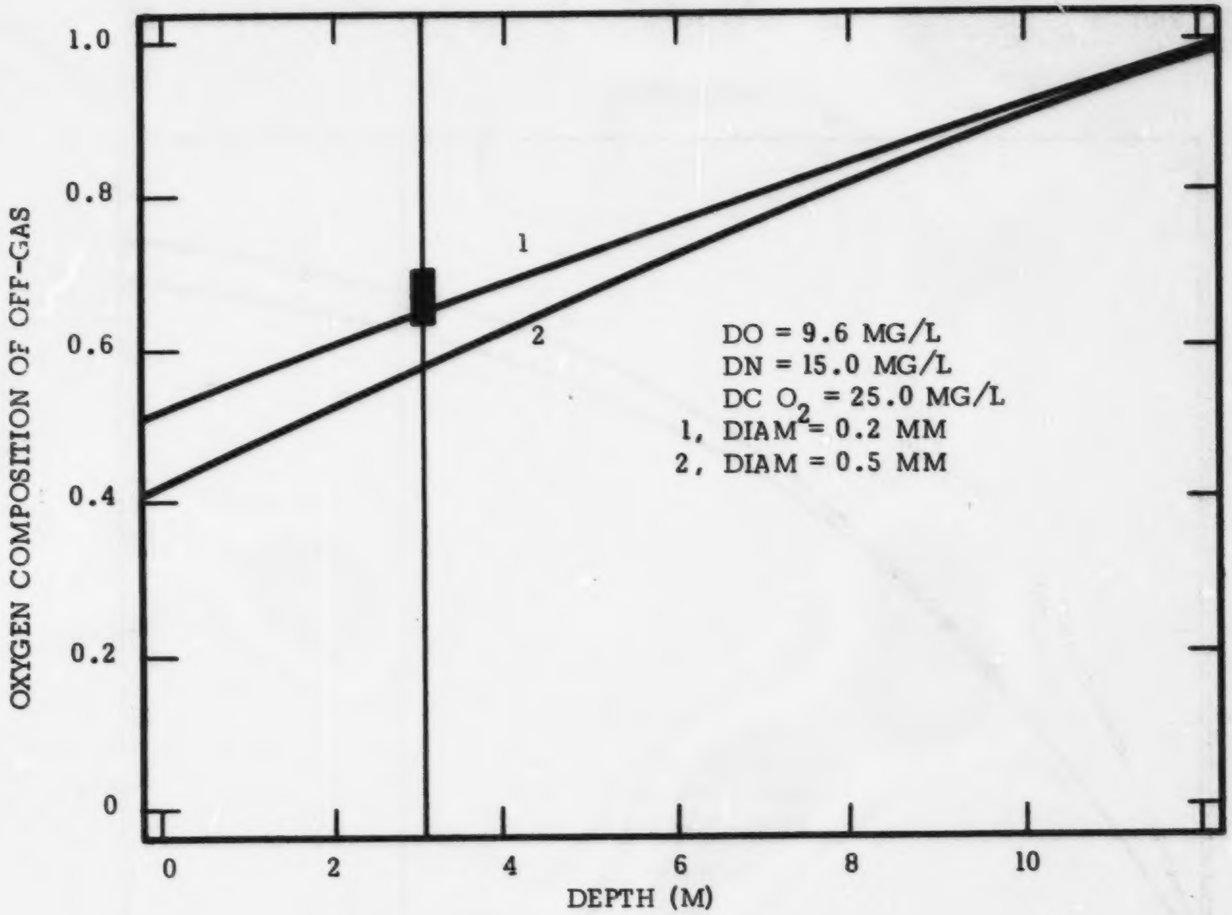

Fig. 19 OXYGEN COMPOSITION OF OFF-GAS VS DEPTH

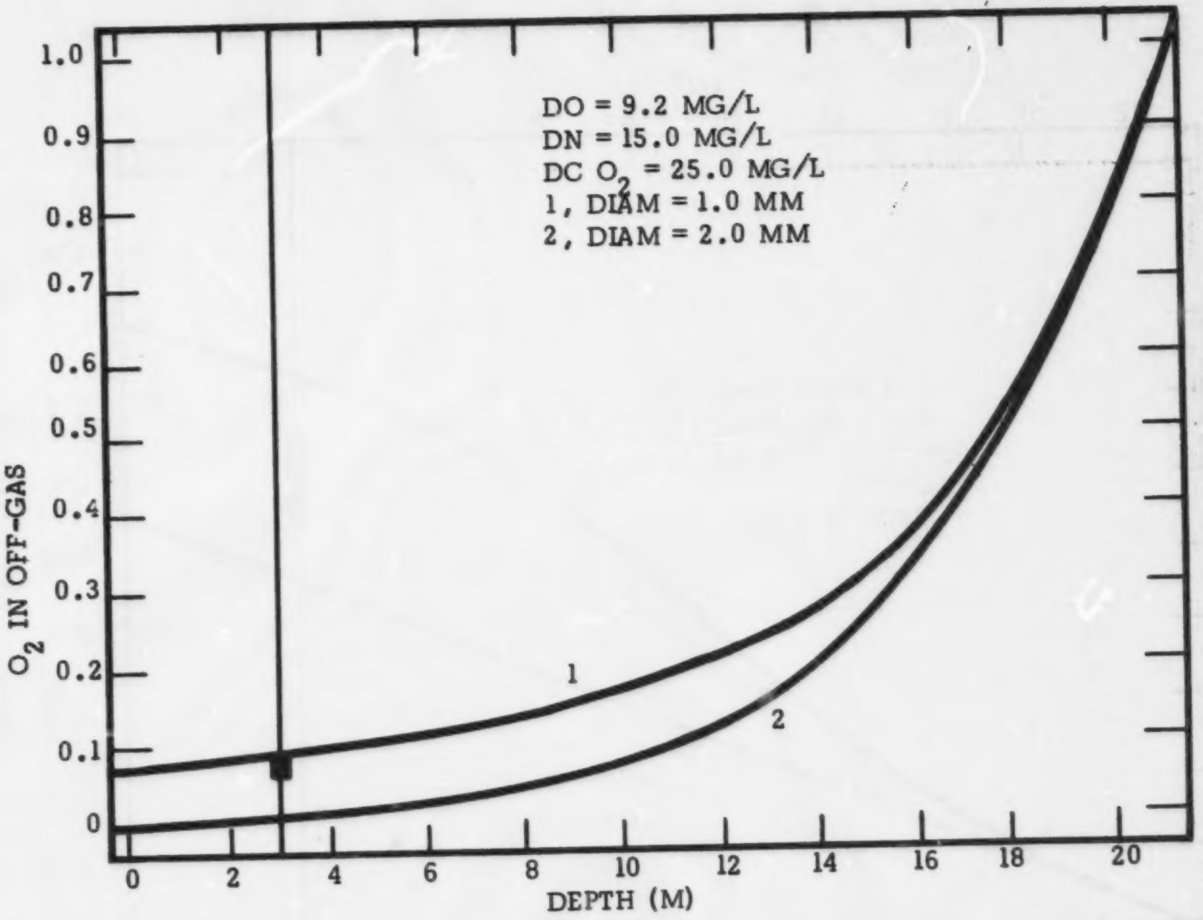

Fig. 20 FRACTION OF ORIGINAL AMOUNT OF O_2 IN OFF-GAS VS DEPTH - PURE OXYGEN

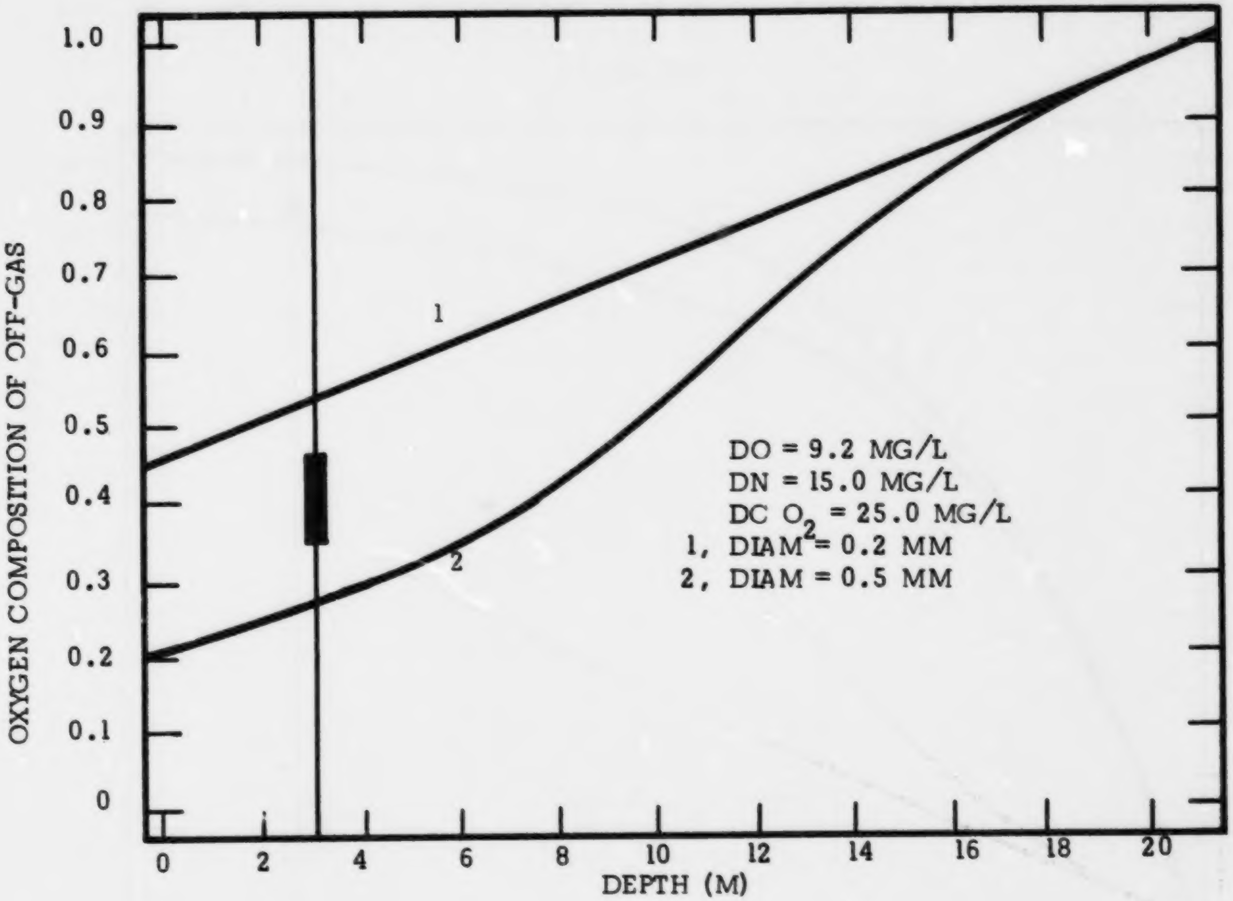

Fig. 21 OXYGEN COMPOSITION OF OFF-GAS VS DEPTH

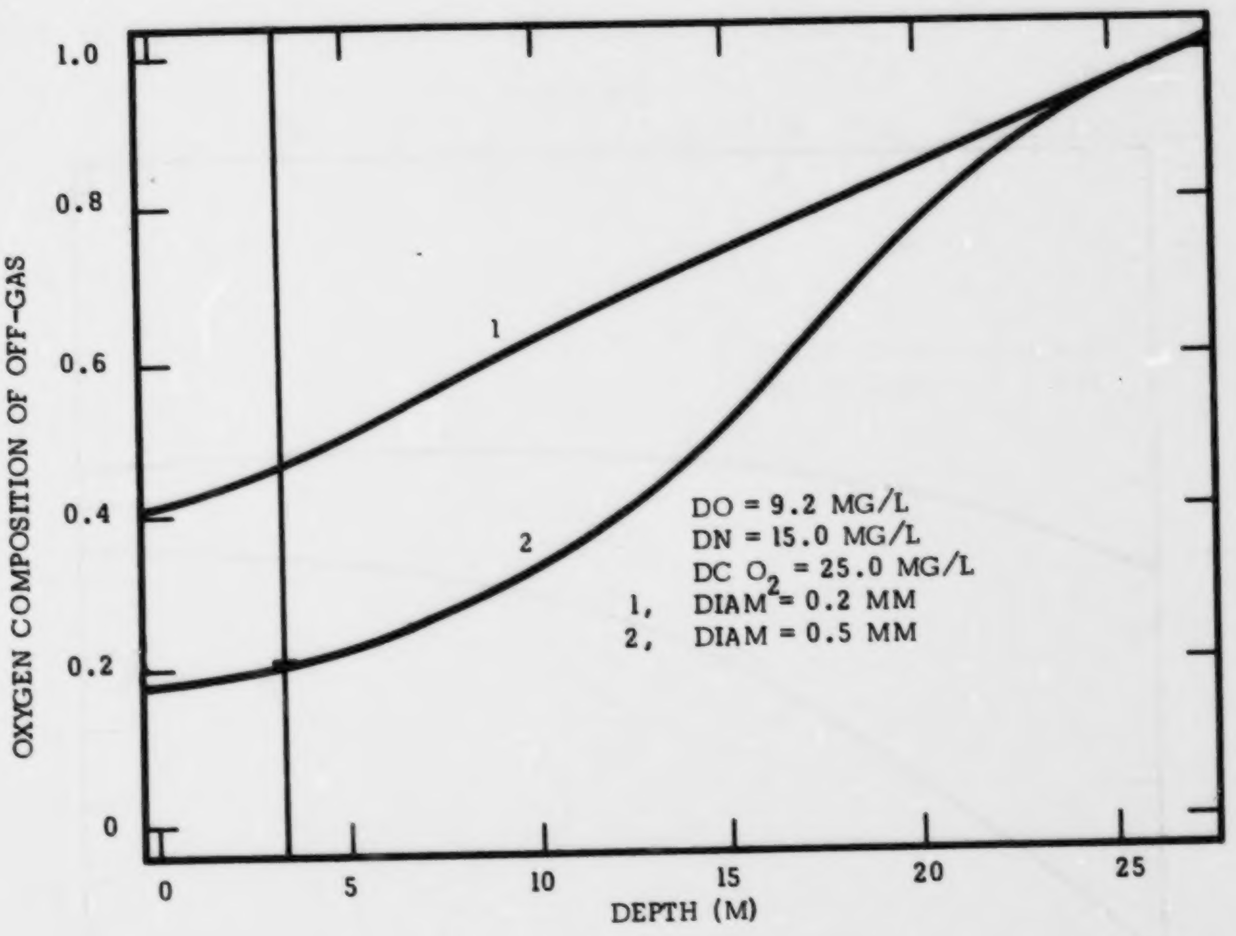

Fig. 22 OXYGEN COMPOSITION OF OFF-GAS VS DEPTH

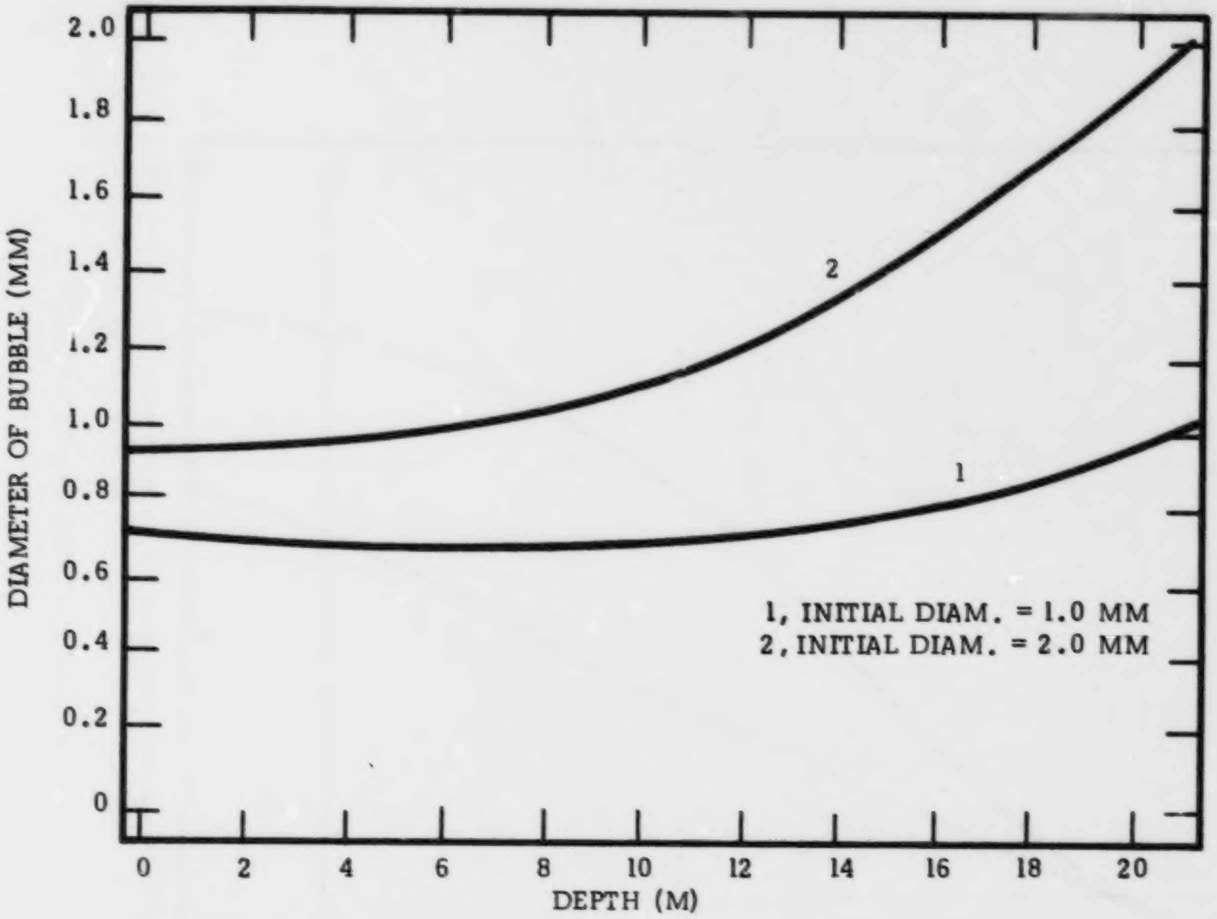

Fig. 23 DIAMETER OF BUBBLE AS A FUNCTION OF DEPTH

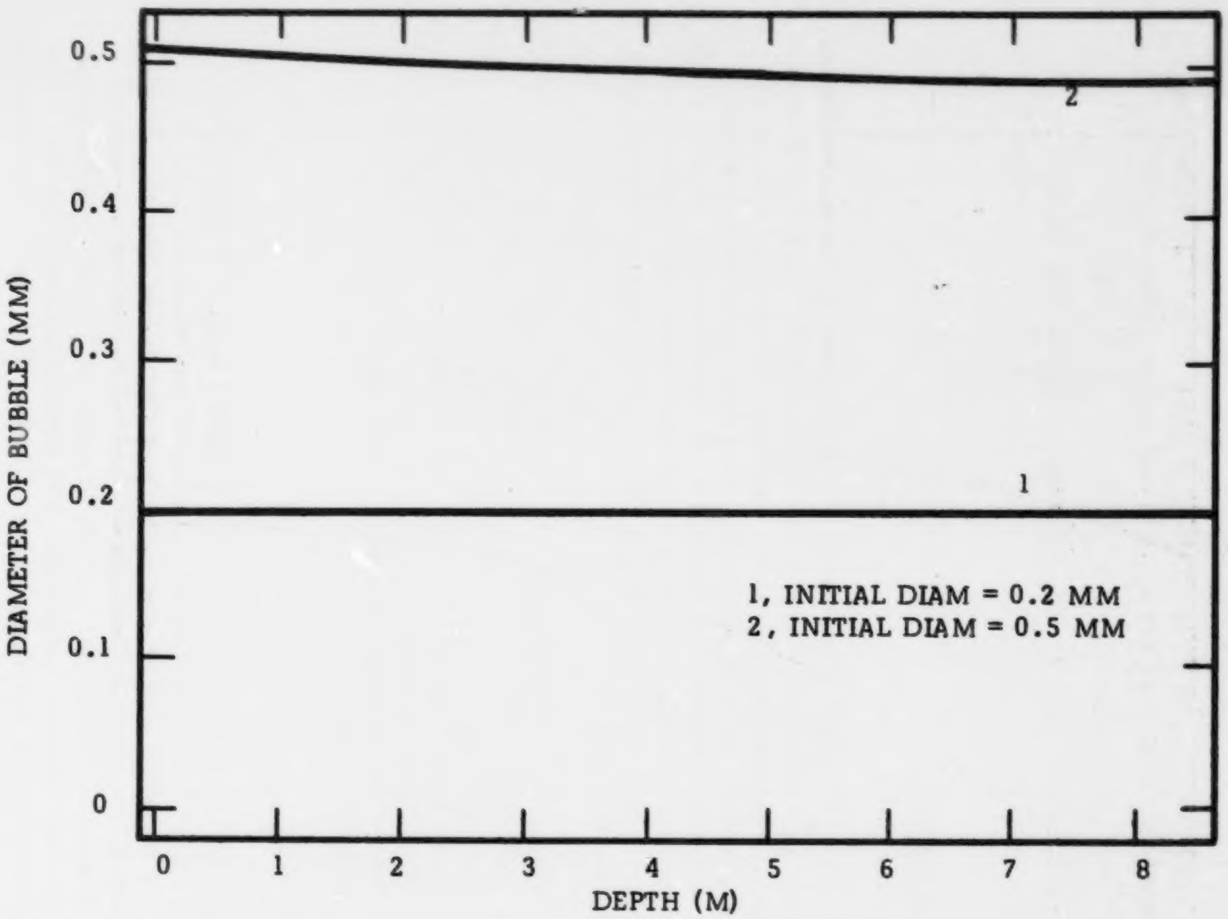

Fig. 24 DIAMETER OF BUBBLE AS A FUNCTION OF DEPTH

The change in the relative volume of gas at any depth with respect to the volume injected can also be traced with rise. This can be of interest to determine the volume of gas which is not absorbed within the hypolimnion and hence will be responsible for the degree of mixing which will occur between the hypolimnion and metalimnion. Figures 25 and 26 show the changes in relative volume for the 21.2 m and 8.5 m injection depths, respectively.

The newly developed K_L function is compared to Barnhart's function in Figure 27.

Sensitivity of Model

The sensitivity of the model to the various parameters can be demonstrated. The variables which are used in the model are the initial bubble diameter, injection depth, temperature, dissolved oxygen concentration, dissolved nitrogen concentration, dissolved carbon dioxide concentration, and the relative slip velocity between the rising bubble and the water mass. For this example, certain conditions were held in common while each parameter was investigated separately to show its effect on the model. The common conditions are as follows:

Initial Bubble Diameter = 0.20 mm
Injection Depth = 40 m
Temperature = 10°C
Dissolved Oxygen = 0 mg/l
Dissolved Nitrogen = 15 mg/l
Dissolved Carbon Dioxide = 25 mg/l
Slip Velocity = 0

Initial Bubble Diameter

The sensitivity of the model to the initial bubble diameter is first demonstrated. The initial bubble diameters which are compared are 0.2, 0.5, 1.0 and 2.0 mm. Figures 28 and 29 show the reduction in the fraction of the original amount of oxygen and the oxygen composition of the off-gas for each bubble diameter. An initial bubble diameter of 2.0 mm results in the best absorption performance. However, the absorption capabilities of the other three diameters are not appreciably different from the 2.0 mm case as can be seen in Figure 28. Figure 29 shows the reduction in oxygen composition with rise. More information concerning the absorption efficiency of different initial bubble diameters is included in the section which follows on design applications.

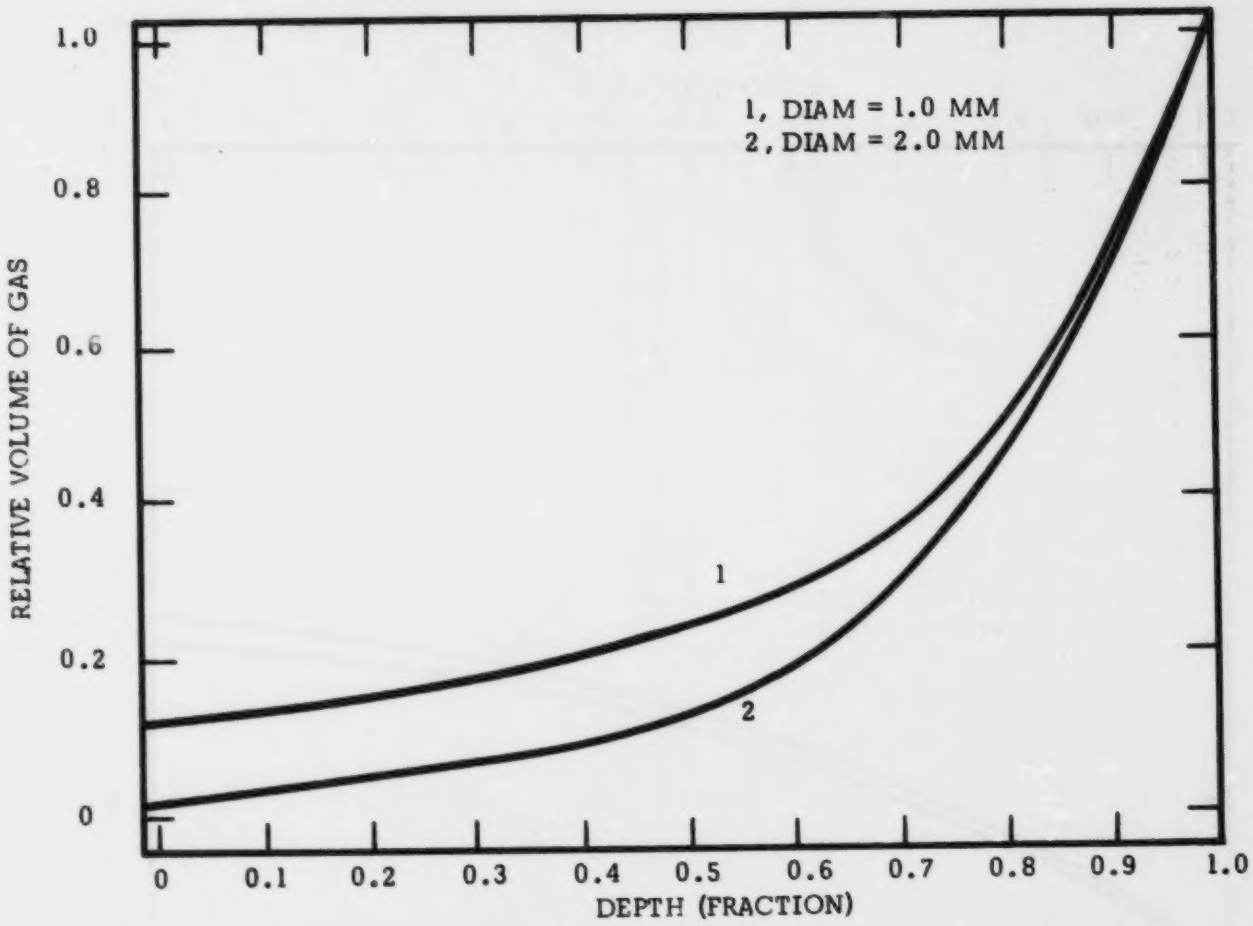

Fig. 25 RELATIVE VOLUME OF GAS VS DEPTH

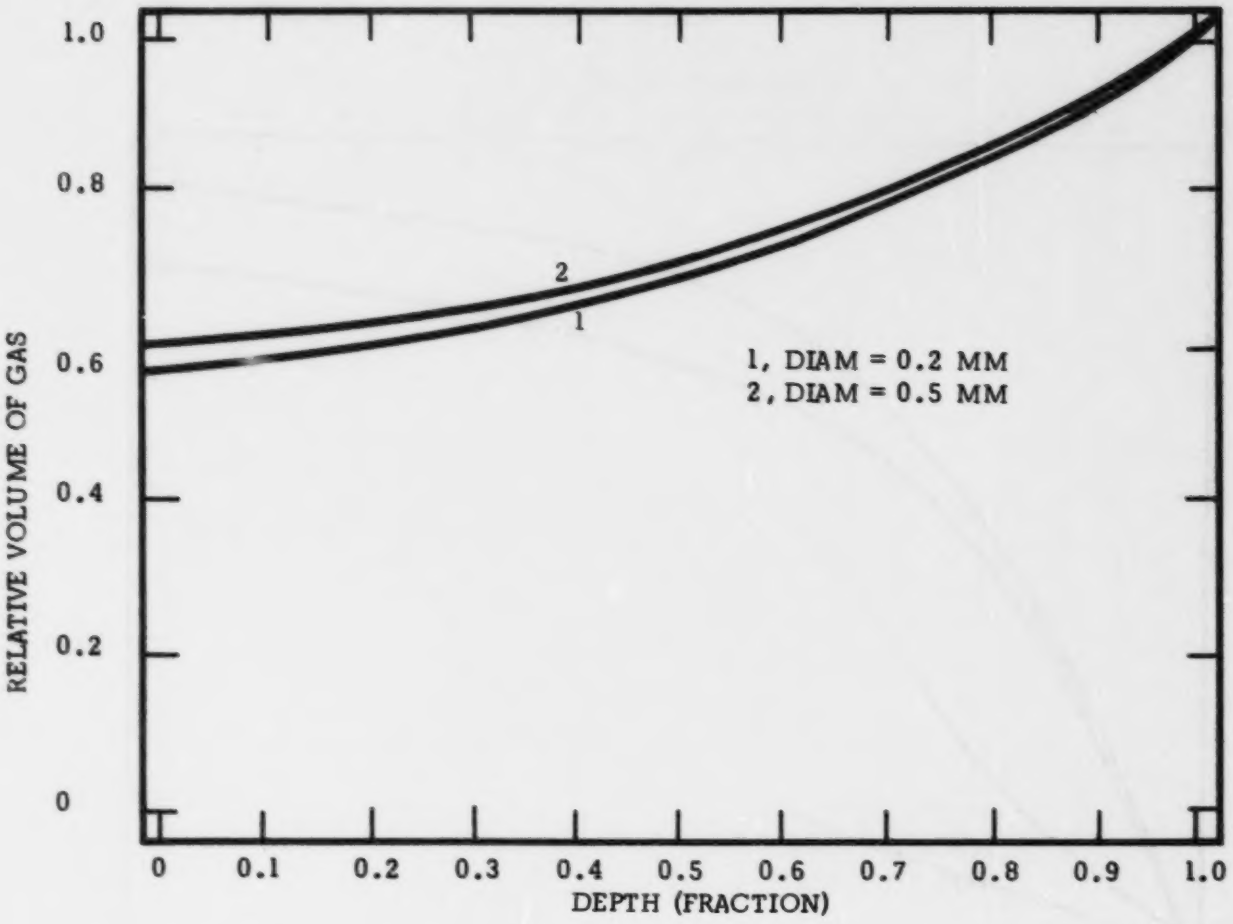

Fig. 26 RELATIVE VOLUME OF GAS VS DEPTH

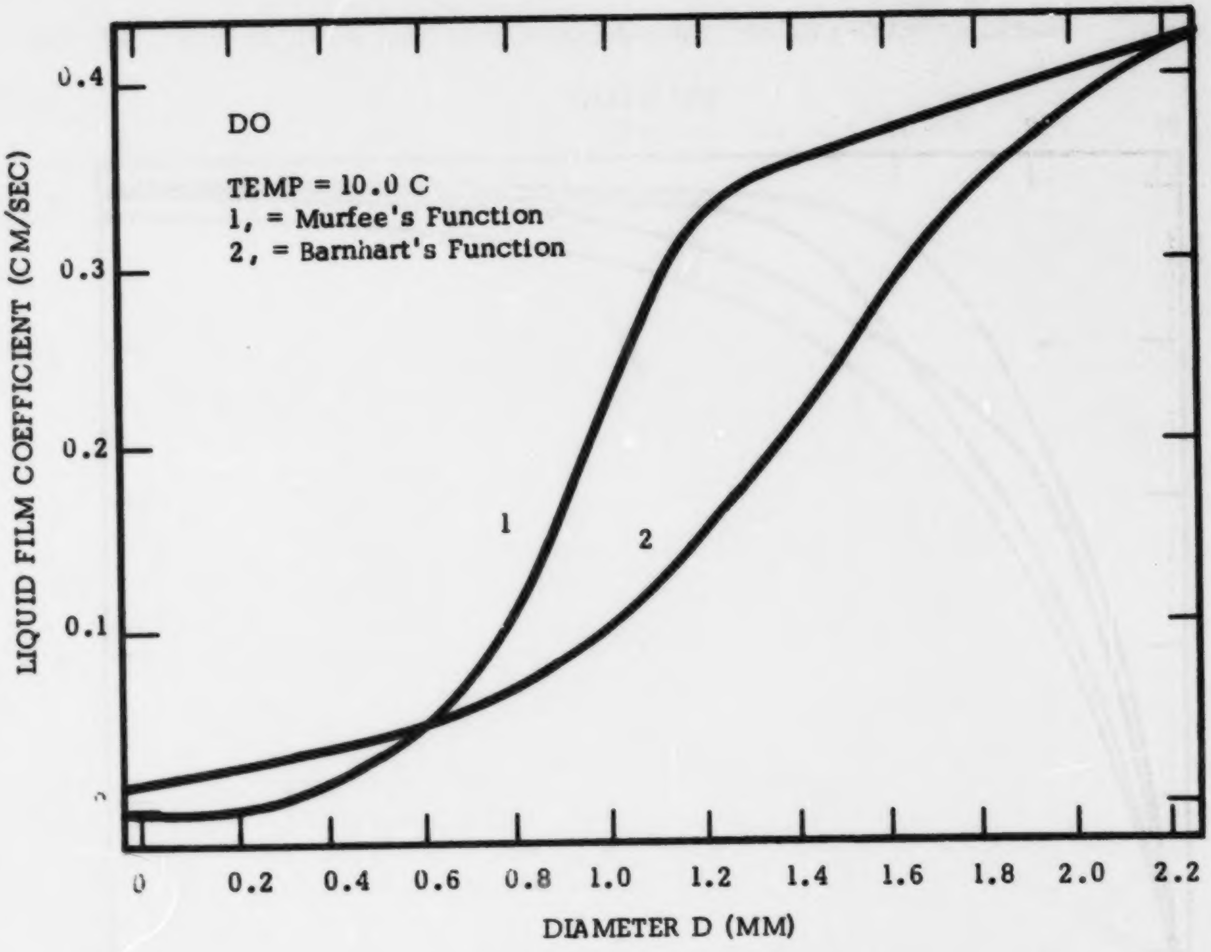

Fig. 27 LIQUID FILM COEFFICIENT VS DIAMETER, D

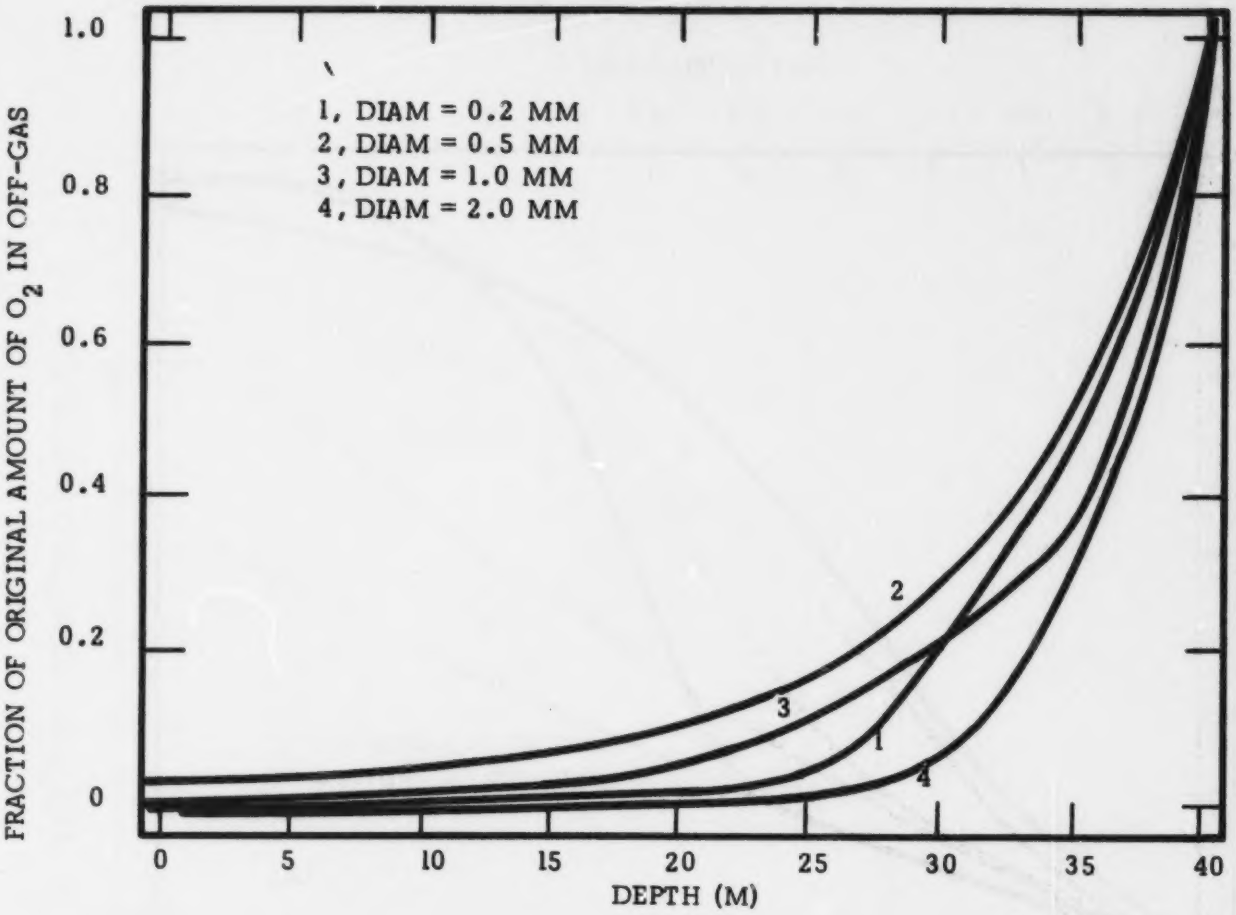

Fig. 28 FRACTION OF ORIGINAL AMOUNT OF O_2 IN OFF-GAS VS DEPTH

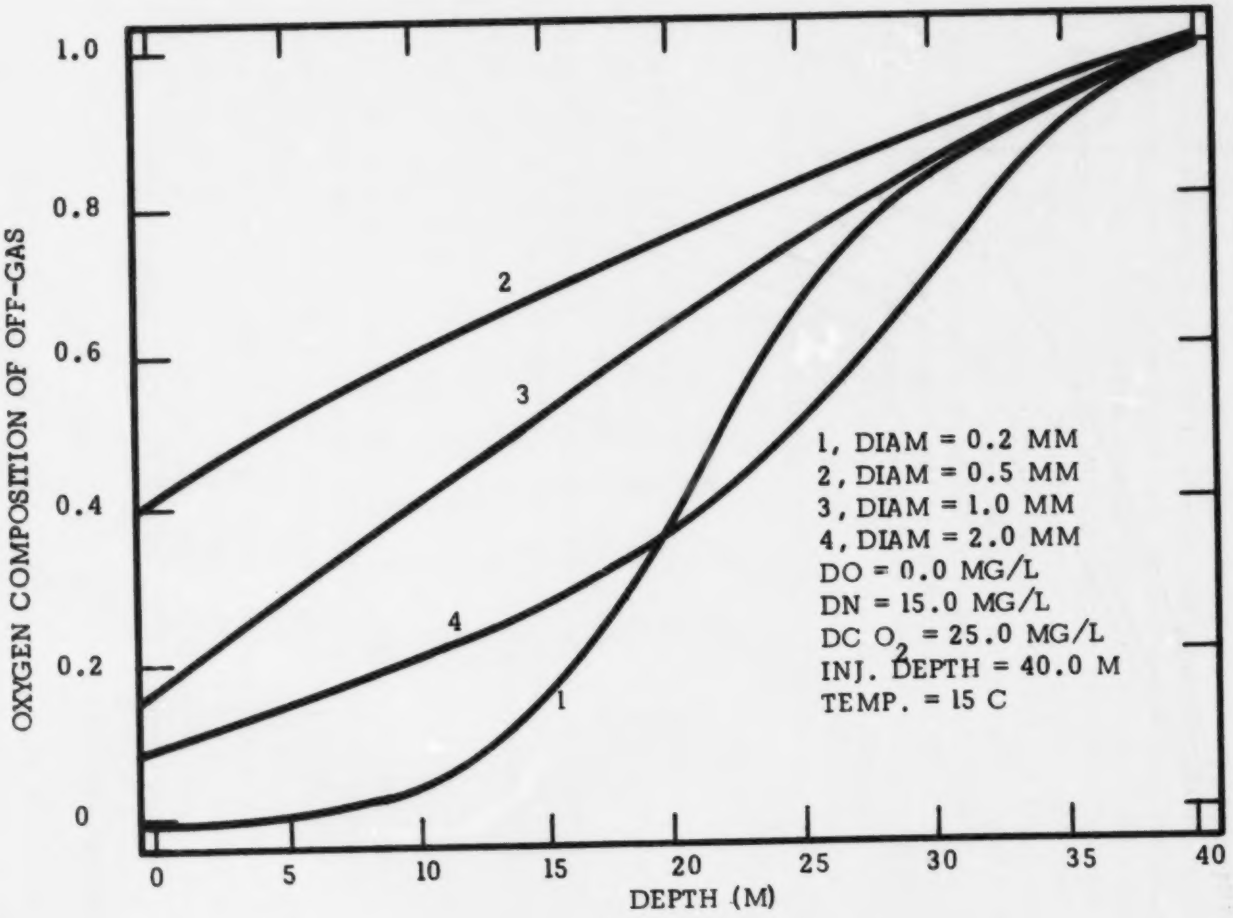

Fig. 29 OXYGEN COMPOSITION OF OFF-GAS VS DEPTH

Injection Depth

Figures 30 and 31 illustrate the predicted reductions in original oxygen and oxygen composition for injection depths of 20, 40, 60, and 80 m. The predictions are plotted against the fraction of the original injection depth. Notice, on Figure 30, the rise heights associated with any particular value for the fraction of original amount of oxygen are approximately the same. For instance, for 30% of the original amount of oxygen the fraction of the depth for 20, 40, 60, and 80 m is 0.60, 0.80, 0.87, and 0.90, respectively. The rise height at which 30% of the original amount is remaining is equal to the fraction of the depth at which 30% is remaining substracted from 1.0 and multiplied times the injection depth. For example, 20 meters (1-0.6) = 8 m; 40 meters (1-0.8) = 8 meters etc. For each case the rise height is approximately 8 m. Notice in Figure 31 that the oxygen composition of the bubbles for all four injection depths is 88 - 92% of the total volume at the time when 30% of the original oxygen mass is left.

Temperature

The temperature was set at 10, 20, and 30°C. Figures 32 and 33 show the absorption of oxygen and the reduction of oxygen in the gas bubbles as a function of depth. The higher the temperature the greater the absorption efficiency. This is due to the fact that the liquid film coefficient increases exponentially with the temperature; whereas, the DC deficit decreases relatively little at higher temperatures.

Dissolved Cxygen

A dissolved oxygen concentration of 0 mg/l was compared to one of 10 mg/l (Figure 34). The absorption efficiency is approximately the same; mainly, because the dissolved oxygen saturation concentration, C_s, is considerably higher than the range of values for dissolved oxygen concentration which are normally encountered in a body of water. Therefore, the dissolved oxygen deficit, $C_s - C_L$, is approximately the same for each case. For example, at 40 meters the DC deficit is equal to 373 mg/l and 363 mg/l for actual DO concentrations of 0 mg/l and 10 mg/l, respectively.

Dissolved Nitrogen and Dissolved Carbon Dioxide

The transfer of oxygen from a bubble to a water mass is independent of the concentrations of nitrogen and carbon dioxide in the water. The composition of the bubble gas, however, is altered because the nitrogen and/or carbon dioxide which is stripped will influence the partial pressure of

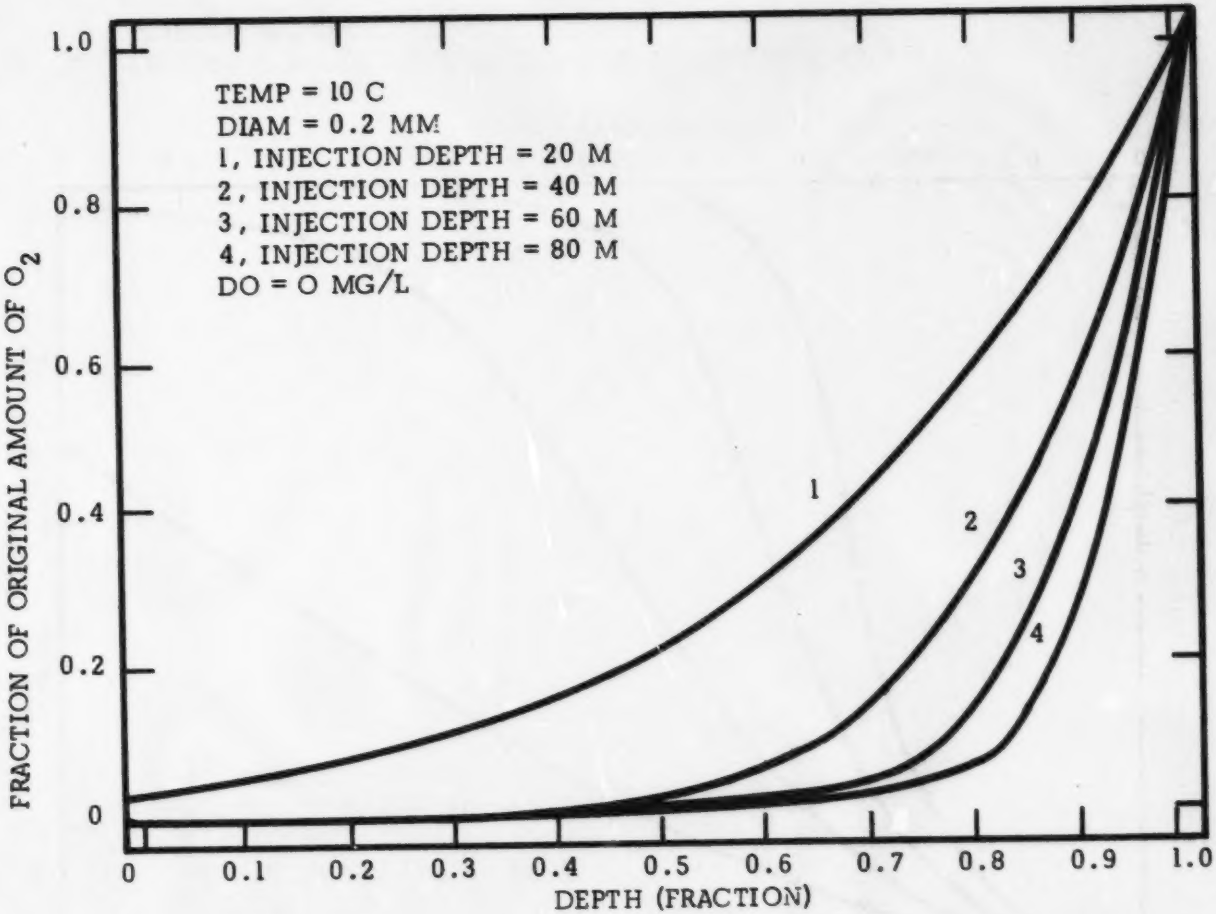

Fig. 30 FRACTION OF ORIGINAL AMOUNT OF O_2 VS FRACTION OF INITIAL INJ ECTION DEPTH

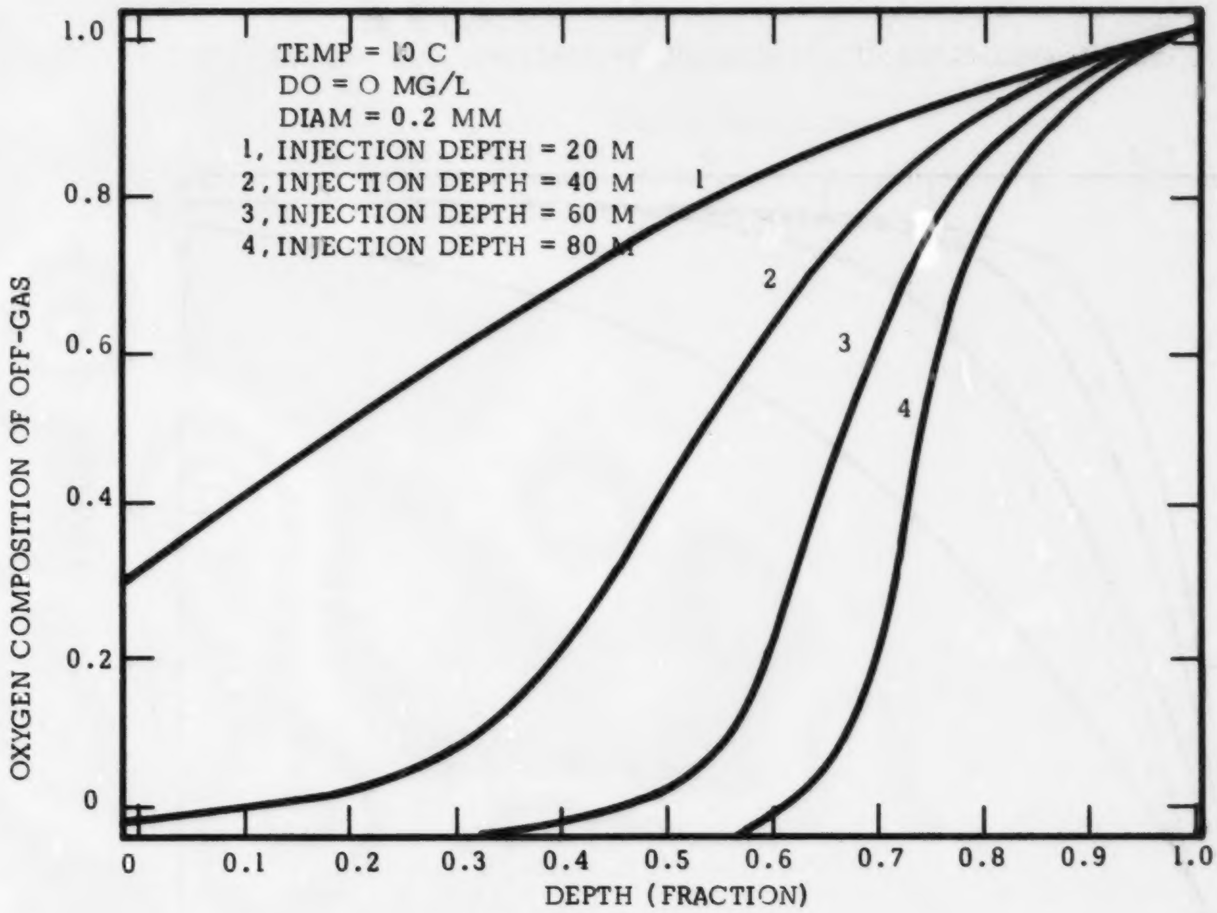

Fig. 31 OXYGEN COMPOSITION OF OFF-GAS VS FRACTION OF INITIAL INJECTION DEPTH

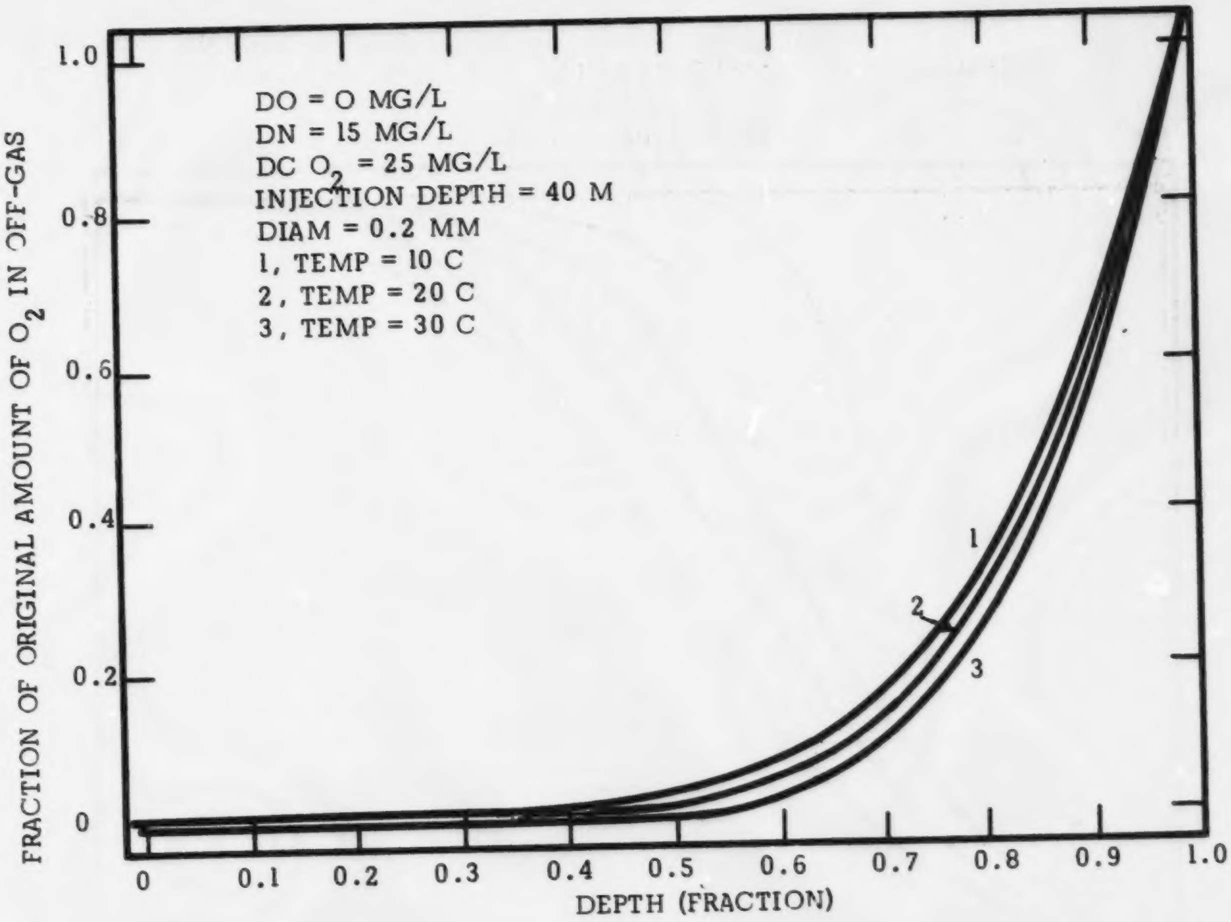

Fig. 32 FRACTION OF ORIGINAL AMOUNT OF O_2 IN OFF-GAS VS DEPTH (FRACTION)

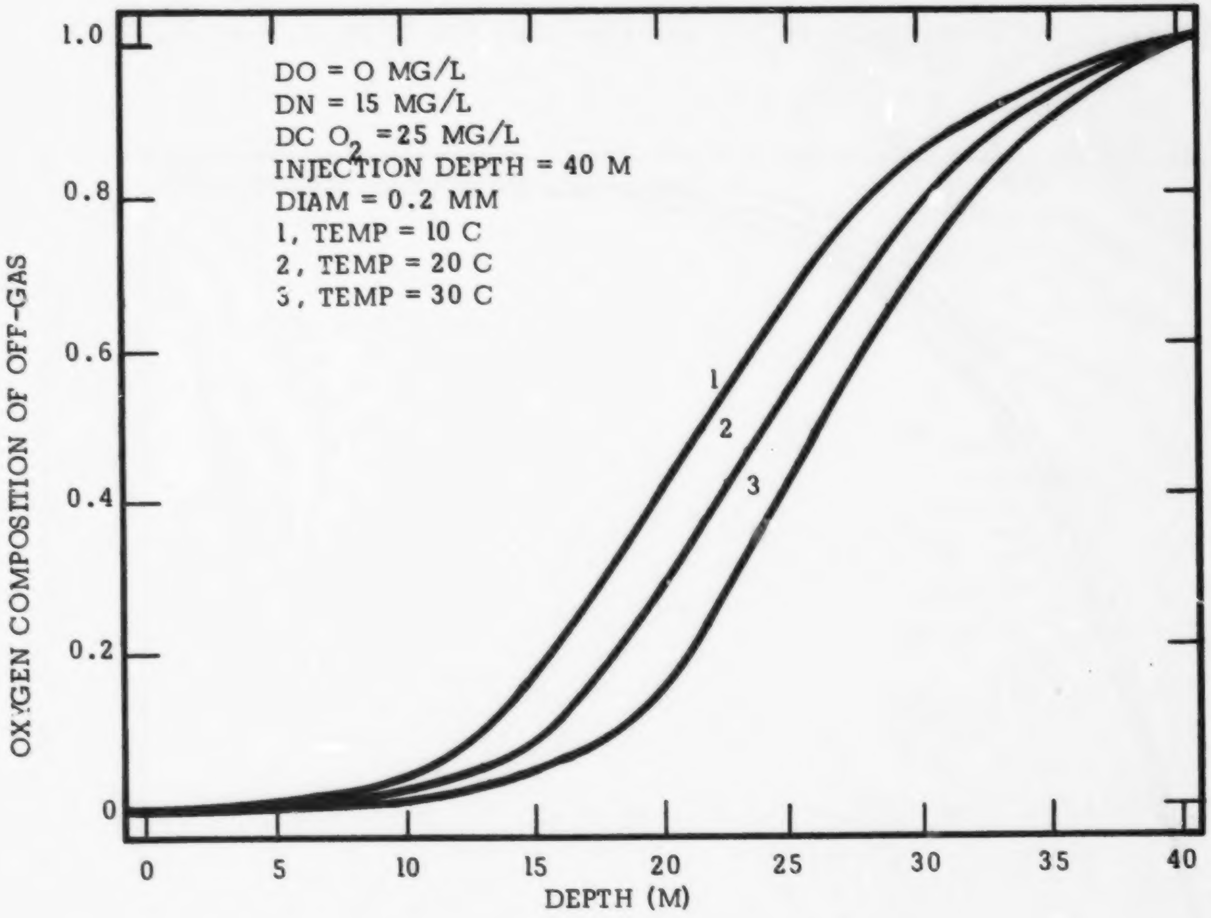

Fig. 33 OXYGEN COMPOSITION OF OFF-GAS VS DEPTH

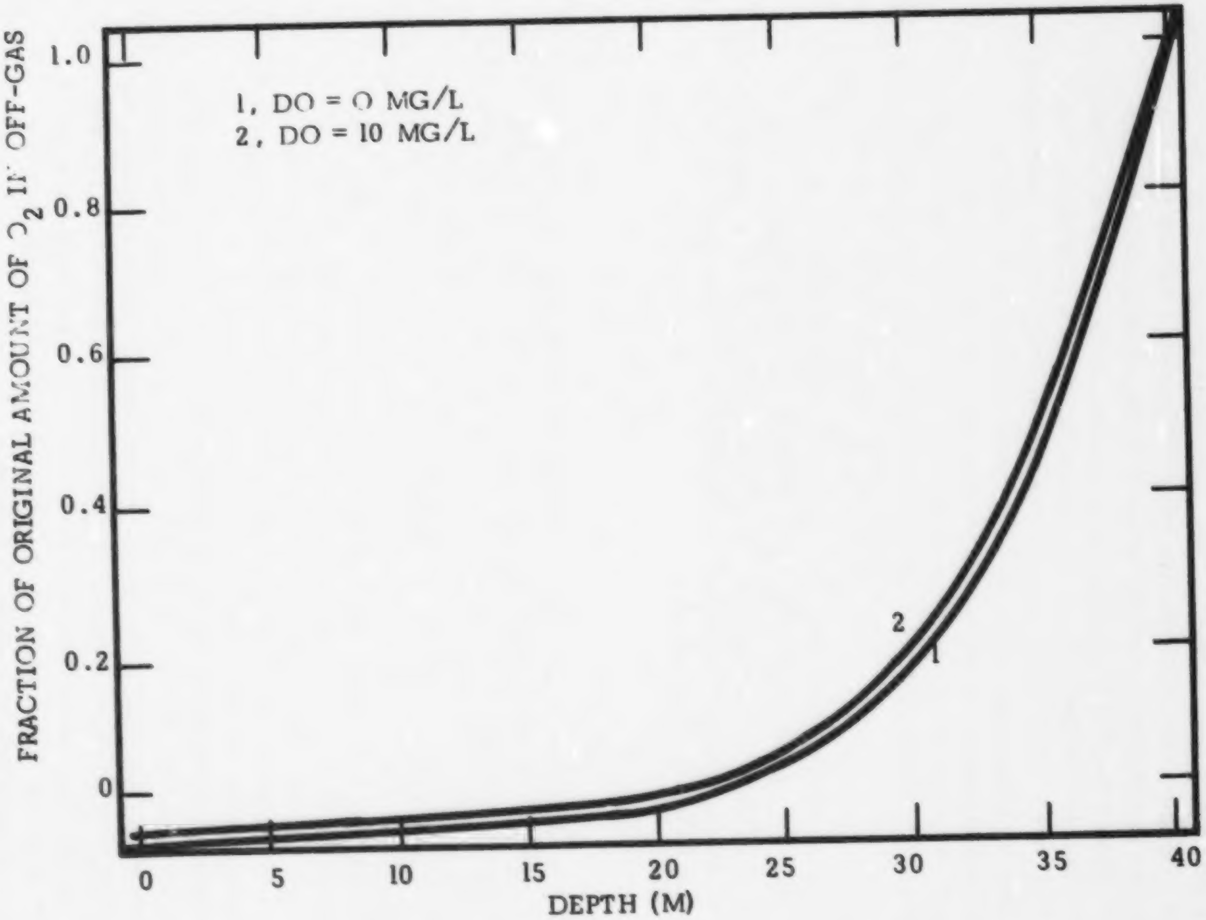

Fig. 34 FRACTION OF ORIGINAL AMOUNT OF O_2 IN OFF-GAS VS DEPTH

oxygen within the bubble. Figure 35 is a plot of how the fraction of the original amount of oxygen changes with rise for two dissolved nitrogen concentrations of 0 mg/l and 15 mg/l. The reduction in oxygen is not affected by the changes in dissolved nitrogen. Figure 36 shows the changes in oxygen composition for the same two dissolved nitrogen concentrations. Notice with the dissolved nitrogen set at 0 mg/l the bubble is completely absorbed by the time it reaches a depth of 20 meters. The bubble is not absorbed completely until it reaches a depth of 4 meters when the concentration of dissolved nitrogen in the water mass is 15 mg/l. This points up an advantage of using a hypolimnion aeration system. If the rise of some gas bubbles from the hypolimnion through the metalimnion can be tolerated, dissolved nitrogen can be stripped out of the hypolimnion if need be.

Figures 37 and 38 show the behavior for changes in dissolved carbon dioxide in the water. The saturation concentration for dissolved carbon dioxide is very low hence, the transfer of carbon dioxide is of a negligible magnitude. Therefore, the concentration of dissolved carbon dioxide need not be considered in aeration problems.

Slip Velocity

The computer model assumes zero slip velocity. That is, the velocity with which a bubble rises is due only to its buoyancy. For 100 per cent slip velocity, the velocity is due to its buoyancy plus the velocity of the plume generated by the bubbles. It has been shown by Rayyan (13) that relative slip velocity is a function of the bubble diameter as well as the injection rate. Figure 39 shows the predicted center line velocities of plumes generated by a 2.0 mm bubble for the cases of zero and non-zero slip. Center line velocity for zero slip is approximately double that for non-zero slip at a height of 27 meters above the injection depth. Hence, a conservative approximation of 100 per cent slip would be to double the terminal velocity of the bubble. Rayyan also showed that for bubbles less than 0.5 mm in diameter there is no difference between zero and non-zero slip on the rate of gas transfer. Figure 40 shows the effect of zero and 100 per cent slip on the reduction in the original amount of oxygen for a 2.0 mm bubble. As can be seen, the absorption efficiency is reduced somewhat when 100 per cent is used. However, the approximation for 100 per cent slip as used in this calculation is quite crude and a more precise investigation into the terminal velocity of bubbles in a plume is needed.

The possibility exists that in some cases it may be desirable to reduce the plume velocity so as to insure that the rate of bubble rise is due to

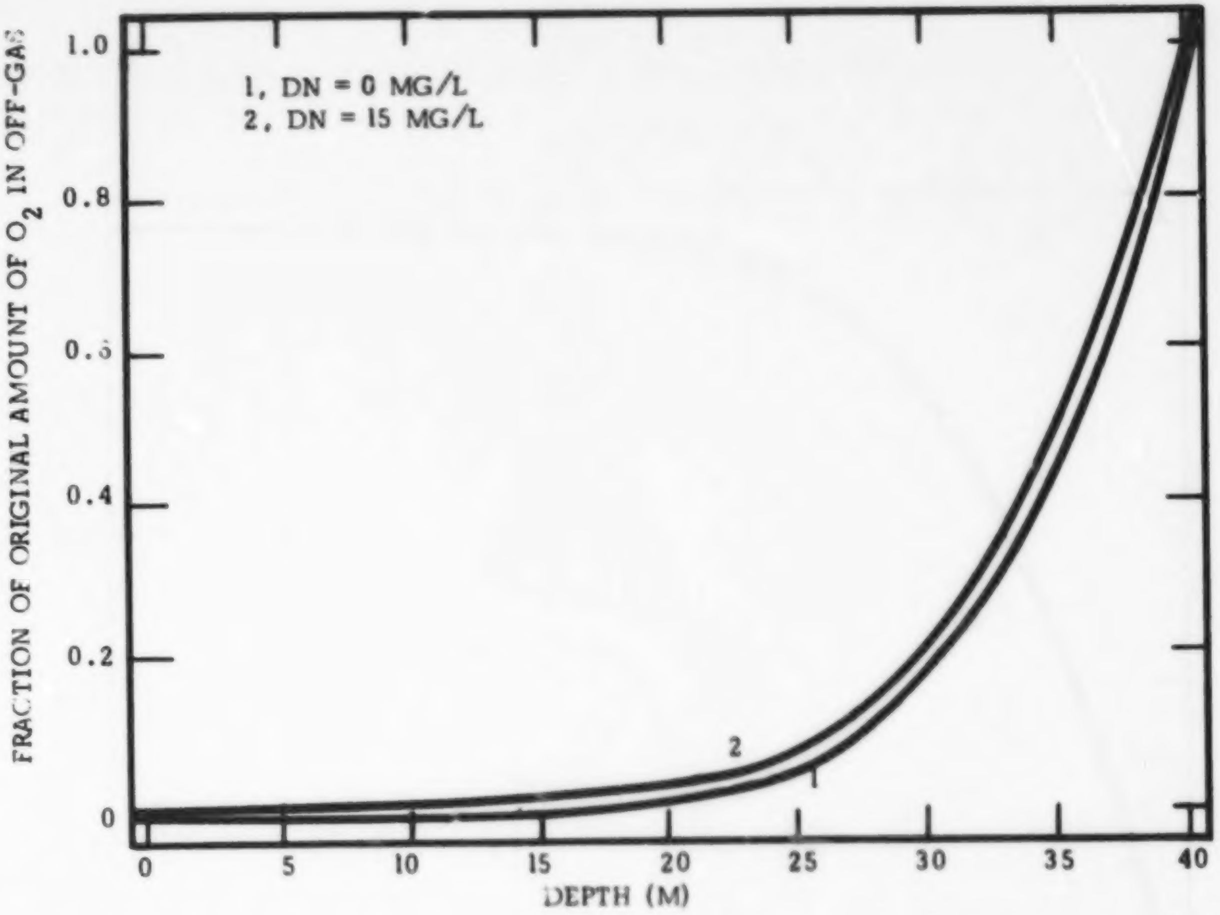

Fig. 35 FRACTION OF ORIGINAL AMOUNT OF O_2 IN OFF-GAS VS DEPTH

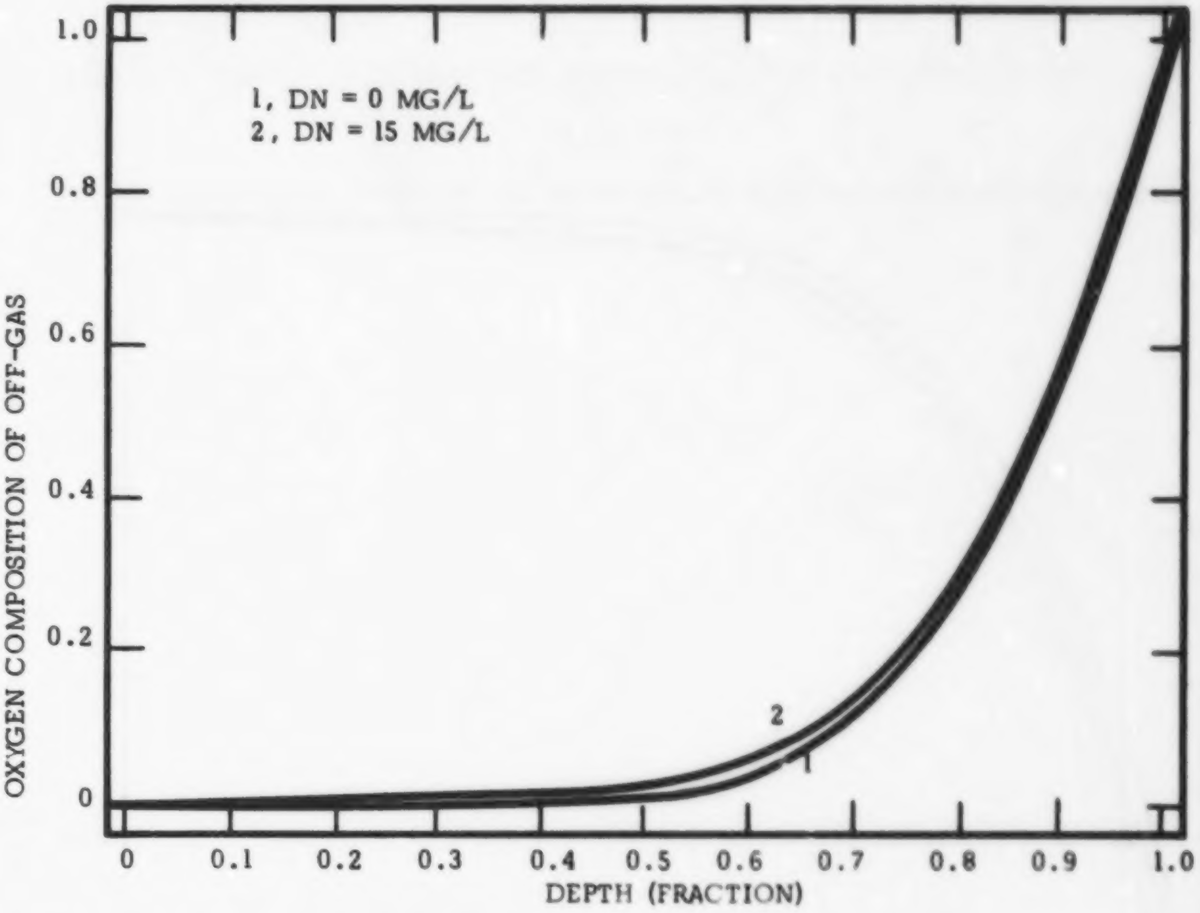

Fig. 36 OXYGEN COMPOSITION OF OFF-GAS VS FRACTION OF DEPTH

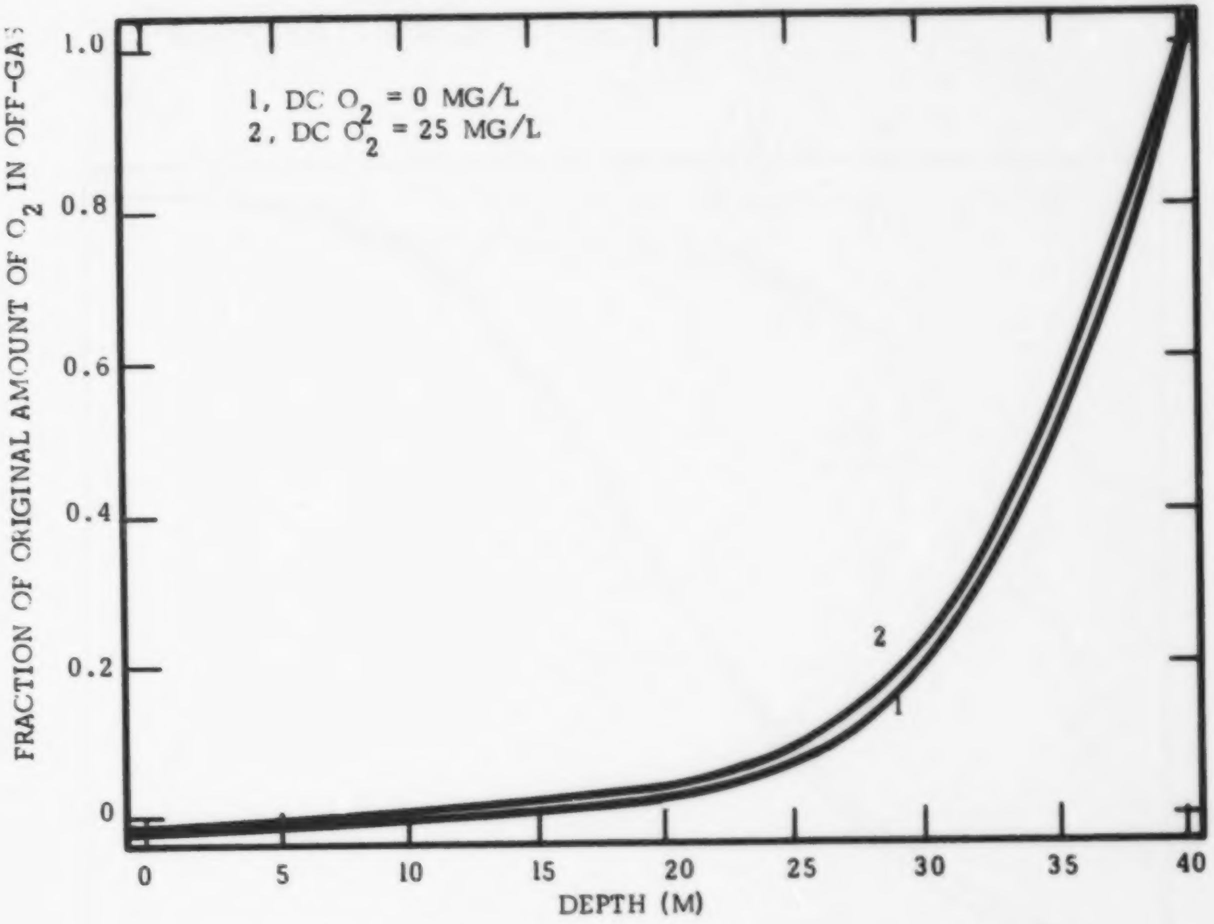

Fig. 37 FRACTION OF ORIGINAL AMOUNT OF O_2 IN OFF-GAS VS DEPTH

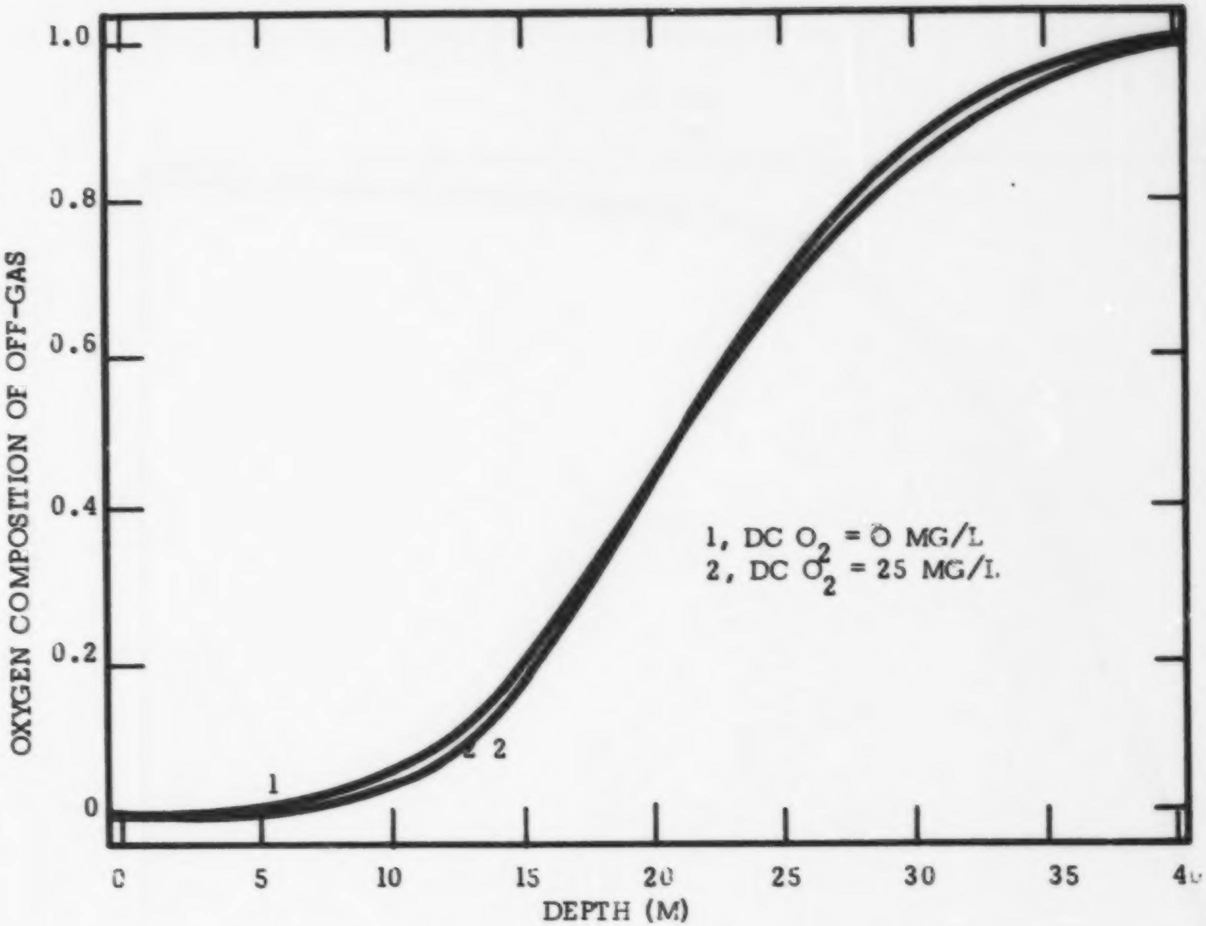

Fig. 38 OXYGEN COMPOSITION OF OFF-GAS VS DEPTH

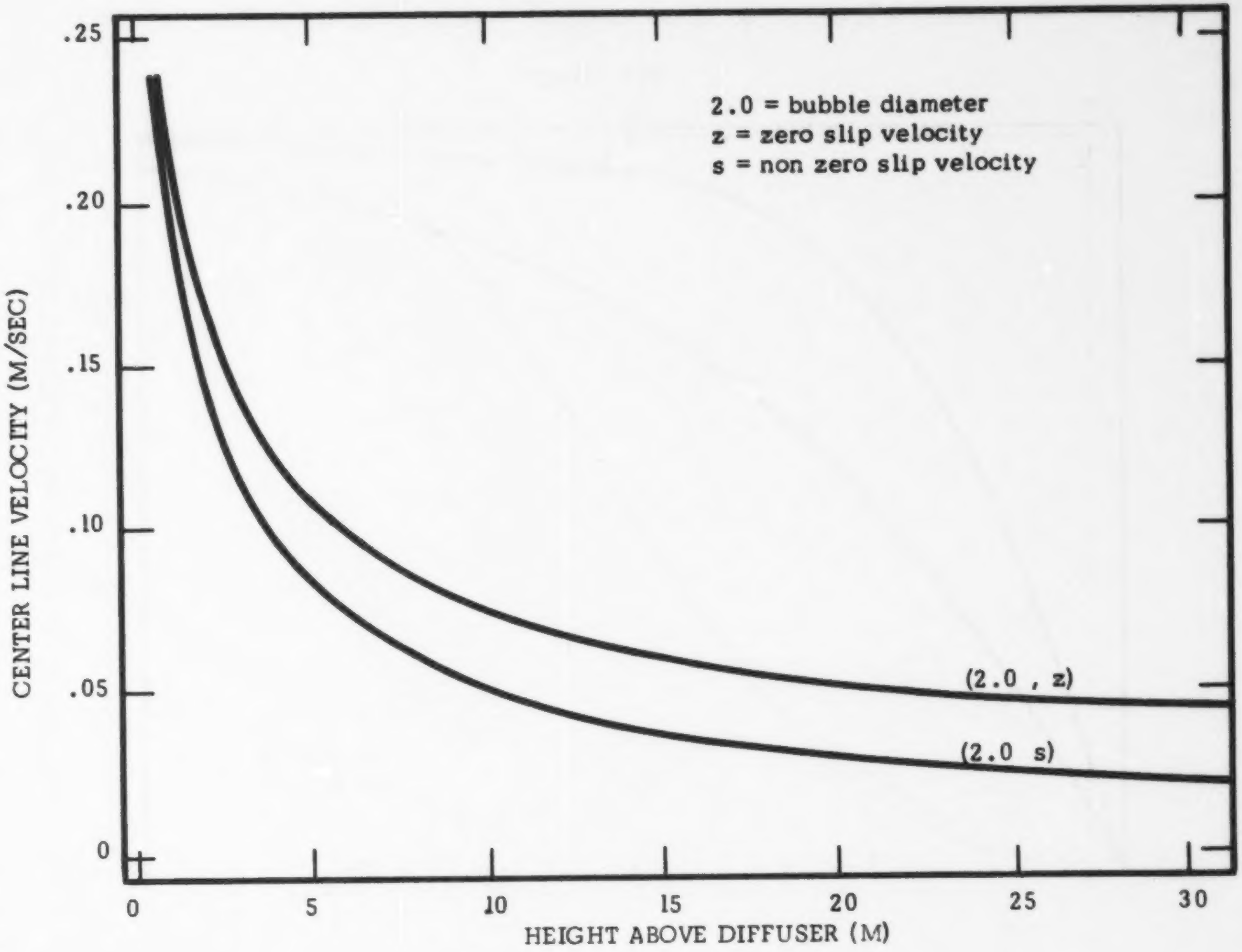

Fig. 39 CENTER LINE VELICITY VS HEIGHT ABOVE DIFFUSER

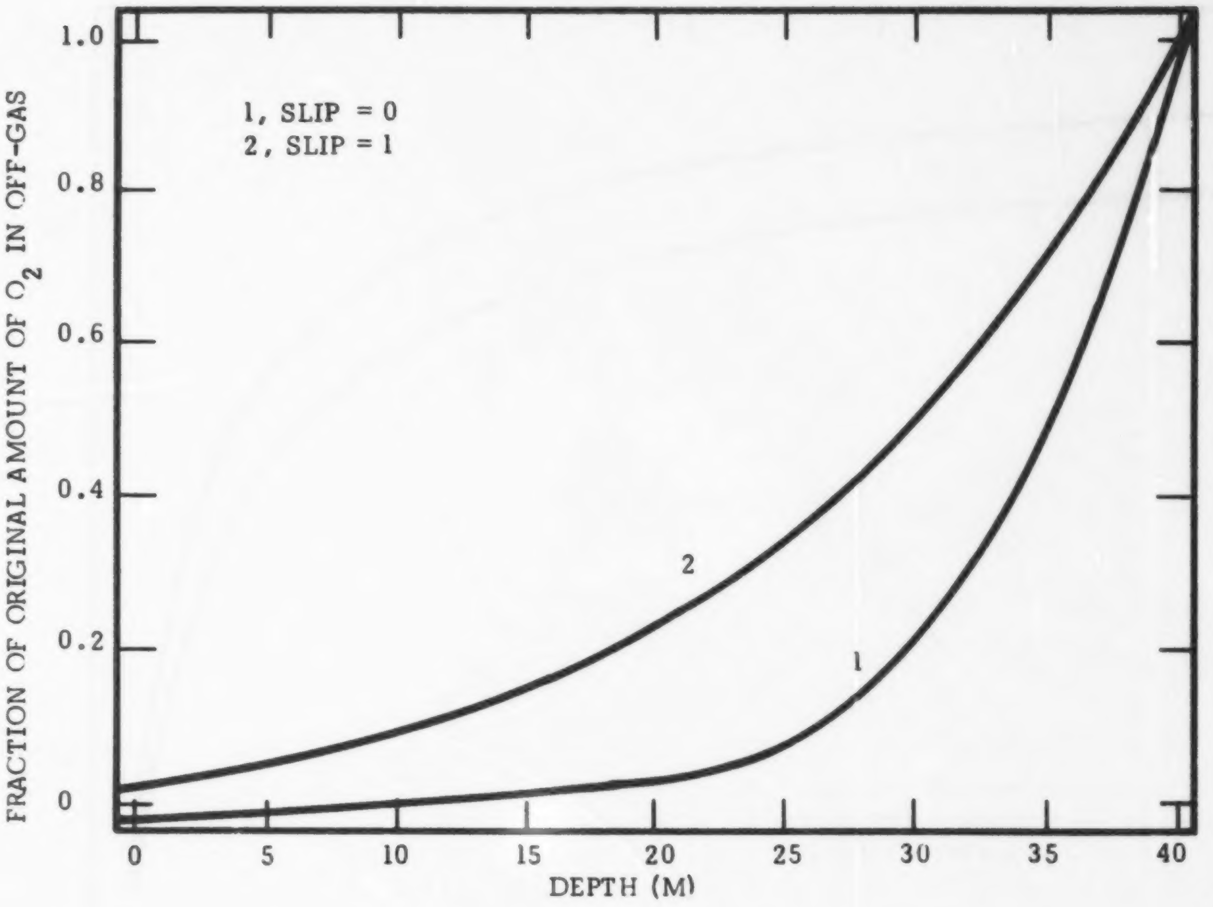

Fig. 40 FRACTION OF ORIGINAL AMOUNT OF O_2 IN OFF-GAS VS DEPTH

buoyancy only. This can be accomplished by installing baffles at an intermediate height above the diffuser.

Internal Pressure of Small Bubbles

In the calculation of the gas mass-transfer, the saturation concentration of the gas in the liquid is of considerable importance. It is calculated by the equation,

$$C_s = (A)\ (FO)\ (TO) \tag{19}$$

where:
A = Pressure in atmospheres
FO = Partial pressure of the gas in the bubble
TO = C_{sat} of the gas per atmosphere of partial pressure.

A, the pressure in atmospheres is calculated by the equation,

$$A = 1.0 + D/10.36 \tag{20}$$

D = Depth in meters

It has been noted that the smaller the bubble, the greater the pressure of the gas inside as compared to that outside. Therefore, theoretically the pressure, A, is higher than calculated by equation 15. The pressure difference for small bubbles, however, can be neglected when using this model due to the relative magnitudes of pressure involved. For example, additional increment of pressure is determined by the equation,

$$P = 4\gamma/d \tag{21}$$

where:
γ = energy per unit area
d = bubble diameter, cm

for cxygen, $\gamma = 15.7$ dynes/cm.

For a 0.1 mm bubble, the ΔP is calculated as follows:

$$\Delta P = \frac{4(15.7 \text{ dynes/cm})}{0.01 \text{ cm}} \quad \frac{9.87 \times 10^{-7} \text{ atm}}{\text{dynes/cm}^2}$$

$$\Delta P = 0.0063 \text{ atm}$$

This ΔP is insignificant compared to the hydrostatic pressures of 1 - 4 atmosphere encountered in this study. Therefore, this increased pressure due to small bubbles was neglected in this study.

Design Applications

A methodology for the design of an in-place hypolimnion diffuser aeration system has been developed. It is based on the average rise height above the point of injection to attain a desired per cent of absorption for bubbles with initial diameters up to 2.0 mm. The values for the average rise heights were computed using Speece's mathematical model with a modified K_L function. Figure 41 represents a compilation of these values. The rise height as presented is the average for injection depths of 20, 40, 60, 80 and 160 m. Table 2 shows the rise height associated with each bubble diameter and injection depth. The dissolved oxygen, nitrogen and carbon dioxide concentrations were 10, 15, and 25 mg/l, respectively. The temperature was 10°C.

The general design procedure for a hypolimnion aeration system is as follows:

1. The allowable rise height is computed knowing the maximum injection depth and the depth of the bottom of the metalimnion.

2. Using Figure 41, the possible combinations of initial bubble diameter and per cent of absorption can be determined. Notice that in most cases this will give you two ranges of initial bubble diameter that will insure a desirable absorption efficiency. Normally, these ranges of values will be approximately bubble diameters less than 0.3 mm and between 1.0 and 2.0 mm. Generally, the larger initial bubble diameters will be more economical because the price of diffusers in this range are approximately one half of those producing the much smaller bubbles. Also, fewer problems with clogging of the diffusers will be encountered using the larger bubble size. If, however, a critical situation exists where mixing between the hypolimnion and metalimnion must be kept to a minimum, then it may be more beneficial to use the smaller bubbles.

3. Once the bubble size has been selected, the injection flow rate, F, will be a function of the type of diffuser selected. Bubble size produced by a diffuser is a function primarily of the orifice diameter and the flow rate.

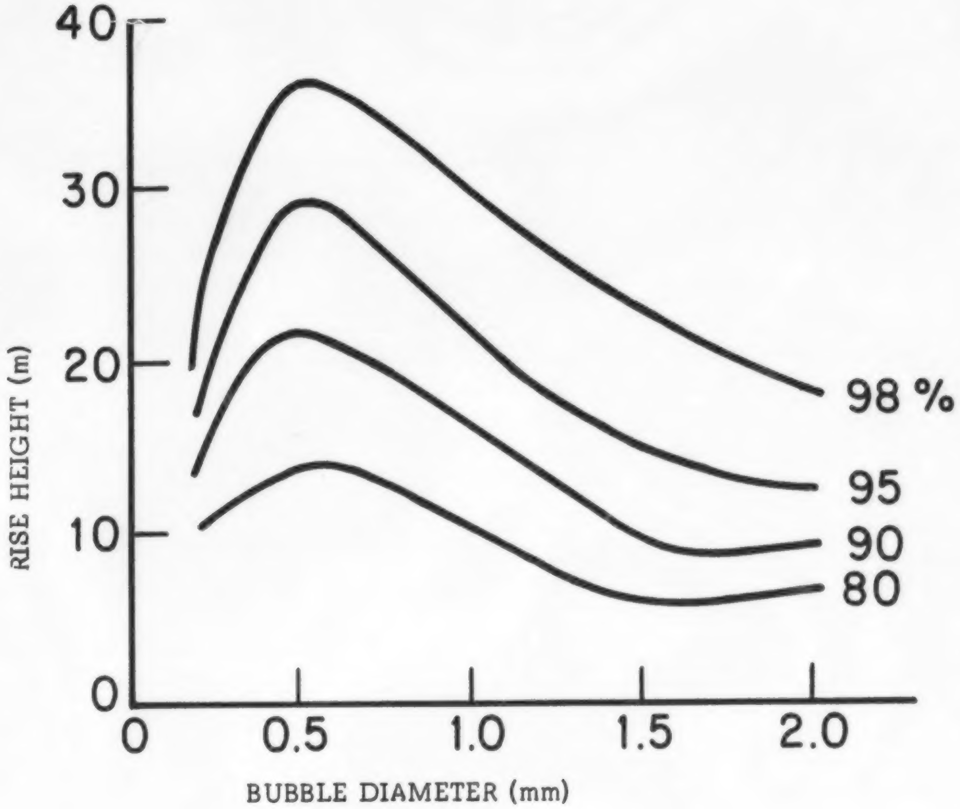

Fig. 41 RISE HEIGHT REQUIRED TO ACHIEVE INDICATED ABSORPTION EFFICIENCY VS BUBBLE DIAMETER

Reproduced from best available copy.

TABLE 2

Rise Heights for Given % Absorption, Injection Depth, and Initial Bubble Diameter

%Abs Inj. Depth, m	Rise Height 80	 90	 95	 98	Initial Bubble Diam, mm
20	11.4	16.3	----	----	0.2
40	10.3	13.7	16.7	20.3	
60	9.9	13.0	15.7	18.6	
80	9.7	12.7	15.2	17.9	
160	9.4	12.3	14.6	17.0	
Avg	10.1	13.6	15.6	18.5	
20	13.9	----	----	----	0.5
40	13.8	21.8	31.9	----	
60	13.9	22.4	29.7	38.4	
80	14.0	22.1	28.8	36.2	
160	14.3	21.7	27.6	33.8	
Avg	14.0	22.0	29.5	36.1	
20	9.9	16.9	----	----	1.0
40	10.6	16.4	22.2	30.6	
60	10.6	16.1	21.6	29.2	
80	10.5	16.0	21.4	29.2	
160	10.5	15.8	21.2	29.9	
Avg	10.4	16.2	21.6	29.7	
20	6.0	9.2	13.2	----	1.5
40	5.9	9.3	14.5	23.4	
60	5.8	9.5	15.4	22.9	
80	5.8	9.7	15.5	22.8	
160	5.8	10.0	15.7	22.7	
Avg	5.9	9.5	14.9	23.0	
20	6.9	10.0	12.8	18.2	2.0
40	6.7	9.1	11.9	16.9	
60	6.5	8.9	11.9	18.0	
80	6.4	8.8	12.0	18.9	
160	6.3	8.7	12.2	19.5	
Avg	6.6	9.1	12.2	18.3	

4. The amount of supplemental reaeration is determined knowing the volume of water time period which is oxygen deficient and the extent of this deficiency.

$$A = Q\,(C_2 - C_1)\,(10^{-6}) \qquad (22)$$

where: A = Supplemental aeration, Kg/day
Q = Volume of water aerated per day, L/day
C_2 = Desired DC concentration, Mg/L
C_1 = Actual DO concentration, Mg/L

5. Next, the daily requirement of injected oxygen is calculated as follows,

$$V = \frac{A}{(X)\,(\rho)} \qquad (23)$$

where: V = Daily volume of injected oxygen, L/day
A = Supplemental aeration required, Kg/day
X = Per cent absorption expressed as a fraction
ρ = The density of oxygen at the depth of injection, Kg/l

is calculated by the formula,

$$\rho = \left(1.0 + \frac{D}{10.36}\right) \text{Atm}\,(Y)\left(\frac{273}{273 + T}\right)(1.43 \times 10^{-3}\ \text{Kg/l-atm}) \qquad (24)$$

where: D = Injection depth, m
Y = Fraction of O_2 in injected gas
T = Temperature, ^{o}C

6. The required area of diffusers is then computed.

$$N = \frac{V}{F}$$

where: N = Area of diffusers required, m^2
V = Daily volume of injected oxygen, L/day
F = Flow rate per surface area of diffuser, $\frac{L/day}{(m)^2}$

7. The arrangement of the diffusers, of course, will be determined by the type of diffuser used. As a general rule, the diffusers should be separated by a minimum distance of 10 m to minimize interaction of plumes. However, if the diffusers are arranged in lines, the minimum distance can be neglected if the diffuser lines are separated by a minimum of 20 meters. Generally speaking, the smaller the allowable rise height and the more critical the effects of mixing between the hypolimnion and the metalimnion, the farther the distance should be separating the diffuser. At present, there is very little information concerning the interactive effects of bubble plumes in water. Therefore, a diffuser system should be designed and built so as to allow for flexibility with respect to the spacing of the diffusers.

To further clarify the previously outlined design procedure an example is furnished.

Design Conditions:

Release flow = 240 m^3/sec

Release duration = 4 hours

Withdrawal depth = 20 m

Injection depth = 25 m

Depth of bottom of metalimnion = 10 m

Width of reservoir bottom = 800 m

Temp of Hypolimnion = 10°C

Dissolved oxygen = 2 mg/l

Dissolved nitrogen = 15 mg/l

Dissolved carbon dioxide = 25 mg/l

Desired dissolved oxygen = 5 mg/l

Calculations:

1. Rise Height = Injection depth - Depth of bottom of metalimnion
   Rise Height = 25 m - 10 m = 15 m

2. Referring to Figure 41, with an allowable rise height of 15 m, bubbles with initial diameter of 1.5 mm will be 95 percent absorbed before reaching the metalimnion.

3. Assume the characteristics of the diffuser are such as to allow the flow rate per unit area to be 200 l/min-m^2.
F= 2.88×10^5 l/day-m^2

4. Required supplemental aeration, A

$$A = Q(C_2 - C_1)(10^{-6})$$

$$Q = 240\ m^3/sec \times 3600\ sec/hr \times 4\ hrs/day = 3.5 \times 10^6\ m^3/day$$

$$C_2 = 5.0\ mg/l$$

$$C_1 = 2.0\ mg/l$$

$$A = (3.5 \times 10^6) m^3 day\ (10^3\ l/m^3)\ (5.0 - 2.0)\ mg/l\ (10^{-6})$$

$$A = 1.05 \times 10^4\ kg/day$$

Using a 4 hour period to reaerate this volume, A = 6.3×10^4 kg/day.

5. Required volume of injected gas per day, V, using pure oxygen.

$$V = \frac{A}{(X)\ (\rho)}$$

$$A = 6.3 \times 10^4\ Kg/day$$

$$X = 0.95$$

$$\rho = (1.0 + \frac{D}{10.36})atm(Y)\ (\frac{273}{273+T})\ (1.43 \times 10^{-3} Kg/l\text{-}atm)$$

$$\rho = (1.0 + \frac{25}{10.36})\ (1.0)\ (\frac{273}{273 + T})\ (1.43 \times 10^{-3})\ Kg/l$$

$$\rho = 4.7 \times 10^{-3}\ Kg/l$$

$$V = \frac{6.3 \times 10^4\ Kg/day}{(0.95)\ (4.7 \times 10^{-3}\ Kg/l)} = 1.41 \times 10^7\ l/day$$

6. Required diffuser area, N

$$N = V/F$$

$$V = 1.41 \times 10^7\ l/day$$

$$F = 2.88\ l/day - m^2$$

$$N = \frac{1.41 \times 10^7\ l/day}{2.88 \times 10^5\ l/day\text{-}m^2} = 49\ m^2$$

A set of reference figures are included in the following section if more specific information is needed concerning the absorption of oxygen.

Stripping of nitrogen from the hypolimnetic waters may be of importance in some cases. Figures 42 - 45 show the transfer of nitrogen into and out of the bubble again for an injection depth of 30 m and using pure oxygen as the injected gas. The dissolved nitrogen concentration is 15 mg/l. The 2.0 mm bubble is the best example. The mass of nitrogen in the bubble increases from zero to a maximum of 0.103 mg at a depth of 20 m. This represents the nitrogen which is stripped out of the hypolimnetic water for a 10 m rise. As the bubble continues to rise the nitrogen is transferred back into the water and the mass of nitrogen in the bubble is reduced to .08 mg at the surface. Figures 46 - 49 show the transfer of nitrogen when air is injected. As can be seen, air will transfer nitrogen into the water at all depths for the bubble sizes used.

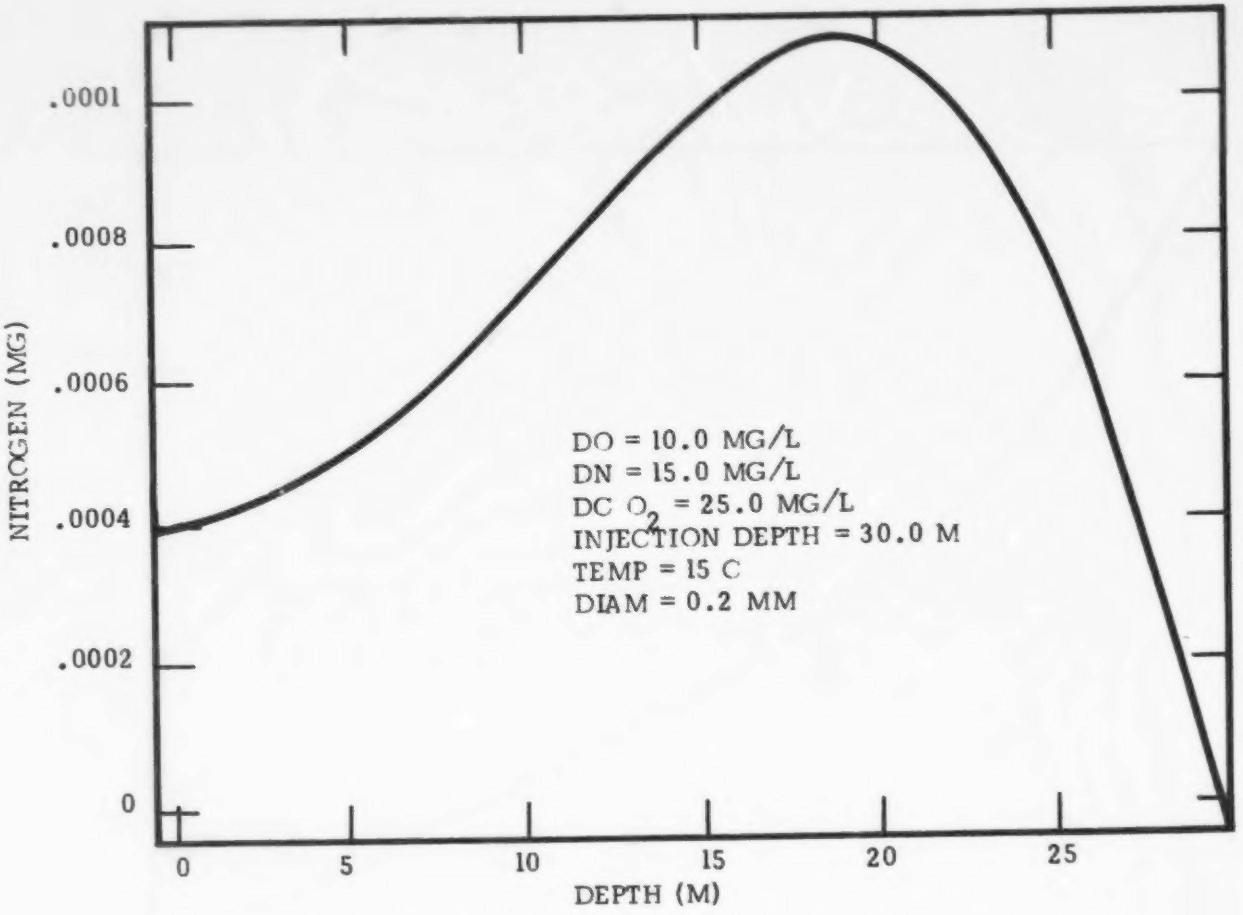

Fig. 42 NITROGEN IN OFF-GAS VS DEPTH - PURE OXYGEN

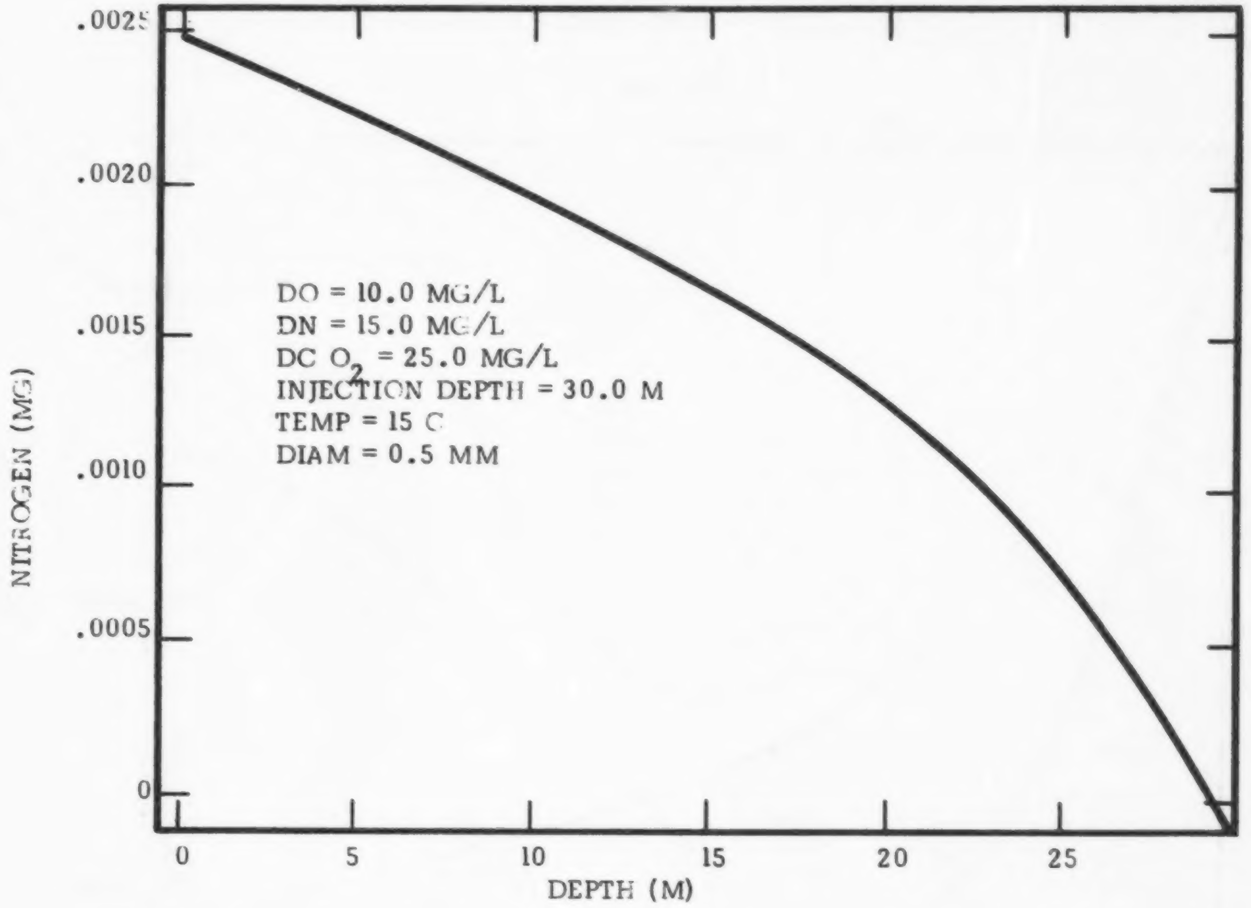

Fig. 43 NITROGEN IN OFF-GAS VS DEPTH - PURE OXYGEN

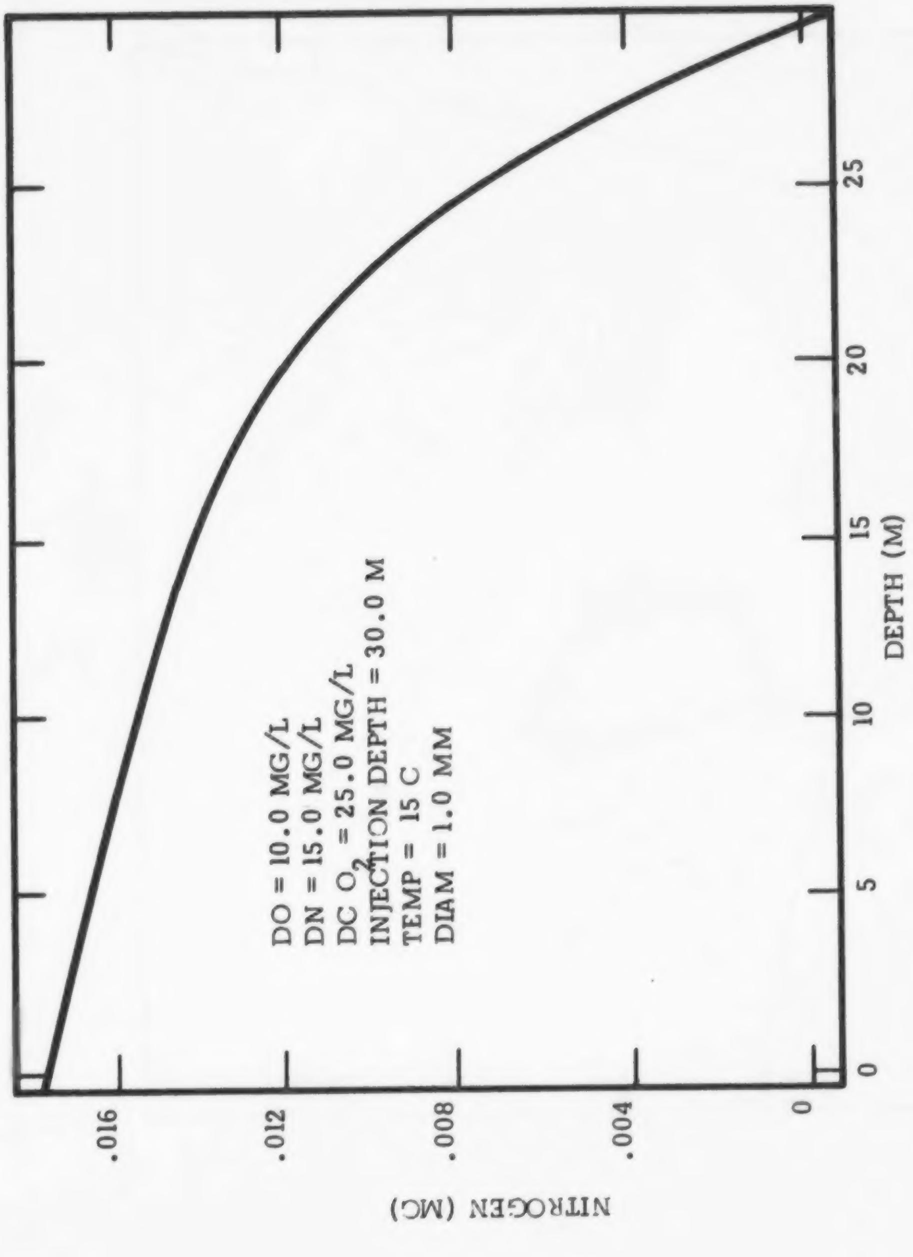

Fig. 44 NITROGEN IN OFF-GAS VS DEPTH - PURE OXYGEN

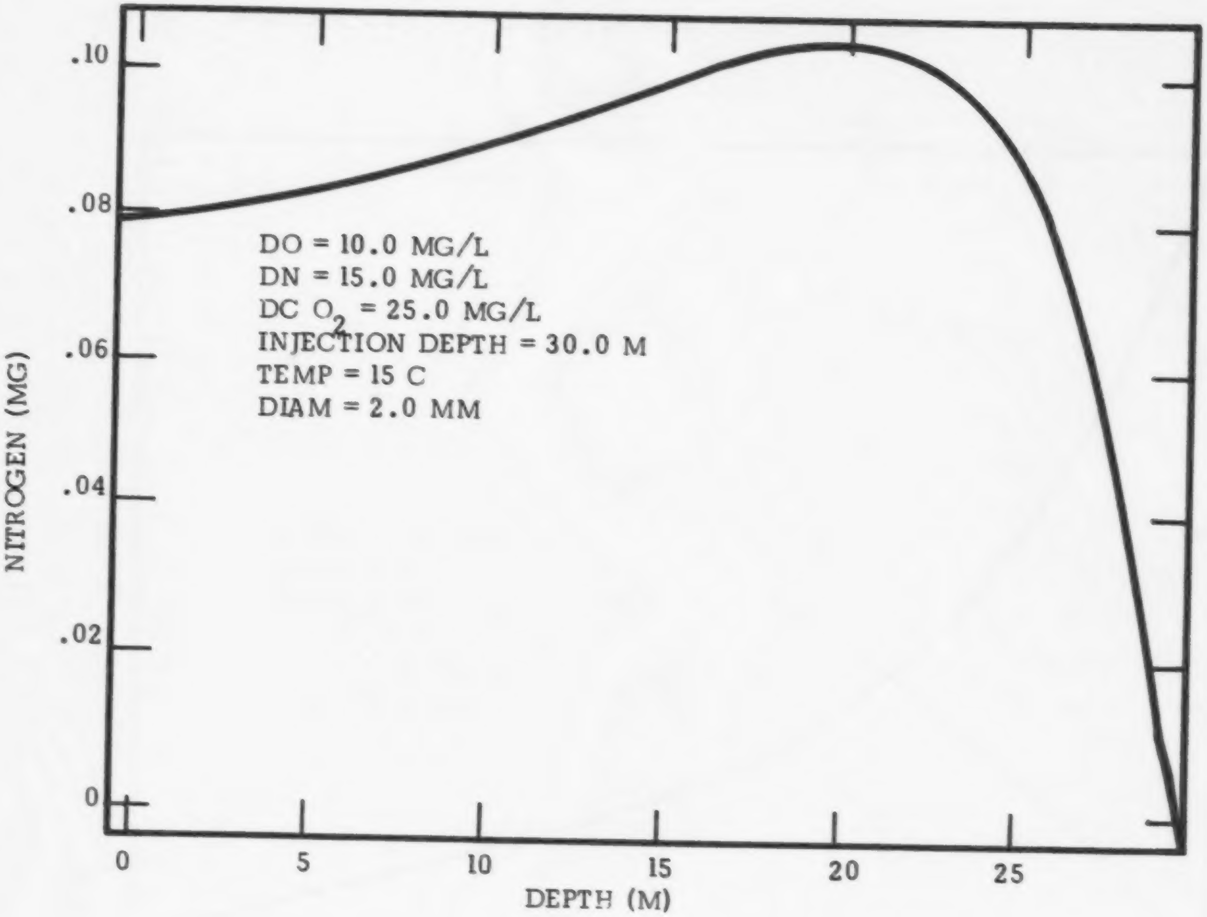

Fig. 45 NITROGEN IN OFF-GAS VS DEPTH - PURE OXYGEN

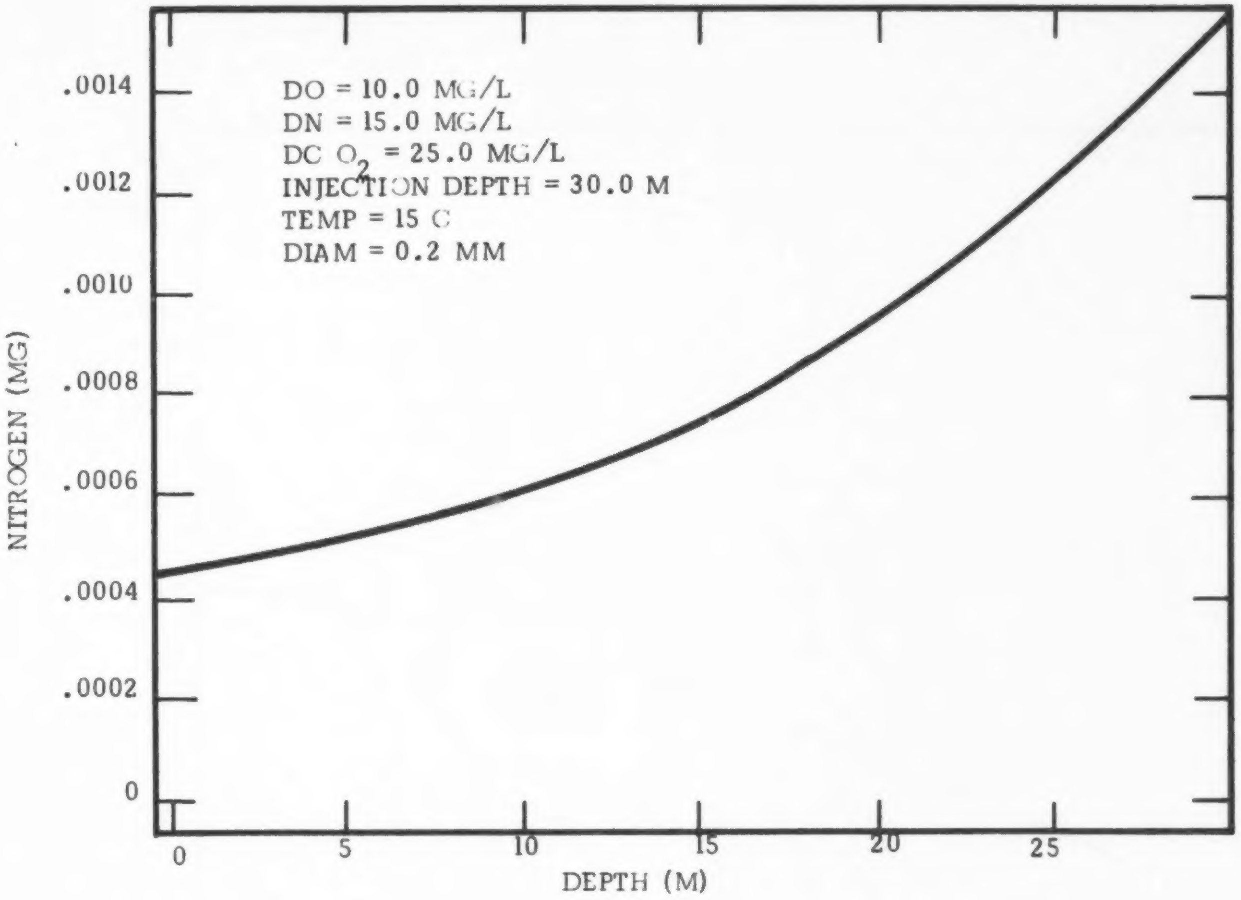

Fig. 46 NITROGEN IN OFF-GAS VS DEPTH - AIR

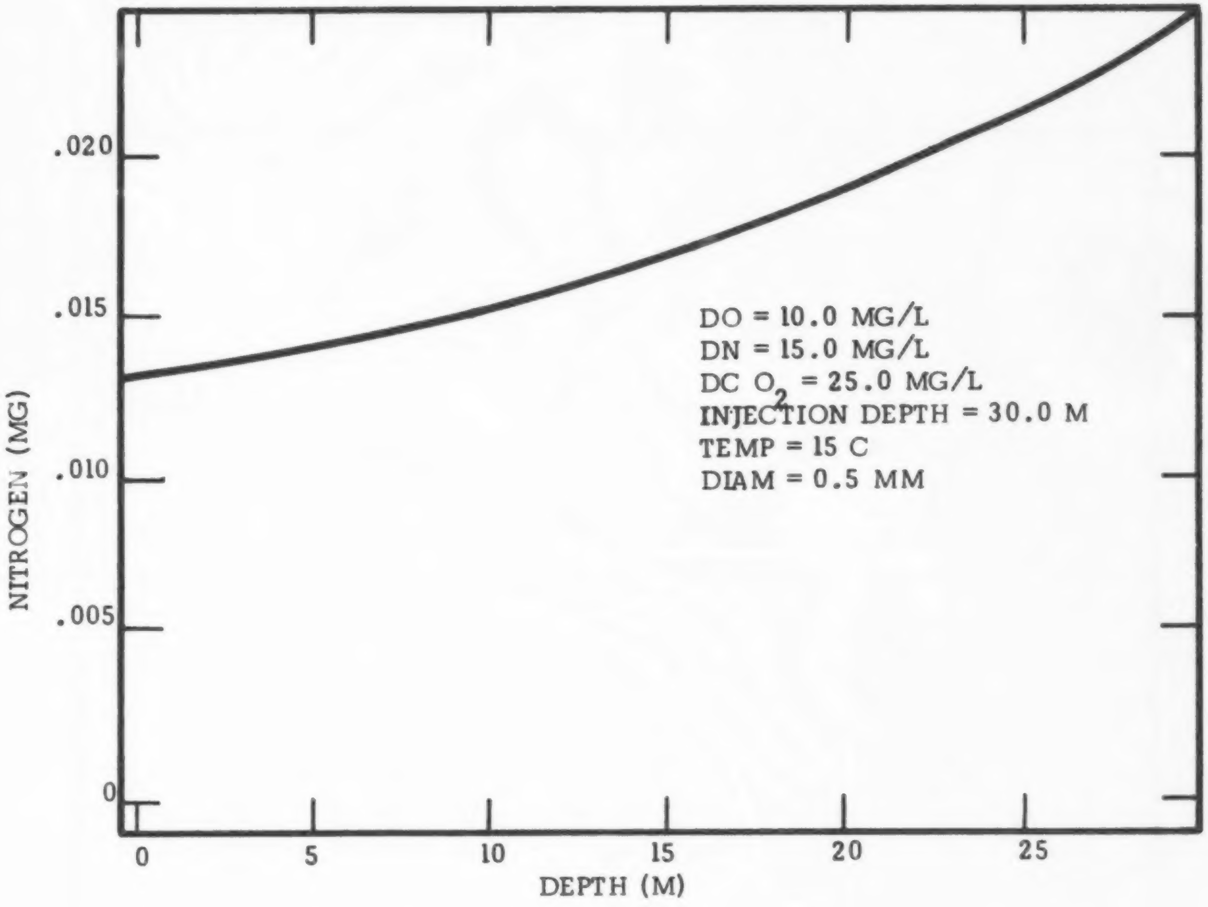

Fig. 47 NITROGEN IN OFF-GAS VS DEPTH - AIR

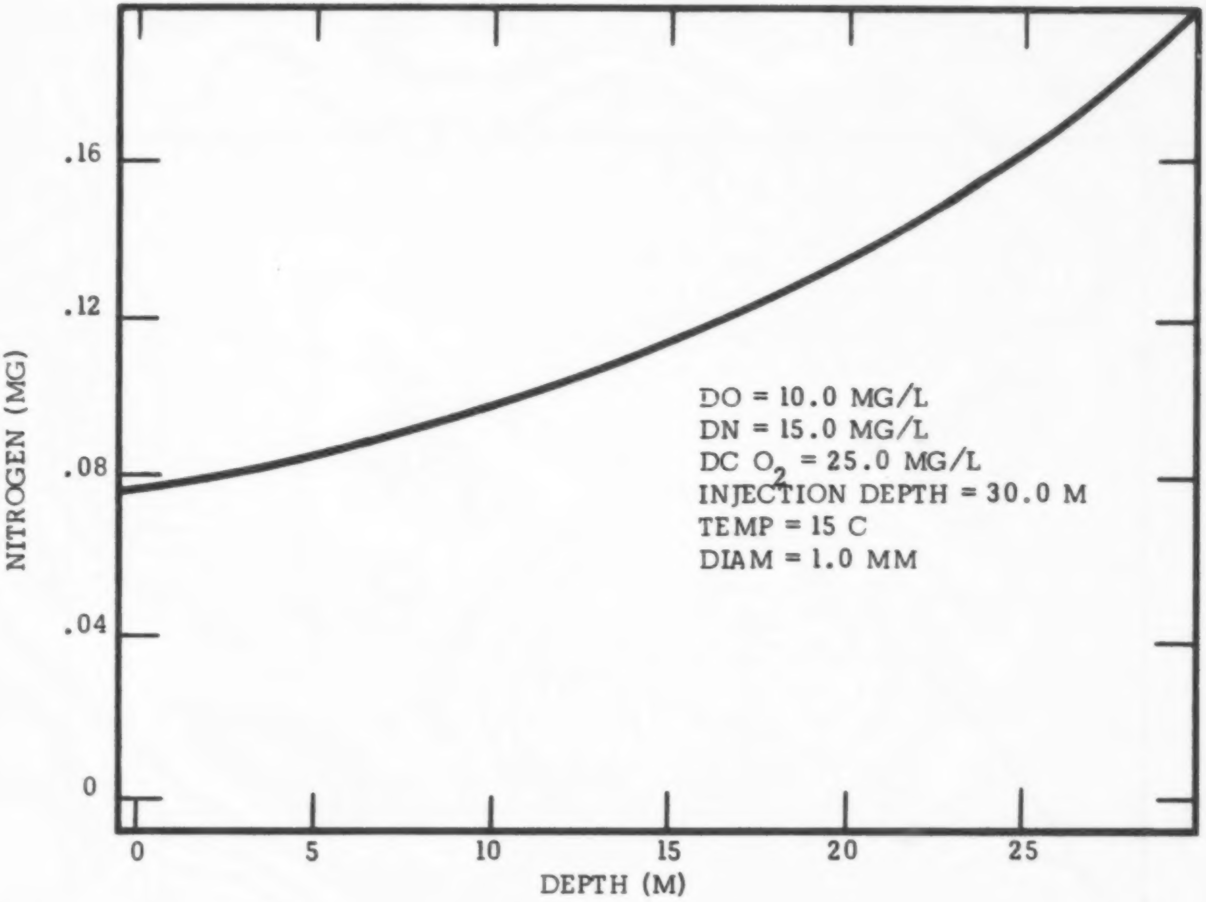

Fig. 48 NITROGEN IN OFF-GAS VS DEPTH - AIR

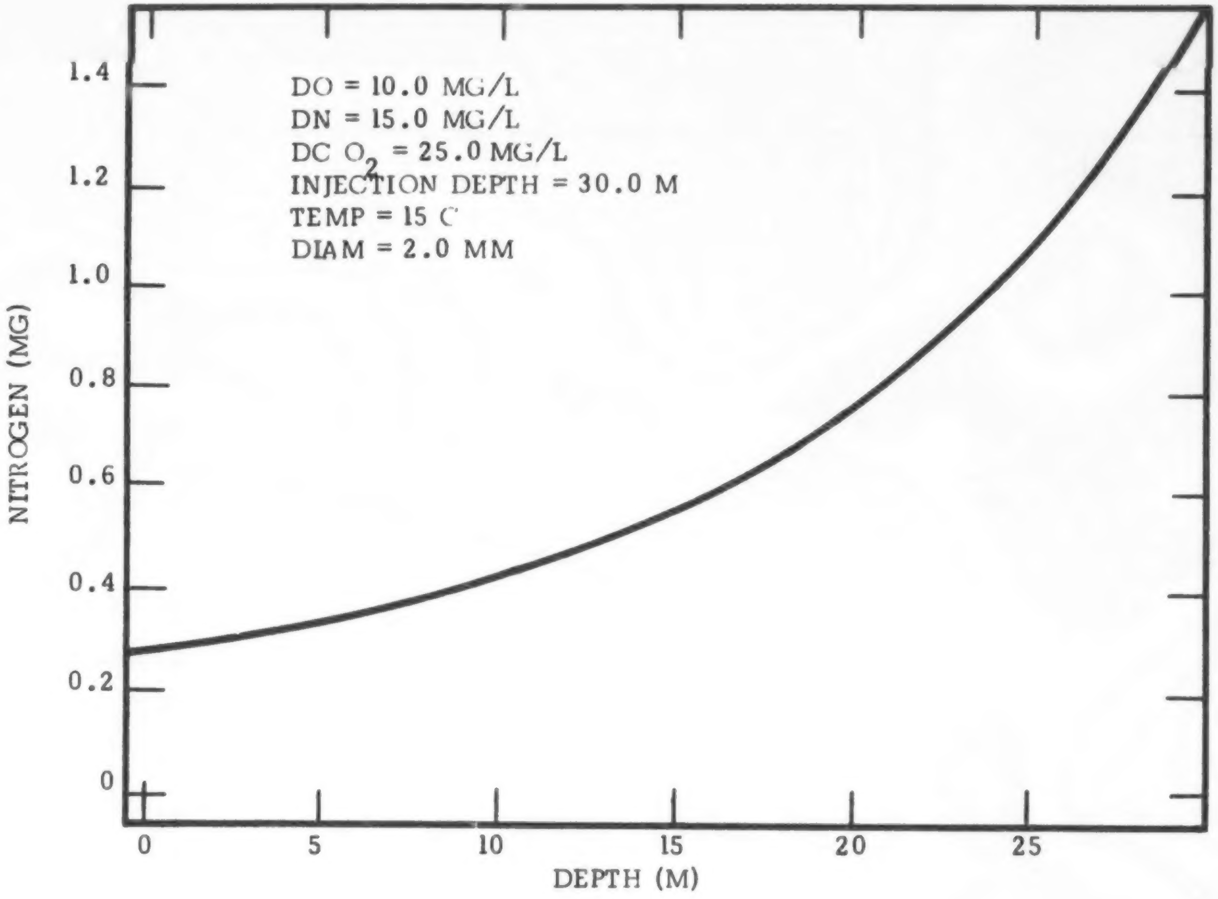

Fig. 49 NITROGEN IN OFF-GAS VS DEPTH - AIR

SECTION VIII

ACKNOWLEDGMENTS

This study was sponsored by the Office of Research and Monitoring, Environmental Protection Agency. Grateful appreciation is extended to Richard Hiller, who was the initial Project Officer and Lowell Leach, who subsequently served as project officer for the major portion of the grant. These men took a genuine interest in the project and whole heartedly supported it. Appreciation is also extended to Dr. Curtis C. Harlin, Jr. for his support of this project as well as the general area of river and impoundment aeration.

The University of Texas at Austin staff of Environmental Health Engineering and Dr. Gus Fruh in particular are gratefully acknowledged for their consultation and encouragement. The staff and facilities of the Center for Research in Water Resources are much appreciated.

SECTION IX

REFERENCES

1. Speece, R. E., "The Use of Pure Oxygen in River and Impoundment Aeration," Proceedings 24th Industrial Waste Conference, Purdue University (1969).

2. Lewis, W. K. and W. E. Whitman, "Principles of Gas Absorption," Industrial and Engineering Chemistry, 16, 1215 - 1220 (1924).

3. Treybal, R. C., Mass Transfer Operations, McGraw-Hill Book Company, New York, New York (1955).

4. Higbie, R., "The Rate of Absorption of a Pure Gas into a Still Liquid During Short Periods of Exposure," Transaction, AICE, 31, 365-389 (1935).

5. Dankwertz, P. V. "Significance of Liquid Film Coefficients in Gas Absorption," Industrial Engineering Chemistry, 43, 1460 (1951).

6. Dobbins, W. E., "Mechanisms of Gas Absorption by Turbulent Liquids," Advances in Water Research, Proceedings First International Conference on Water Pollution Research, Pergamon Press Ltd., London, England, 2, 61 (1964).

7. Eckenfelder, W. W., Jr., "Absorption of Oxygen from Air Bubbles in Water," JSED, ASCE, 85, 95 (1959).

8. Barnhart, E. T., "Transfer of Oxygen in Aqueous Solutions," JSED, ASCE, 95, No. SA3, 645 - 661 (1969).

9. Rosenberg, B., "The Drag and Shape of Air Bubbles Moving in Liquids," David Taylor Model Basin, Navy Department Report 727 (Sept., 1950).

10. Calderbank, P. H., and R. P. Patra, "Mass Transfer in the Liquid Phase During the Formation of Bubbles," Chemical Engineering Science, 1966, 21, 719.

11. Montgomery, J. O., "Relative Ratio of Nitrogen-to-Oxygen Transfer Coefficients in Aqueous Solutions," M. S. Thesis, New Mexico State University, (March, 1970).

Preceding page blank

12. Standard Methods for the Examination of Water and Wastewater, American Public Health Association, New York, New York, 12th Ed., (1965).

13. Rayyan, Fawzi, "Dynamics of Bubble Plumes Incorporating Mass Transfer," M. S. Thesis , University of Texas at Austin, (August, 1972).

14. Adamson, A. W., Physical Chemistry of Surfaces, Interscience Publishers, New York, New York (1970).

SECTION X

LIST OF PUBLICATIONS

One publication, to date, has resulted from this project. It is entitled "Alternative Considerations in the Oxygenation of Reservoir Discharges and Rivers" by R. E. Speece, Fawzi Rayyan, George Murphee. It is a publication in the Conference Proceedings - Applications of Commerical Oxygen the Water and Wastewater Systems University of Texas Press (In Press).

No patents resulted from this study.

SECTION XI

APPENDICES

Preceding page blank

APPENDIX A

DESIGN FIGURES - O_2 and Air

1) Fractional Absorption from Bubbles vs Rise Height

2) Relative Volume in Bubbles vs Rise Height

DESIGN FIGURES

The figures in this section can be used as additional material in the design of hypolimnion aeration systems. The figures which are included are the fraction of the original amount of oxygen injected versus depth and the volume of gas remaining at any depth relative to the volume of gas injected. Bubble diameter and bubble composition vs injection depth figures are included in the Appendix. These figures are divided into two sets. The first set is for the case where pure oxygen is used and the second set is for the use of air as the injected gas. On each figure, the behavior of four initial bubble diameters is represented. The four diameters are 0.2, 0.5, 1.0, and 2.0 mm. The injections depths are 8, 16, 24, 32, 48, 64, and 96 m. The dissolved oxygen, nitrogen, and carbon dioxide concentrations were set at 10, 15, and 25 mg/l, respectively. The temperature was set at 15°C. The '=' indicates more than one point is plotted in that space.

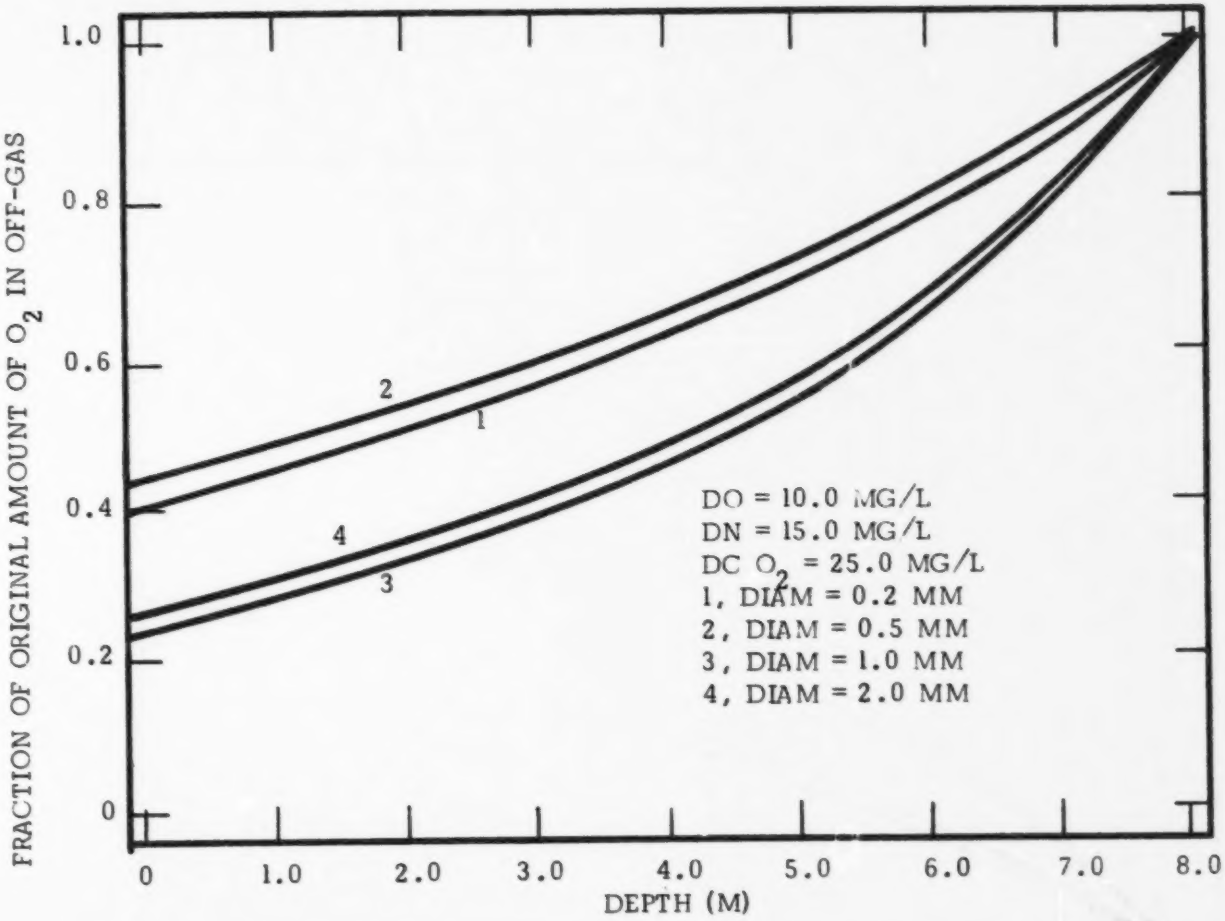

Fig. 50 FRACTION OF ORIGINAL AMOUNT OF O_2 IN OFF-GAS VS DEPTH - PURE OXYGEN

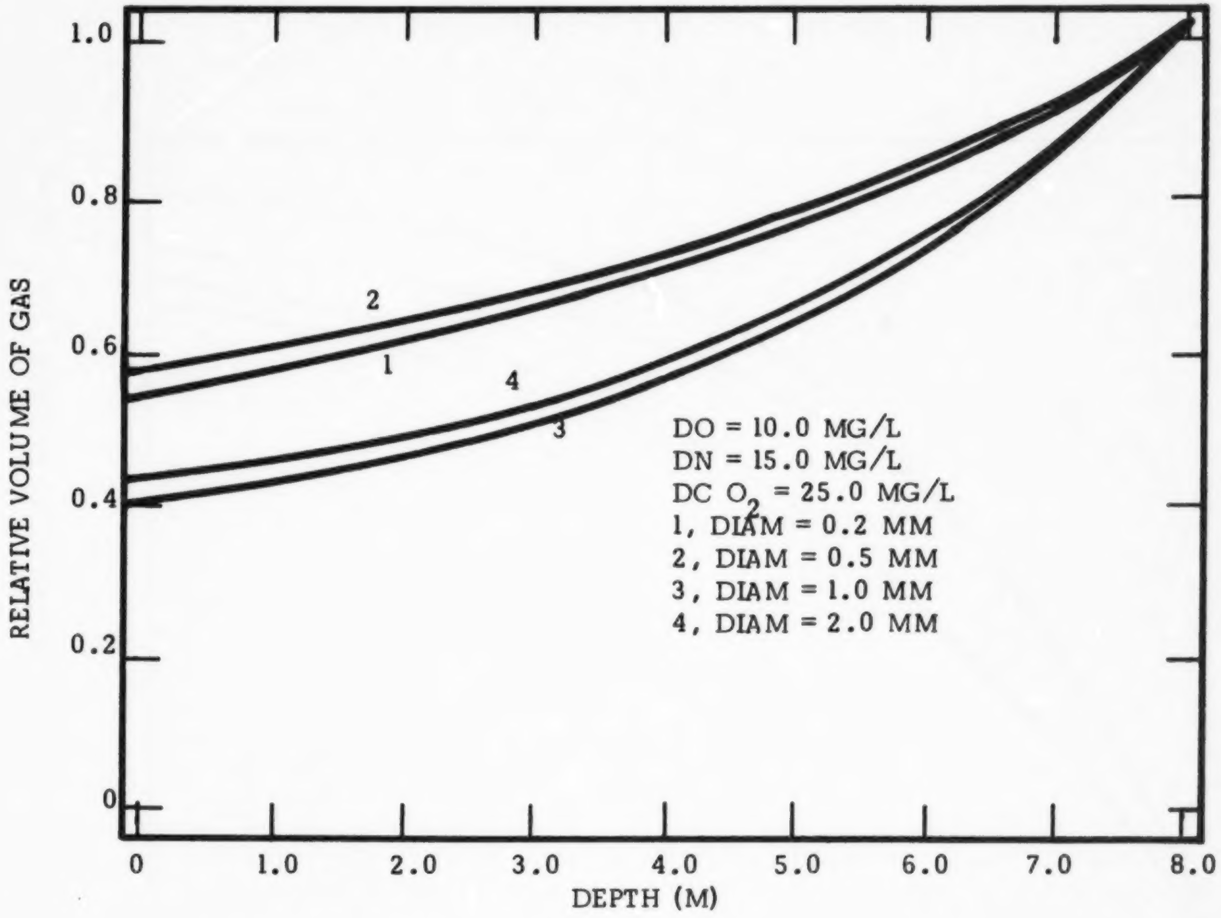

Fig. 51 RELATIVE VOLUME OF GAS VS DEPTH (M) - PURE OXYGEN

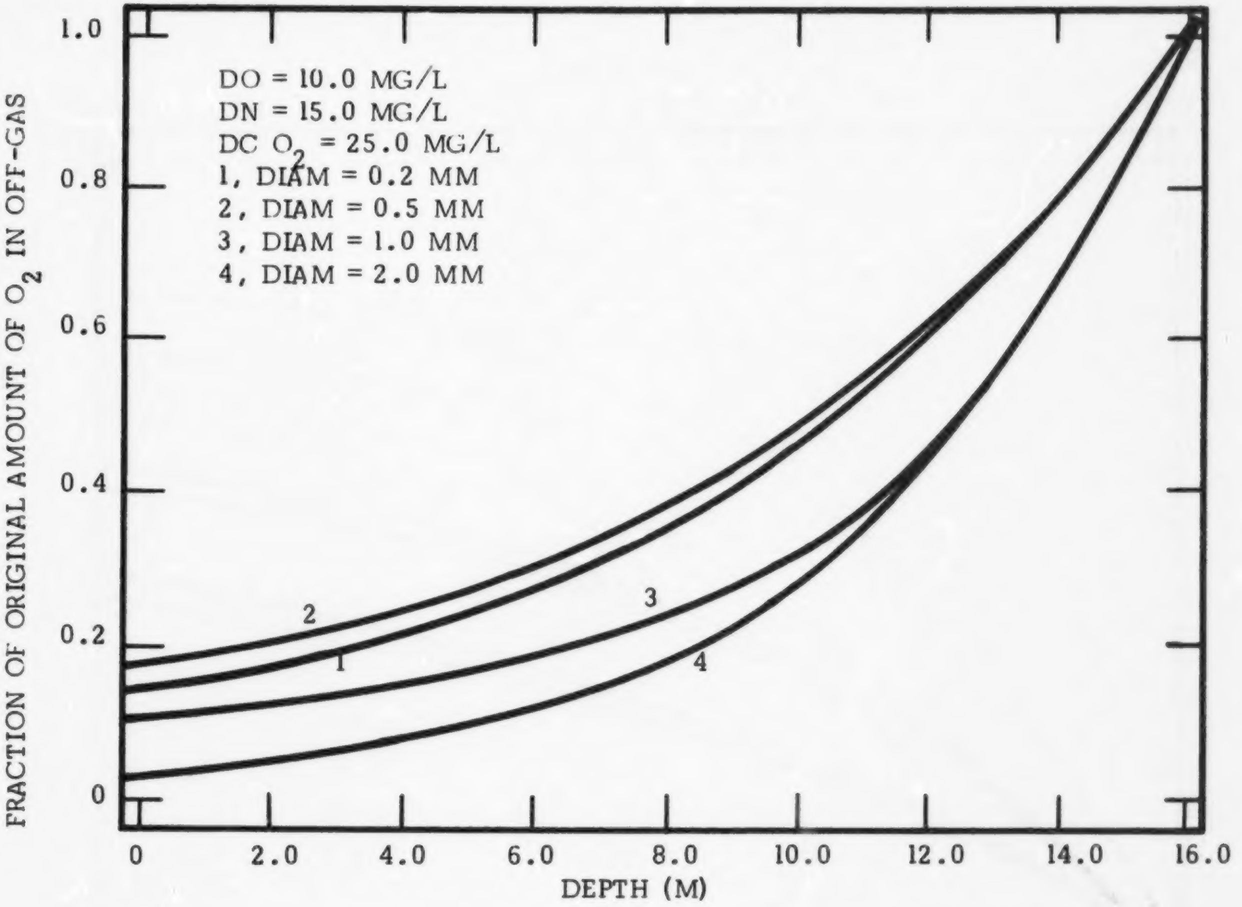

Fig. 52 FRACTION OF ORIGINAL AMOUNT OF O_2 IN OFF-GAS VS DEPTH - PURE OXYGEN

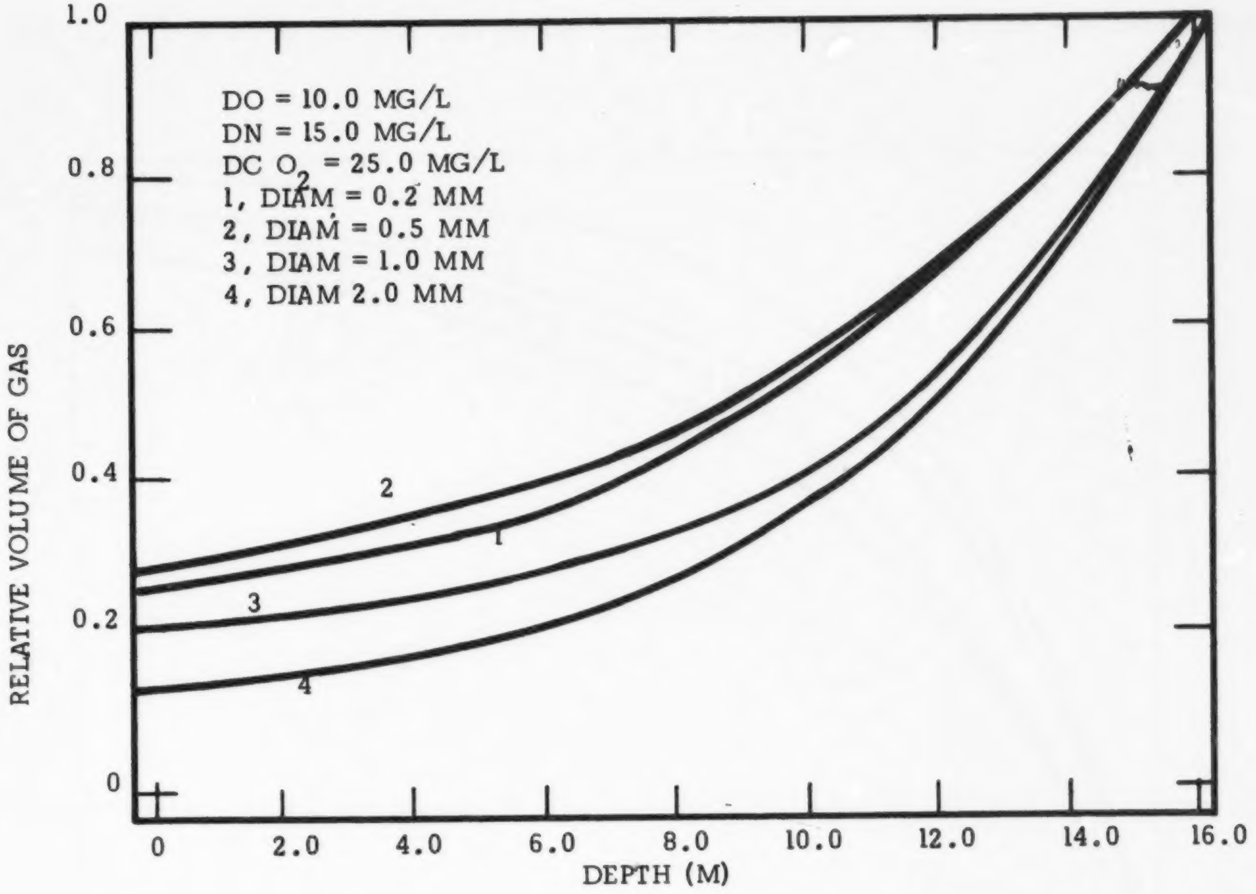

Fig. 53 RELATIVE VOLUME OF GAS VS DEPTH - PURE OXYGEN

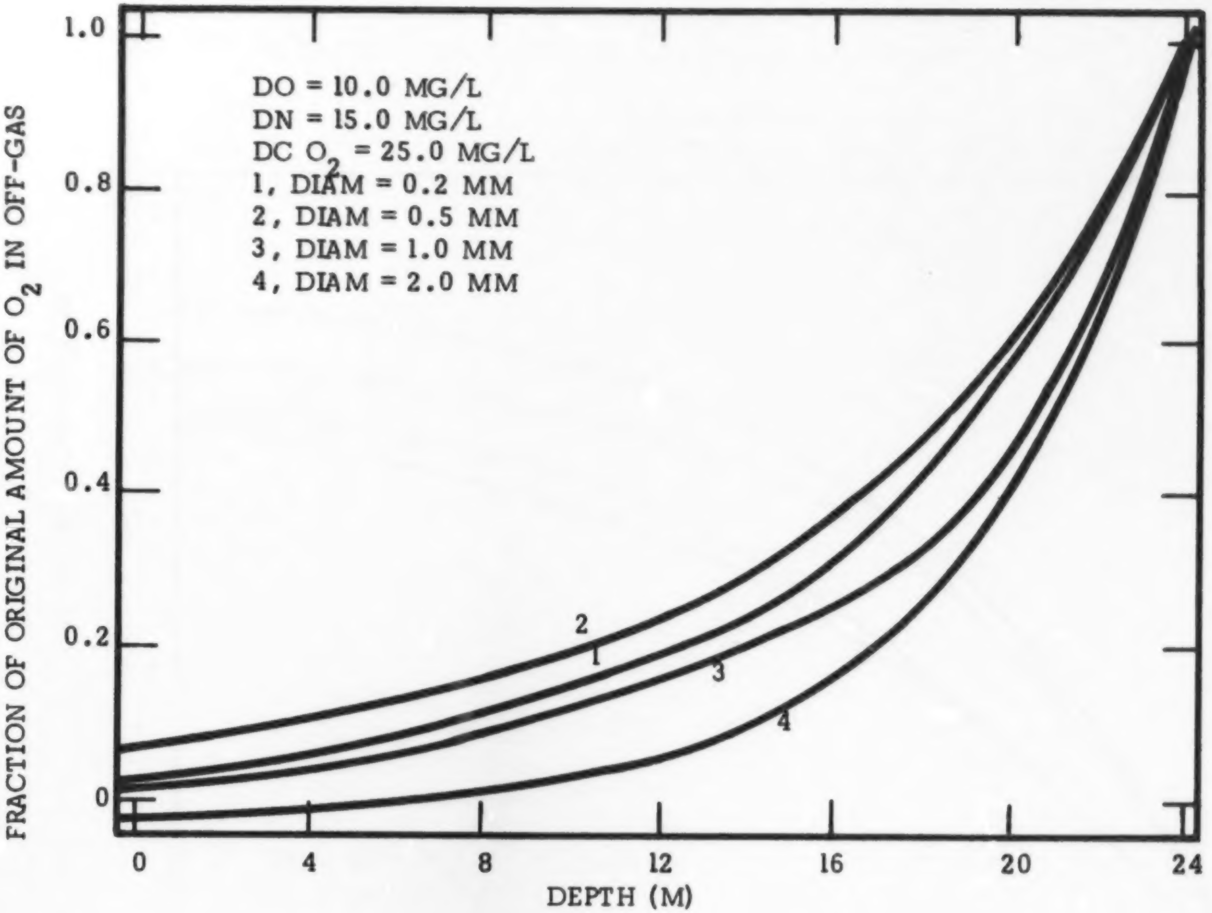

Fig. 54 FRACTION OF ORIGINAL AMOUNT OF O_2 IN OFF-GAS VS DEPTH - PURE OXYGEN

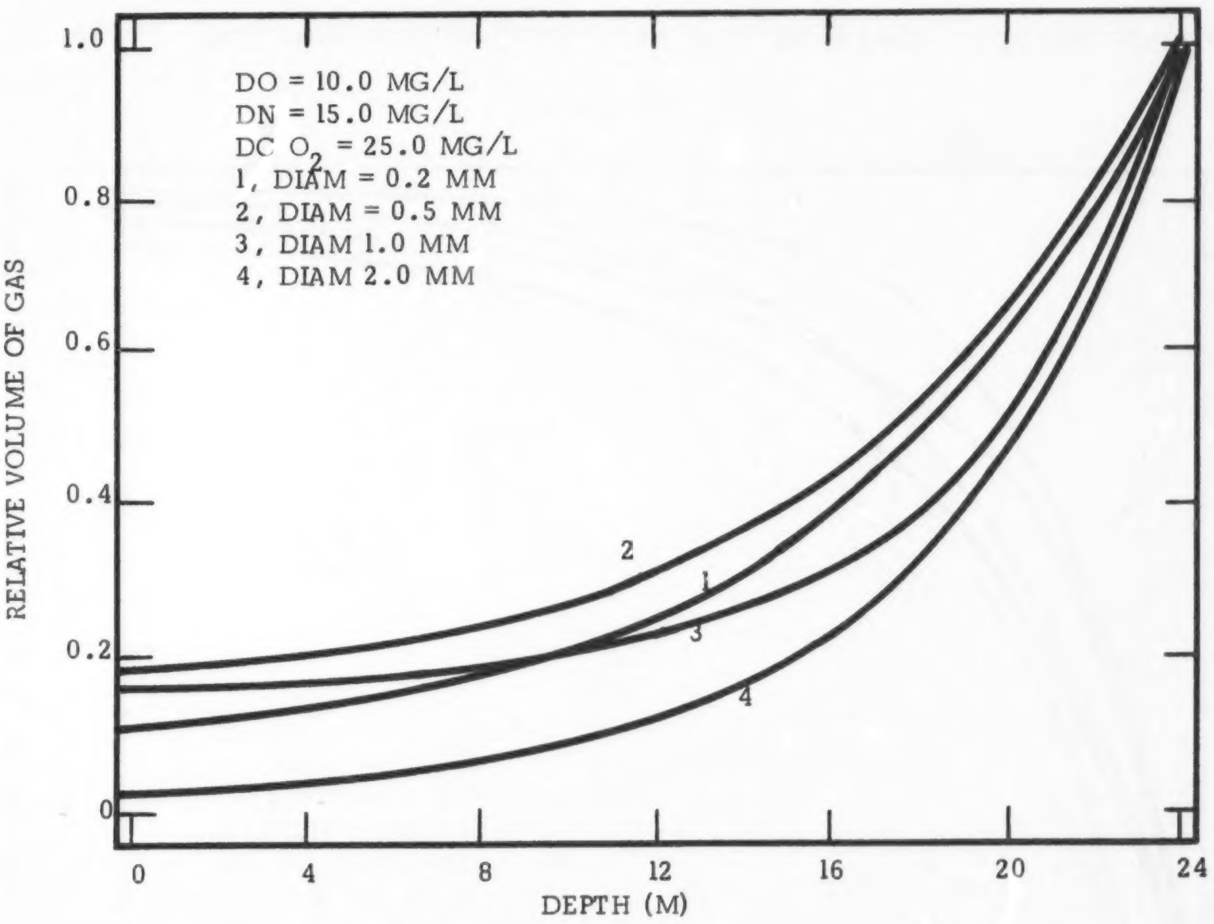

Fig. 55 RELATIVE VOLUME OF GAS VS DEPTH - PURE OXYGEN

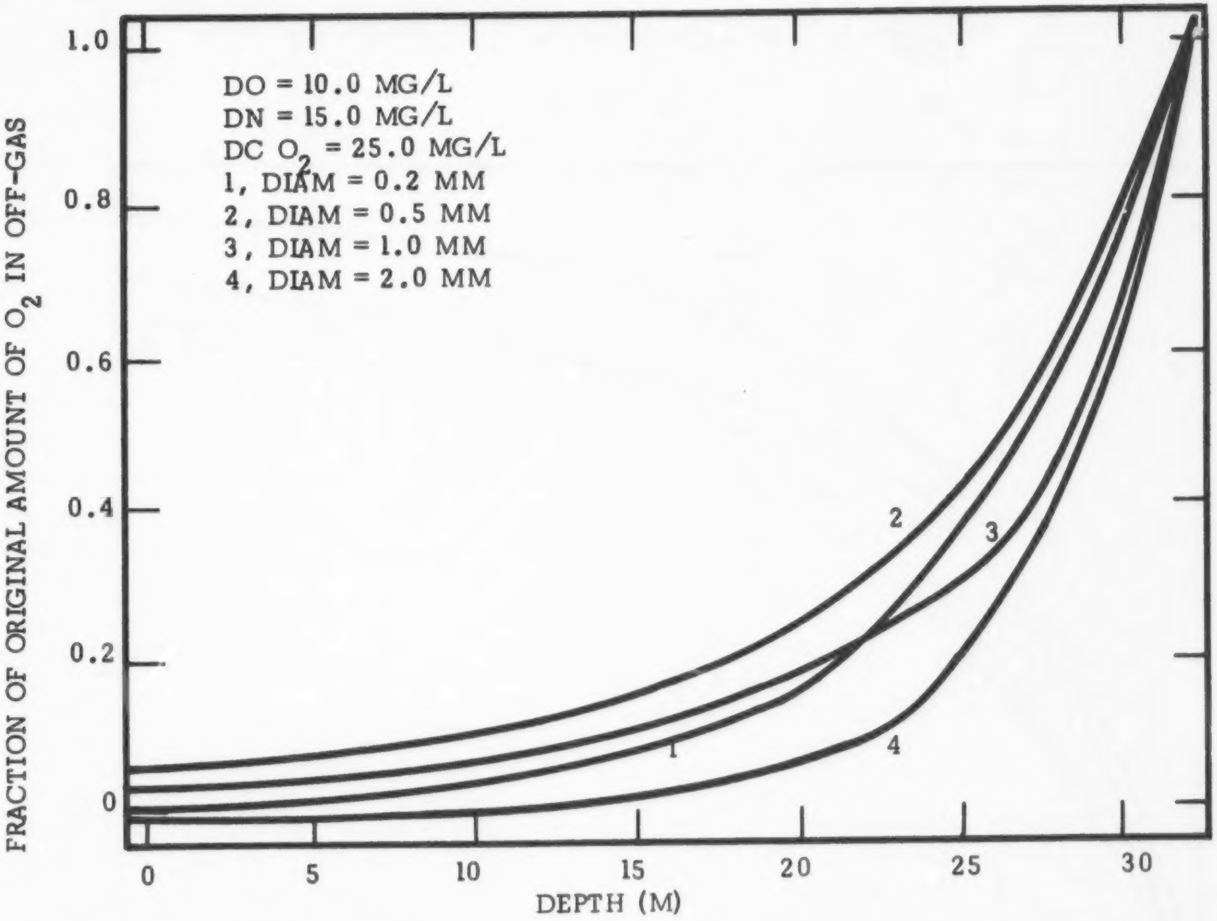

Fig. 56 FRACTION OF ORIGINAL AMOUNT OF O_2 IN OFF-GAS VS DEPTH - PURE OXYGEN

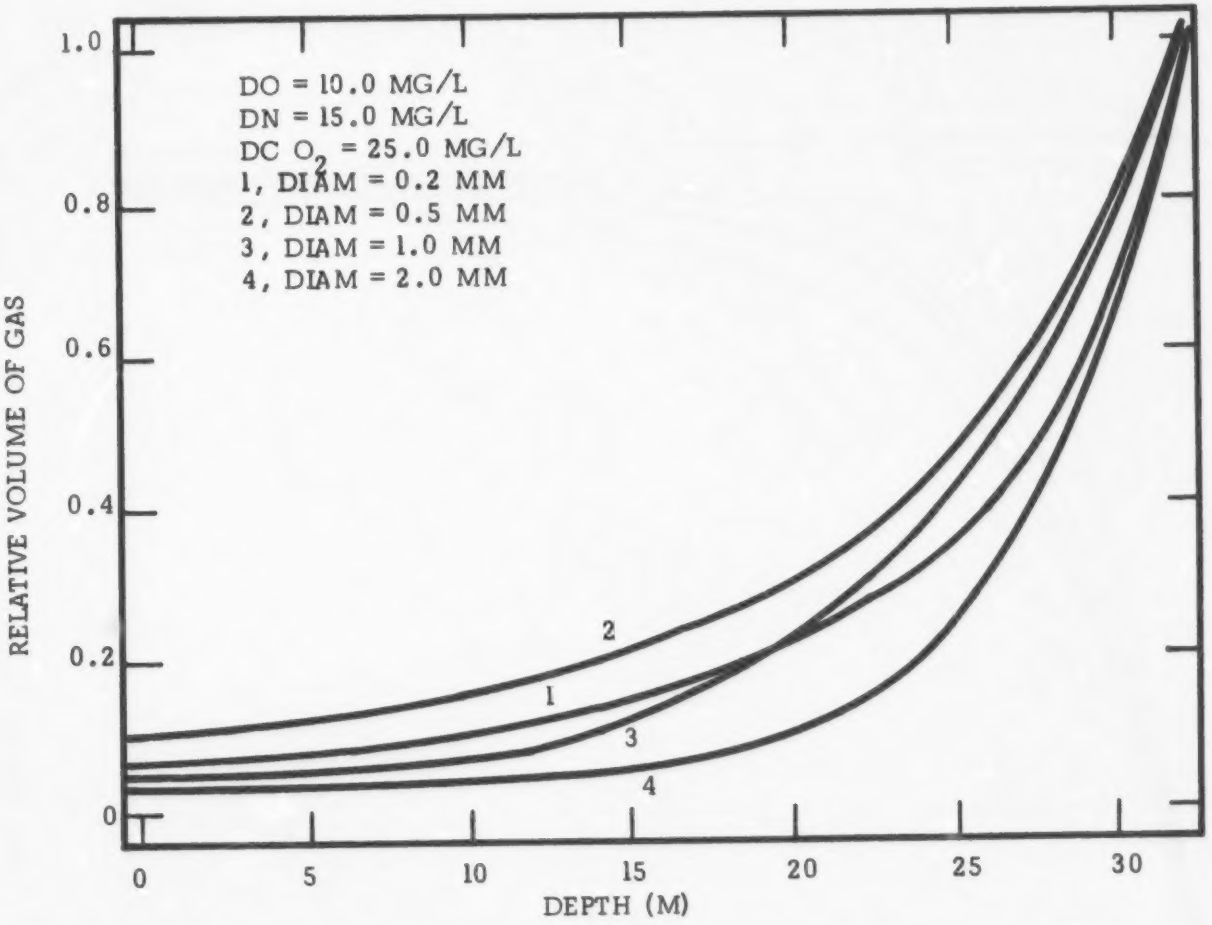

Fig. 57 RELATIVE VOLUME OF GAS VS DEPTH - PURE OXYGEN

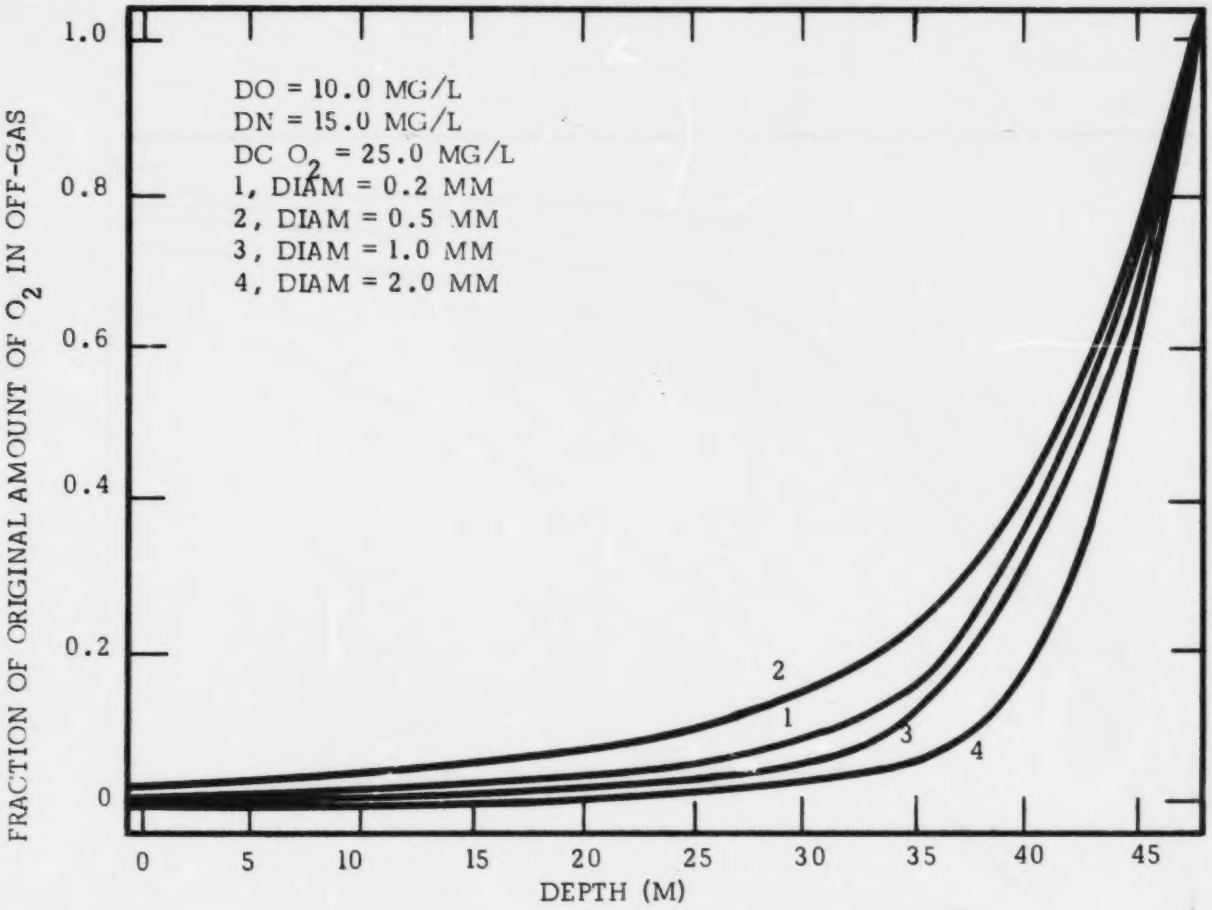

Fig. 58 FRACTION OF ORIGINAL AMOUNT OF O_2 IN OFF-GAS VS DEPTH - PURE OXYGEN

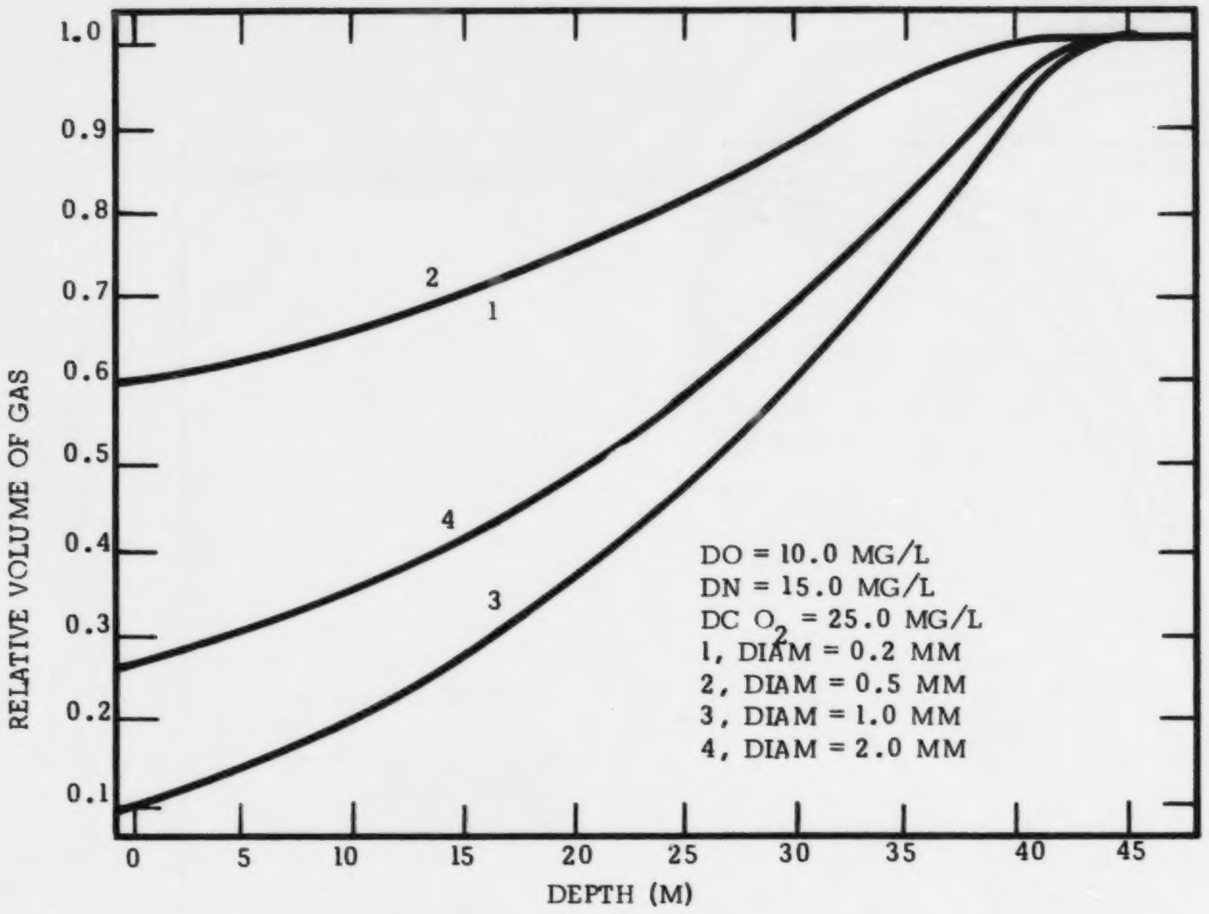

Fig. 59 RELATIVE VOLUME OF GAS VS DEPTH - PURE OXYGEN

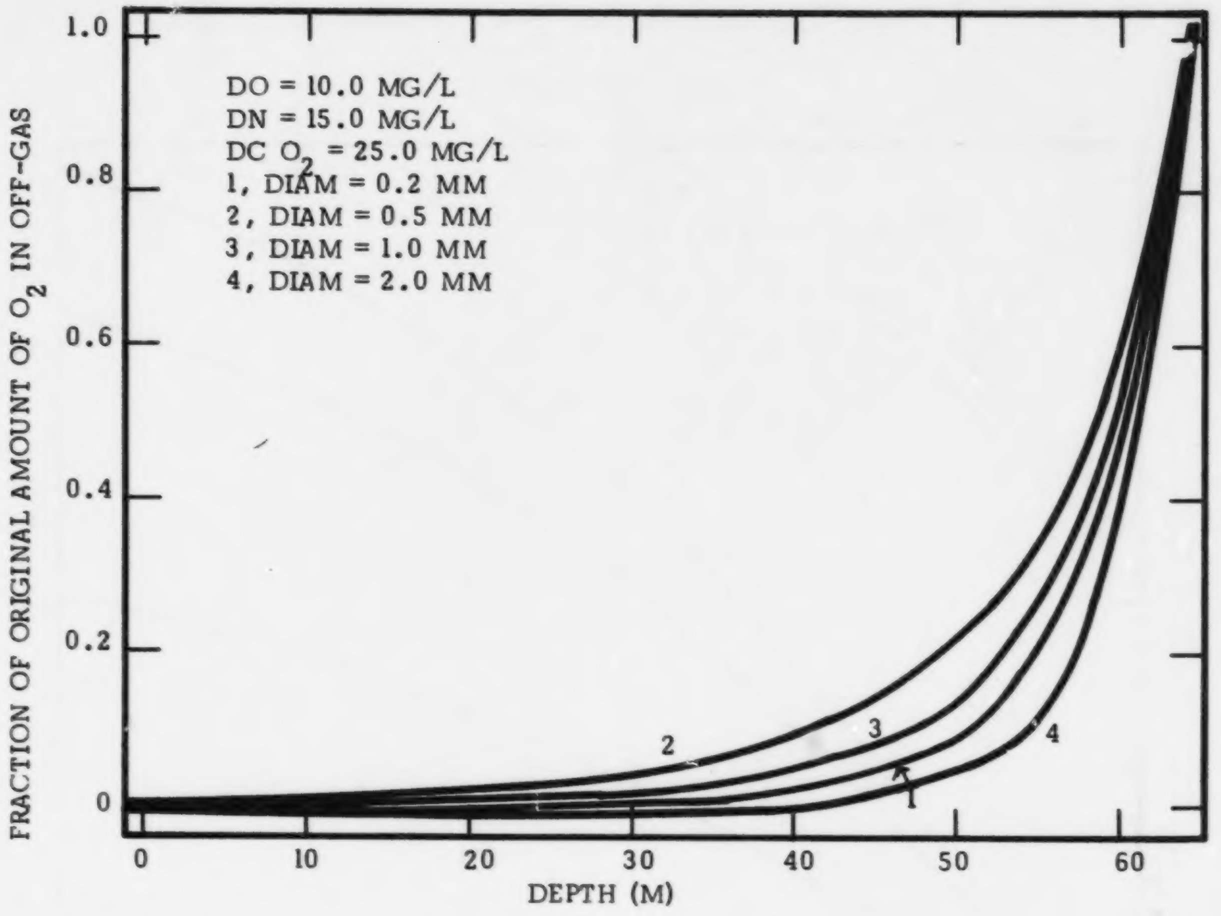

Fig. 60 FRACTION OF ORIGINAL AMOUNT OF O_2 IN OFF-GAS VS DEPTH - PURE OXYGEN

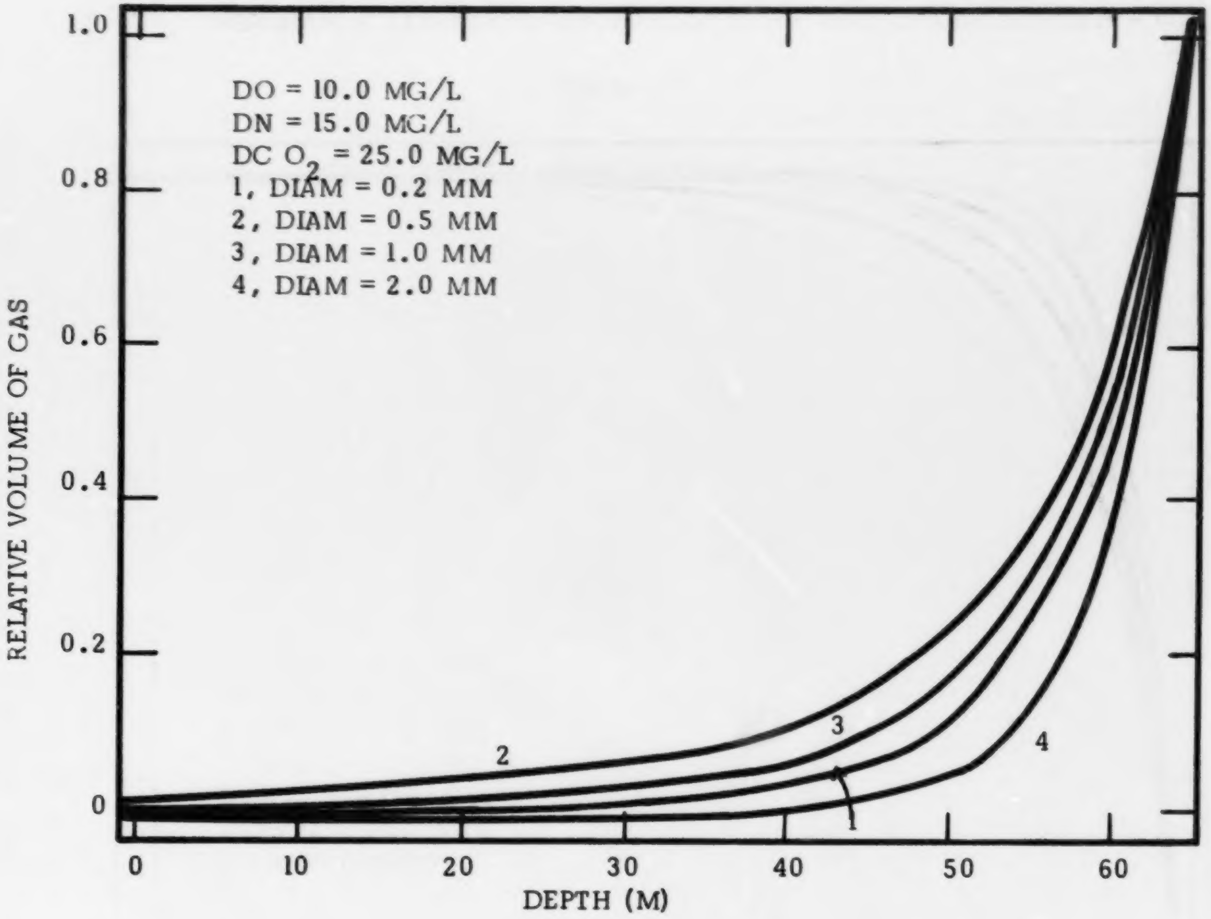

Fig. 61 RELATIVE VOLUME OF GAS VS DEPTH - PURE OXYGEN

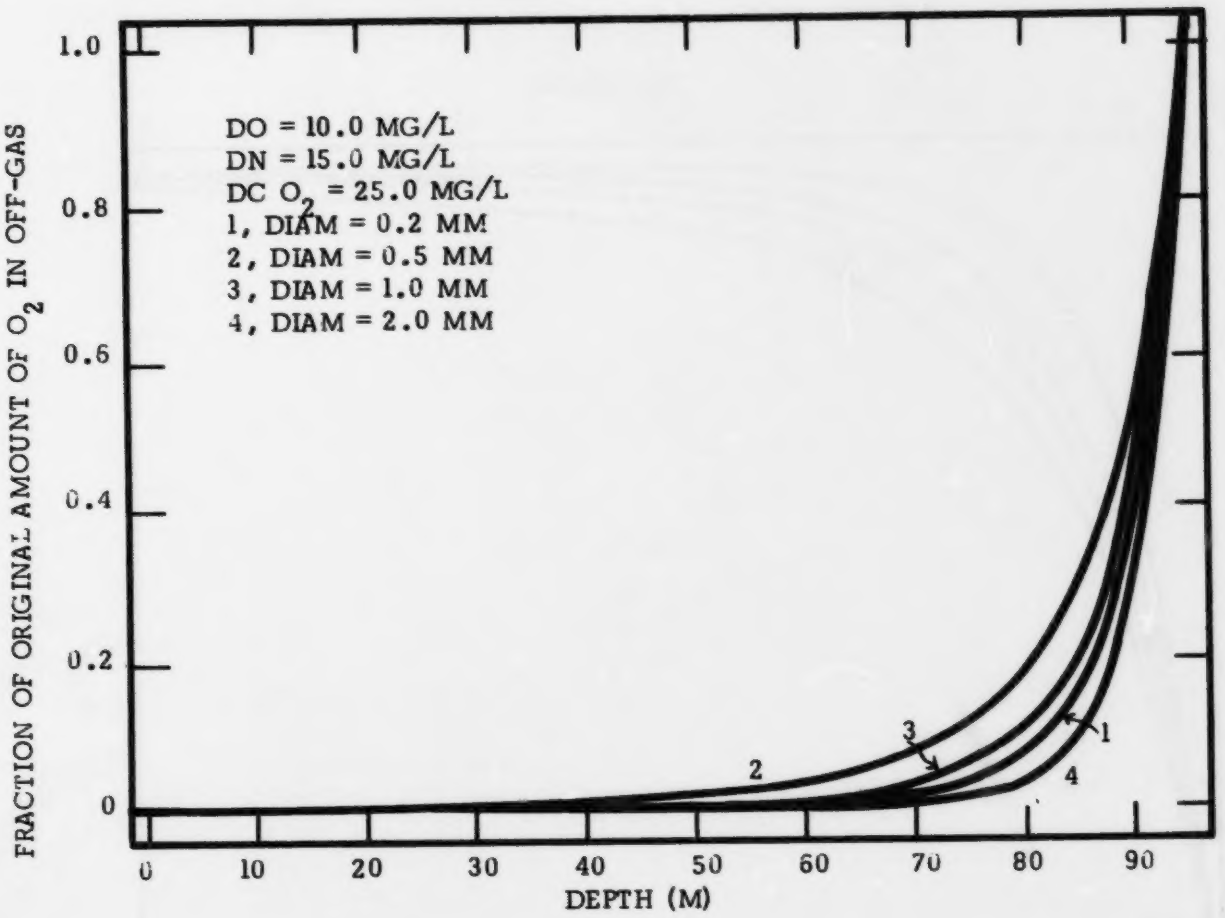

Fig. 62 FRACTION OF ORIGINAL AMOUNT OF O_2 IN OFF-GAS VS DEPTH - PURE OXYGEN

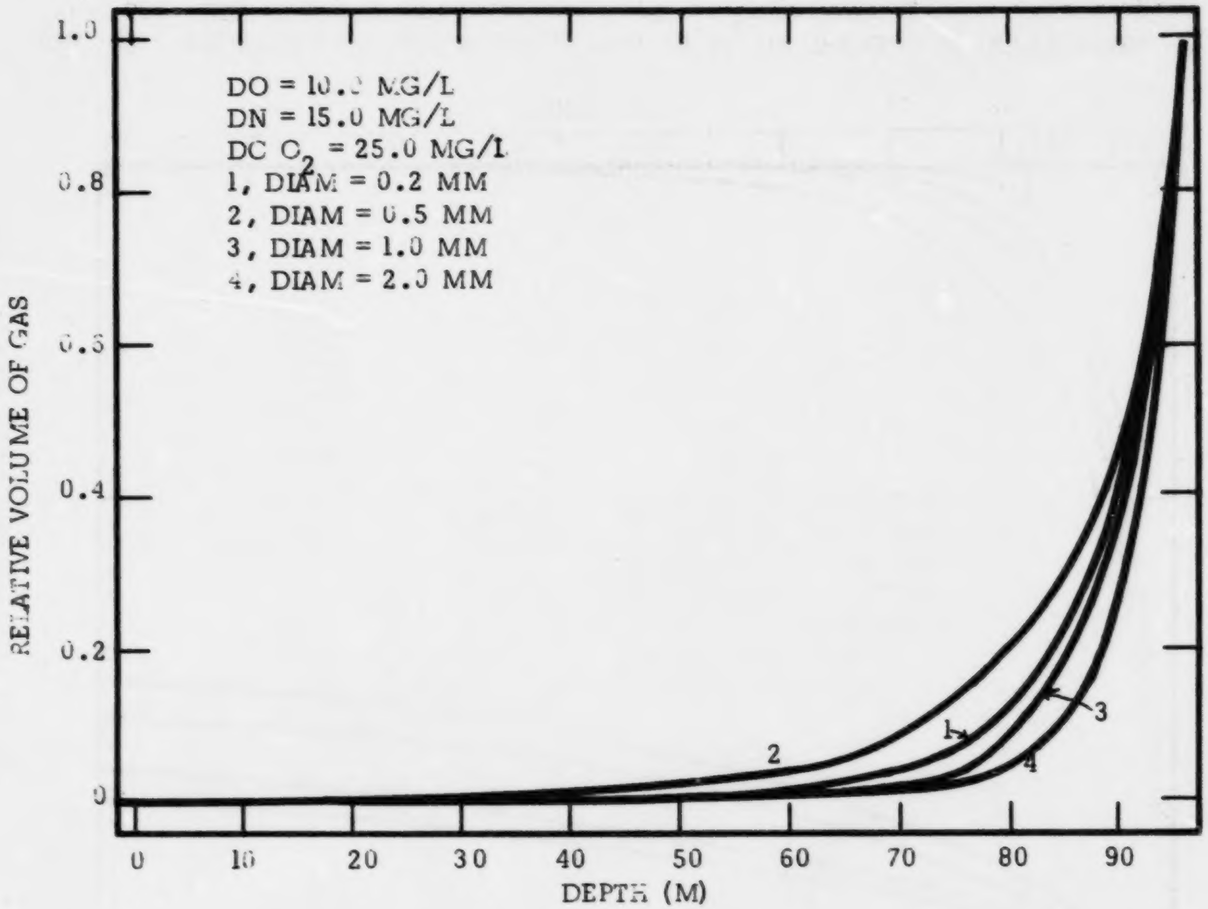

Fig. 63 RELATIVE VOLUME OF GAS VS DEPTH - PURE OXYGEN

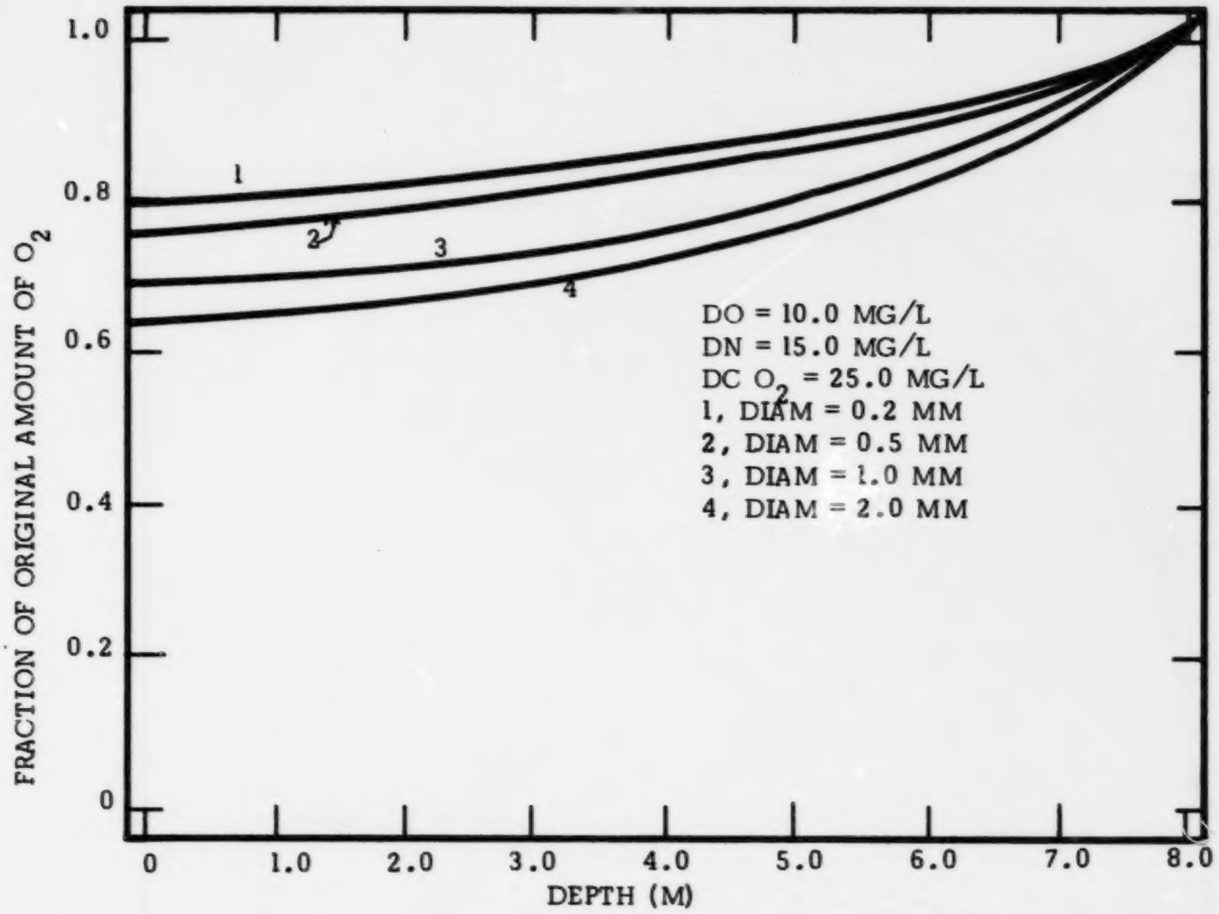

Fig. 64 FRACTION OF ORIGINAL AMOUNT OF O_2 IN OFF-GAS VS DEPTH - AIR

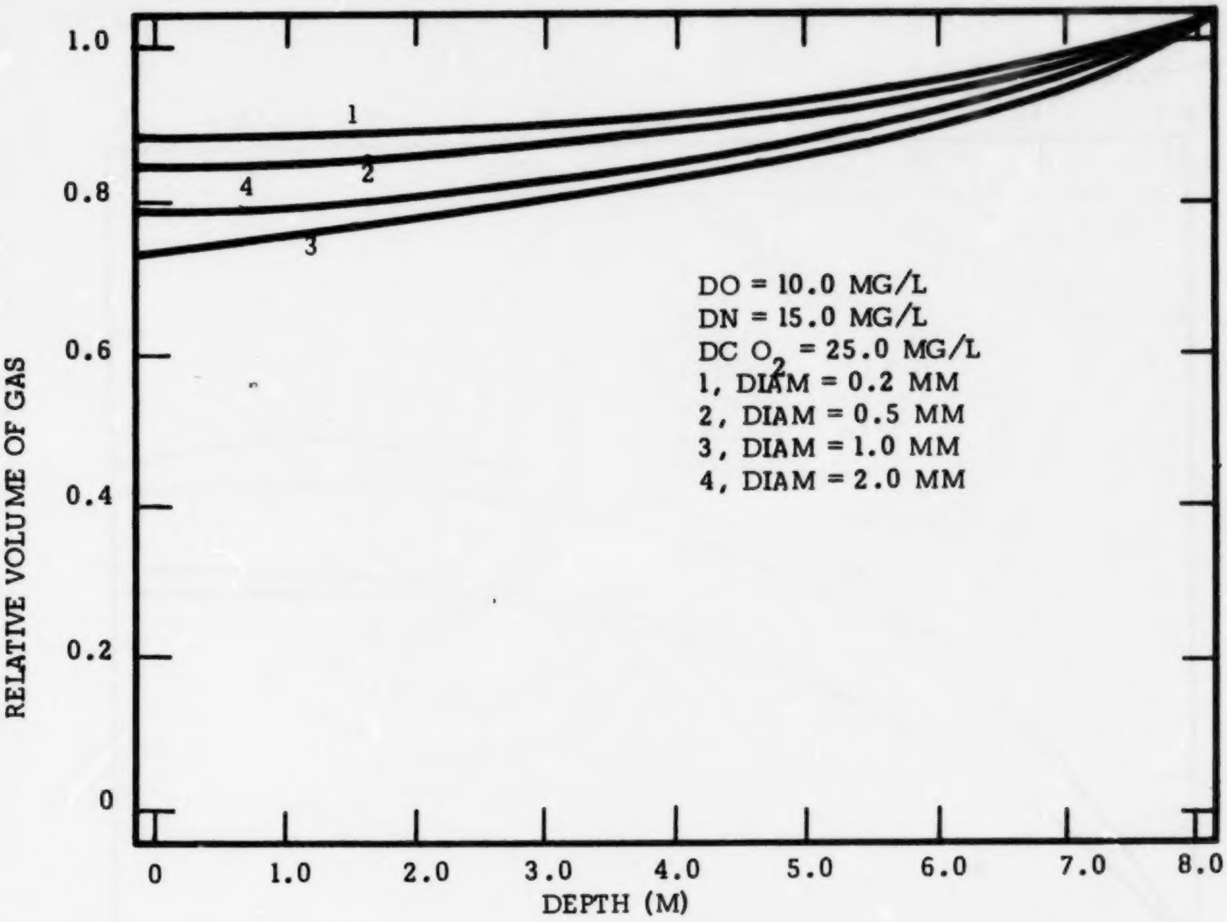

Fig. 65 RELATIVE VOLUME OF GAS VS DEPTH - AIR

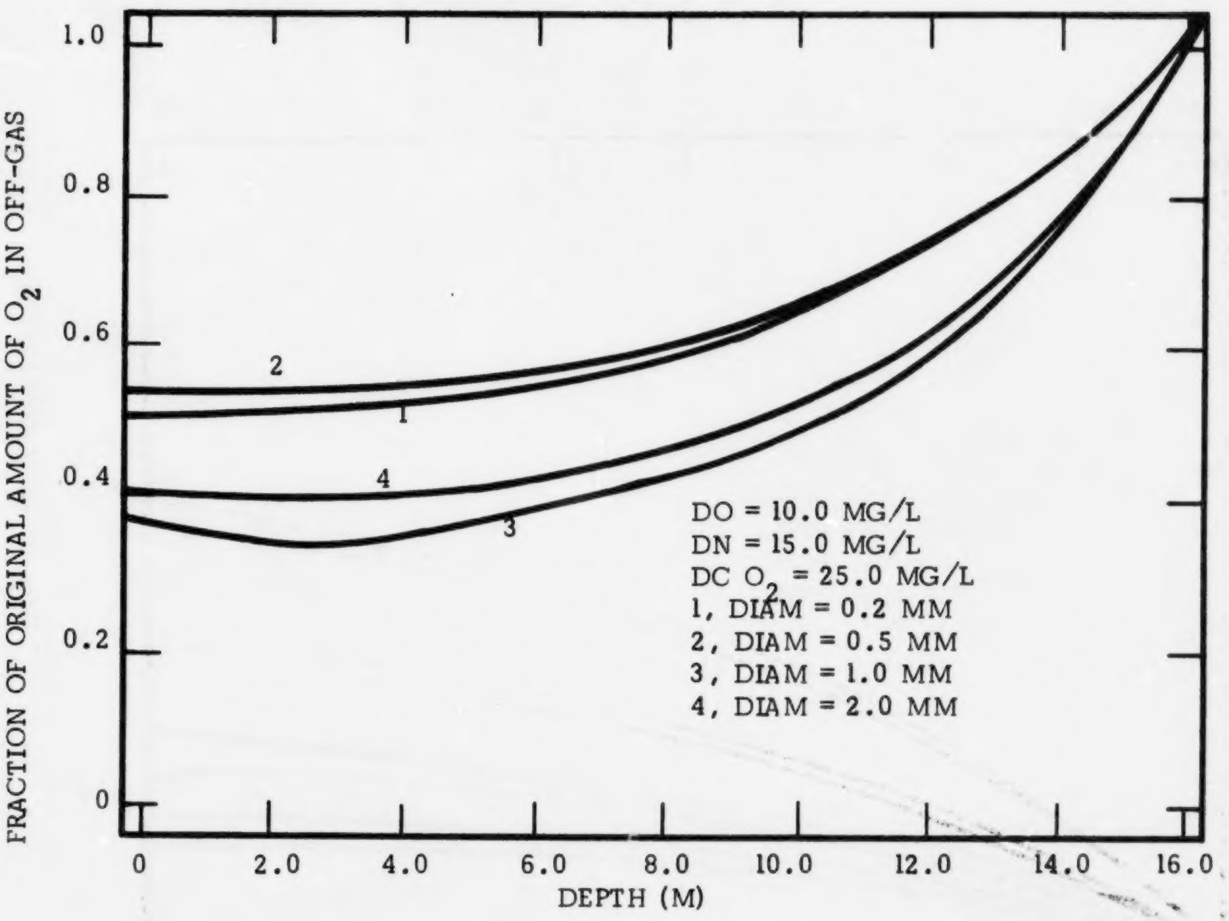

Fig. 66 FRACTION OF ORIGINAL AMOUNT OF O_2 IN OFF-GAS VS DEPTH - AIR

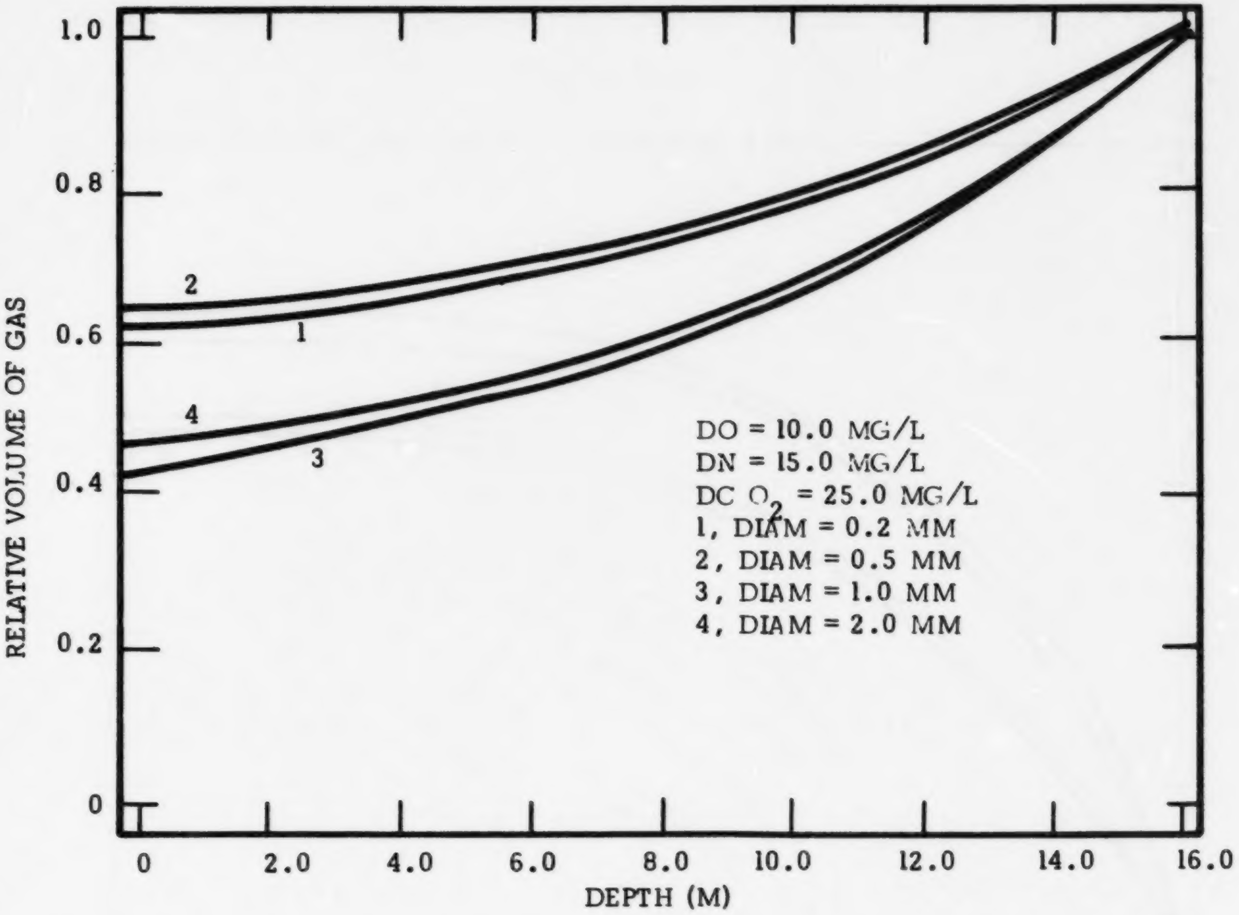

Fig. 67 RELATIVE VOLUME OF GAS VS DEPTH - AIR

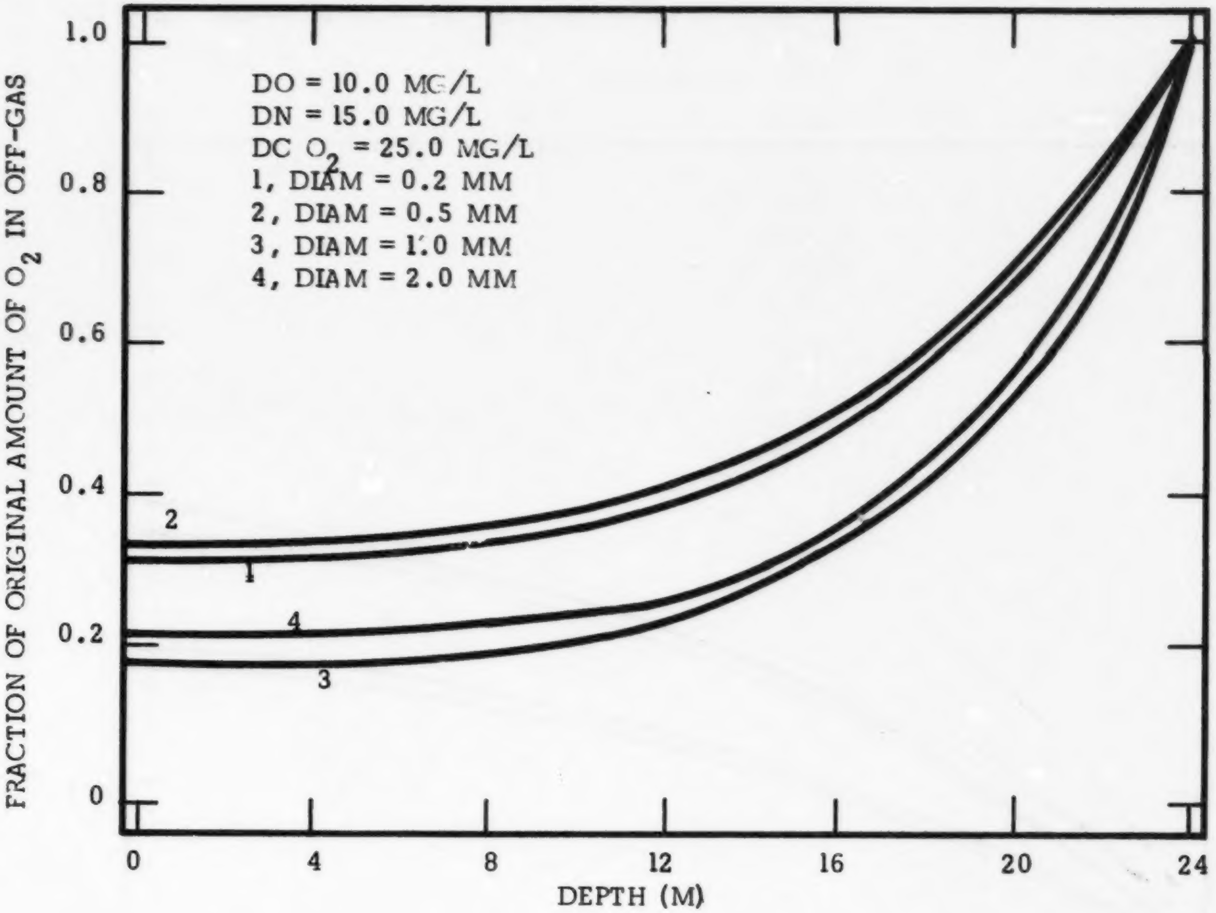

Fig. 68 FRACTION OF ORIGINAL AMOUNT OF O_2 IN OFF-GAS VS DEPTH - AIR

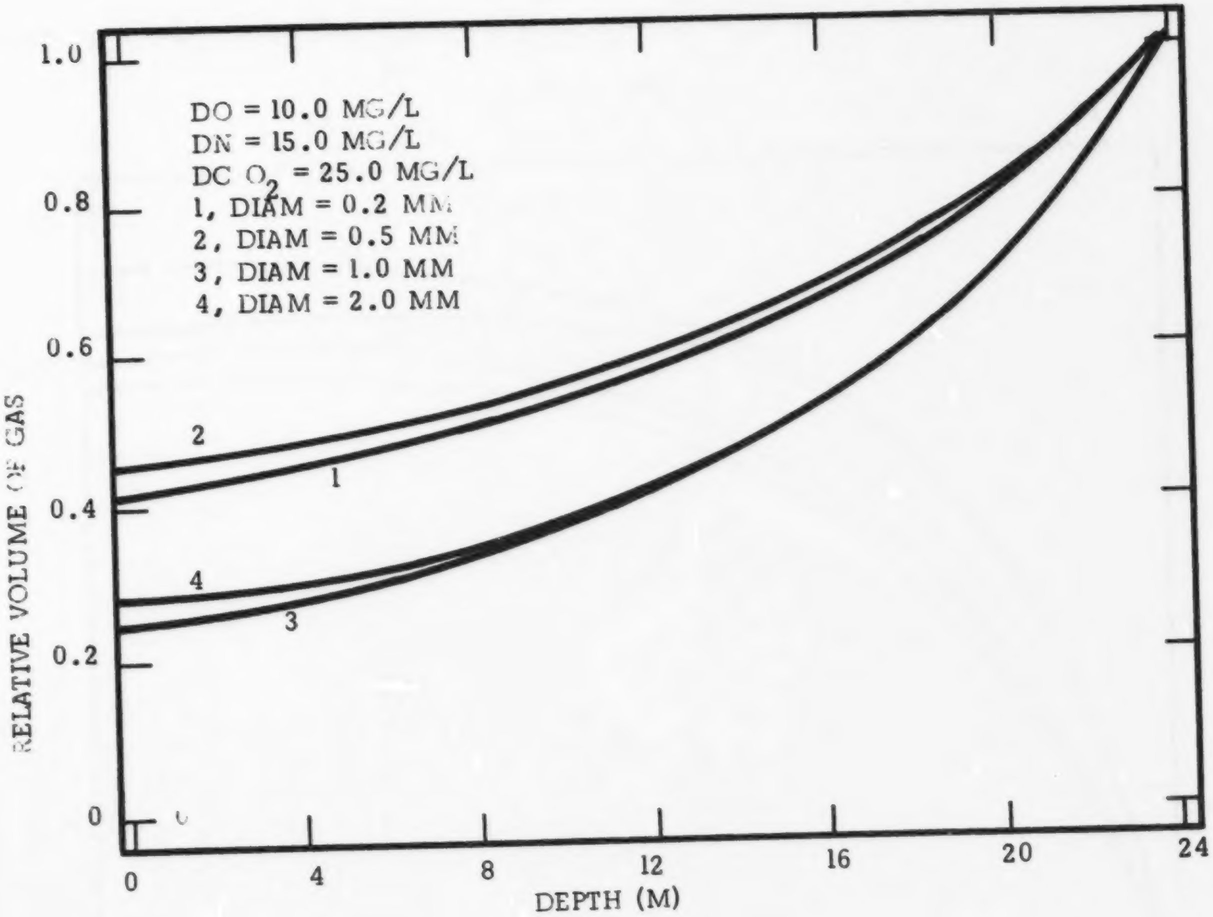

Fig. 69 RELATIVE VOLUME OF GAS VS DEPTH - AIR

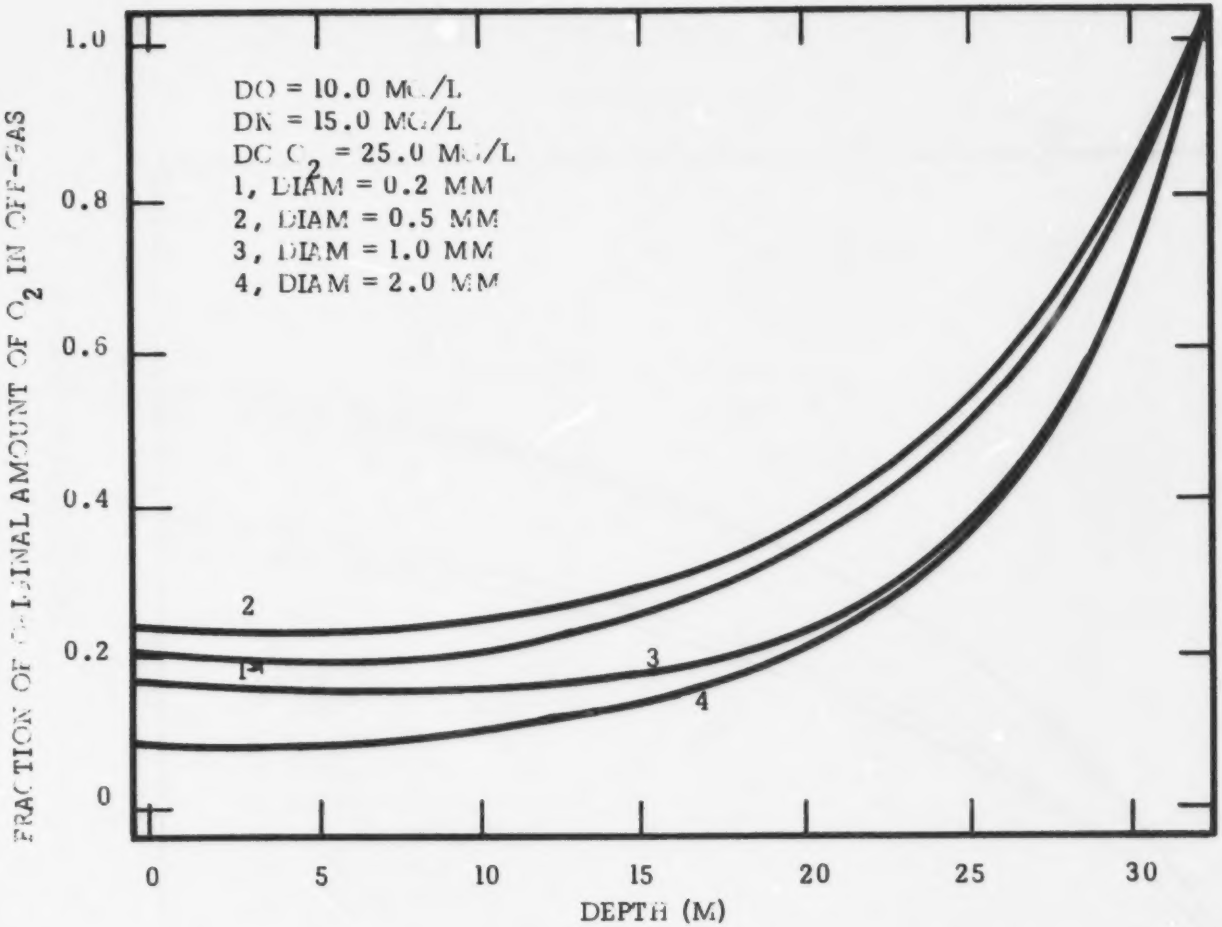

Fig. 70 FRACTION OF ORIGINAL AMOUNT OF O_2 IN OFF-GAS VS DEPTH - AIR

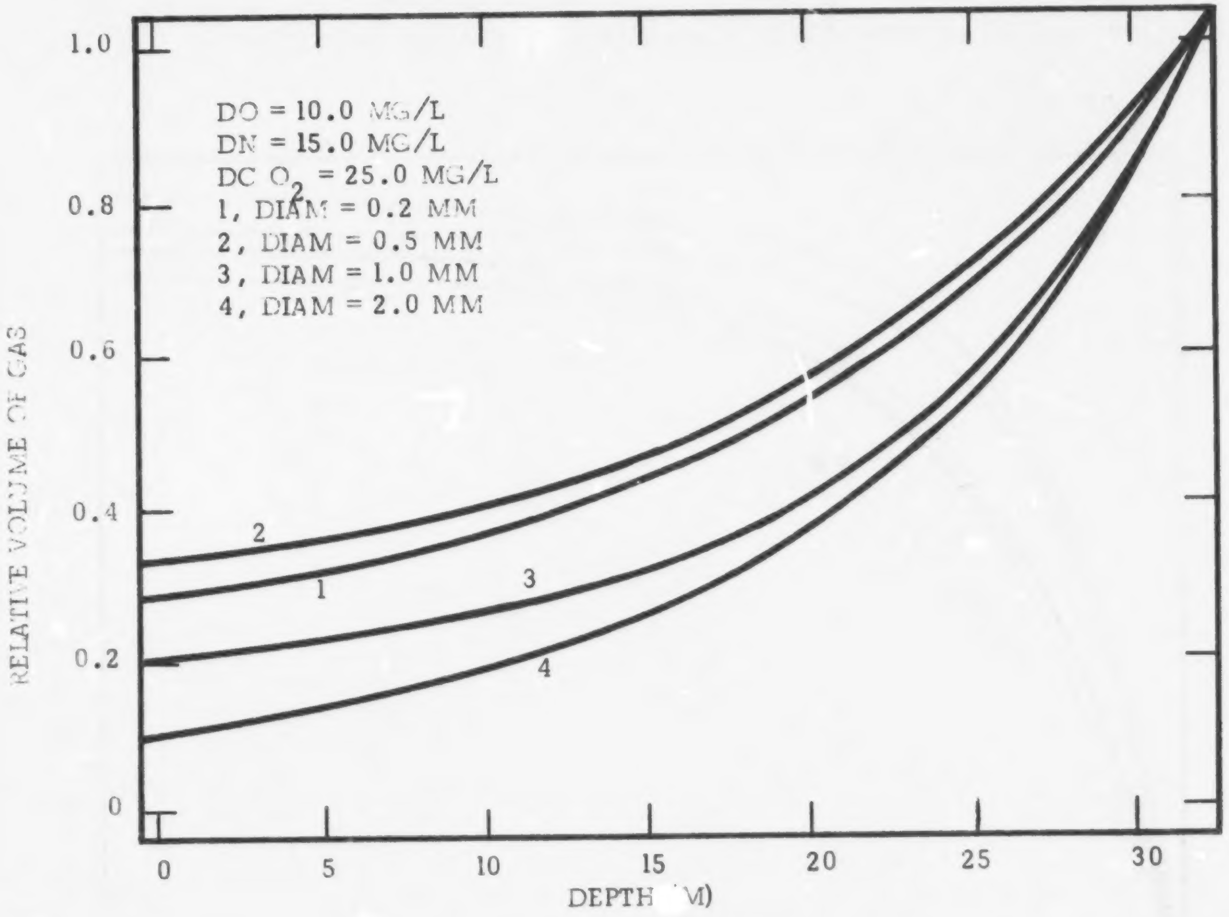

Fig. 71 RELATIVE VOLUME OF GAS VS DEPTH - AIR

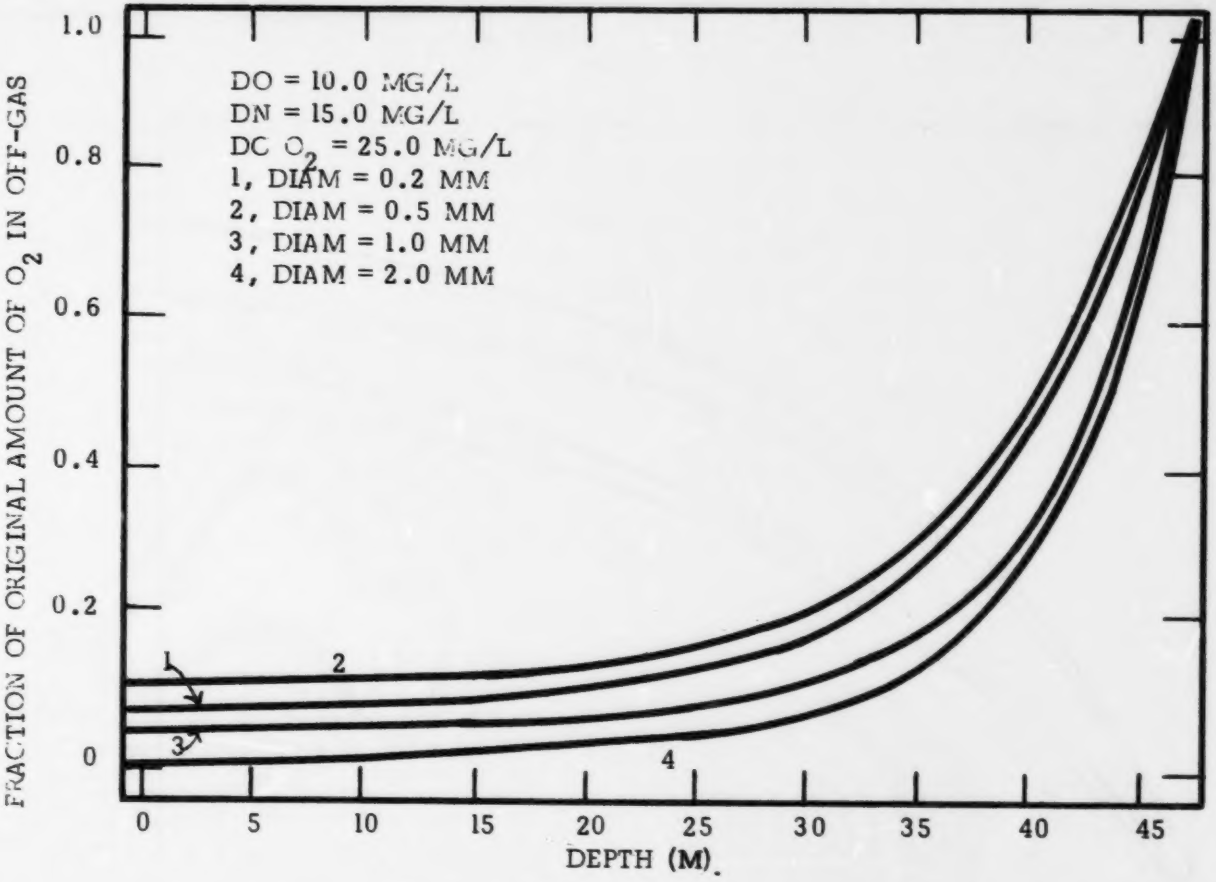

Fig. 72 FRACTION OF ORIGINAL AMOUNT OF O_2 IN OFF-GAS VS DEPTH - AIR

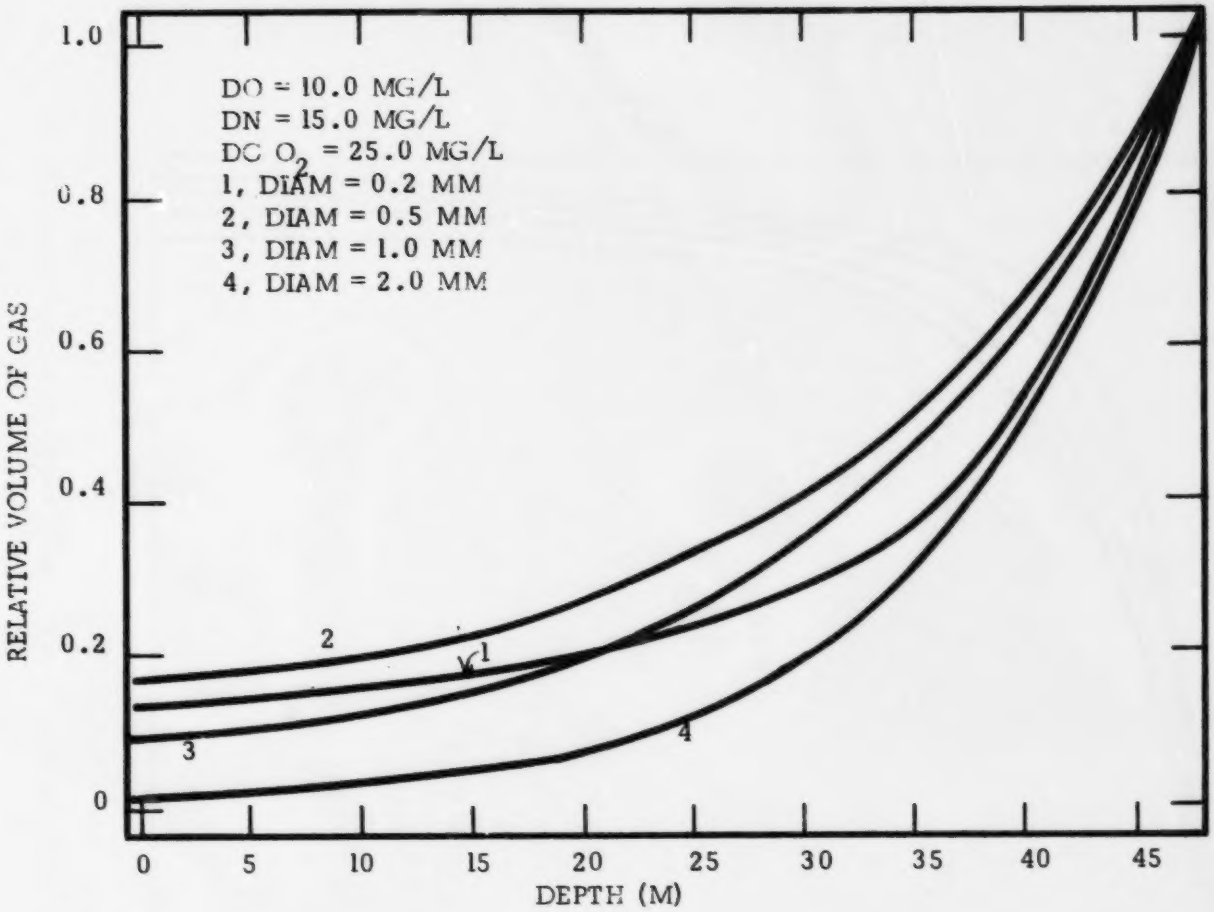

Fig. 73 RELATIVE VOLUME OF GAS VS DEPTH - AIR

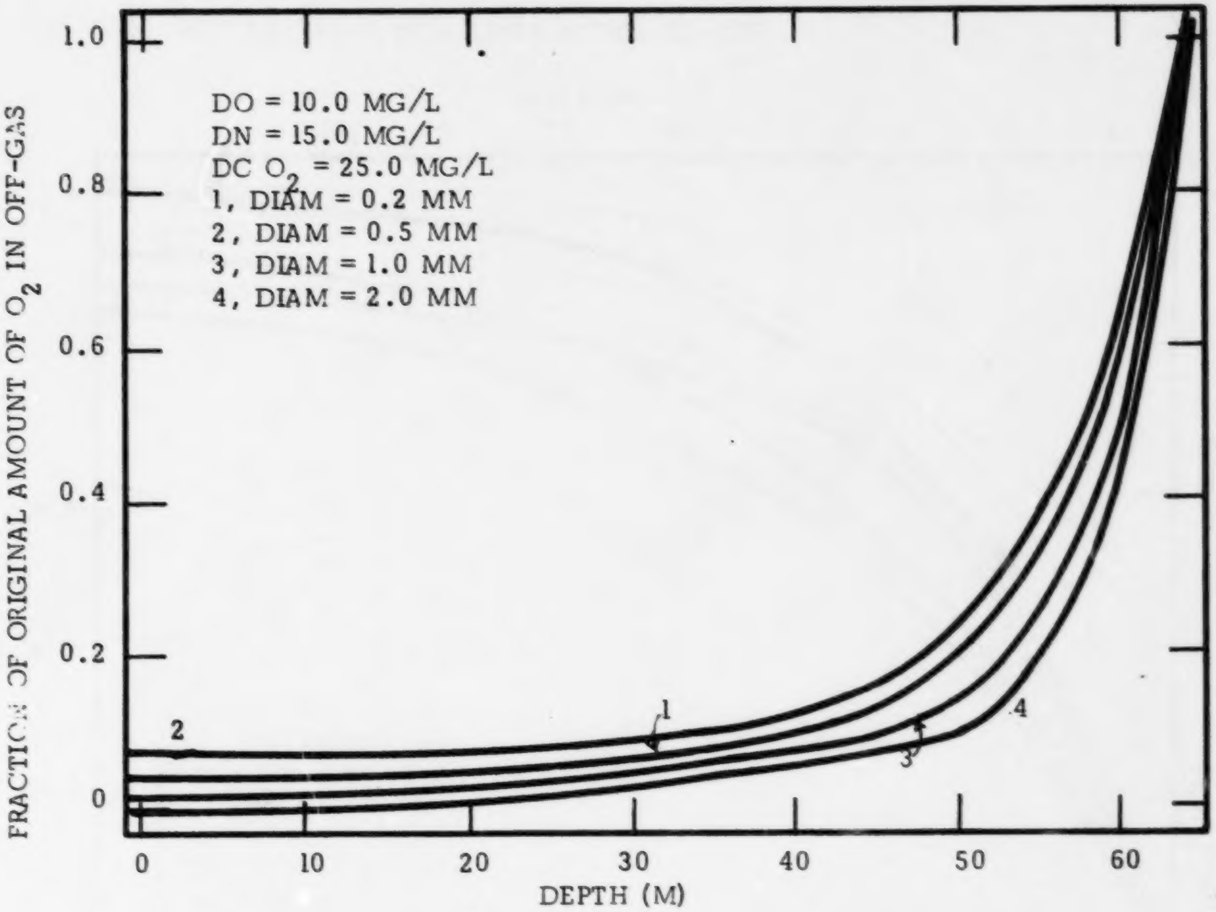

Fig. 74 FRACTION OF ORIGINAL AMOUNT OF O_2 IN OFF-GAS VS DEPTH - AIR

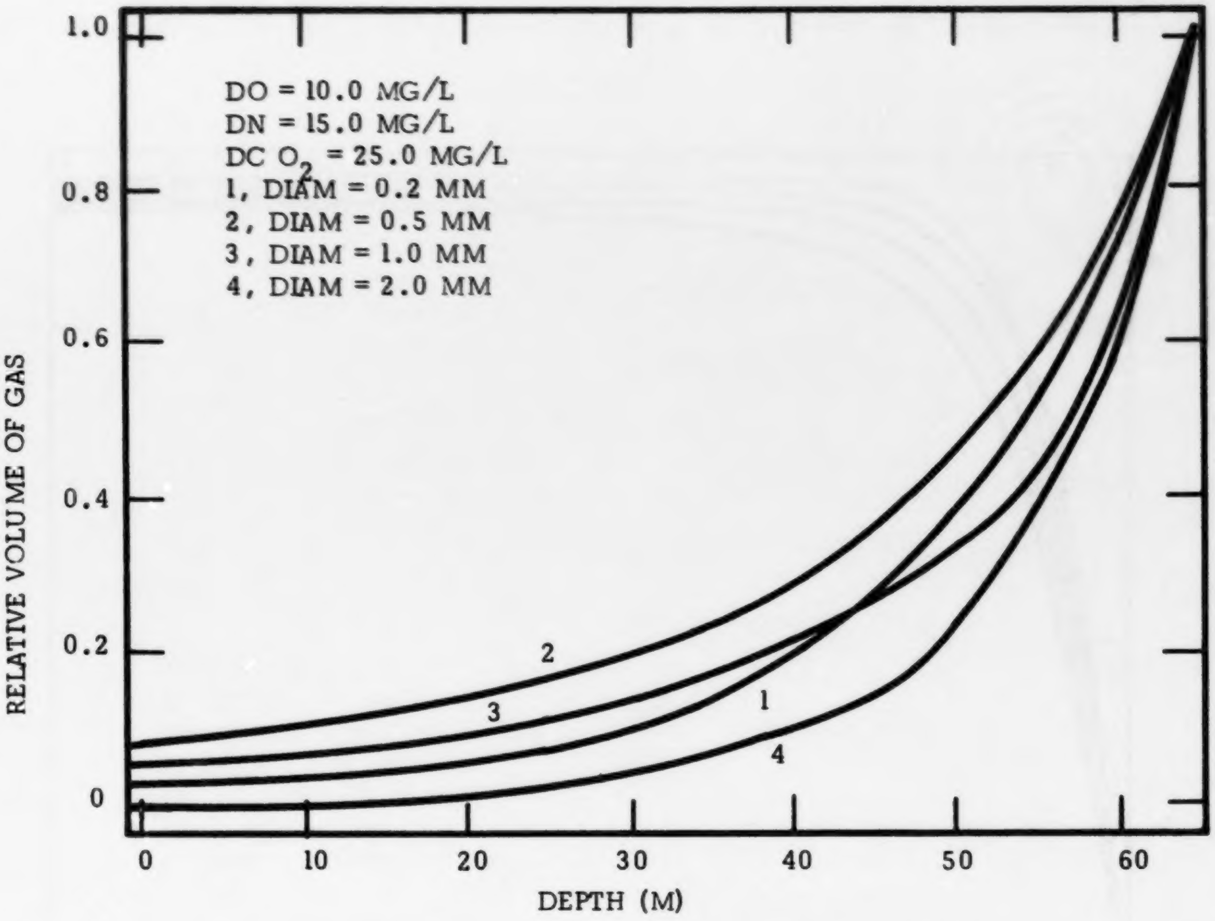

Fig. 75 RELATIVE VOLUME OF GAS VS DEPTH - AIR

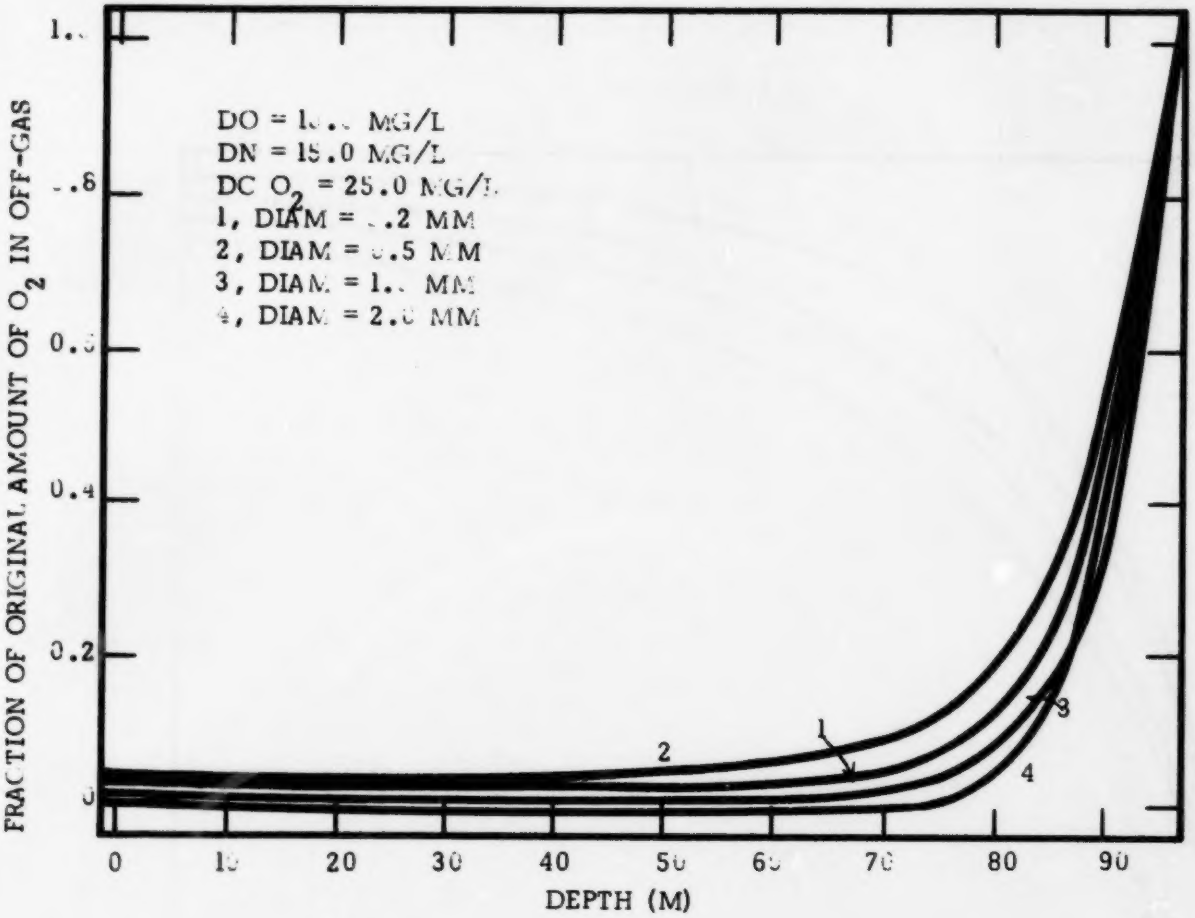

Fig. 76 FRACTION OF ORIGINAL AMOUNT OF O_2 IN OFF-GAS VS DEPTH - AIR

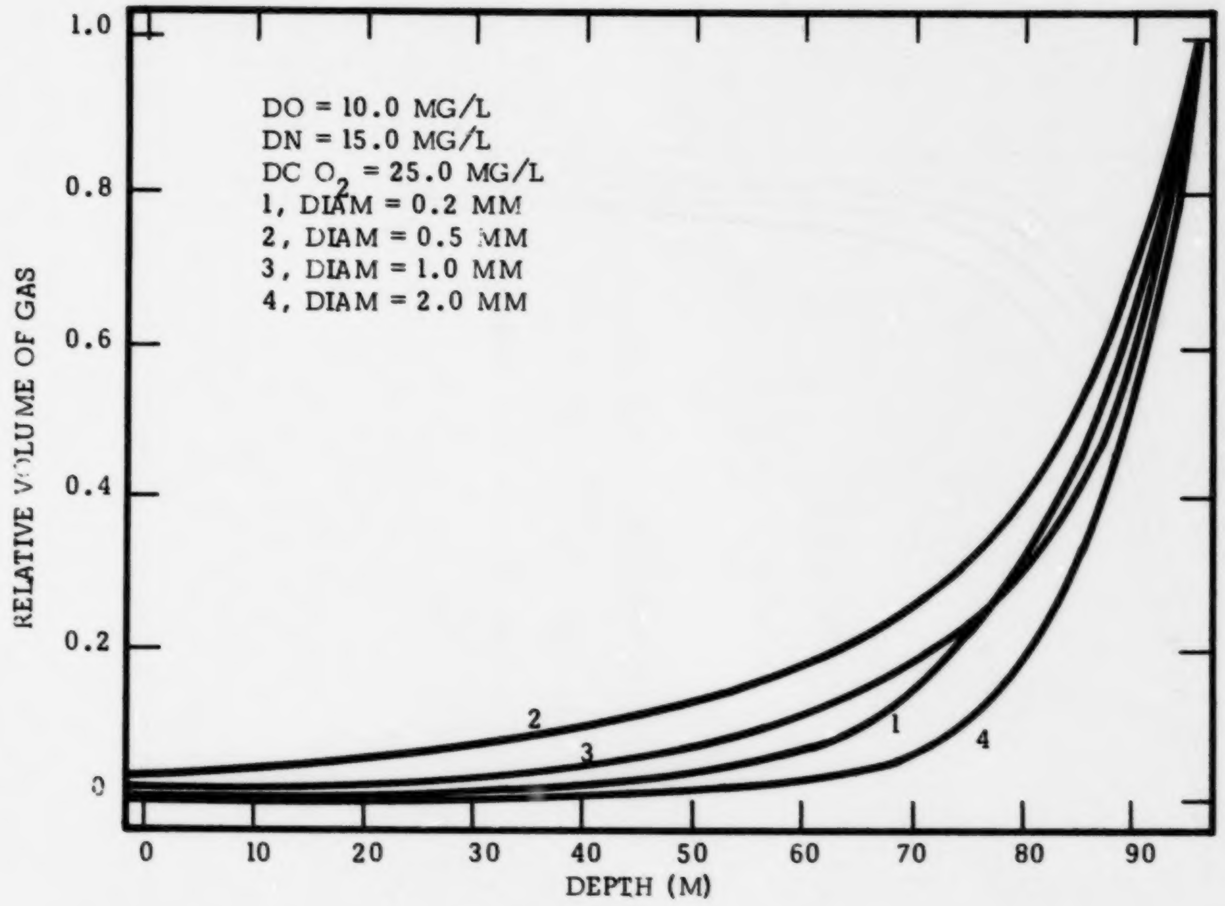

Fig. 77 RELATIVE VOLUME OF GAS VS DEPTH - AIR

APPENDIX B

DESIGN FIGURES - O_2 and Air

1) Diameter vs Rise Height
2) O_2 Composition vs Rise Height

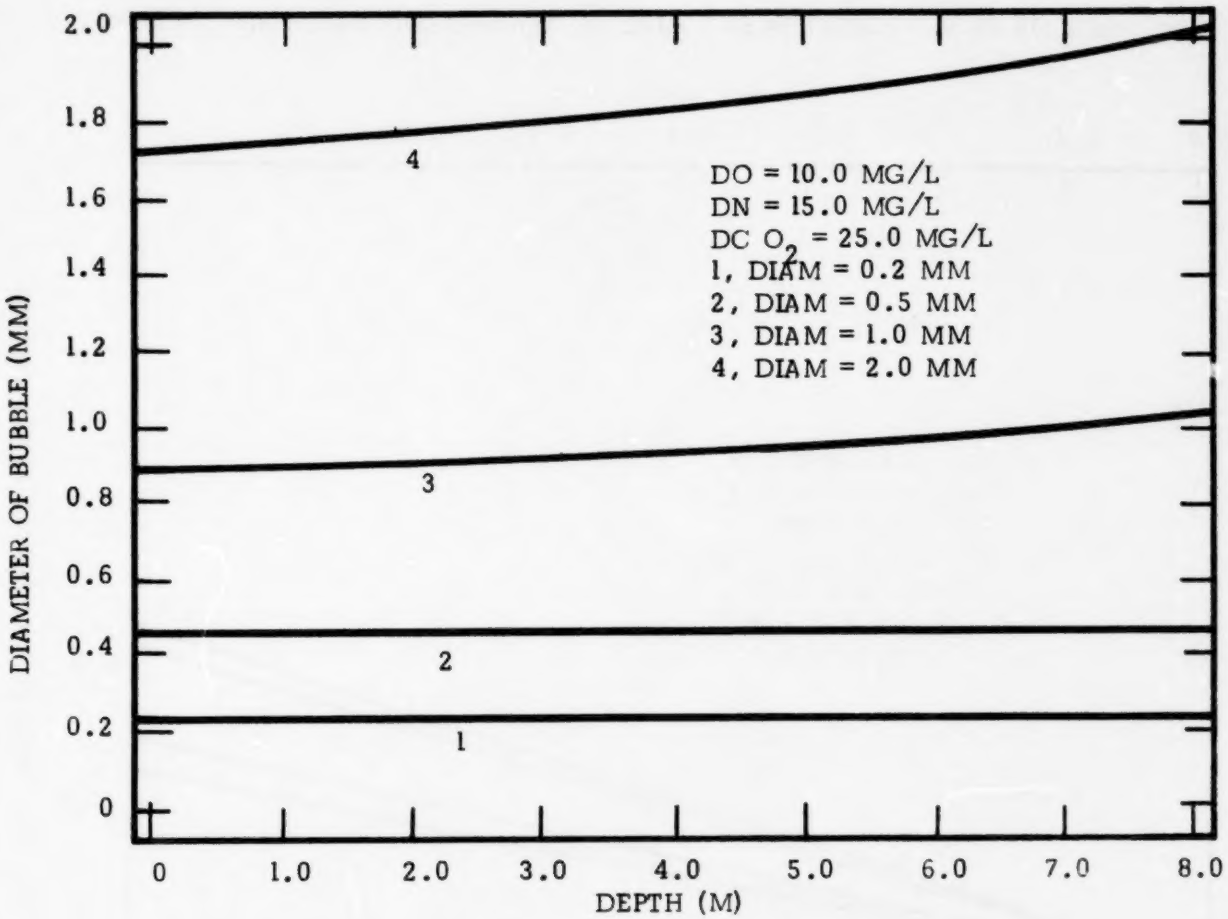

Fig. 78 DIAMETER OF BUBBLE AS A FUNCTION OF DEPTH – PURE OXYGEN

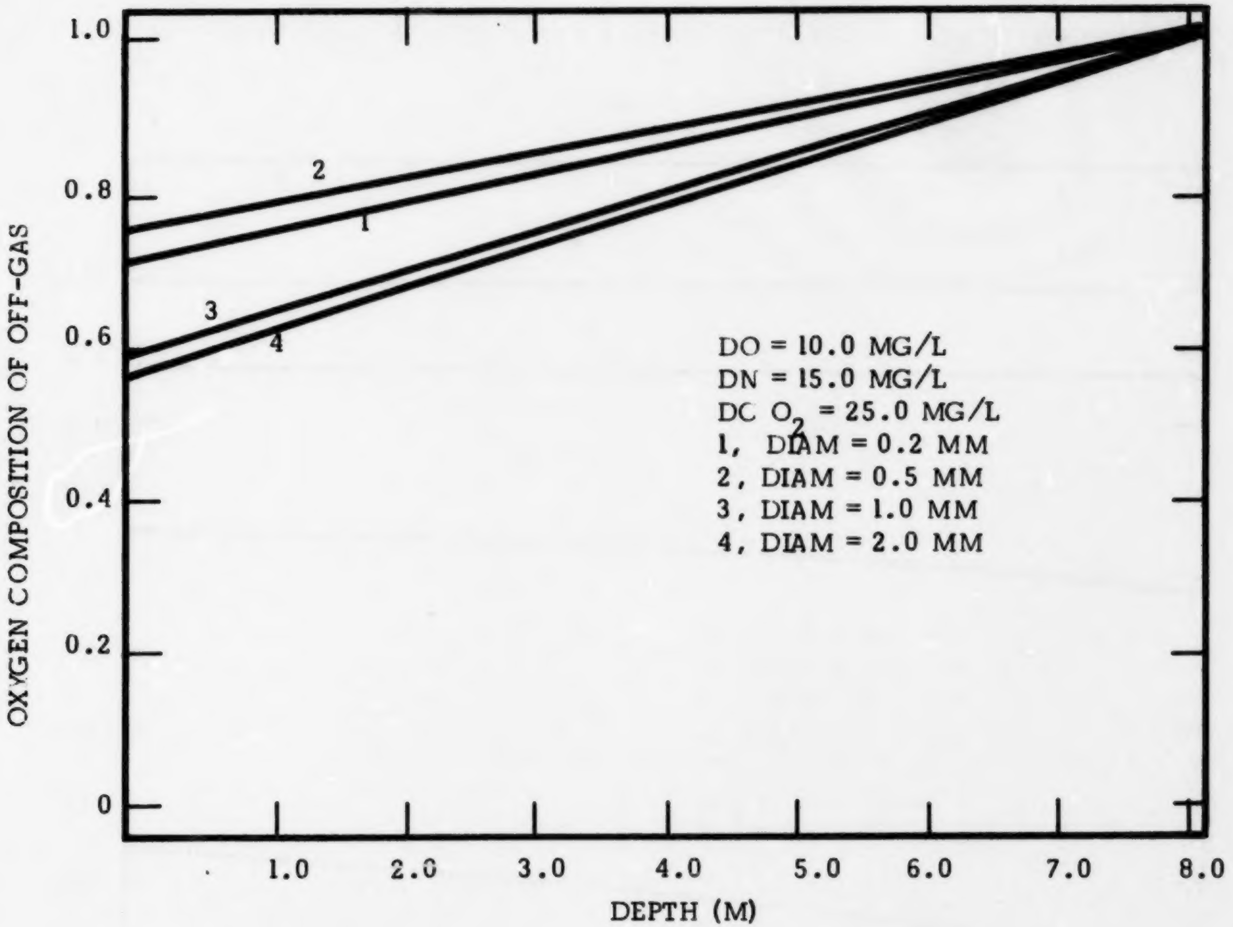

Fig. 79 OXYGEN COMPOSITION OF OFF- GAS VS DEPTH - PURE OXYGEN

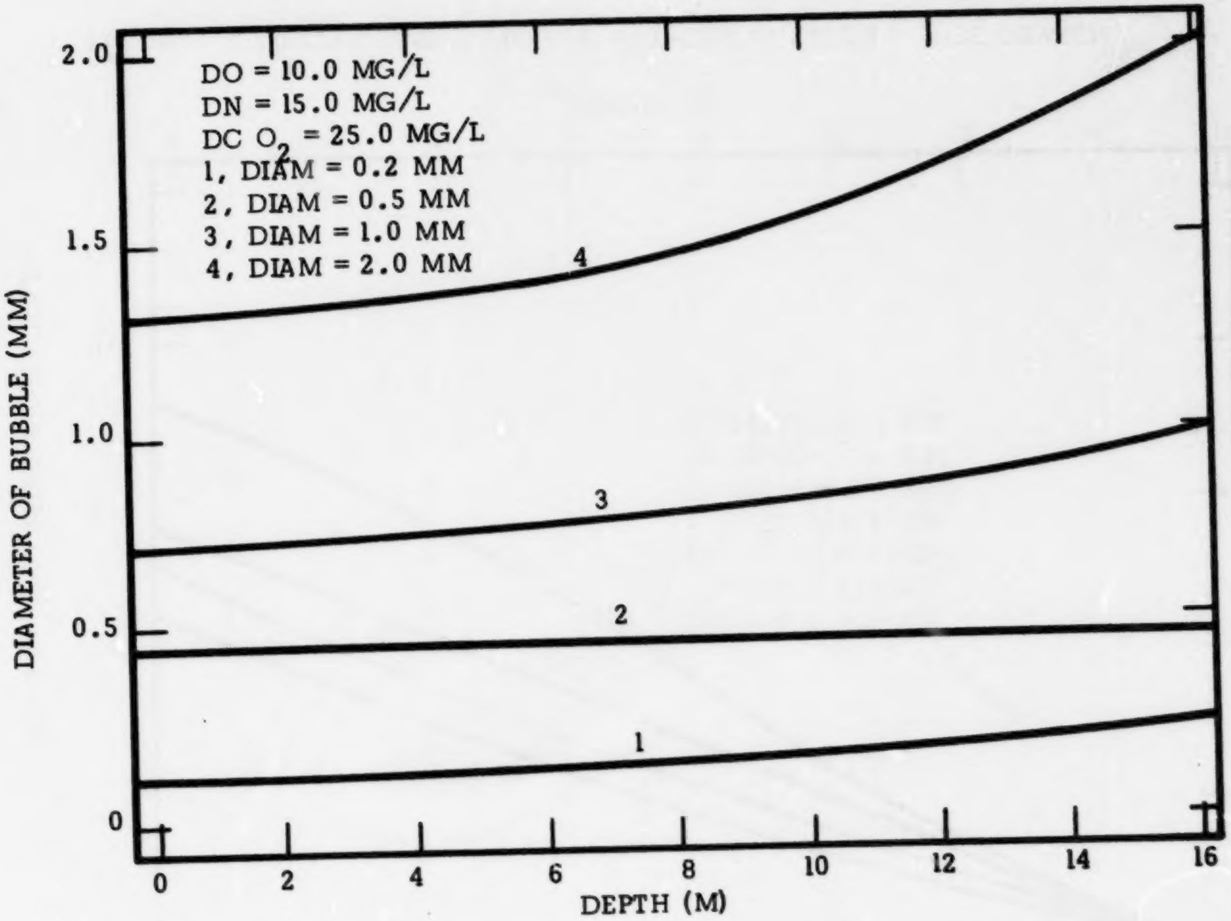

Fig. 80 DIAMETER OF BUBBLE AS A FUNCTION OF DEPTH - PURE OXYGEN

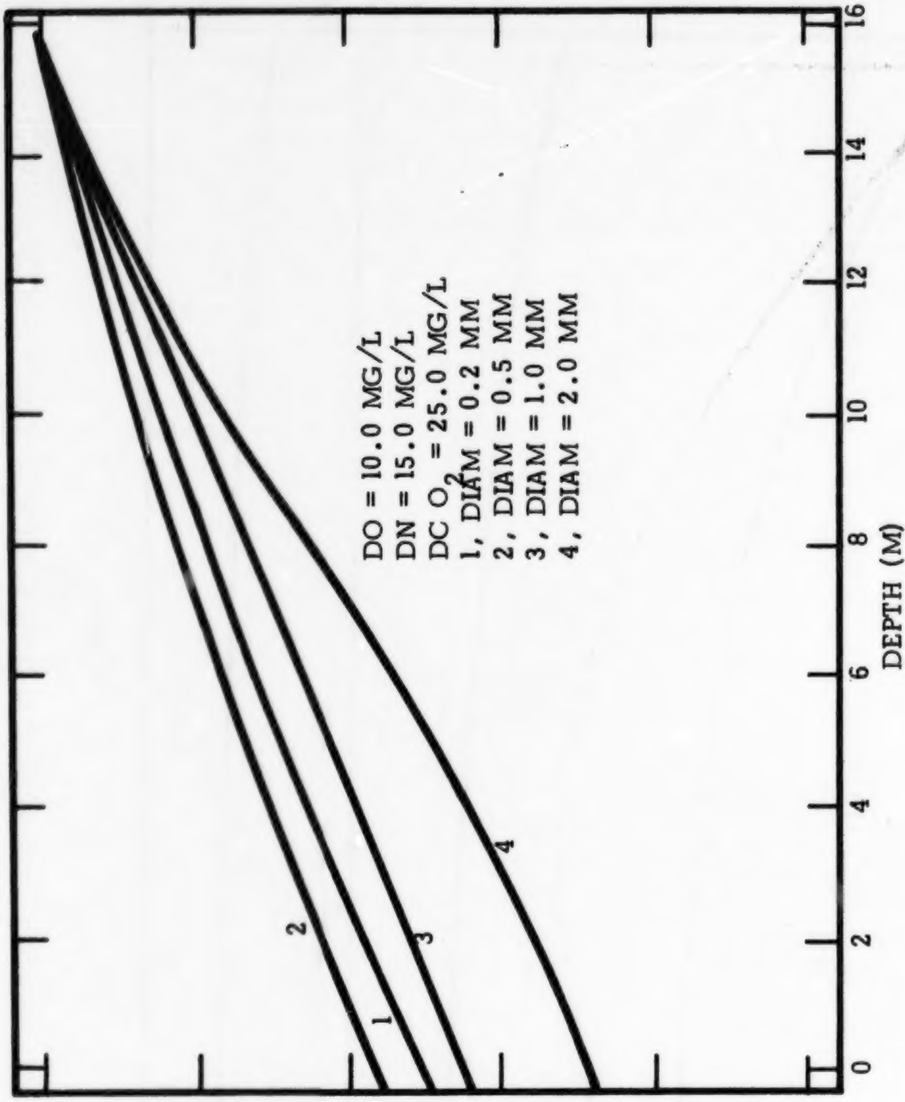

Fig. 81 OXYGEN COMPOSITION OF OFF-GAS VS DEPTH - PURE OXYGEN

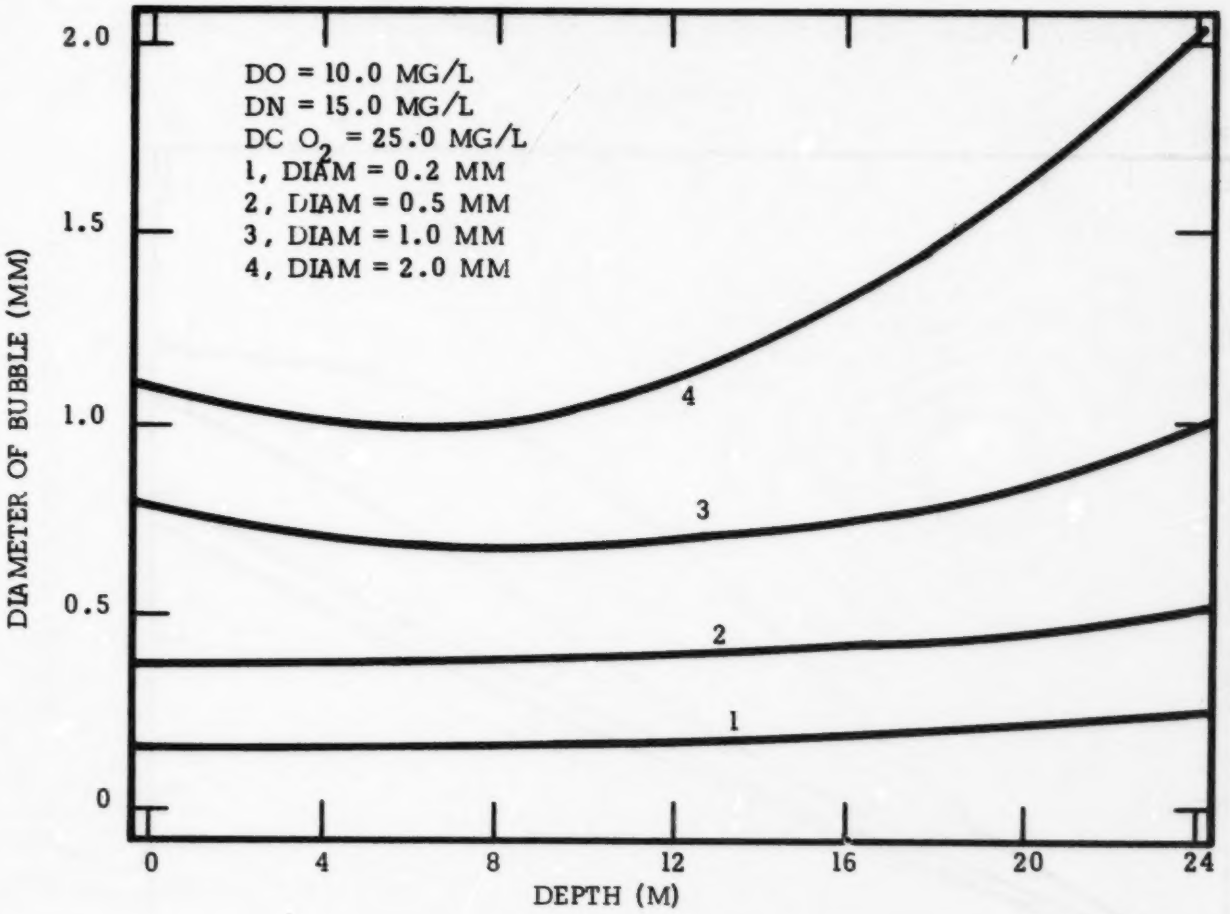

Fig. 82 DIAMETER OF BUBBLE AS A FUNCTION OF DEPTH - PURE OXYGEN

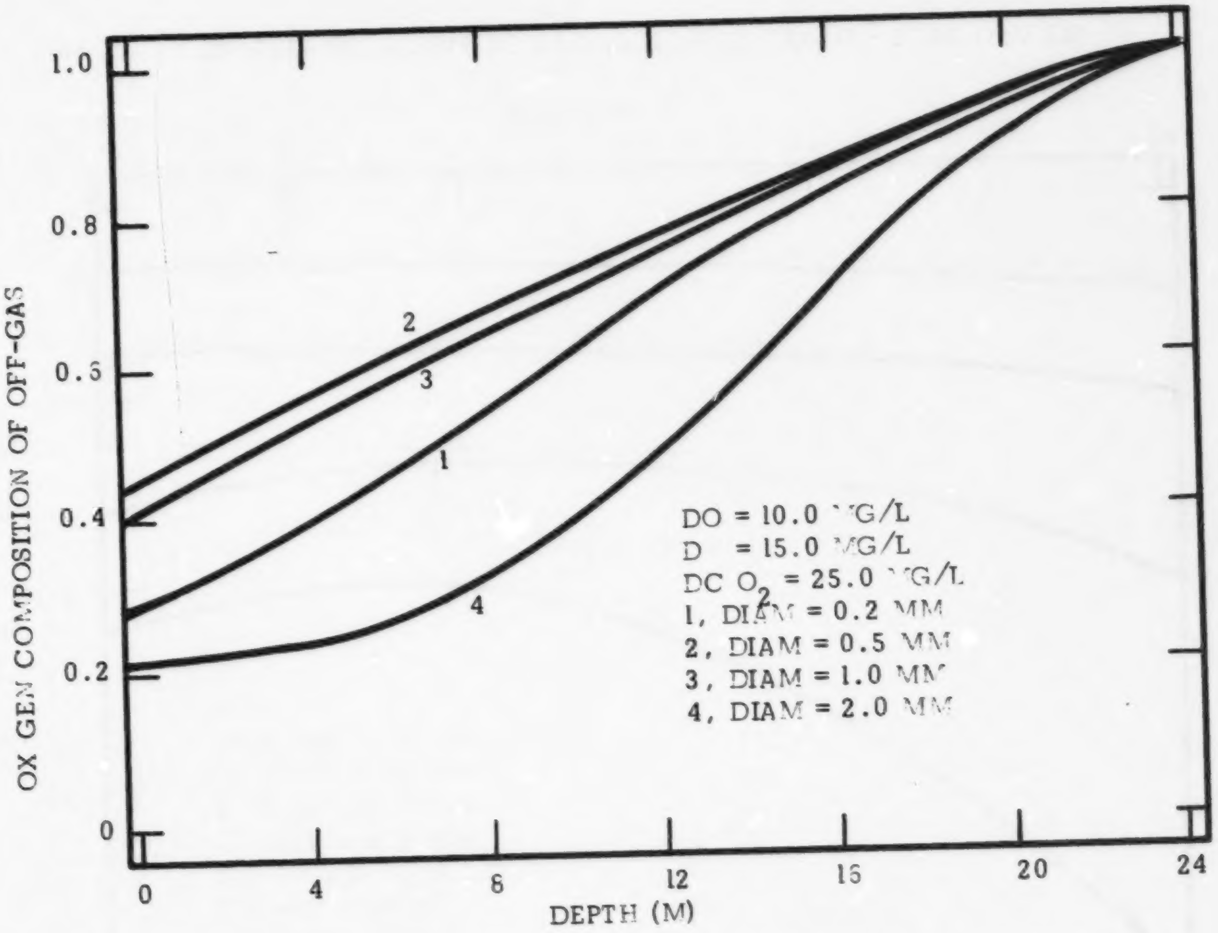

Fig. 83 OXYGEN COMPOSITION OF OFF-GAS VS DEPTH - PURE OXYGEN

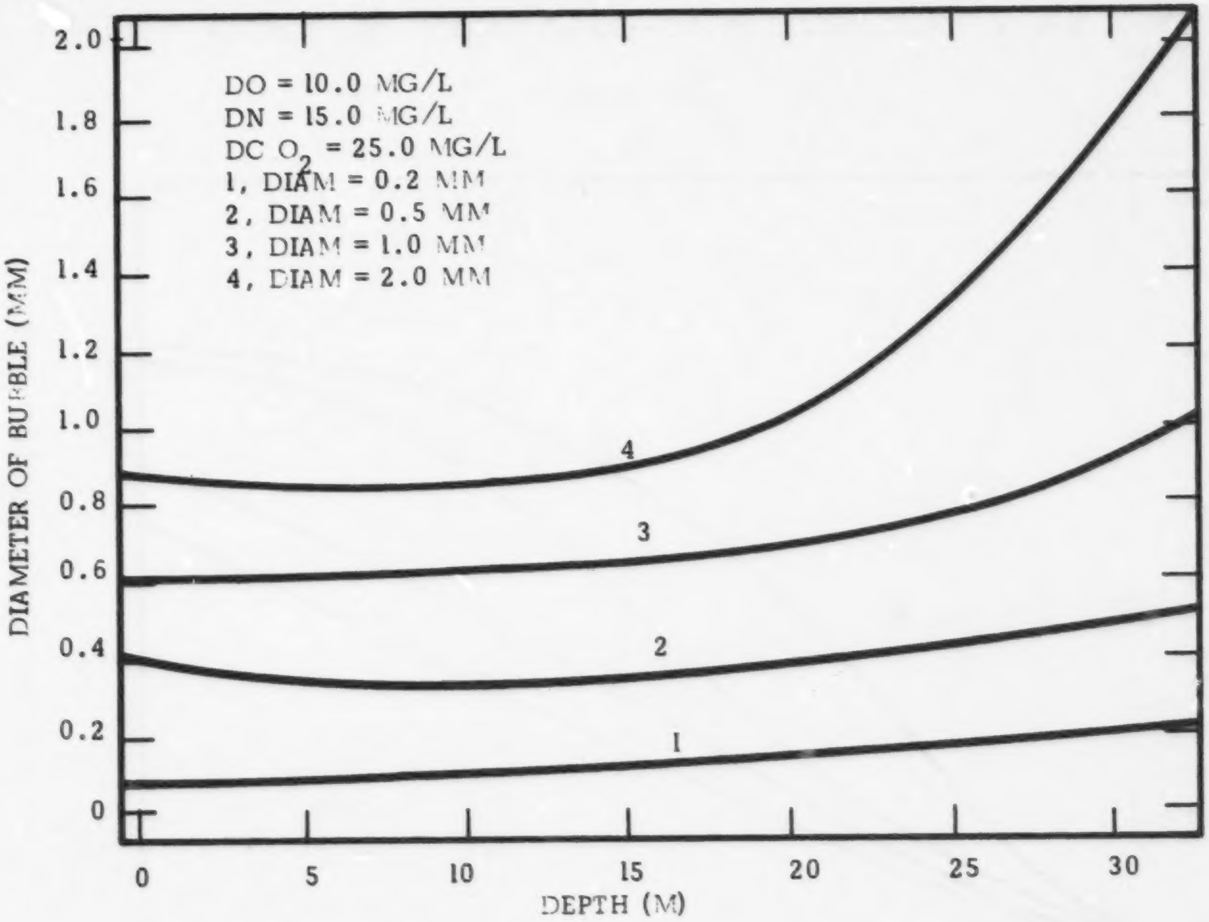

Fig. 84 DIAMETER OF BUBBLE AS A FUNCTION OF DEPTH - PURE OXYGEN

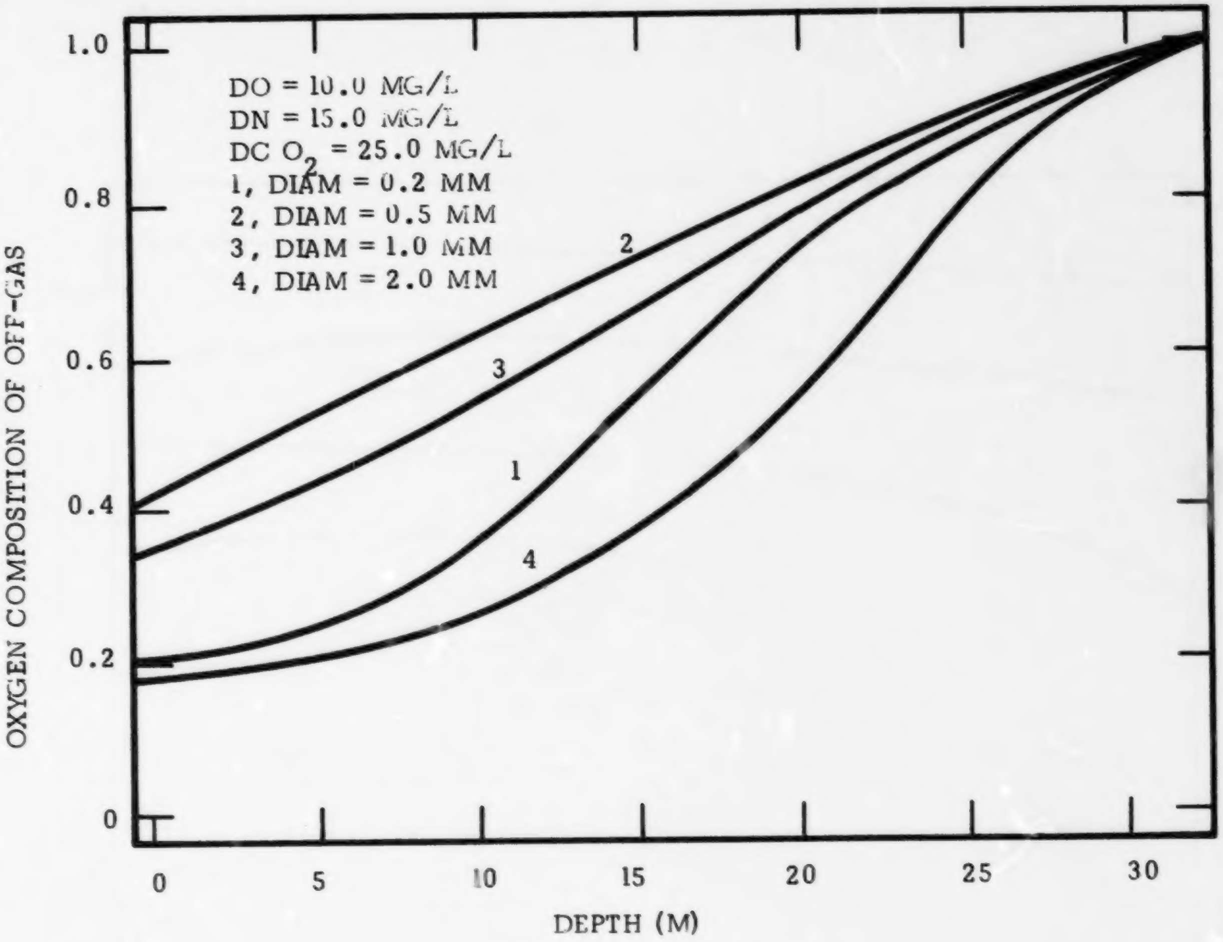

Fig. 85 OXYGEN COMPOSITION OF OFF-GAS VS DEPTH - PURE OXYGEN

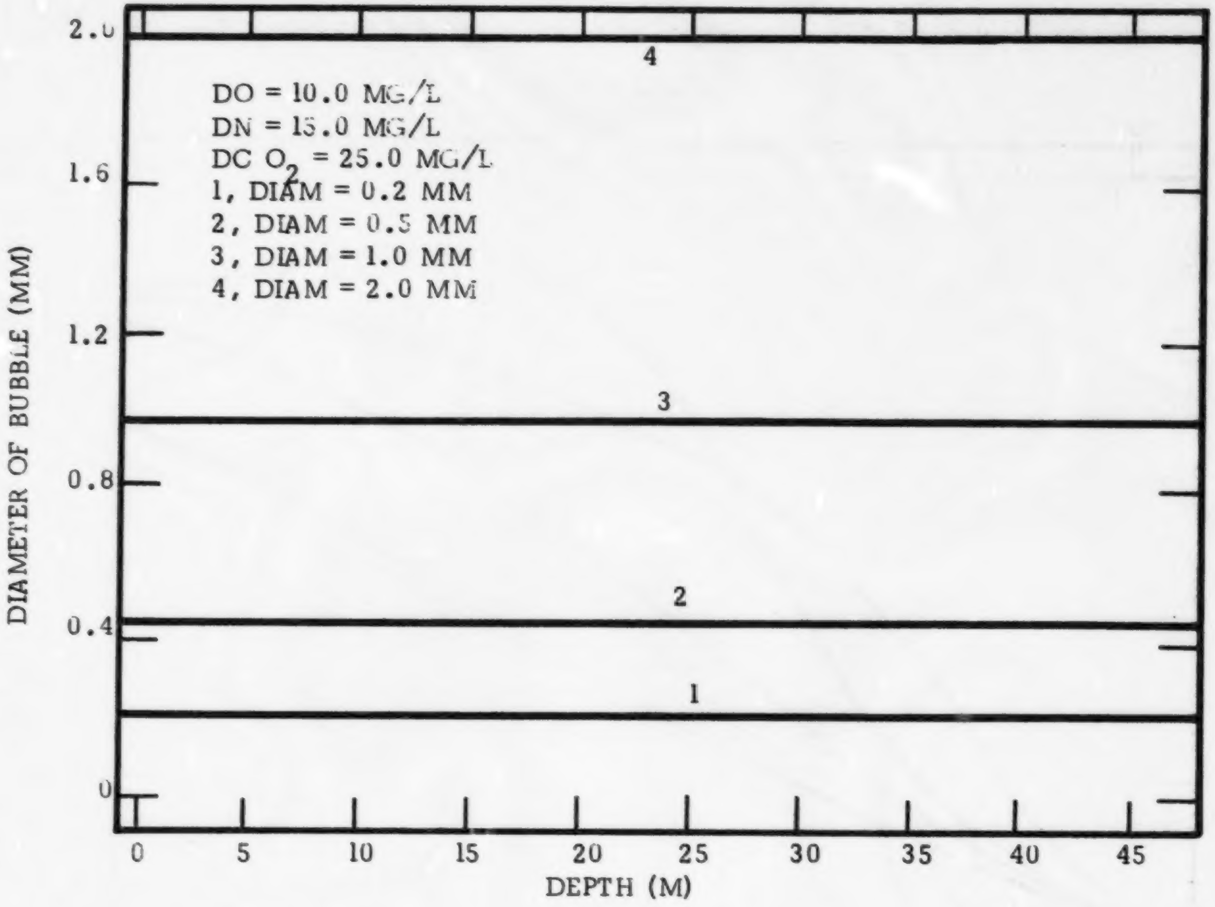

Fig. 86 DIAMETER OF BUBBLE AS A FUNCTION OF DEPTH - PURE OXYGEN

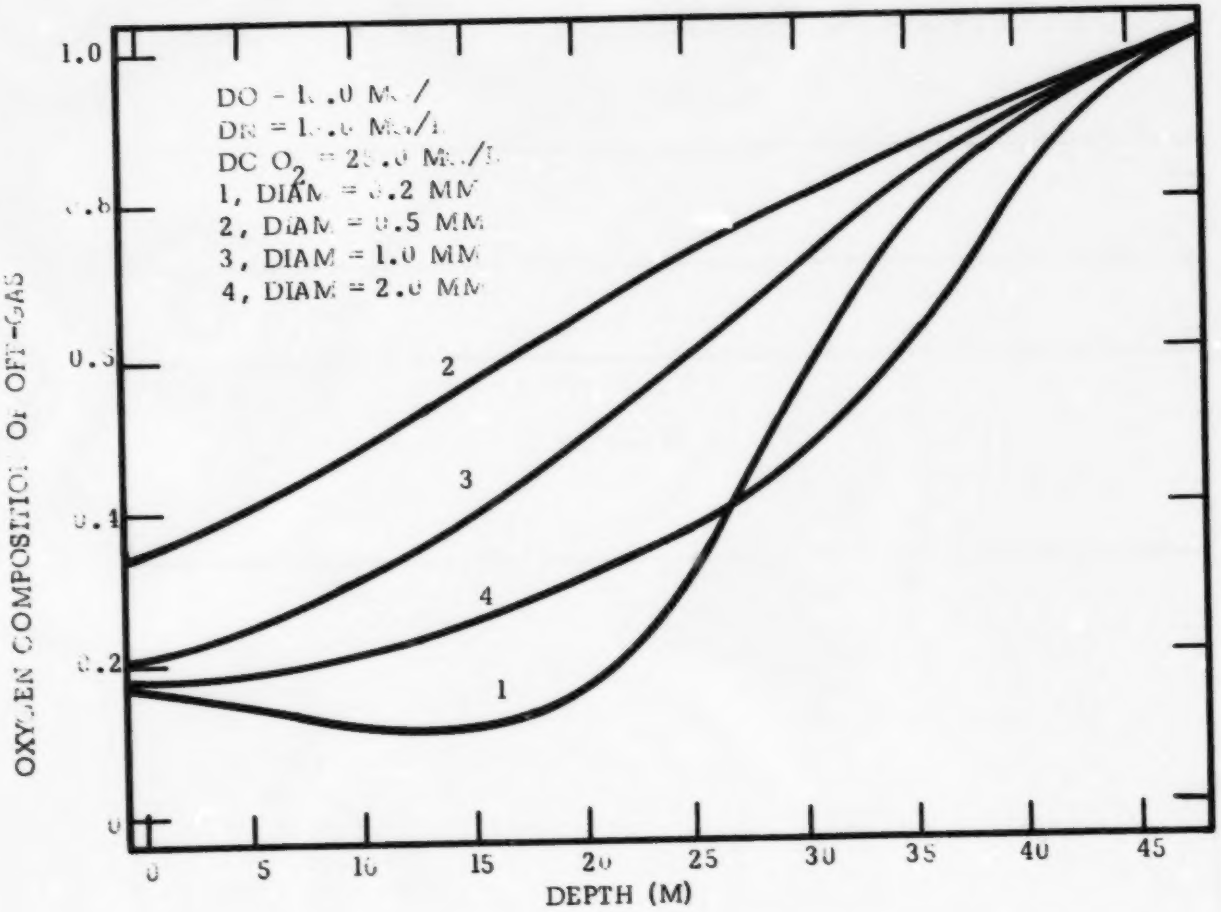

Fig. 87 OXYGEN COMPOSITION OF OFF-GAS VS DEPTH - PURE OXYGEN

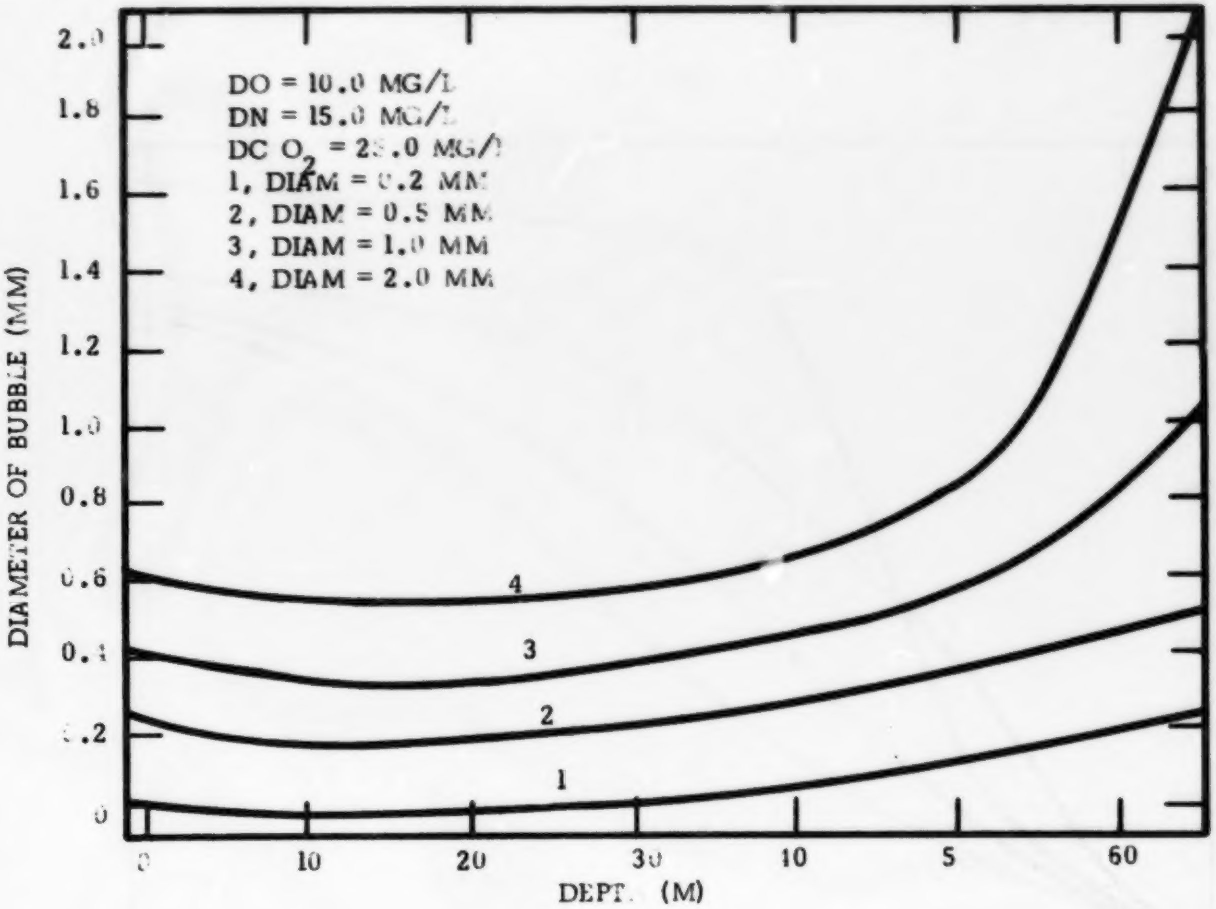

Fig. 88 DIAMETER OF BUBBLE AS A FUNCTION OF DEPTH - PURE OXYGEN

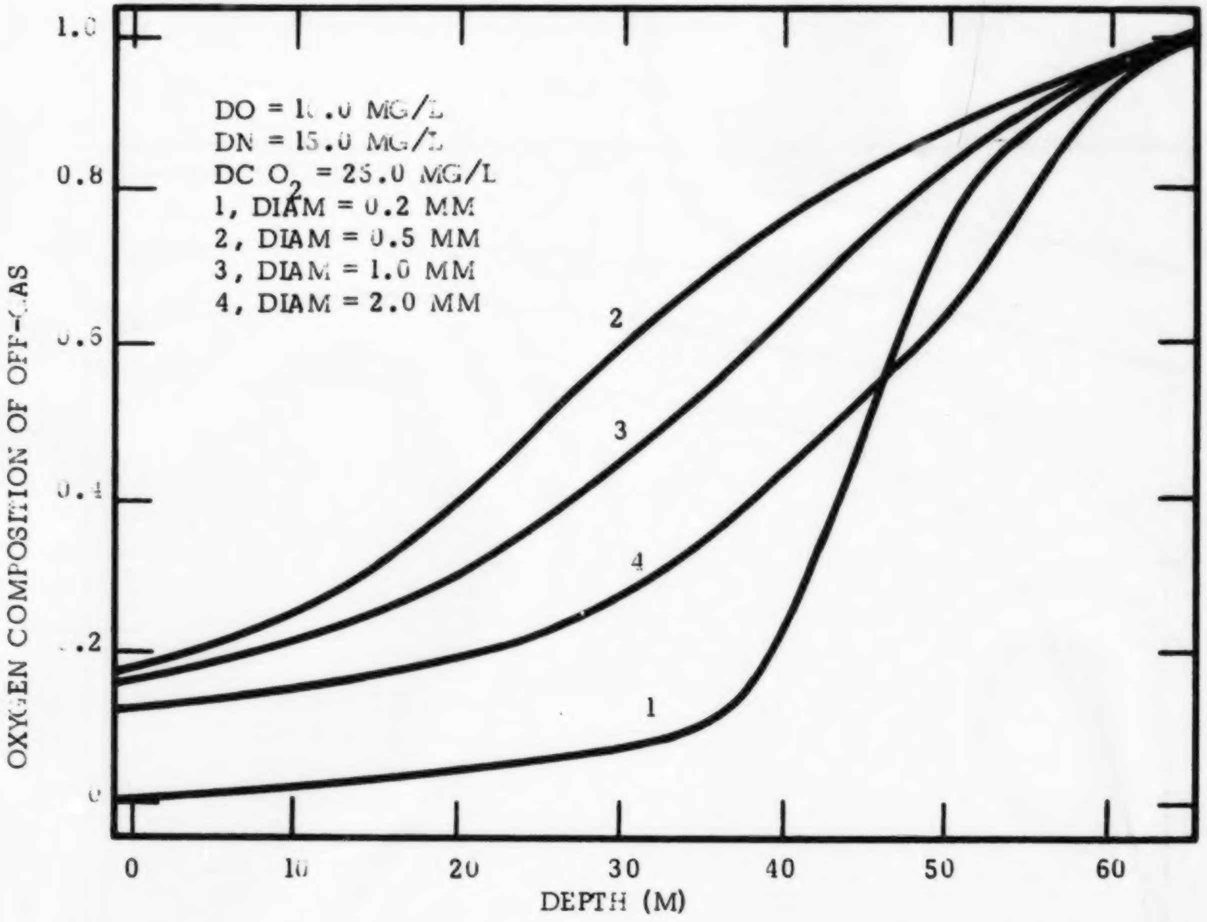

Fig. 89 OXYGEN COMPOSITION OF OFF-GAS VS DEPTH - PURE OXYGEN

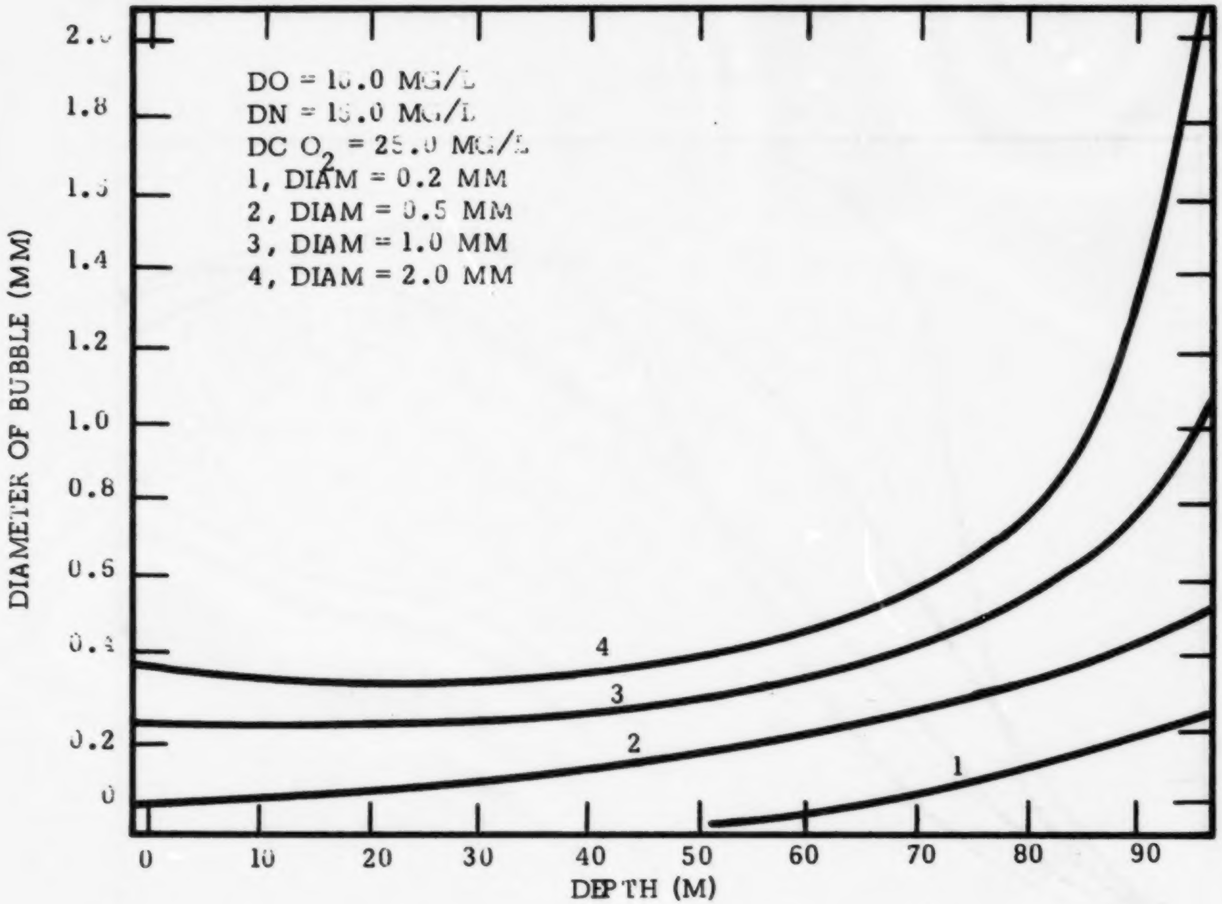

Fig. 90 DIAMETER OF BUBBLE AS A FUNCTION OF DEPTH - PURE OXYGEN

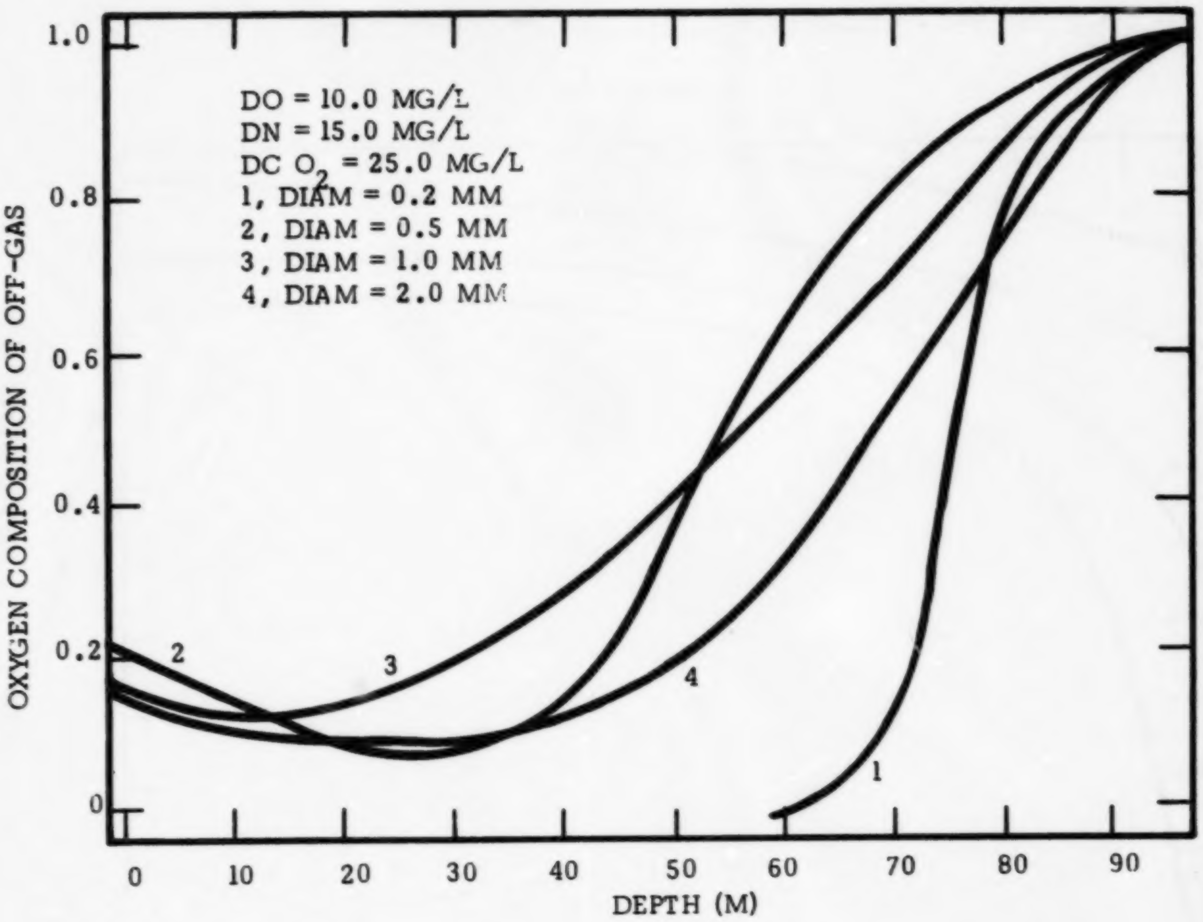

Fig. 91 OXYGEN COMPOSITION OF OFF-GAS VS DEPTH - PURE OXYGEN

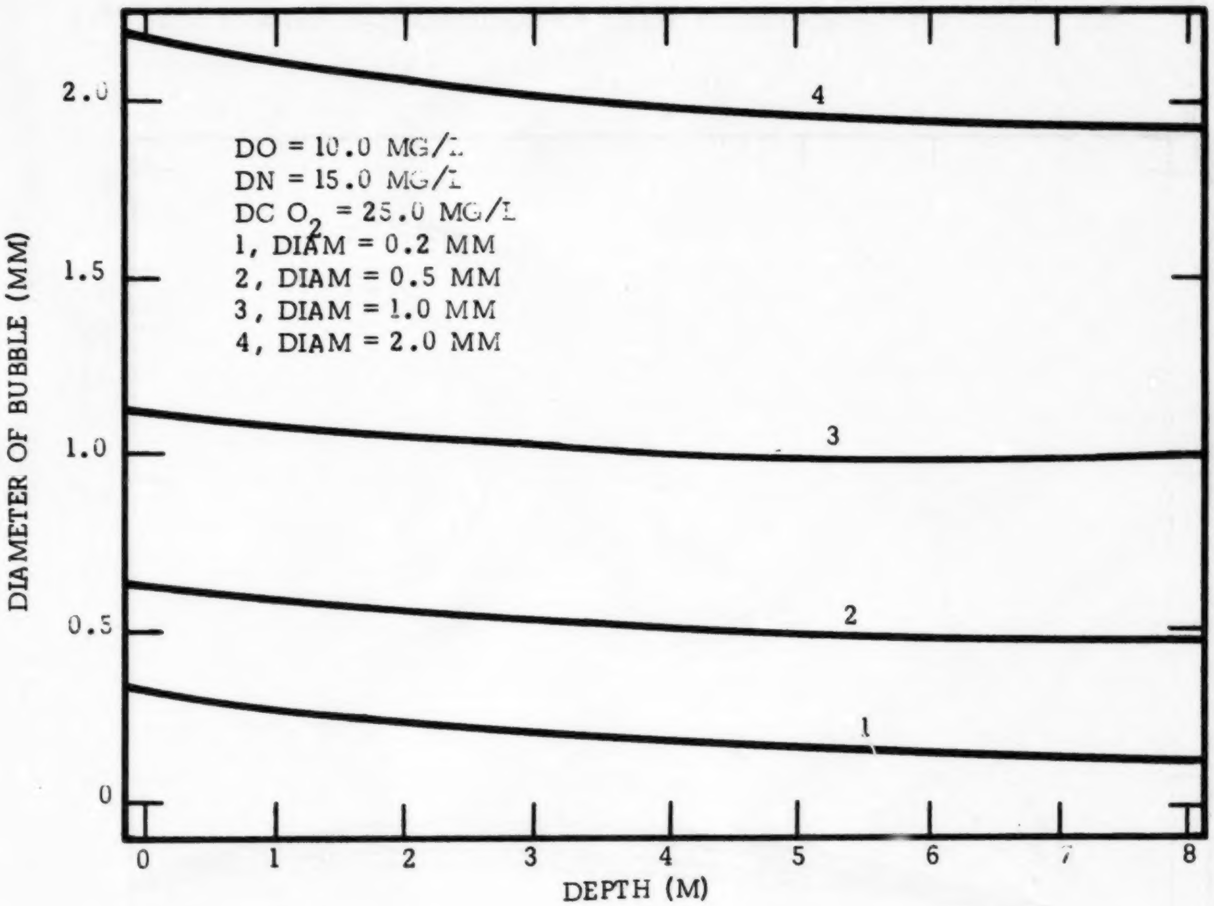

Fig. 92 DIAMETER OF BUBBLE AS A FUNCTION OF DEPTH - AIR

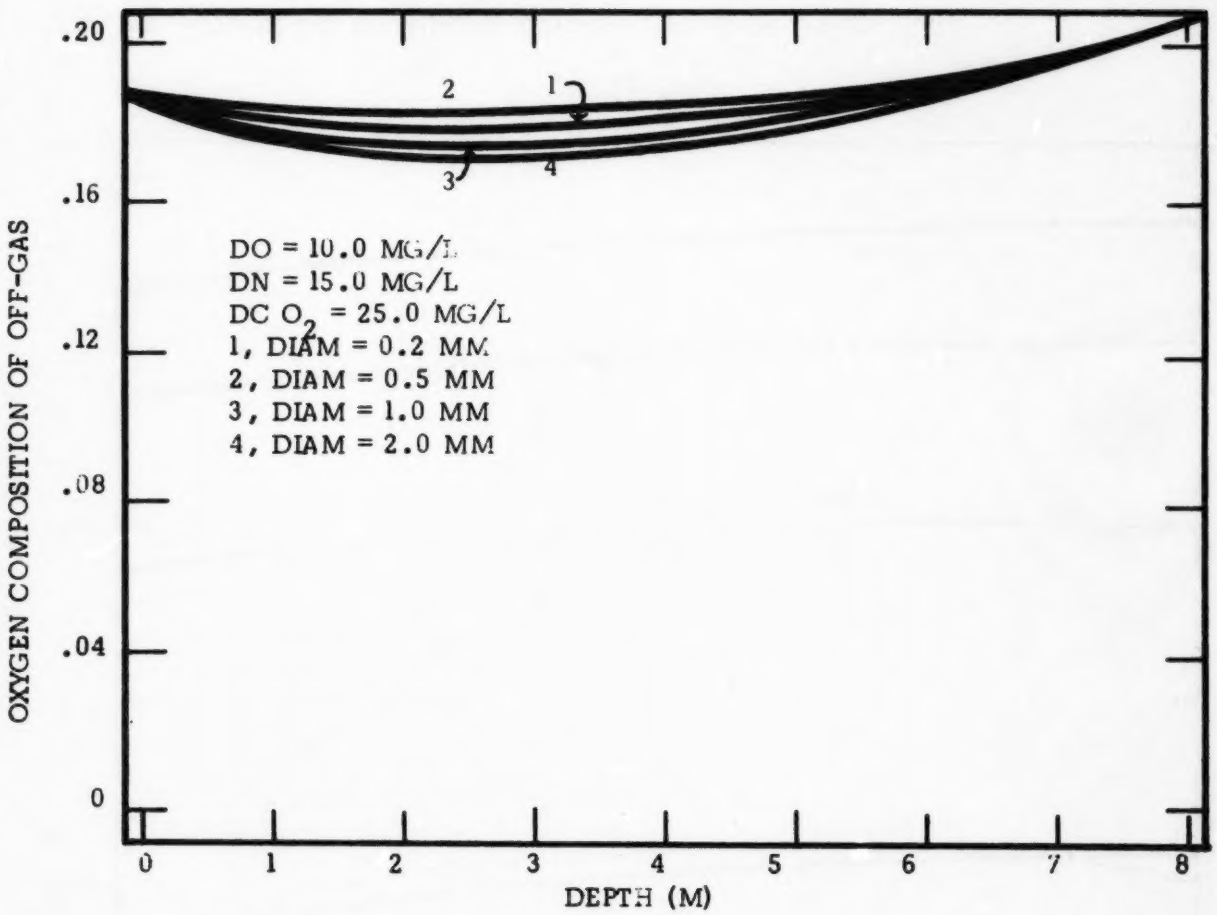

Fig. 93 OXYGEN COMPOSITION OF OFF-GAS VS DEPTH - AIR

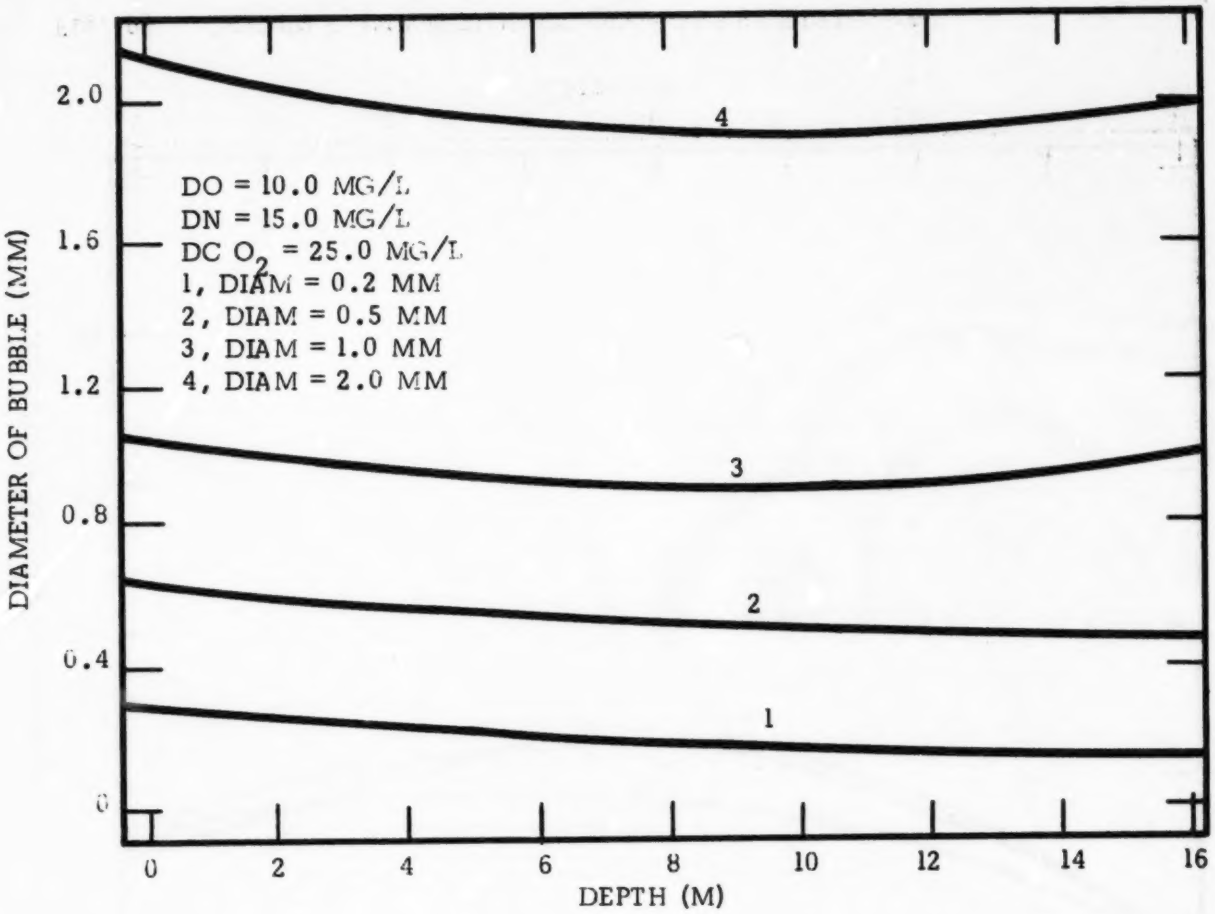

Fig. 94 DIAMETER OF BUBBLE AS A FUNCTION OF DEPTH - AIR

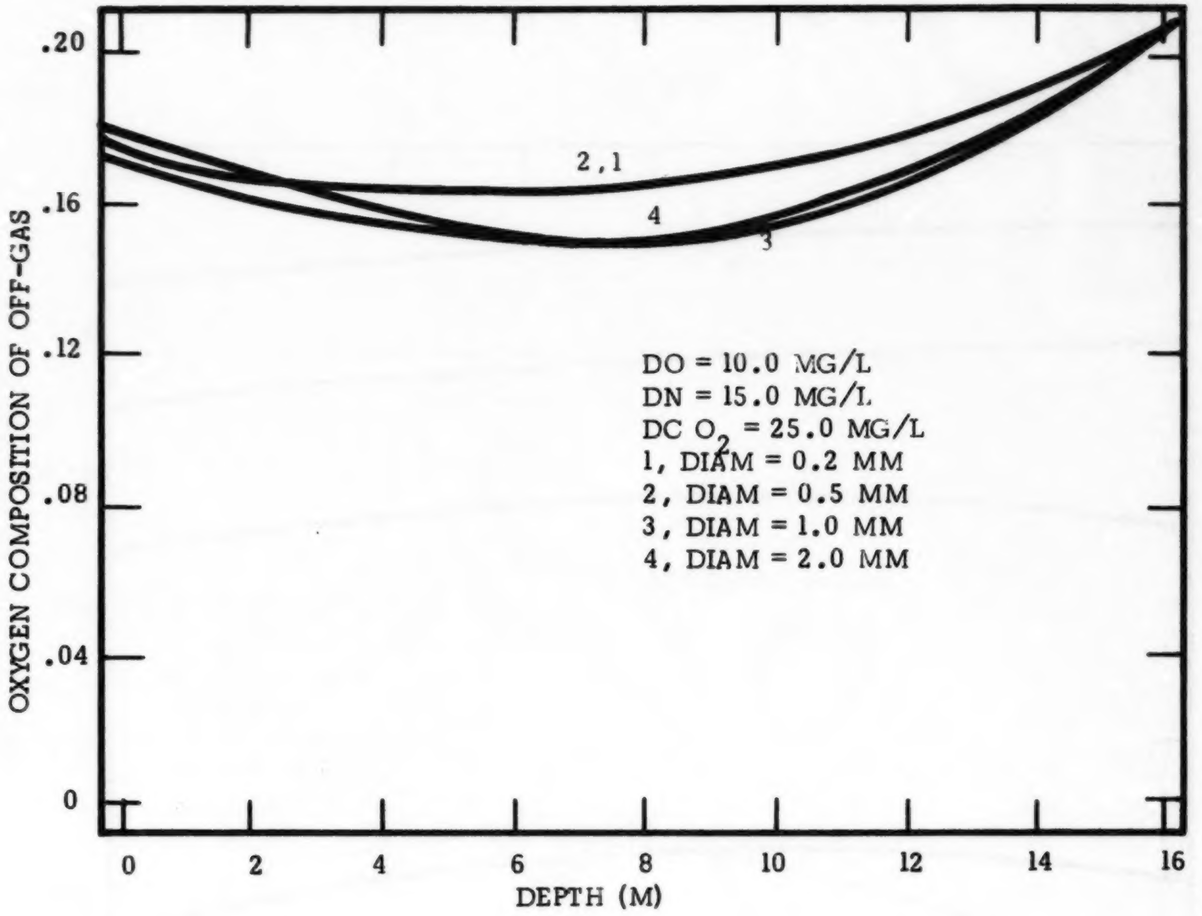

Fig. 95 OXYGEN COMPOSITION OF OFF - GAS VS DEPTH - AIR

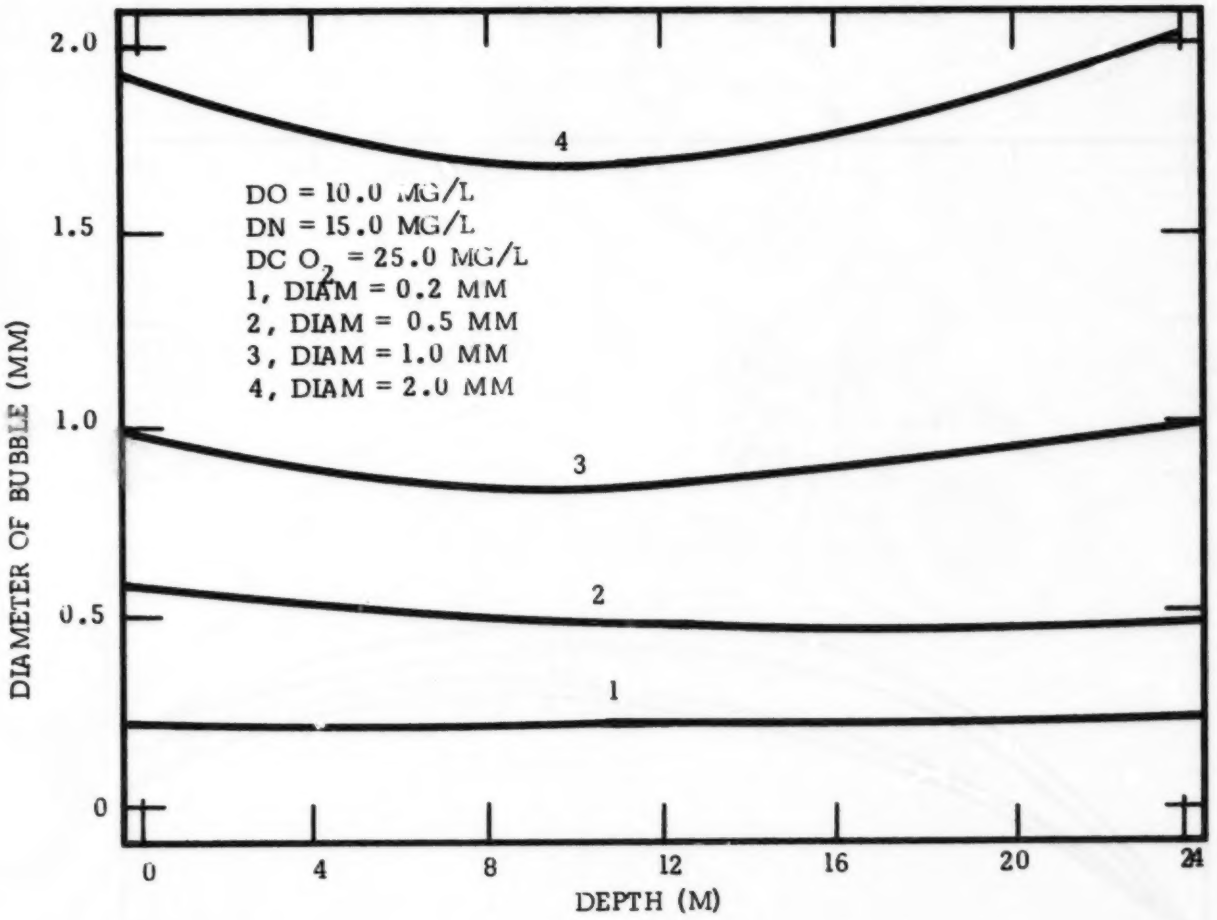

Fig. 96 DIAMETER OF BUBBLE AS A FUNCTION OF DEPTH - AIR

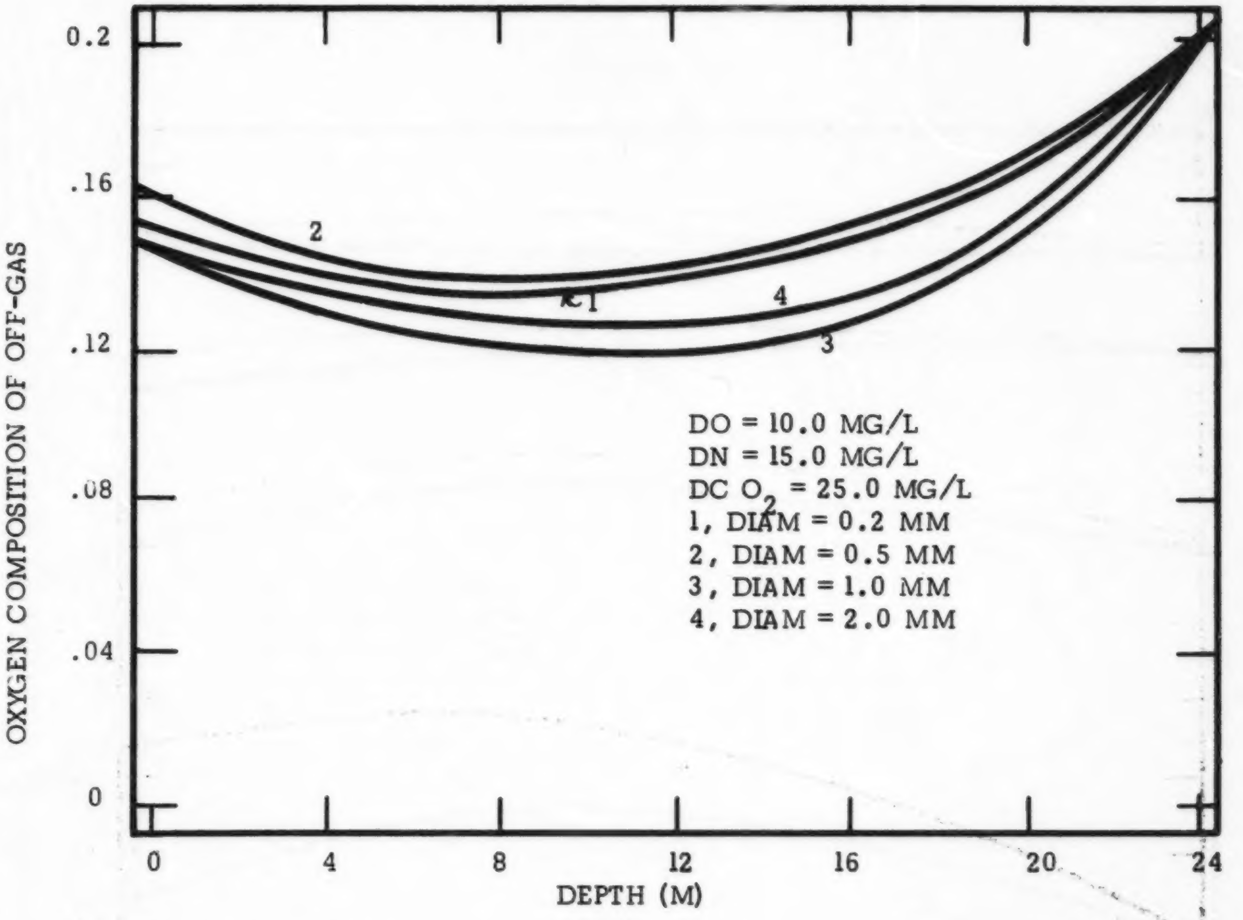

Fig. 97 OXYGEN COMPOSITION OF OFF-GAS VS DEPTH - IAR

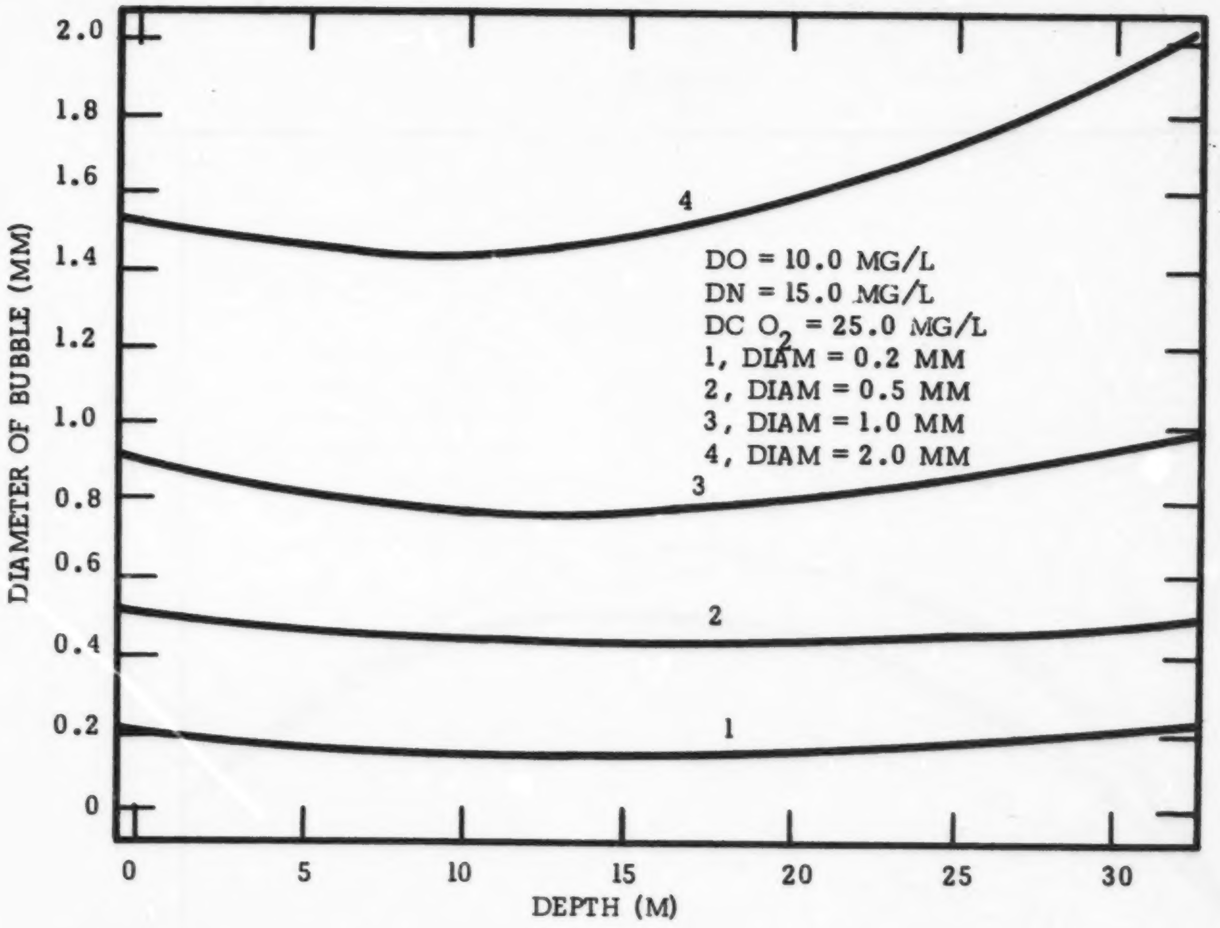

Fig. 98 DIAMETER OF BUBBLE AS A FUNCTION OF DEPTH - AIR

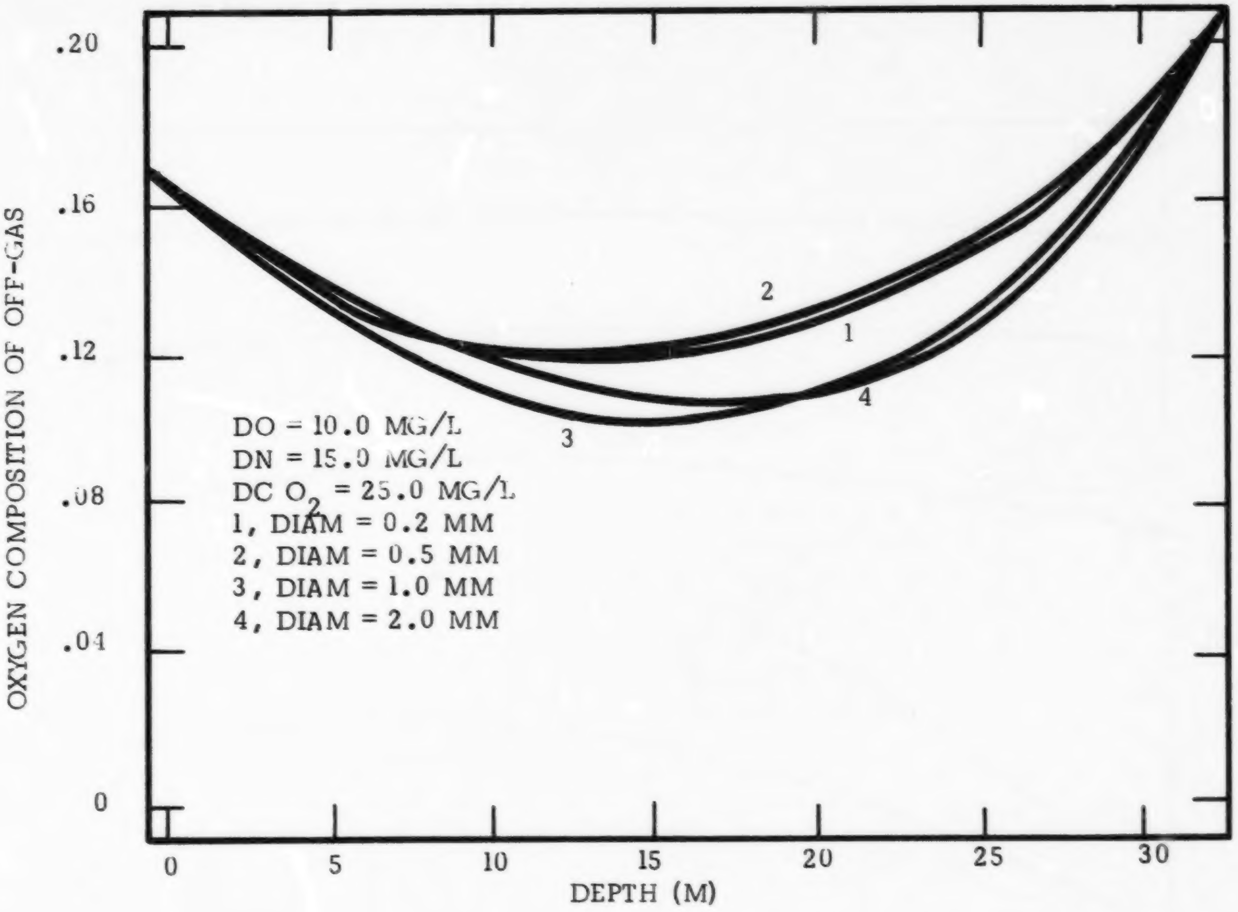

Fig. 99 OXYGEN COMPOSITION OF OFF-GAS VS DEPTH - AIR

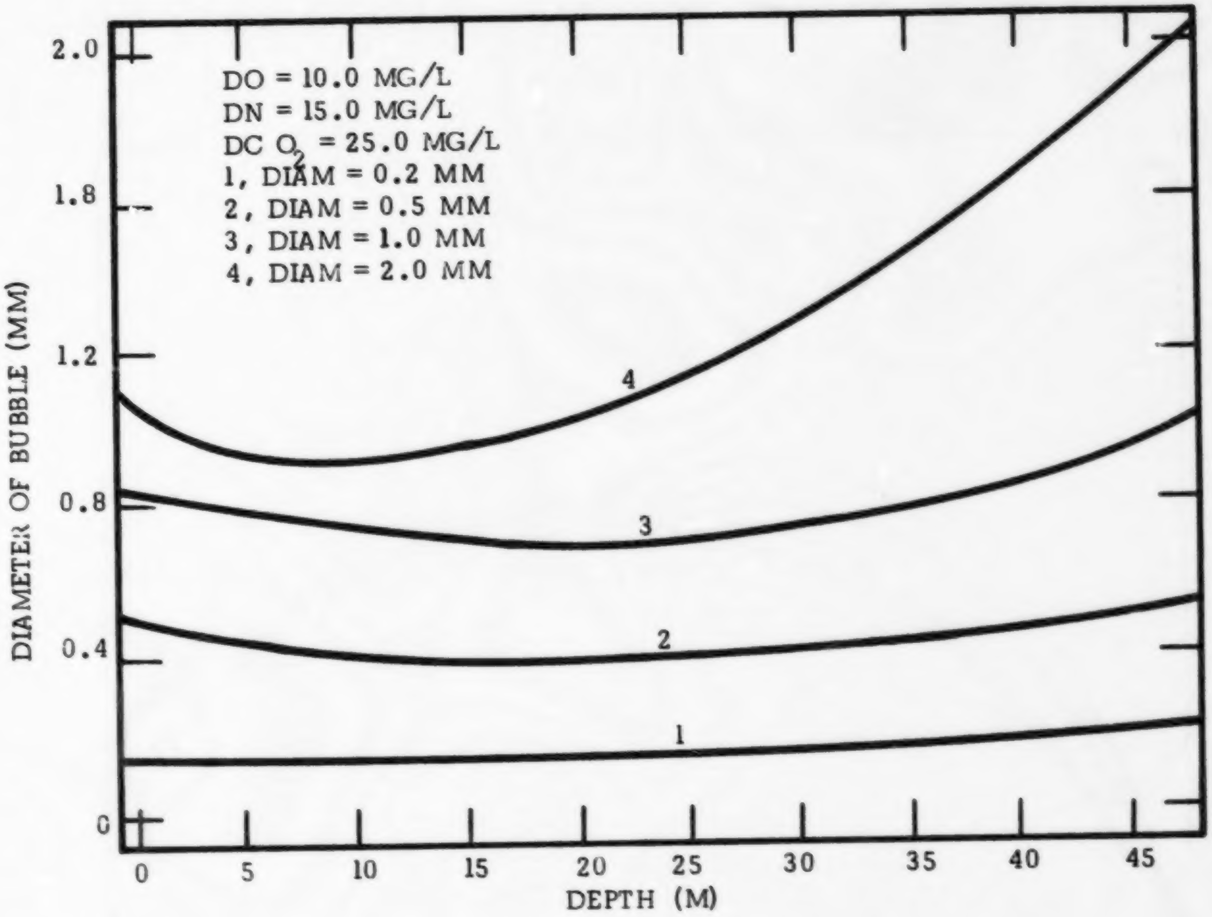

Fig. 100 DIAMETER OF BUBBLE AS A FUNCTION OF DEPTH - AIR

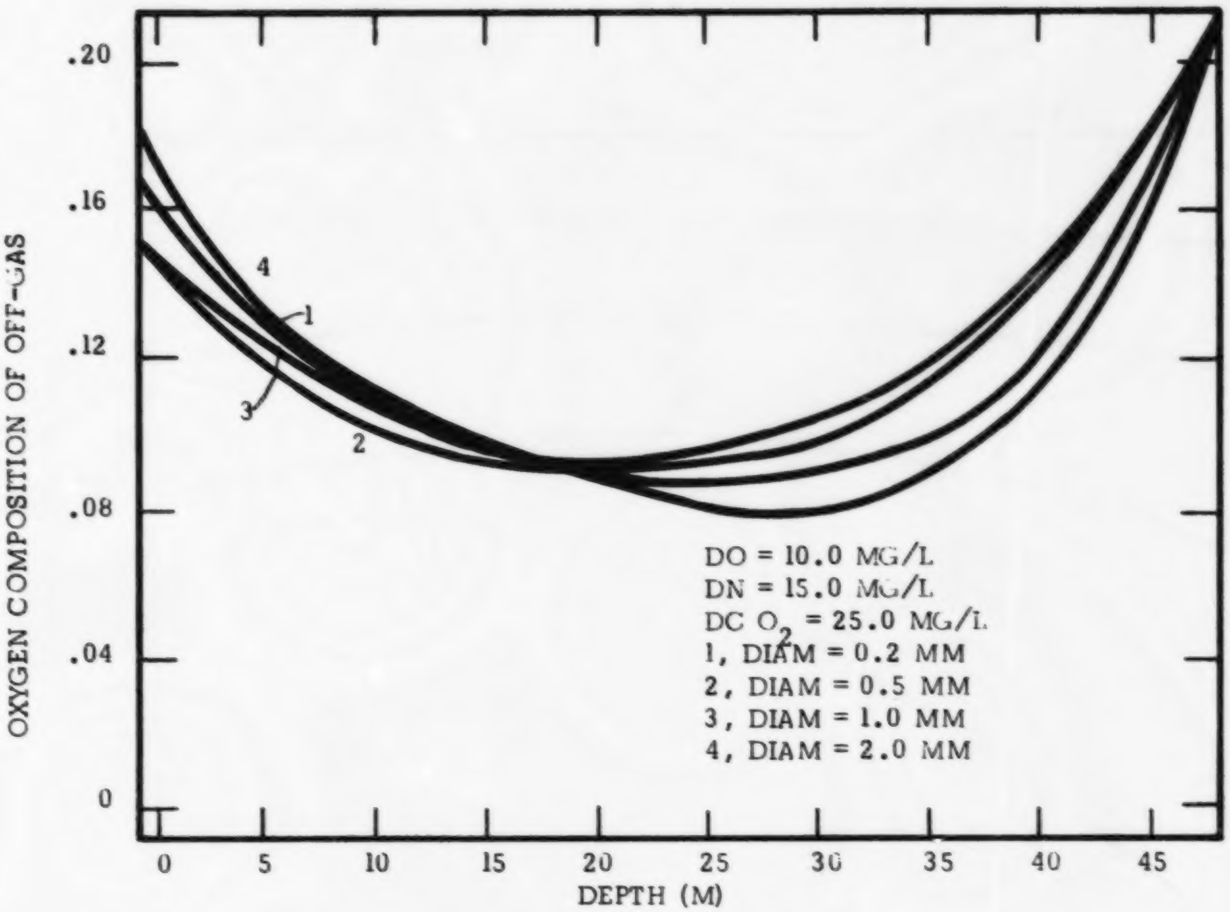

Fig. 101 OXYGEN COMPOSITION OF OFF-GAS VS DEPTH - AIR

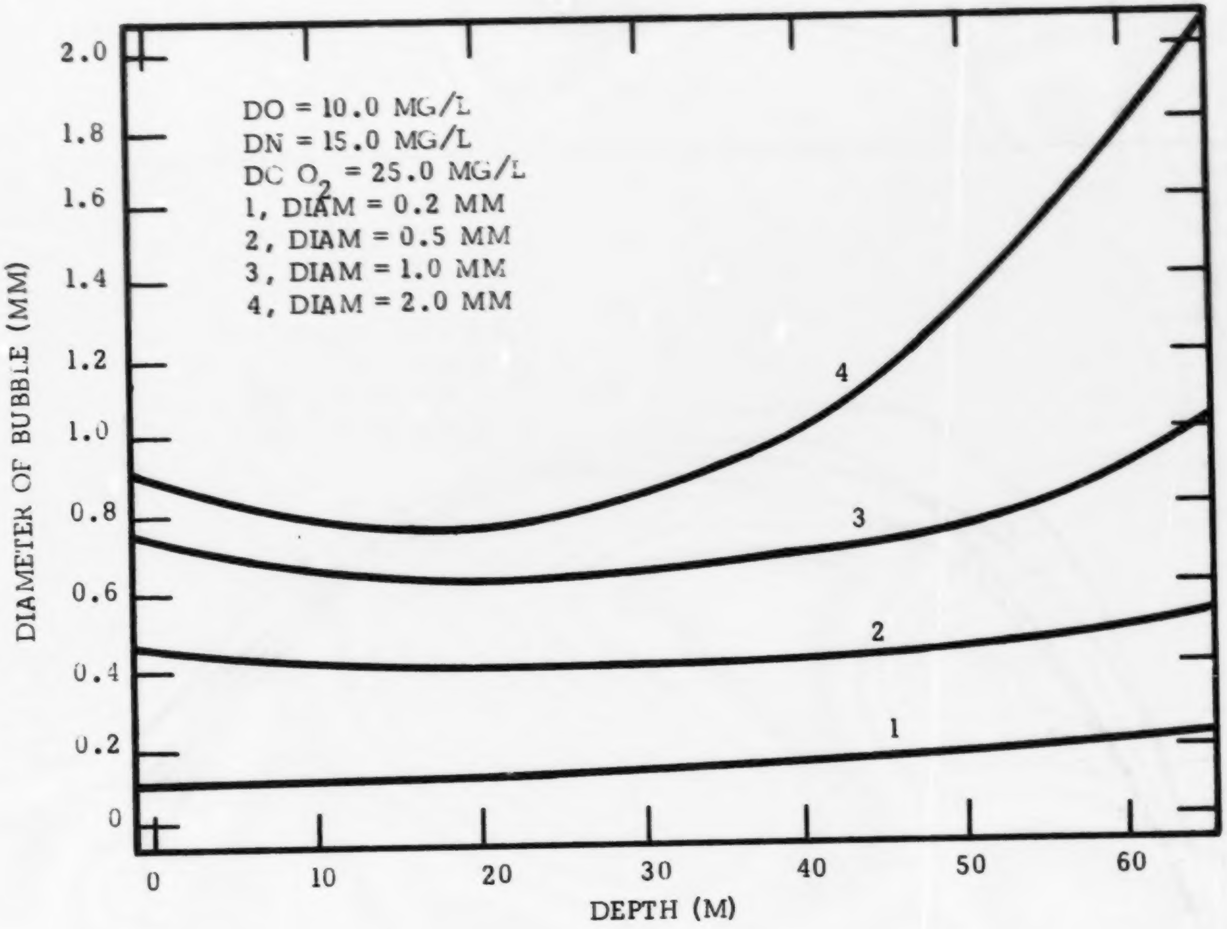

Fig. 102 DIAMETER OF BUBBLE AS A FUNCTION OF DEPTH - AIR

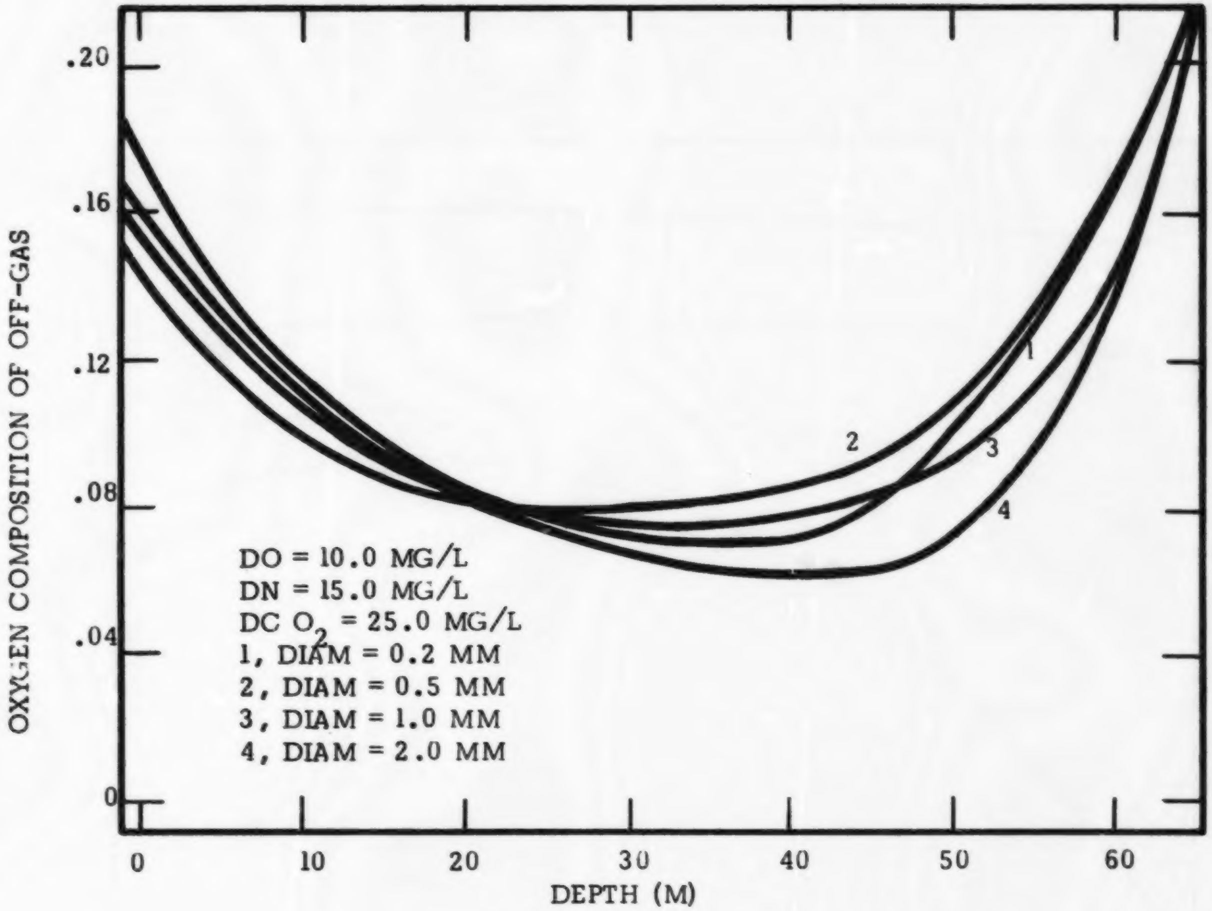

Fig. 103 OXYGEN COMPOSITION OF OFF-GAS VS DEPTH - AIR

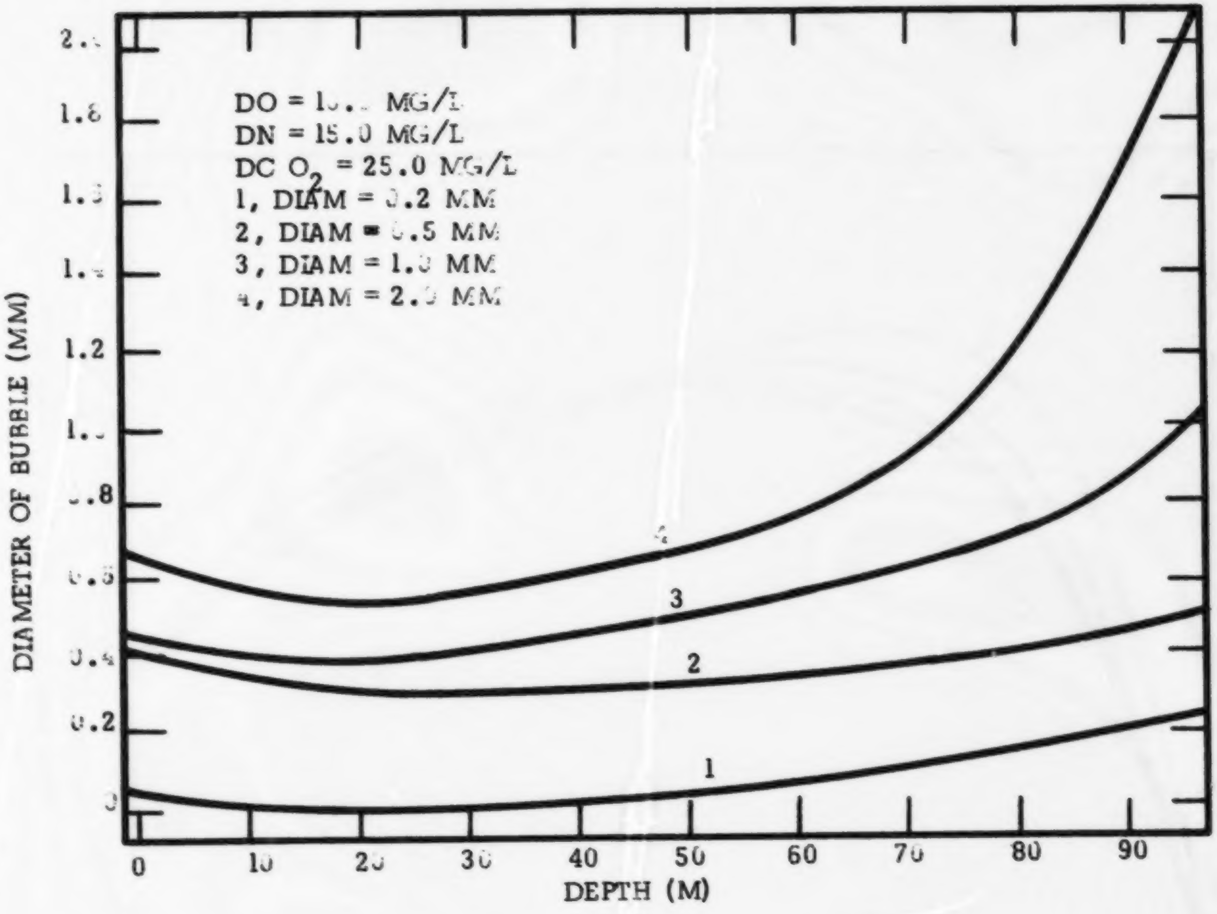

Fig. 104 DIAMETER OF BUBBLE AS A FUNCTION OF DEPTH - AIR

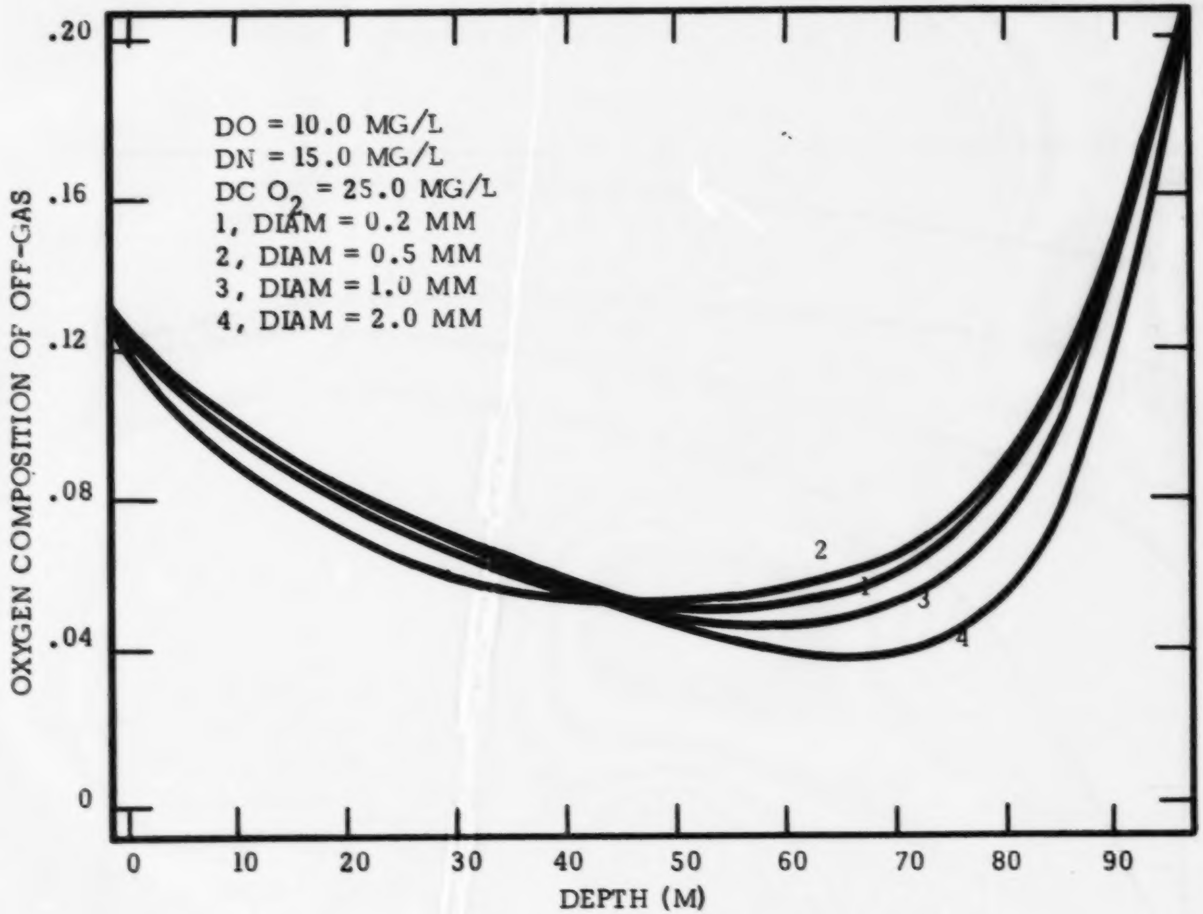

Fig. 105 OXYGEN COMPOSITION OF OFF-GAS VS DEPTH - AIR

☆U.S. GOVERNMENT PRINTING OFFICE: 1974 546-114/209 1-3